Faculty of Science and Engineering

Influence of Rock Wettability on Reservoir-Scale CO_2 Geo-Sequestration

Emad Abdulhusain Fakher Al-Khdheeawi

This thesis is presented for the Degree of
Doctor of Philosophy
of
Curtin University

June 2020

Declaration of Academic Integrity

To the best of my knowledge and belief this thesis contains no material previously published by any other person except where due acknowledgment has been made.

This thesis contains no material which has been accepted for the award of any other degree or diploma in any university.

Signature: **(Emad Abdulhusain Fakher Al-Khdheeawi)**

Date: 11 of June 2020

Copyright

Signature: **(Emad Abdulhusain Fakher Al-Khdheeawi)**

Date: 11 of June 2020

Dedication

I would like to dedicate my thesis to all those people who are source of my motivation!
To my mother, for your unconditional love, support, and prayers.

To the memory of my father (Peace be upon him).

To my wife, Doaa, for your unconditional love, support and understanding, and for all the encouragement and humour that kept me going. Without your support, it would have been difficult to complete this thesis. Thank you from the bottom of my heart.

To my lovely Kids, Mohammed and Lareen. You have always inspired me to keep on and gave me a reason to smile after long hours in the office.

My sincerest gratitude and appreciation to my brothers, sisters, and friends for their support, and prayers and encouragement.

Acknowledgement

First of all, I would like to express my utmost sincere appreciation to my main supervisors, Professor Stefan Iglauer and Associate Professor Ahmed Barifcani. Professor Stefan Iglauer, Thank you for your support through this process and over the years. Thank you for pushing me hard towards productivity. Associate Professor Ahmed Barifcani, your words of encouragement have driven me to work hard. I am grateful for your continual guidance and knowledge, which have provided the energy for me to push through the difficulties during my PhD research.

I also express my deepest appreciation to the co-supervisors, Dr. Stephanie Vialle, and Dr. Mohammad Sarmadivaleh. Dr. Stephanie Vialle, thank you for your excellent support, contributions, and encouragement, you never held back in ensuring continuous study progress and always offered positive guidance, and motivation through my study period. Dr. Mohammad Sarmadivaleh, thank you for your support and contributions towards my work progress.

I would like to thank the other professors, lecturers, research and administrative staff in the Department of Petroleum Engineering at Curtin University for their support, as well as my colleagues and office-mates who have offered their friendship, advice, and support.

I would like to thank the HCED for sponsoring my study.

In addition, my sincere thanks and gratitude go to my family, especially my mother for her encouragement, prayers. I would also like to thank my brothers, sisters, family and friends for their cheer throughout this long process.

My final and most significant acknowledgement must be given to my wife, Doaa, my son, Mohammed, and my daughter, Lareen, for their patience while I was working on this thesis research. Without their help, love, and forbearance, this thesis would not have been done.

Abstract

Concerning the underground storage of CO_2 in geological formations, CO_2 flow through porous media and CO_2 storage efficiency are significantly influenced by various parameters. Rock wettability, which is the tendency of the rock surface to be preferentially in contact with one fluid when more than one fluid is present in the same system, is one key parameter. It has been shown that wettability can vary from strongly water-wet to strongly CO_2-wet depending on the chosen reservoir. Moreover, wettability can strongly vary within a selected reservoir. Despite its importance, rock wettability has received little attention in CO_2 storage studies; specifically, rock wettability controls relative permeability, capillary pressures, residual fluid saturations, CO_2-brine interfacial areas, and CO_2 cluster morphologies.

Thus, the main focus of this research is to investigate the direct influence of rock wettability on CO_2 movement through porous media. By performing different multiphase flow reservoir simulations on a hectometre scale, this research investigates the effects of wettability and wettability spatial distribution on the efficiency of CO_2 trapping mechanisms. Further, this research includes a sensitivity analysis of the effect of factors affecting wettability on CO_2 movement and trapping capacities, including formation water salinity, reservoir temperature, and permeability and porosity spatial heterogeneity. This research also compares the efficiency of different CO_2 injection technologies, including injection well configurations (horizontal versus vertical injection wells) and CO_2 injection scenarios (continuous, intermittent injection, and water-alternating-gas injection (WAG)).

The results of this research show that reservoir wettability significantly influences CO_2 storage efficiency. CO_2-wet reservoirs have the highest vertical CO_2 plume migration while water-wet reservoirs have the best CO_2 retention. In addition, less residual CO_2 but more dissolved CO_2 is obtained in a CO_2-wet reservoir. Moreover, the results of this investigation clearly show that wettability heterogeneity significantly accelerates the vertical CO_2 migration distance, CO_2 mobility, and solubility trapping while reducing residual trapping. Further, the results of this research also show that formation water salinity, reservoir temperature, and permeability and porosity heterogeneity all affect CO_2 geo-sequestration efficiency. Lower salinity decreases CO_2 mobility and migration distance, and enhances residual and solubility trapping

significantly. Higher temperatures significantly increase vertical CO_2 migration, mobile CO_2, and dissolution trapping capacities while reducing the residual trapping capacity. Permeability and porosity heterogeneity reduces vertical CO_2 migration and induces significant horizontal migration but shows lower residual and solubility storage capacities. Moreover, this research demonstrates that a smart choice of CO_2 injection technology can significantly enhance CO_2 storage efficiency. Horizontal wells have reduced CO_2 plume migration, CO_2 mobility, and CO_2 solubility trapping and improved CO_2 residual trapping. WAG injection results in more favourable CO_2 storage outcomes when compared with continuous or intermittent injections. Specifically, residual and solubility trapping were significantly improved while vertical CO_2 migration was reduced.

This thesis concludes that water-wet rock and homogeneous wettability improve CO_2 storage capacity and containment security. Further, this work concludes that low porosity and permeability heterogeneity, low formation water salinities, low reservoir temperatures, using horizontal injection wells, and WAG injection all enhance CO_2 geo-sequestration capacity.

Publications by the Author

Journal Articles forming part of thesis as standalone chapters

1. **Emad A. Al-Khdheeawi,** Stephanie Vialle, Ahmed Barifcani, Mohammad Sarmadivaleh, and Stefan Iglauer. (2017). Influence of CO_2-wettability on CO_2 migration and trapping capacity in deep saline aquifers. Greenhouse Gases: Science and Technology, 7(2), 328-338. doi:10.1002/ghg.1648
2. **Emad A. Al-Khdheeawi,** Stephanie Vialle, Ahmed Barifcani, Mohammad Sarmadivaleh, and Stefan Iglauer. (2017). Impact of reservoir wettability and heterogeneity on CO_2-plume migration and trapping capacity. International Journal of Greenhouse Gas Control, 58, 142-158. doi: 10.1016/j.ijggc.2017.01.012.
3. **Emad A. Al-Khdheeawi**, Stephanie Vialle, Ahmed Barifcani, Mohammad Sarmadivaleh, and Stefan Iglauer. (2017). Influence of injection well configuration and rock wettability on CO_2 plume behaviour and CO_2 trapping capacity in heterogeneous reservoirs. Journal of Natural Gas Science and Engineering, 43, 190-206. doi: 10.1016/j.jngse.2017.03.016
4. **Emad A. Al-Khdheeawi,** Stephanie Vialle, Ahmed Barifcani, Mohammad Sarmadivaleh, and Stefan Iglauer. (2018). Effect of wettability heterogeneity and reservoir temperature on CO_2 storage efficiency in deep saline aquifers. International Journal of Greenhouse Gas Control, 68, 216-229.
5. **Emad A. Al-Khdheeawi,** Stephanie Vialle, Ahmed Barifcani, Mohammad Sarmadivaleh, Yihuai Zhang, and Stefan Iglauer. (2018). Impact of salinity on CO_2 containment security in highly heterogeneous reservoirs. Greenhouse Gases: Science and Technology, 8(1), 93-105. doi:10.1002/ghg.1723
6. **Emad A. Al-Khdheeawi,** Stephanie Vialle, Ahmed Barifcani, Mohammad Sarmadivaleh, and Stefan Iglauer. (2018). Enhancement of CO_2 trapping efficiency in heterogeneous reservoirs by Water Alternating Gas injection. Greenhouse Gases: Science and Technology, 8(5), 920-931. doi:10.1002/ghg.1805

Journal Articles relevant to the thesis but not forming part of it

7. **Emad A. Al-Khdheeawi,** Stephanie Vialle, Ahmed Barifcani, Mohammad Sarmadivaleh, and Stefan Iglauer. (2017). Effect of brine salinity on CO2 plume migration and trapping capacity in deep saline aquifers. The APPEA Journal, 57(1), 100-109.
8. **Emad A. Al-Khdheeawi,** Stephanie Vialle, Ahmed Barifcani, Mohammad Sarmadivaleh, and Stefan Iglauer. (2017). Influence of Rock Wettability on CO2 Migration and Storage Capacity in Deep Saline Aquifers. Energy Procedia, 114, 4357-4365.
9. **Emad A. Al-Khdheeawi,** Stephanie Vialle, Ahmed Barifcani, Mohammad Sarmadivaleh, and Stefan Iglauer. (2018). Impact of injected water salinity on CO2 storage efficiency in homogenous reservoirs. The APPEA Journal, 58(1), 44-50.
10. **Emad A. Al-Khdheeawi,** Stephanie Vialle, Ahmed Barifcani, Mohammad Sarmadivaleh, and Stefan Iglauer. (2019). Effect of the number of water alternating CO_2 injection cycles on CO_2 trapping capacity. The APPEA Journal, 59, 357-363.

Refereed Conference Papers:

11. **Emad A. Al-Khdheeawi,** Stephanie Vialle, Ahmed Barifcani, Mohammad Sarmadivaleh, and Stefan Iglauer. (2017). CO_2 trapping capacity as a function of CO_2 injection scenarios in weakly water-wet reservoirs. Paper presented at the 2017 One Curtin Postgraduate Conference, 10-12 December 2017, Miri, Sarawak, Malaysia.
12. **Emad A. Al-Khdheeawi,** Stephanie Vialle, Ahmed Barifcani, Mohammad Sarmadivaleh, and Stefan Iglauer. (2018). Impact of Injection Scenario on CO2 Leakage and CO_2 Trapping Capacity in Homogeneous Reservoirs. Paper presented at the Offshore Technology Conference Asia, 20-23 March 2018, Kuala Lumpur, Malaysia.
13. **Emad A. Al-Khdheeawi,** Stephanie Vialle, Ahmed Barifcani, Mohammad Sarmadivaleh, and Stefan Iglauer. (2018). The effect of $WACO_2$ ratio on CO_2 geo-sequestration efficiency in homogeneous reservoirs. Paper presented at the

Applied Energy Symposium and Forum, Carbon Capture, Utilization and Storage, CCUS 2018, 27–29 June 2018, Perth, Australia.

14. **Emad A. Al-Khdheeawi,** Stephanie Vialle, Ahmed Barifcani, Mohammad Sarmadivaleh, and Stefan Iglauer. (2018). Implementation of different CO_2-rock-water wettability conditions in TOUGH2. Paper presented at TOUGH symposium 2018, 8–10 October 2018, Berkeley, California, USA.
15. **Emad A. Al-Khdheeawi,** Stephanie Vialle, Ahmed Barifcani, Mohammad Sarmadivaleh, and Stefan Iglauer. (2018). Implementation of Wettability in TOUGH2 for improved estimates of CO_2 storage capacity. Paper presented at the Second Biennial Meeting of Australian Chapter of InterPore, 31 October–2 November 2018, Melbourne, Australia.

Table of Contents

List of Figures

List of Tables

Chapter 1 Introduction

1.1 Background

CO_2 injection into oil reservoirs is an essential technology for enhancing oil recovery (CO_2-EOR). Further, CO_2-EOR is a good option for long-term CO_2 geological sequestration, which is a significant method of mitigating anthropogenic carbon emission (Bachu, 2008). This is done by capturing CO_2 and injecting it into geological sites, such as depleted oil and gas reservoirs, unminable coal seams, and deep saline aquifers (Metz et al., 2005). Owing to their high geo-sequestration capacity and wide geographical spread, saline aquifers are the most preferable CO_2 geo-sequestration formations (Lackner, 2003). Typically, the CO_2 injection depth should be deeper than 800m, where the associated reservoir conditions (i.e., temperature and pressure) are higher than the critical temperature (31.04 °C) and the critical pressure (7.39 MPa) of CO_2. Thus, the injected CO_2 remains in a supercritical state (Pruess et al., 2003). However, the injected CO_2's density is lower than that of formation water; therefore, injected CO_2 migrates upwards as a result of the buoyancy forces (Flett et al., 2007). This upward migration can be reduced by four trapping mechanisms: structural, residual, dissolution, and mineral trapping. Once the CO_2 is injected into the reservoirs, some of it will be trapped by impermeable seals (i.e., by structural trapping) (Hesse et al., 2008; Iglauer et al., 2015a). In addition, large volumes of the injected CO_2 will be immobilised by the capillary trapping mechanism, which is controlled by capillary forces (Pentland et al., 2011; Iglauer et al., 2011). Some of the supercritical CO_2 will be dissolved in formation water to be trapped as dissolution trapping, which is a function of the CO_2 and water interface area (Lindeberg and Wessel-Berg, 1997; Spycher et al., 2003; Iglauer, 2011). Finally, some of the CO_2 will be trapped by the mineral trapping mechanism, which results from chemical reactions between the reservoir minerals and dissolved CO_2 (Xu et al., 2004; Gaus, 2010). Only the first three trapping mechanisms are treated in this thesis. The capacity of these trapping mechanisms and CO_2 movement in porous media are affected by many caprock and reservoir parameters. Rock wettability is one of these parameters, which, despite its importance, has received little attention in CO_2 geo-sequestration reservoir simulations (Iglauer et al., 2015a). Specifically, rock wettability has a significant

effect on capillary pressure (Anderson, 1987a; Batycky et al., 1981; Heiba et al., 1983; Melrose, 1965; Morrow, 1976), relative permeability (Owens and Archer, 1971; McCaffery and Bennion, 1974; Heiba et al., 1983; Anderson, 1987b; Krevor et al., 2012; Levine et al., 2014), residual CO_2 saturations (Iglauer et al., 2011; Anderson, 1987b; Chaudhary et al., 2013), reservoir fluid displacement mechanisms, and phase distribution in the reservoir (Morrow, 1990). Based on the experimental observations, rock wettability can vary tremendously from strongly CO_2-wet to strongly water-wet. This wettability variation is a result of factors such as reservoir temperature (Broseta et al., 2012; Al-Yaseri et al., 2016; Arif et al., 2016a,b), salinity and ion type (Al-Yaseri et al., 2016; Arif et al., 2016b; Chiquet et al., 2007; Espinoza and Santamarina, 2010; Wang et al., 2012), reservoir pressure (Al-Yaseri et al., 2016; Arif et al., 2016a,b; Chiquet et al., 2007; Broseta et al., 2012), and surface chemistry (Iglauer et al., 2015a,b). Experimental studies have shown that low salinity water flooding changes the rock wettability towards a more water-wet state (Morrow and Buckley, 2011; Myint and Firoozabadi, 2015; Sheng, 2014). Importantly, experimental measurements performed at laboratory scale (mm to cm) clearly investigated that rock wettability affects residual trapping (Iglauer et al., 2011; Iglauer, 2017; Andrew et al., 2013; Chaudhary et al., 2013; Rahman et al., 2016) and structural trapping (Naylor et al., 2011; Iglauer et al., 2015; Iglauer, 2017).

Moreover, most of the previous studies assumed that the reservoir has a homogeneous wettability (strongly water-wet) state. However, this is unlikely (Iglauer, 2017). Based on experimental investigations at different laboratory scales (ranging from the microscale to the macroscale) rock wettability is distributed heterogeneously (Aspenes et al., 2003; Chaouche et al., 1994; Graue et al., 2002; Masalmeh, 2002; Morrow et al., 1986; Spinler et al., 2002; Standnes and Austad, 2000; Vizika and Duquerroix, 1997). This heterogeneous wettability distribution is a result of various factors, including pore-surface roughness heterogeneity, mineral surface chemical heterogeneity, grain size heterogeneity, permeability heterogeneity and the associated fluid flow, adsorption of organics, reservoir depth, and chemistry variations of the rock surface (Crocker and Marchin, 1988; Drelich and Miller, 1994; Gaydos and Neumann, 1987; Iglauer et al., 2015a,b; Iglauer, 2017; Jafari and Jung, 2016; Laroche et al., 1999; Li, 1996; Lin et al., 1993; Morrow et al., 1986; Saghafi et al., 2014; Van Lingen et al., 1996; Vizika and Duquerroix, 1997). Regardless that it has been demonstrated that this heterogeneous wettability distribution significantly affects phase distribution

during EOR processes and displacement mechanisms (Laroche et al., 1999; Anderson, 1986, 1987a,b; Chang et al., 1997; Morrow, 1990; Bertin et al., 1998; Blunt, 1997; Kiriakidis et al., 1993), its influence on CO_2 storage efficiency has not been investigated previously.

Thus, in this research, we develop various multiphase flow reservoir simulation models on a hectometre-scale to investigate the influence of the rock wettability and wettability heterogeneity on CO_2 storage efficiency and CO_2 movement through porous media. This thesis also includes a sensitivity analysis on effect of other parameters, such as reservoir temperature, formation water salinity, reservoir permeability and porosity heterogeneity, injection well configurations (i.e., vertical and horizontal wells), and the CO_2 injection scheme (i.e., continuous injection, intermittent injection, and water-alternating-gas (WAG) injection), on CO_2 geo-sequestration and CO_2 flow through porous media.

1.2 Research Objectives

The main objective of this research is to investigate the influence of rock wettability on CO_2 storage efficiency and CO_2 movement through porous media. The specific objectives of this research are described below:

1- Investigating the influence of rock wettability on CO_2 storage efficiency and CO_2 movement in homogeneous reservoirs by testing the CO_2 trapping capacity and CO_2 plume migration for five wettability conditions (i.e., strongly water-wet, weakly water-wet, intermediate-wet, weakly CO_2-wet, and strongly CO_2-wet) in a homogeneous reservoir.

2- Investigating the effect of reservoir wettability on CO_2 trapping capacities and CO_2 mobility in heterogeneous reservoirs (reservoirs with a heterogeneous distribution of permeability and porosity).

3- Investigating the impact of heterogeneous wettability distribution (at isothermal and non-isothermal conditions) on vertical CO_2 plume migration and dissolution and residual trapping storage capacities.

4- Investigating the effect of geological parameters affecting rock wettability (i.e. reservoir temperature, brine salinity, and reservoir heterogeneity) on CO_2 geo-sequestration efficiency.

5- Optimizing CO_2 injection technology by investigating the effect of two important technical parameters: the CO_2 injection scheme (i.e., continuous injection, intermittent injection, and water-alternating-gas (WAG) injection) and the injection well configuration (i.e., vertical and horizontal wells) on CO_2 trapping efficiency.

1.3 Thesis Outline and Organisation

This thesis comprises nine chapters, including the introduction (Chapter 1), literature review (Chapter 2), methodology, results, and discussion (chapters 3 – 8), and conclusions, recommendations and outlook for future work (Chapter 9). The structure of the thesis objectives (Chapters 3 – 8) is presented in Figure 1-1. The nine chapters are detailed below:

Chapter 1 — *Introduction* **—** Presents a brief introduction and background of the thesis, research objectives, and thesis outline and organisation.

Chapter 2 — *Literature Review* **—** Provides an overview of the previous studies on rock wettability and CO_2 geo-sequestration processes. First, some fundamentals concerning oil-water-rock and CO_2-water-rock systems are presented. Then, we discuss the various existing wettability measurement methods, as well as the key parameters affecting rock wettability. We also give an overview of the different carbon geo-sequestration processes. Finally, we present a comprehensive review of the previous simulation studies regarding the influence of wettability on CO_2 storage capacity.

Chapter 3 — *Influence of CO_2-wettability on CO_2 migration and trapping capacity in deep saline aquifers. Greenhouse Gases: Science and Technology. 7(2): 328-338 (2017); doi:10.1002/ghg.1648* **—** Investigates the effect of CO_2 wettability on CO_2 plume migration, CO_2 mobility, and the capacity of residual and solubility trapping in homogeneous reservoirs and demonstrates its key importance. In this chapter, multiphase flow reservoir simulations on a homogeneous reservoir have been

performed using five relative permeability and capillary pressure curves that represent five characteristic wettability scenarios from strongly water-wet to strongly CO_2-wet.

Chapter 4 — *Impact of reservoir wettability and heterogeneity on CO_2-plume migration and trapping capacity. International Journal of Greenhouse Gas Control. 58: 142-158 (2017); doi: 10.1016/j.ijggc.2017.01.012* **—** Investigates the impact of reservoir wettability on storage capacities (i.e., residual trapping and dissolution trapping), mobile CO_2 capacity, and CO_2 plume migration patterns in heterogeneous reservoirs using 3D reservoir simulation models. This chapter also demonstrates the impact of permeability and porosity heterogeneity within the reservoir on CO_2 storage efficiency.

Chapter 5 — *Influence of injection well configuration and rock wettability on CO_2 plume behaviour and CO_2 trapping capacity in heterogeneous reservoirs. Journal of Natural Gas Science and Engineering. 43: 190-206 (2017); doi: 10.1016/j.jngse.2017.03.016* **—** Investigates the impact of the CO_2 injection well configuration (vertical versus horizontal) and rock wettability on the CO_2 geo-storage efficiency. In this chapter, three-dimensional multiphase flow simulations have been developed in a heterogeneous reservoir using four injection well scenarios: one vertical well, two vertical wells, four vertical wells, and one horizontal well with different wettability conditions.

Chapter 6 — *Effect of wettability heterogeneity and reservoir temperature on CO_2 storage efficiency in deep saline aquifers. International Journal of Greenhouse Gas Control. 68: 216-229 (2018); doi: 10.1016/j.ijggc.2017.11.016* **—** Investigates the influence of heterogeneous wettability distribution (at isothermal and non-isothermal conditions) and reservoir temperature on the CO_2 geo-storage efficiency in heterogeneous porosity and permeability reservoirs.

Chapter 7 — *Impact of salinity on CO_2 containment security in highly heterogeneous reservoirs. Greenhouse Gases: Science and Technology. 8(1): 93-105 (2018); doi: 10.1002/ghg.1723* **—** Computationally examines the effect of salinity (in the range 3-20 wt%) on CO_2 geo-sequestration efficiency using a highly heterogeneous 3D reservoir scale model.

Chapter 8 — *Enhancement of CO_2 trapping efficiency in heterogeneous reservoirs by water- alternating gas injection. Greenhouse Gases: Science and Technology.*

00:1–12 (2018); doi: 10.1002/ghg.1805 — Investigates the influence of CO_2 injection scenarios, namely continuous CO_2 injection, intermittent CO_2 injection, and water alternating gas injection on CO_2 trapping efficiency. In this chapter, numerical multiphase flow simulations have been used in a highly heterogeneous, hectometre-sized storage reservoir.

Chapter 9 — *Conclusions, Recommendations and Outlook for Future Work* — Concludes the thesis and provides recommendations for future research.

Note: Chapters 3 – 8 have all been published by the author in peer-reviewed journals (please refers to the section "Publications by the Author" on page VII) and are reproduced in this thesis as individual chapters. Due to the selected format, some details may appear more than once across different chapters and reader may like to read them separately. Appendix B contains the relevant copyright agreements between the author and the respective journals.

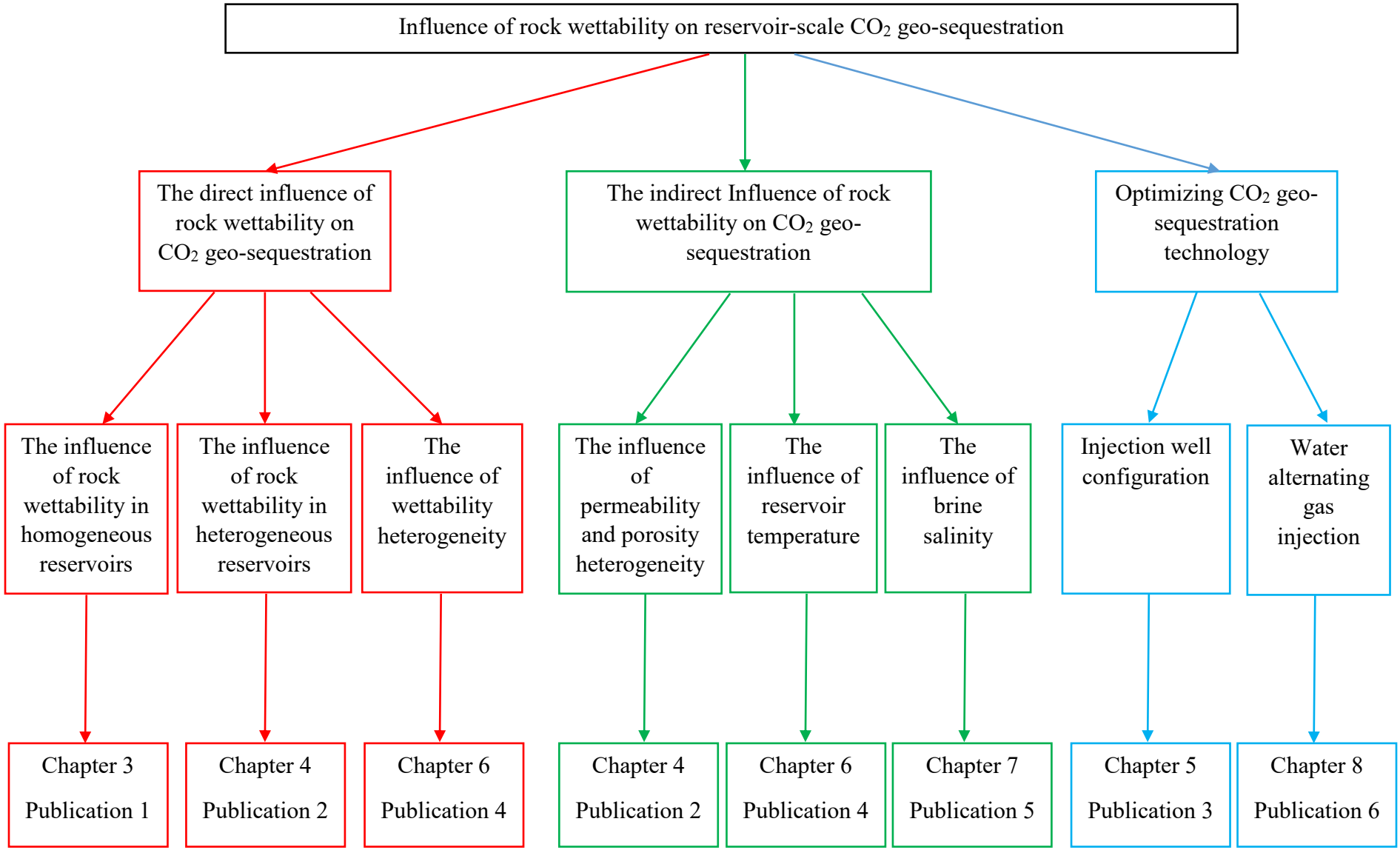

Figure 1-1 Thesis objectives and structural layout

Chapter 2 Literature Review

2.1 Introduction

This chapter provides an overview of previous studies on rock wettability and how it affects CO_2 geo-sequestration processes. First, this chapter presents the fundamentals of wettability in oil-water-rock and CO_2-water-rock systems. Methods of wettability measurements are then discussed in detail, including the contact angle methods, the Amott method, the USBM method, the imbibition method, relative permeability methods, the permeability-residual saturation relationship method, and capillary pressure methods. Among the contact angle methods, which are direct measurement methods, this chapter details the captive bubble method, the tilting plate method, the Wilhelmy balance method, capillary rise at a vertical plate, direct measurement on fibres method, and the capillary tube method. Next, the chapter discusses various chemical and geological factors affecting CO_2/water/rock wettability such as surface chemistry, surface roughness, reservoir pressure, reservoir temperature, brine composition (salinity and ion type), and impurities in the injected CO_2 stream. An overview of the technology of carbon geo-sequestration is then presented; this encompasses CO_2 storage sites (i.e., depleted oil and gas reservoirs, unminable coal seams, and deep saline aquifers) and carbon geo-sequestration trapping mechanisms (i.e., structural trapping, residual trapping, mineral trapping, and solubility trapping). Finally, the chapter is concluded with a comprehensive review of the previous simulation studies that have been carried out on the effect of wettability on CO_2 storage capacity.

2.2 Fundamentals of wettability

Wettability is the tendency of the solid surface to be in contact with a particular fluid relative to other existing fluids in the system (Abdallah et al., 1986; Al-Khdheeawi et al., 2017b, c; Iglauer et al., 2015a). Rock wettability strongly controls relative permeability, capillary pressures, the residual saturation of water, and the residual saturation of non-aqueous phase liquids that significantly control multiphase fluid flow through the porous media (Chaudhary et al., 2015; Anderson, 1987a, b; Craig,

1993; Jackson et al., 2005; Morrow, 1990). On a molecular scale, wetting is the result of intermolecular forces and the degree of wetting (or wettability) is determined by the balance between adhesive forces between the liquid and solid and cohesive forces within the liquid.

In oil-water-rock systems, the force vectors are balanced at the point of contact of the oil-water-solid (Figure 2-1). This balance of the forces is represented by Young's equation (Eq.2.1) for the oil-water-solid system, as follows:

$$\sigma_{os} - \sigma_{ws} = \sigma_{ow} \cos \theta \qquad (2.1)$$

where σ_{os} is the oil-solid IFT (interfacial tension), σ_{ws} is the water-solid IFT, σ_{ow} is the oil-water IFT and θ is the contact angle.

Depending on the value of the contact angle, the oil-water-rock system can be classified, in petroleum fundamentals, as three wettability scenarios: water-wet, intermediate-wet and oil-wet (Table 2-1). Thus, the oil and water distribution through the porous medium is controlled by the wettability. In water-wet rocks, water fills small pores and covers most of the rock surface while the remaining pore centres are occupied by oil. However, in oil-wet rocks, oil covers the rock surface and fills small pores while water occupies the remaining pore centres (Figure 2-2) (Anderson, 1986b).

Table 2-1 Contact angle values for the different oil-water-rock system wettability scenarios

Wettability scenario	Dake (1978)	Treiber and Ownes (1972)
Water-wet	$0^o \leq \theta < 90^o$	$0^o \leq \theta < 75^o$
Intermediate-wet	$\theta = 90^o$	$75^o \leq \theta < 105^o$
Oil-wet	$90^o < \theta \leq 180^o$	$105^o \leq \theta \leq 180^o$

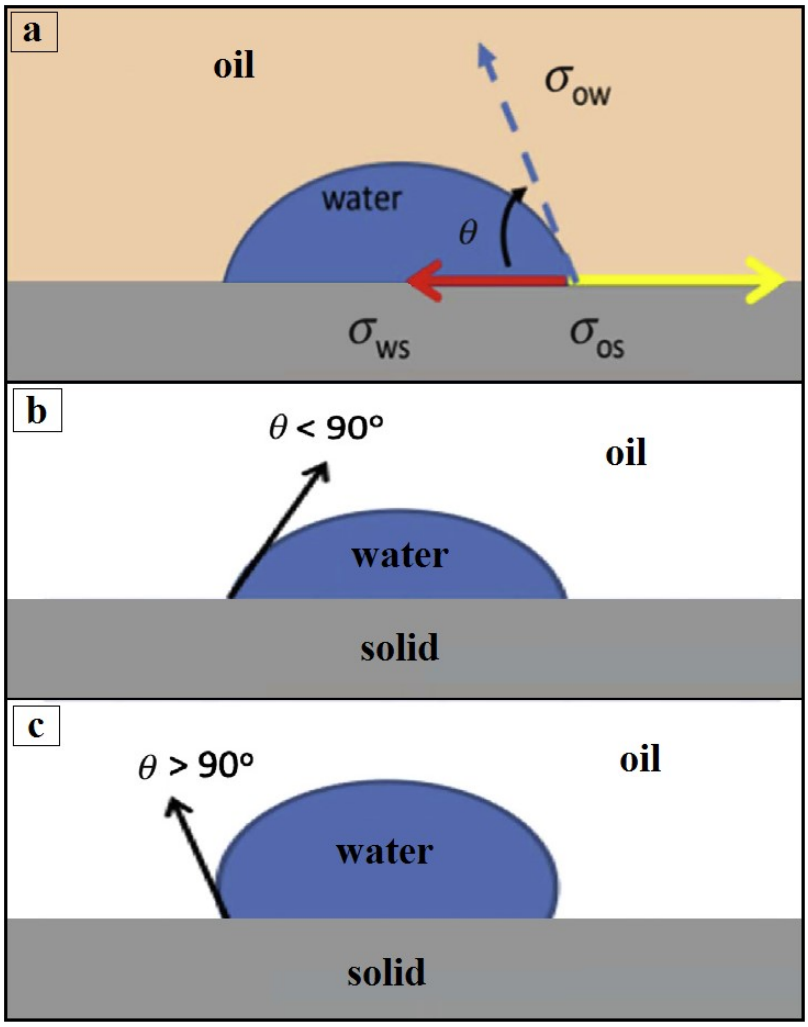

Figure 2-1 An oil-water-solid system showing: (a) interfacial forces interaction (b) contact angle value and the shape of water droplets in a water-wet system and (c) contact angle value and shape of water droplets in the oil-wet system (Wheaton, 2016).

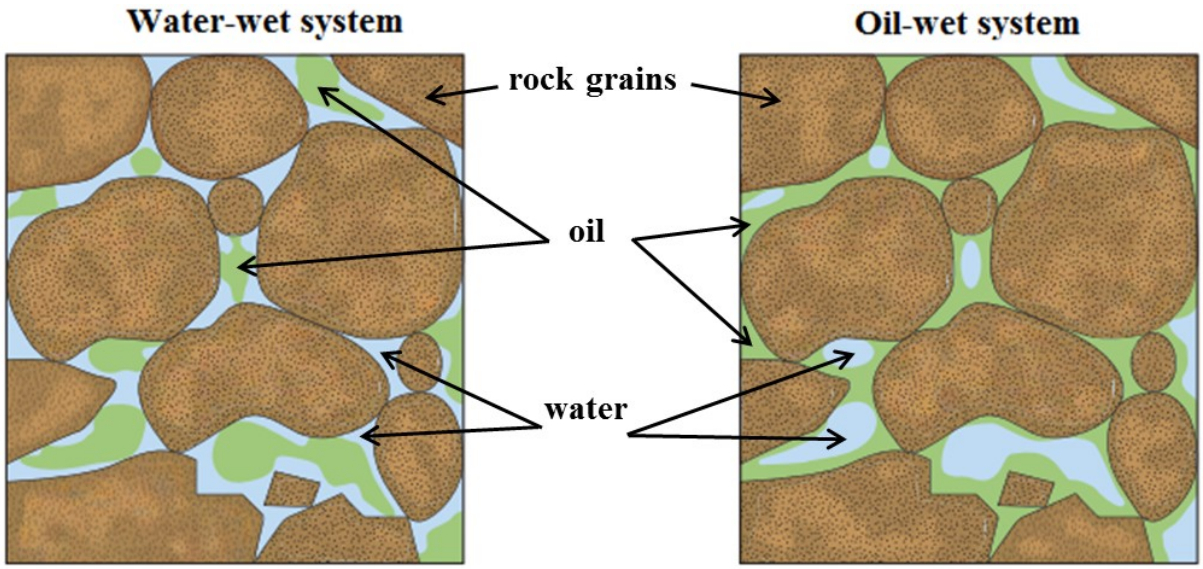

Figure 2-2 Water (blue) and oil (green) distribution in water-wet and oil-wet systems (modified after Abdallah et al., 1986).

In CO_2-water-rock systems, it has been shown that the same wettability classification as the one used for the oil-water-solid system can be used by replacing the oil-wet term by the CO_2-wet term. Thus, based on contact angle measurements, there are different wettability cases for the CO_2-water-rock system ranging from complete wetting of water to complete non-wetting of water (Table 2-2) (Iglauer et al., 2015b).

In the gas (CO_2)-liquid (water)-solid systems, Young's equation (Eq. 2.2) also describes the relationship between surface tension and contact angle, which indicates that contact angle is a function of the forces' balance between the liquid droplet and the solid surface at the line of contact (Figure 2-3). Three surface tension forces result from this liquid-solid surface contact. These are solid-liquid surface tension, liquid-gas surface tension, and solid-gas surface tension, which are used to measure the gas-liquid-rock system wetting state:

$$\sigma_{sg} - \sigma_{sl} = \sigma_{lg} \cos \theta \qquad (2.2)$$

where: σ_{sg}, $\sigma_{sl,}$ and σ_{lg} are the solid-gas, solid-liquid, and liquid-gas interfacial tensions, respectively.

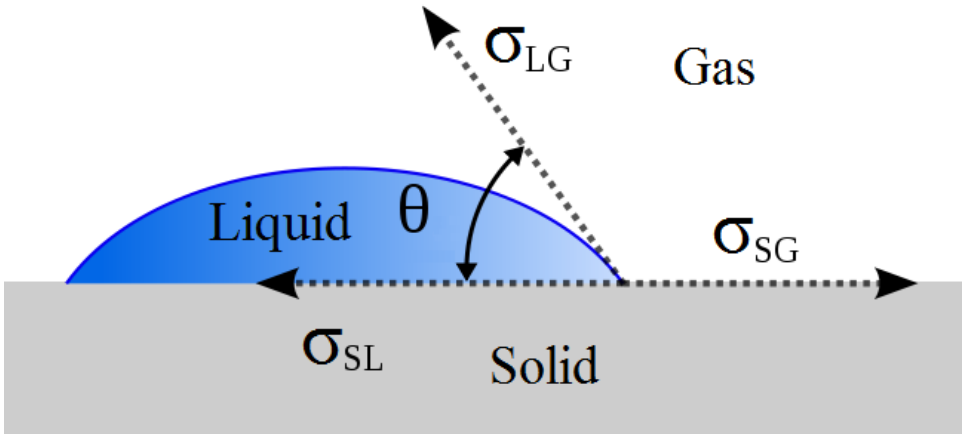

Figure 2-3. Schematic of the gas-liquid-solid system showing the interfacial forces interaction of Young's equation.

Table 2-2 Contact angle values for the different CO_2-water-rock system wettability cases (Iglauer et al., 2015b)

Wettability case	Contact angle
Complete wetting of water	0^o
Strongly water-wet	0^o-50^o
Weakly water-wet	50^o-70^o
Intermediate-wet	70^o-110^o
Weakly CO_2-wet	110^o-130^o
Strongly CO_2-wet	130^o-180^o
Complete non-wetting of water	180^o

2.3 Wettability measurements

Wettability can be measured by different methods, which can be classified as quantitative methods (i.e., contact angle method, imbibition, and forced displacement (Amott) method, and USBM method) and qualitative methods (imbibition rates, microscope examination, floatation, glass side, relative permeability-saturation relationships, and reservoir logs) (Anderson, 1986a).

2.3.1 The contact angle method

The contact angle method is considered the most appropriate quantitative method for measuring wettability. The method is also used for measuring the wettability alteration owing to reservoir fluid flow, in addition to investigating the impact of pressure, temperature, and salinity on rock wettability. However, measuring the contact angles of the reservoir cores involves some difficulties. Contact angle measurements do not include rock heterogeneity, rock roughness, and reservoir rock complex geometry. Thus, great care is needed while sampling and cleaning the reservoir rock cores to obtain more representative contact angle measurements. Please refer to Section 2.2 and Tables (2-1) and (2-2) for more details concerning the relationship between contact angle and wettability for both oil-water-rock and CO_2-water-rock systems. Contact angle can be measured using different methods, which include the direct measurement method, the captive bubble method, the tilting plate method, the Wilhelmy balance method, capillary rise at a vertical plate, individual fibre, capillary tube, the capillary penetration method, and the capillary bridge method (Yuan and Lee, 2013).

2.3.1.1 The direct measurement method

Direct measurement of the contact angle is considered as the most common method. It includes measuring the tangent angle at the fluids-mineral contact point on a sessile drop profile using a telescope-goniometer. Bigelow et al. (1946) were the first to create the telescope-goniometer, which is a simple tool for measuring the contact angle of various liquids on polished plates. Then, at the start of the 1960s, an instrument company (Ramé-Hart) manufactured the first commercial goniometer for measuring the contact angle, which consists of a horizontal platform, a micrometre pipette, a source of illumination, and a telescope containing a protractor eyepiece (Figure 2-4). To measure the contact angle using a telescope-goniometer, the sessile drop profile tangent should be aligned at the point of contact with the surface. The protractor should then be read via the eyepiece. Since the 1960s, various changes have been made to this machine to increase its accuracy (e.g., adding a camera to take drop profile pictures to measure the contact angle at any time (Leja and Poling, 1960); increased accuracy of the examination of the contact profile using high magnification (Smithwich, 1988); employing a motor-driven syringe to measure the dynamic contact angle for sessile

drops (Kwok et al., 1996)). Although, using small volumes of substrate and liquid in this method increases the method's simplicity, this reduces the measurement accuracy owing to increasing the risk of impurities .

To measure the contact angle of the CO_2-water-rock system using this method, the rock is immersed in water then its surface is placed in contact with the CO_2 droplet. Typically, the telescope-goniometer is placed in a high-pressure cell. Owing to the ability to control various factors (e.g., size of the droplet, brine salinity, temperature, and pressure), the high-pressure cell can be used to investigate the impact of these factors on contact angle. Experimentally, during the sessile drop method, a droplet of wetting phase fluid (i.e., water) is positioned at the top of the rock surface, which is surrounded by low-density CO_2. In this method, the contact angle is determined through the water.

Figure 2-4 A direct contact angle measurement device (telescope-goniometer) from Yuan and Lee (2013).

2.3.1.2 The captive bubble method

This method is similar to the sessile drop method. However, in the captive bubble method, instead of positioning a drop of water at the top of the rock surface, a bubble of nonwetting phase fluid (e.g., CO_2) is positioned beneath the rock surface, which is surrounded by water. In this method, the contact angle is determined through the CO_2.

2.3.1.3 The tilting plate method

The tilting plate technique, which was introduced by Adam and Jessop (1925) and improved by Fowkes and Harkins (1940), was once the preferred method for measuring the contact angle owing to its accuracy and simplicity. Here, a solid plate is held on one end and the free end is landed towards a water surface in a rotating motion. When the plate's free end is immersed in the water, a meniscus is formed on the plate's sides. Then, the plate is titled until the meniscus becomes parallel with one of the plate's sides. After that, the contact angle is measured, which represents the angle between the horizontal surface and the plate. This procedure is rarely used because it requires considerable skill and the measured values of the contact angle are affected by liquid contamination and subjectivity. In 1940, the accuracy of the tilting plate technique was improved by Fowkes and Harkins (1940) by adding glass barriers for surface cleaning, film balance for detecting liquid impurities, and a microscope for ensuring the edge of intersection between the plate and the water is positioned on the rotation axis.

2.3.1.4 The Wilhelmy balance method

This technique was first used by Wilhelmy (1863) for indirectly measuring the dynamic contact angle. Experimentally, when a thin and smooth plate of solid immerses in liquid, the plate weight will be changed owing to the balance of the interfacial force (wetting force) and buoyancy force. Note that during the wetting measurement, the gravitational force will not be changed. The wetting force (F_W) is represented by the following equation (Eq. 2.3):

$$F_w = \sigma_{lg}\, p \cos\theta \qquad (2.3)$$

where σ_{lg} = surface tension of liquid-gas, P = the plate perimeter, and θ = contact angle.

while the buoyancy force is represented by the following equation (Eq. 2.4):

$$F_b = V\Delta\rho g \tag{2.4}$$

Where:

V = displaced liquid volume.

$\Delta\rho$ = liquid-air density difference.

g = gravity acceleration.

Therefore, the following relationship (Eq. 2-5) represents the total measured force balance (F) during the Wilhelmy balance technique measurements:

$$F = \sigma_{lg}\, p \cos\theta - V\Delta\rho g \tag{2.5}$$

Thus, if the plate perimeter and the liquid's surface tension are known, the contact angle can be estimated using equation (Eq. 2.5) after measuring F experimentally. In some scenarios, for a zero contact angle with a given solid perimeter, the detected force is directly identified with the liquid's surface tension.

2.3.1.5 The capillary rise at a vertical plate

This method is used to measure the contact angle using the capillary effect by measuring the capillary rise h when a liquid contacts an infinitely wide and vertical plate. Here, the following integrated Laplace equation is used to estimate the contact angle θ (Cain et al., 1983):

$$\sin\theta = 1 - \frac{\Delta\rho g h^2}{2\sigma_{lg}} \tag{2.6}$$

The infinite wide theoretical requirement will be satisfied for a plate width of approximately 2 cm. When such a plate, with a homogeneous surface, is immersed in a moderate surface tension liquid (e.g., water), the contact line will be at the plate's centre. Experimentally, the capillary rise h can be measured using an optical instrument (i.e., cathetometer). This method is suitable for measuring the contact angle at various temperatures (Neumann and Good, 1979). In addition, this method can measure dynamic contact angles by pulling or pushing the plate.

2.3.1.6 Direct measurement on fibres method

The direct measurement of contact angle on fibres was first established by Schwartz and Minor (1959). In this method, a fibre surface should be suspended horizontally in a microscope field. A drop profile will be made from depositing large drops on the fibre surface. The angle of this drop profile, which can be measured using a goniometer eyepiece, represents the contact angle. This method can be used to measure the contact angle hysteresis, advancing contact angle, and receding contact angle for homogeneous and smooth fibre surfaces.

2.3.1.7 Capillary tube method

In this method, the Wilhelmy and capillary rise methods are both applied. As the Wilhelmy method is not limited to flat surfaces only, it can be used to determine the contact angles of different geometries, such as capillaries, plates, wires, rods, and tubes. The perimeter p for the tube geometry in the Wilhelmy method represents the sum of the outer and inner perimeters. Secondly, the capillary rise method can be applied to determine the contact angle of the very narrow vertical capillaries. Here, the meniscus is deemed to have a spherical geometry. The experimental measurements of capillary rise h and the capillary radius r are used to estimate the contact angle:

$$h = \frac{2\sigma_{lg}\cos\theta}{\Delta\rho g r} \tag{2.7}$$

2.3.2 The Amott method

The Amott method is an important quantitative method for measuring the average wettability of reservoir fluids and core samples by combining the imbibition and centrifugal (forced) displacement (Anderson, 1986a). The wettability measurement theory of this method is derived from the fact that the wetting fluid tends to imbibe, spontaneously, into the rock pores and displaces other fluids available in the rock (i.e., nonwetting fluid). The measurement steps in this method are summarised as follows: a) immerse the rock sample in oil for a 20-hour period and measure the volume of water spontaneously displaced (V_{wsp}) by oil imbibition; b) displace the remaining water by oil (using forced displacement) until irreducible water saturation (S_{wi}) is achieved and measure the total displaced water volume by both spontaneous and forced displacement processes (V_{wt}); c) immerse the rock sample in brine for a 20-hour period and measure the volume of the oil spontaneously displaced (V_{osp}) by imbibition of water; d) displace the remaining oil by water (using forced displacement) until irreducible oil saturation (S_{oi}) is achieved and measure the total displaced oil volume by both spontaneous and forced displacement processes (V_{ot}) (Anderson, 1986a). Then, the ratios of displacement by oil (δ_o) and by water (δ_w) can be estimated as follows:

$$\delta_o = \frac{V_{wsp}}{V_{wt}} \tag{2.8}$$

$$\delta_w = \frac{V_{osp}}{V_{ot}} \tag{2.9}$$

Thus, the wettability of core sample is estimated using these ratios as follows:

Water-wet sample: δ_w = positive and $\delta_o = 0$

Strongly water-wet: $\delta_w = 1$ and $\delta_o = 0$

Neutral-wet sample: $\delta_w = 0$ and $\delta_o = 0$

Oil-wet sample: $\delta_w = 0$ and δ_o = positive

Strongly oil-wet: $\delta_w = 0$ and $\delta_o = 1$

2.3.3 United States Bureau of Mines (USBM) method

This method was first established by Donaldson et al. (Donaldson et al., 1969; Donaldson et al., 1980; Donaldson, 1981) for quantitatively measuring the wettability

of the oil-water-rock system. In this method, the required work for displacing a certain fluid by another fluid are compared. Generally, displacing the wetting fluid from the rock sample by nonwetting fluid requires more work than required for displacing the nonwetting fluid, from the same rock sample, by the wetting fluid. Morrow (1970) and Leverett (1941) reported that this required work for fluid displacement is a function of the area below the capillary pressure curve. Specifically, for water-wet rocks, displacing oil by water process has a smaller area below the capillary pressure curve than the process of displacing water by oil. This is due to the fact that most of the water will be spontaneously imbibed inside the water-wet rock and the area below the capillary pressure curve will be small for the process of displacing oil by water. The ratios of these two different areas below the capillary pressure curves are used in the USBM method for calculating the wettability index (W) as follows:

$$W = \log (A_1/A_2) \tag{2.10}$$

where A_1 = the area below the oil-drive curve and A_2 = the area below the brine-drive curve.

Thus, the wettability estimation depends on the wettability index value (W). If the W value is near 1, the rock is water-wet while if the W value is near -1 (i.e., less than zero), the rock is oil-wet. If the W value is near zero, the rock is neutral-wet **(**Figure 2-5**).**

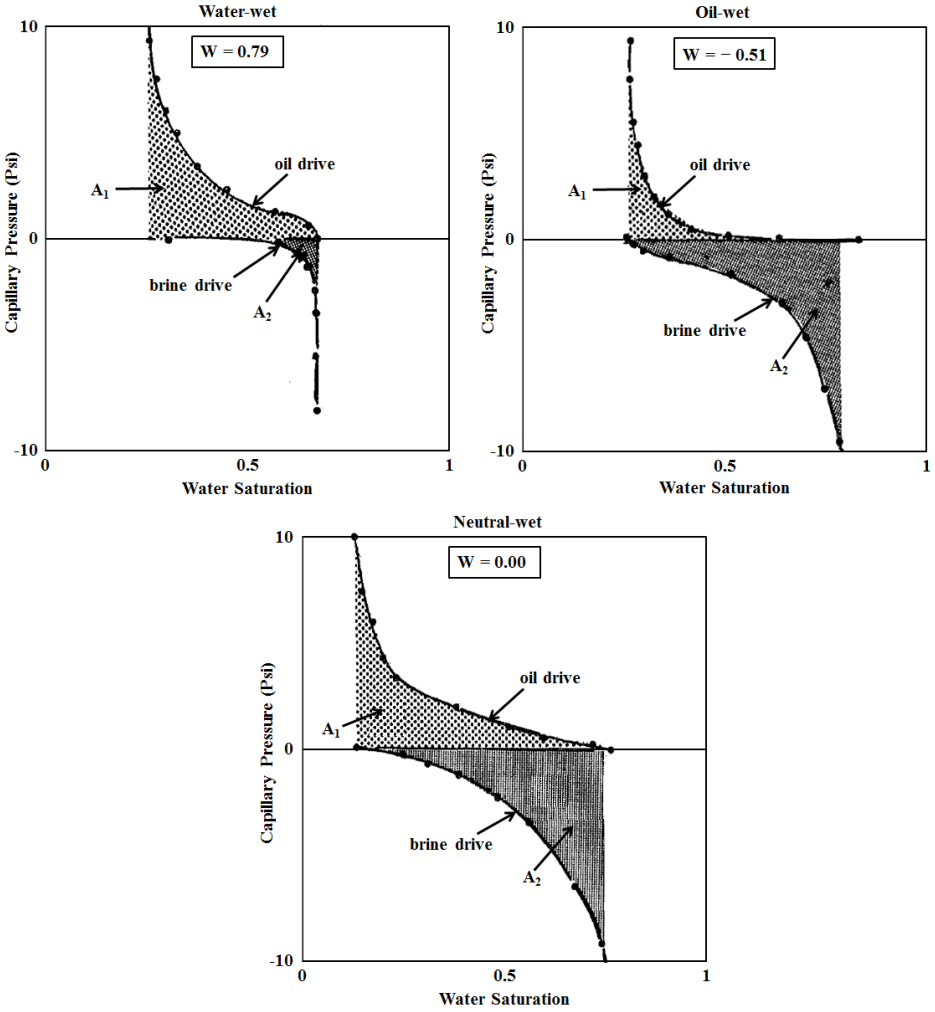

Figure 2-5 Illustration of wettability measurement using the USBM method for three different wettability conditions: water-wet, oil-wet, and neutral-wet. *W* is the USBM wettability index (modified after (Anderson, 1986a)).

2.3.4 The imbibition method

As a result of its simplicity and rapidity, the imbibition method is a common method for qualitatively measuring wettability. The original method can only measure the wettability at room conditions (temperature and pressure; Bobek et al., 1958). However, the apparatus modified by Kyte et al. (1961) was able to measure the wettability at reservoir conditions. To estimate the wettability using this method, a core sample, at initial water saturation, is immersed in water to simulate an imbibition process and measure the volume of displaced oil, caused by the water imbibition, over time. The rock sample is considered strongly water-wet if the water imbibition process is rapid and weakly water-wet if the water imbibition process is slow. However, for

neutral-wet and oil wet rocks, no water will be imbibed. In this latter case, when no water is imbibed, the core sample should be driven to residual oil saturation and immersed in oil. Then, the volume of displaced water, owing to the oil imbibition, is measured as a function of time. The rock sample is oil-wet if it imbibes oil. The oil imbibition process rapidity will be used to indicate the degree of oil-wetness (i.e., strongly oil-wet rocks will have a rapid oil imbibition process while weakly oil-wet rocks will have slow oil imbibition). If neither water nor oil imbibition occurs, the rock is considered to have neutral wettability. However, if both the water and oil imbibition processes occur, the rock is either mixed-wet or fractional-wet. Importantly, the imbibition rate is not only a function of wettability but it also depends on other factors, such as initial saturation, pore structure, interfacial energy, viscosity, and relative permeability (Anderson, 1987a; Dullien, 1979). Thus, this is considered as the main problem of the imbibition method. This dependency can be decreased by comparing the measured core sample imbibition volumes with a strongly water-wet imbibition measurement (i.e., with a reference measurement).

2.3.5 Relative permeability methods

Relative permeability is an important qualitative method for wettability measurement. Generally, if more than one phase (e.g., gas, water, and oil) flows simultaneously in a system, the relative permeability of a particular phase represents the ratio of the effective phase permeability, which is the permeability of one fluid if more than one fluid is available in the system, to the absolute permeability. Relative permeability for a particular phase has a direct relationship with the phase saturation and the phase relative permeability increases with increasing the phase saturation. For each phase, the relative permeability ranges from zero to 1. Thus, for a given phase saturation, the relative permeability of each phase can be calculated as follows:

$$K_{rg} = \frac{K_g}{K} \tag{2.11}$$

$$K_{rw} = \frac{K_w}{K} \tag{2.12}$$

$$K_{ro} = \frac{K_o}{K} \tag{2.13}$$

Where K_{rg}, K_{rw}, and K_{ro} are the relative permeability of gas, water, and oil, respectively, K_g, K_w, and K_o are the effective permeability of gas, water, and oil, respectively, and K is the absolute permeability.

Thus, if two fluids are flowing simultaneously in a system, Darcy's equation will be modified by using the relative permeability concept to calculate the flow rate for each phase as follows:

$$Q_o = -\mathrm{A}\frac{K\,K_{ro}\,\Delta P}{\mu_o\,\Delta L} \tag{2.14}$$

$$Q_w = -\mathrm{A}\frac{K\,K_{rw}\,\Delta P}{\mu_w\,\Delta L} \tag{2.15}$$

where Q_o = oil flow rate, Q_w = water flow rate, A= cross sectional area, μ_o= oil viscosity, μ_w = water viscosity, ΔP = pressure drop through the flow system, and ΔL = length of the flow system.

Based on the well-known fact that wettability affects relative permeability curves and the associated residual oil, water, and gas saturation (Owens and Archer, 1971; McCaffery and Bennion, 1974; Anderson, 1987b; Craig, 1993; Batycky et al., 1981), many methods were investigated to qualitatively estimate the rock wettability. Craig (1993) proposed important rules of thumb to distinguish the differences between oil-wet and water-wet rocks, which is considered an important relative permeability method for estimating the rock wettability (Anderson, 1987b). Craig's rules of thumb estimate the rock wettability based on the values of three main relative permeability curve's characteristics: the residual water saturation, the water saturation where the relative permeability of oil and the relative permeability of water are equal, and water relative permeability at floodout (i.e. at maximum water saturation; Table 2-3 and Figure 2-6). Later, in this work, we use Craig's rules of thumb for modelling different wettability cases in our simulations.

Table 2-3 Typical characteristics of water-wet and oil-wet relative permeability curves (Craig, 1993)

Characteristic	Water-wet	Oil-wet
Residual water saturation (S_{wr}, %)	$20 < S_{wr} \leq 25$	$S_{wr} < 10$
Water saturation where relative permeability of oil and relative permeability of water are equal (S_w, %)	$S_w > 50$	$S_w < 50$
Water relative permeability at floodout (K_{rw}, %)	$K_{rw} < 30$	$50 \leq K_{rw} \leq 100$

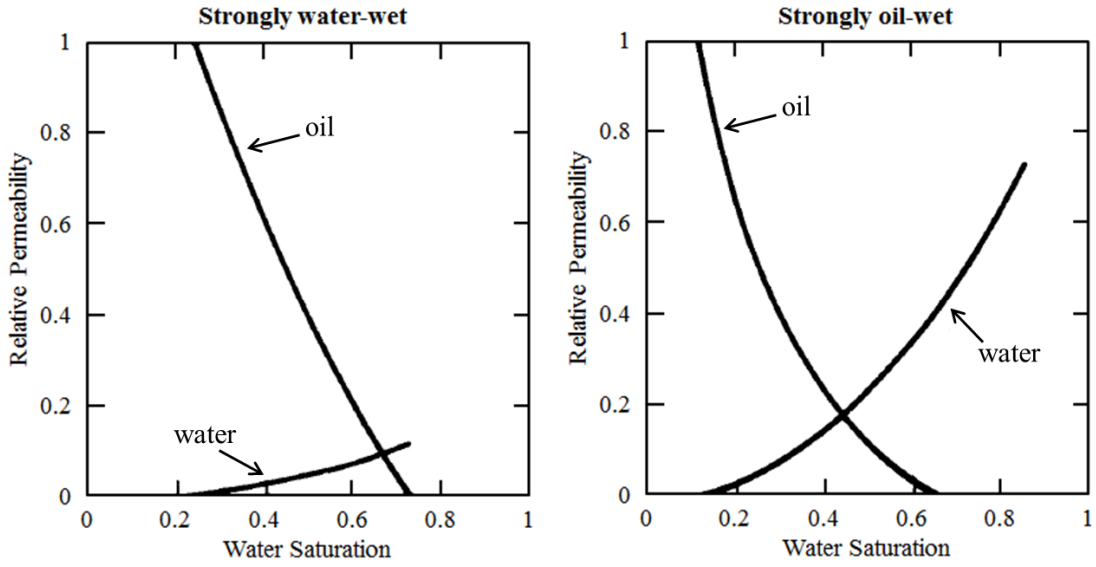

Figure 2-6 Typical relative permeability curves for strongly water-wet and strongly oil-wet rocks (Craig, 1993).

The second method for evaluating rock wettability using relative permeability measurements is presented by Treiber and Owens (1972). In this method, the relative permeability curves of water-oil, oil-gas, and water-gas are compared. Then, the wettability is estimated based on the fact that the strongly wetting phase relative permeability is a function of that same phase saturation only (Craig, 1993; Owens and Archer, 1971). Importantly, for water-wet rock, the oil phase is the preferable wetting phase compared to the gas phase. Thus, in this method, the rock is considered as strongly water-wet when the oil relative permeability in the gas-oil system is found to be a continuation to the water relative permeability in the oil-water system (Owens

and Archer, 1971), as shown in Figure 2-7. However, the rock is not strongly water-wet if the oil relative permeability (in the gas-oil measurement) is significantly different from the water relative permeability (in the oil-water measurement).

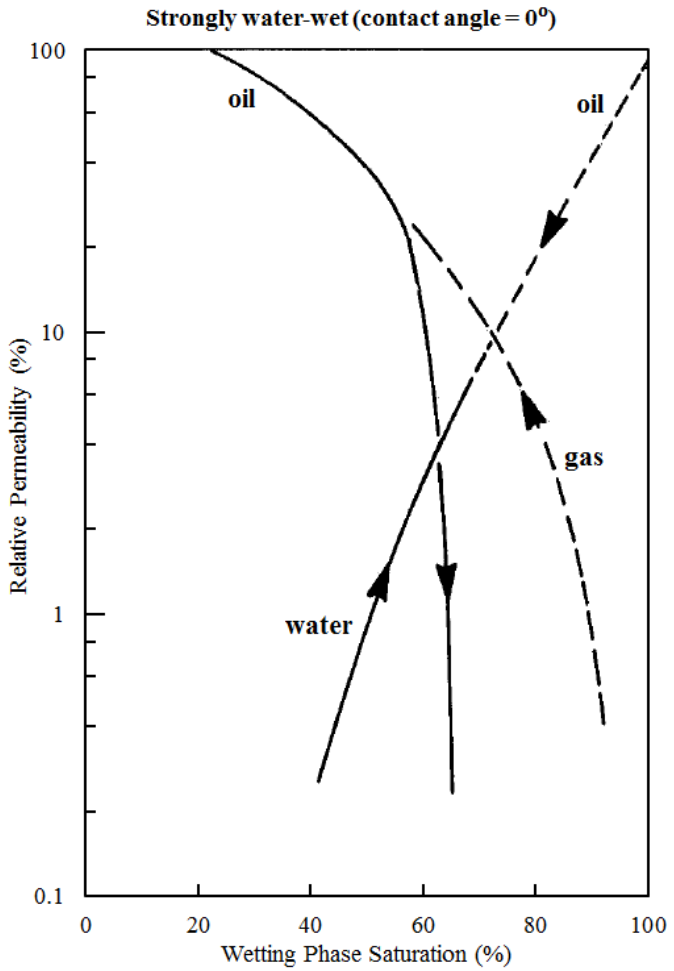

Figure 2-7 Comparison of the oil-gas drainage (dashed lines) and water-oil imbibition (solid lines) relative permeability curves measured in a strongly water-wet rock (Torpedo sandstone). The relative permeability of water in the water-oil test is a continuation of the relative permeability of oil in the oil-gas test. Thus, the rock is strongly water-wet (Owens and Archer, 1971).

2.3.6 The permeability-residual saturation relationship method

Proposed by Raza et al. (1968), this method is used to qualitatively determine rock wettability based on the relationship between air permeability and residual water saturation. The rock wettability is estimated by plotting the air permeability versus the

residual water saturation. The average residual water saturation of oil-wet rock is usually lower than that of the water-wet rock. Thus, if the best-fitting line for the residual water saturation-permeability relationship is found to be approximately vertical and it is extended over a small residual water saturation range, the rock is considered oil-wet. However, if the best-fitting line is found to be inclined with a low vertical gradient and it covers a large residual water saturation range, the rock is water-wet (Figure 2-8).

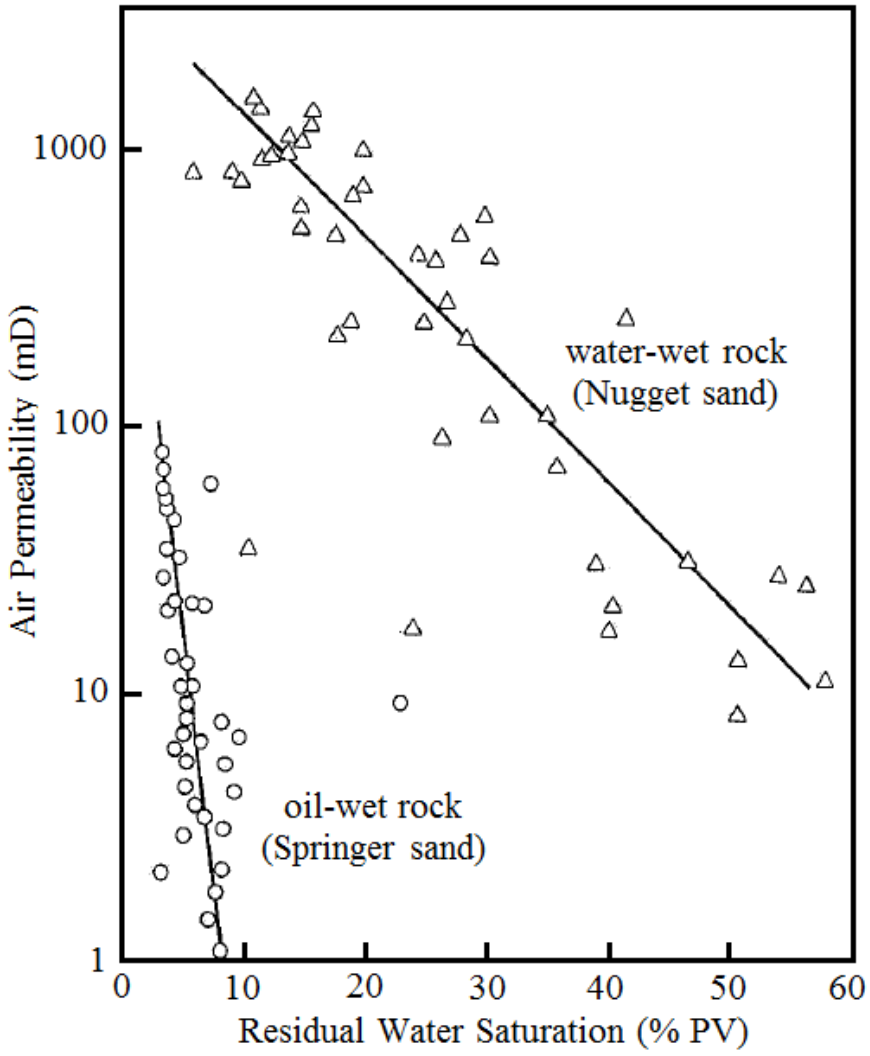

Figure 2-8 Permeability-residual water saturation relationship for water-wet and oil-wet rocks (Raza et al., 1968).

2.3.7 Capillary pressure methods

Capillary pressure (P_c) is the pressure difference between two immiscible fluids coexisting in the same porous medium, which are separated by an interface. Capillary pressure is considered as an important rock property that controls the multiphase flow

in porous media. Specifically, in reservoir engineering fundamentals, capillary pressure (P_c) is defined as the pressure difference between the non-wetting phase and wetting phase as follows:

$$P_c = P_{non-wetting} - P_{wetting} \quad (2.16)$$

In addition, capillary pressure is affected by rock-fluid interfacial tensions, pore size distribution, and rock-wetting characteristics. Thus, the capillary pressure can be calculated using the following relationship:

$$P_c = \frac{2\sigma \cos\theta}{r} \quad (2.17)$$

where σ is the interfacial tension between the wetting and non-wetting fluids, θ is the contact angle, and r is the capillary radius.

The use of capillary pressure curves in estimating rock wettability was first suggested by Calhoun (1951) while the first attempt to use the area below the capillary pressure curve to predict wettability was done by Gatenby and Marsden (1957). They used the areas surrounded by both the imbibition and drainage curves, for negative and positive capillary pressures, to investigate the relationship between capillary pressure and rock wettability. According to the results, they concluded that there is no clear relationship between these capillary pressure areas and rock wettability. However, Donaldson et al. (1969) suggested that only the areas below the water-drive and oil-drive curves should be used when estimating rock wettability.

Another capillary pressure method for estimating the rock wettability is called the method of displacement capillary pressure. In this method, the threshold (or displacement) capillary pressure is used to calculate the apparent contact angle θ_a. Threshold capillary pressure refers to the minimum required capillary pressure for the nonwetting phase to enter a rock that is fully saturated with the wetting phase (Benner et al., 1942; Bartell and Osterhof, 1927). The apparent contact angle can be predicted using the following relationship (Dullien, 1979):

$$P_T = \frac{2\sigma \cos\theta_a}{r_{max}} \quad (2.18)$$

where P_T = Threshold capillary pressure, r_{max} = pore radius by which the nonwetting phase starts to enter the rock, and θ_a = apparent contact angle.

As increasing the pore radius leads to reducing the capillary pressure required for injecting the nonwetting phase, the average radii of the biggest pores of the rock is used to represent r_{max}. There are two limitations of this method. These are the effect of the pore geometry on the measured contact angle and the capability of examining the largest pore wettability only (Anderson, 1986a).

2.4 Factors affecting CO_2/water/rock wettability

CO_2-wettability can differ substantially within the reservoir from strongly CO_2-wet to strongly water-wet (Iglauer, 2017). This CO_2-wettability variation is a result of chemical and geological factors such as surface chemistry, surface roughness, reservoir pressure, reservoir temperature, brine composition (salinity and ion type), and impurities. The influence of these factors on CO_2 wettability is discussed in the sections that follow.

2.4.1 Rock surface chemistry

The chemistry of the rock surface has a significant impact on the CO_2-wettability. Generally, hydrophilic surfaces have a high affinity for water (i.e., water-wet) while hydrophobic surfaces have a low affinity for water (i.e., CO_2- wet) (Iglauer, 2017). Thus, because of their hydrophilicity, the clean rock-forming minerals such as mica, calcite, quartz, and feldspar are water-wet. Moreover, it was shown that wettability is strongly influenced by the degree of surface deprotonation and hydroxylation (Chen et al., 2015b). However, it was reported that owing to their hydrophobicity, oil-wet rocks are intermediate-wet or CO_2-wet (Iglauer et al., 2015b). Importantly, the measured contact angle on the clean surface is significantly lower than the actual contact angle in the reservoir as mineral surfaces in the reservoir are unlikely clean.

In summary, wettability can vary in subsurface formations, at reservoir conditions, from strongly CO_2-wet to strongly water-wet. Thus, in this work, different wettability scenarios (from strongly CO_2-wet to strongly water-wet) have been accurately simulated and the effect of this wettability variation on CO_2 storage capacity and contaminate security has been investigated.

2.4.2 Reservoir pressure

Reservoir pressure, also known as hydrostatic pressure or formation pressure, is the pressure of fluids within the reservoir. In CO_2 geo-sequestration processes, reservoir pressure is usually computed from the hydrostatic pressure gradient of 10 MPa/km (Dake, 2007). Pressure is an important influencing factor on CO_2-wettability (Iglauer, 2017). Previous experimental studies performed on various minerals clearly showed that increasing pressure leads to increased CO_2-wettability (i.e., increasing pressure leads to increasing the advancing and receding contact angle) (Iglauer et al., 2014; Chiquet et al., 2007; Broseta et al., 2012; Farokhpoor et al., 2013). This increase in CO_2-wettability (i.e., contact angle) with increasing pressure is mainly a result of the highly increasing CO_2 density with pressure, which, in turn, leads to enhancing the intermolecular interactions between the CO_2 molecules and minerals (Iglauer et al., 2012).

2.4.3 Reservoir temperature

By reason of the impact of temperature on various factors affecting wettability (e.g., water-CO_2 interfacial energies, fluid dielectric constant, and fluid density), there is an intricate relationship between temperature and contact angle. Thus, previous studies have indicated two different trends of the effect of temperature on water-CO_2-mineral contact angle. Some literature studies observed that the contact angle of quartz substrate in the CO_2-water-mineral system decreases with increased temperature (Yang et al., 2005; Yang et al., 2008a; Bikkina, 2011; Saraji et al., 2013). However, other studies observed that the contact angle of the same substrate (i.e., quartz) increases with temperature (Farokhpoor et al., 2013; Sarmadivaleh et al., 2015). Further, Iglauer et al. (2012) showed that the contact angle decreases with temperature using molecular dynamics simulations. In summary, the effect of temperature on the water-CO_2-mineral system is considered as an open research area and more research work is required to understand its fundamentals (Iglauer, 2017).

2.4.4 Brine composition: salinity and ion type

Brine salinity is widely varied in CO_2 geo-sequestration formations. Previous studies have clearly demonstrated that brine salinity significantly affects CO_2-wettability.

Many previous experimental studies qualitatively investigated that the CO_2-water-mineral contact angle increases with increased salinity for various substrates (Espinoza and Santamarina, 2010; Broseta et al., 2012; Wang et al., 2012; Jung and Wan, 2012; Farokhpoor et al., 2013; Saraji et al., 2014; Sarmadivaleh et al., 2015). Mechanistically, the rock surface is charged and this charge is affected by the mineral type and PH value. In brine, the positive ions move toward the negative surface charges; this reduces the surface potential and polarity. This surface potential and polarity reduction leads to reduced hydrophilicity and the contact angle is thus increased (i.e., CO_2-wettability will be increased at higher salinities) (Iglauer, 2017). Further, the dissolved ion type in brine also affects the CO_2-wettability. The ionic strength and the ratios of the charge to volume in the high-valency ions (e.g., Al^{3+}, Mg^{2+}, SO_4^{2-} and Ca^{2+}) are higher than that of the monovalent ions (Cl^{1-}, Na^{+} and K^{+}), which results in a more effective shielding to the surface charge, which results in increasing the contact angle (i.e., increasing the CO_2 wettability).

2.4.5 Impurities in injected CO_2 stream

The CO_2 injected in the CO_2 geo-sequestration process could contain impurities such as H_2S, H_2, N_2, O_2, CH_4, CO, SOx, NOx, and Ar (Iglauer, 2017). According to the used separation method, the injected CO_2 impurity ranges from 0.05% to 5% by volume (Porter et al., 2015). Moreover, in some petroleum production operations, the produced gas, which could be highly contaminated with H_2S, is reinjected into the reservoir to enhance oil recovery. Thus, it is important to test the impact of these impurities on CO_2-wettability. For instance, previous experimental studies observed that pure CO_2 is more CO_2-wet (i.e., higher contact angle) than the N_2 and CO_2-N_2 mixture (Kaveh et al., 2014; Iglauer, 2017) and less CO_2-wet (i.e., lower contact angle) than H_2S (Broseta et al., 2012).

2.4.6 Surface roughness

It is well established that surface roughness affects the CO_2-water-mineral wettability. Surface roughness affects the CO_2-water-mineral contact angle as represented by the Wenzel equation (Wenzel, 1949):

$$\cos\theta_{rough} = \mathrm{r}\cos\theta_{smooth} \quad (2.19)$$

where θ_{rough}: apparent (measured) contact angle, θ_{smooth}: Young contact angle on ideal surface (i.e. totally flat surface), and *r*: the roughness factor, which represents the ratio of the measured surface area to the ideal surface area; thus, for the ideal surfaces, *r* =1). Typically, surface wetting increases by increasing surface roughness. Thus, in water-wet rock, increasing surface roughness leads to increasing the water wetting state while in CO_2-wet rock, increasing surface roughness results in increasing the CO_2 wetting state. Wang et al. (2013) observed a significant difference in contact angle between smooth (RMS = 5.8 nm) and rough (RMS = 2300 nm) silica surfaces. They found that the contact angle of a smooth silica surface ranged from 31° to 38° while it was only 1° for the rough silica surface, measured at the same pressure (0 to 20 MPa), temperature (323 K), and salinity (1.5 M NaCl).

2.5 Carbon geo-sequestration

Carbon geo-sequestration, also known as geological CO_2 sequestration, is an effective strategy for anthropogenic carbon emissions mitigation. In the carbon geo-sequestration process, CO_2 is captured from large CO_2 sources (e.g., heat supply processes, fossil fuel, power generation, solid fuels burning) and injected, normally as a supercritical fluid, into an accurately selected geological site (Pruess et al., 2003). For many decades, the technology of CO_2 injection into geological formations (e.g., oil and gas reservoirs) has been used for enhanced oil recovery purpose. However, in recent years, this technology has been applied for the purpose of long-term CO_2 geo-sequestration. It is important to mention that the first commercial CO_2 injecting project for CO_2 geo-sequestration and enhanced oil recovery purposes was developed in 2000 in the Weyburn oilfield in Canada (Preston et al., 2005).

There are various geological sites for CO_2 geo-sequestration (Figure 2-9). The CO_2 geo-sequestration site must satisfy some fundamental characteristics such as having high permeability, being overlaid by a caprock seal, being economically feasible, and being environmentally safe (Metz et al., 2005). It was estimated that for a carefully selected and evaluated CO_2 geo-sequestration formation, approximately 99% of the total injected CO_2 can be retained over a long-term storage period (1000 years) and the CO_2 storage period can be extended for millions of years (Metz et al., 2005).

Mainly, CO_2 can be stored in three various storage formations: depleted oil and gas reservoirs, unminable coal seams, and deep saline aquifers. Table 2-4 summarises the estimated storage capacity for the different geological storage sites. These sites are described in more detail in sections that follow.

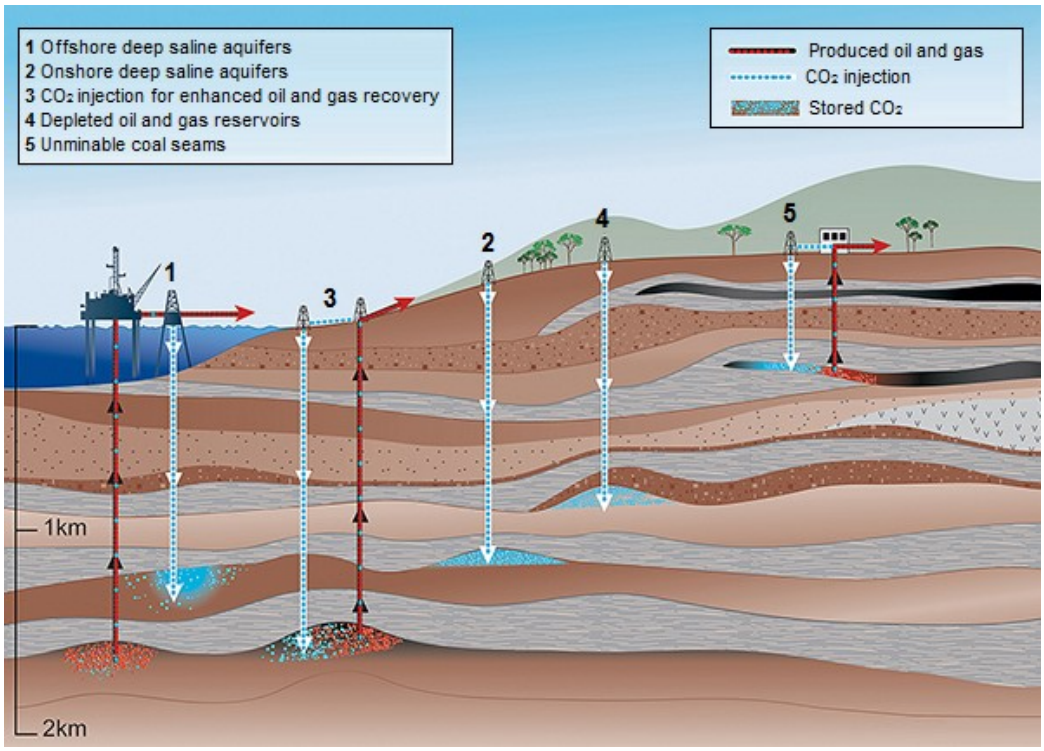

Figure 2-9 An overview of CO_2 injection and geological storage sites (modified after Metz et al., 2005).

Table 2-4 Storage capacity for different storage sites (modified After Metz et al., 2005)

Storage site	Lower estimate for the CO_2 storage volume (Gt)	Upper estimate for the CO_2 storage volume (Gt)
Unminable Coal Seams	3-15	200
Depleted Oil and Gas Reservoirs[a]	675	900
Deep Saline Aquifers	1000	Approximately 10000

[a]These lower and upper estimates for the storage volume of depleted oil and gas reservoirs may be increased by 25% after including the undiscovered hydrocarbon fields.

2.5.1 Depleted oil and gas reservoirs

Depleted oil and gas reservoirs are considered as economical carbon geo-sequestration sites owing to various reasons such as the well-understood geology during the oil and gas exploration operations, the wide use of CO_2 injection into oil and gas reservoirs to enhance hydrocarbon recovery, and the availability, in place, of the surface and underground infrastructure, which can be used to inject CO_2 for geo-sequestration purposes (Li et al., 2006). Thus, CO_2 injection into oil and gas reservoirs improves hydrocarbon production and reduces CO_2 emissions. It was estimated that the CO_2 storage capacity in depleted oil reservoirs is approximately 60% of the injected CO_2 (Shaw and Bachu, 2002). However, approximately 40% of the injected CO_2 is produced with oil, which can be reinjected into the oil reservoir (Shaw and Bachu, 2002). CO_2 storage capacity in depleted oil and gas reservoirs is estimated to be approximately 50 Gton worldwide (Firoozabadi and Myint, 2010). The Weyburn CO_2 capture and storage project in Canada and CO2CRC Otway project in Australia are examples of CO_2 geo-sequestration in depleted oil and gas reservoirs, respectively. In the Weyburn CO_2 capture and storage project, 5000t/day CO_2 is injected in the Weyburn oil field for enhanced oil recovery and CO_2 sequestration purposes (Bachu, 2008). However, in the CO2CRC Otway project, carbon dioxide is collected from a natural gas field (Buttress filed, which contains 20% methane and 80% carbon dioxide) and injected into a small gas filed (Naylor gas filed), which has an estimated initial gas volume of 5.4 Bscf (Underschultz et al., 2011).

2.5.2 Unminable coal seams

CO_2 sequestration in unminable coal seams is an important technology for reducing CO_2 emissions to the atmosphere (Shi and Durucan, 2005). Recently, CO_2 sequestration in unminable coal seams, particularly in conjunction with enhanced coal-bed methane (ECBM) recovery, has attracted significant attention (Zhang et al., 2016b). This technology is important because of its capability of long-term CO_2

sequestration in addition to producing methane, especially in high-methane-content coal, which assists in reducing the cost of the CO_2 sequestration process (Shi and Durucan, 2005). Physically, CO_2 injected into deep unminable coal formations adsorbs on the coal surface and displaces the existing methane because of its higher affinity to adsorb onto coal compared to methane. This technology was performed in many locations worldwide (e.g., the CO_2 sequestration in deep unminable coal seams and enhanced coalbed methane recovery project in the San Juan Basin (New Mexico) by Burlington Resources) (Stevens et al., 1998).

2.5.3 Deep saline aquifers

Deep saline aquifers are porous rocks layers at depths of over 800 m. They usually contain formation waters with high salinity, which don't have any commercial value (Metz et al., 2005). However, deep saline aquifers are the most preferred CO_2 storage sinks, as they provide the largest CO_2 storage capacity compared to other CO_2 geological sinks (Metz et al., 2005). In deep saline aquifers, for efficiency and safety considerations, CO_2 must be injected at depths deeper than 800 m, where the CO_2 remains in a supercritical phase owing to the associated temperature (higher than critical temperature of CO_2; 31.04^{o}C) and pressure (higher than critical pressure of CO_2; 7.39 MPa) (Holloway and Savage, 1993). Table 2-5 summarises the current and planned projects for CO_2 injection and storage in saline aquifers.

Table 2-5 List of current and planned CO_2 geo-sequestration projects in saline aquifers (Metz et al., 2005)

Name	Location	Type	Injection start	Injection rate (t/day)	Total storage (Mt)
MRCSP (Cincinnati Arch)	USA	Pilot	2009	500	0.001
Frio	USA	Pilot	2004	177	0.0016
SECARB Mississippi	USA	Pilot	2008	160	0.00275
Nagaoka	Japan	Pilot	2003	40	0.01

MRCSP (Michigan Basin)	USA	Pilot	2008	300-600	0.06
Ketzin	Germany	Pilot	2006	100	0.06
MGSC Decatur	USA	Demonstration	2010	1000	1
SECARB Early	USA	Demonstration	2009	2700	1.5
In Salah	Algeria	Commercial	2004	3500	17
Sleipner	Norway	Commercial	1996	2700	20
Snøhvit	Norway	Commercial	2008	2000	23
Gorgon	Australia	Commercial	2014	12300	129

2.6 Carbon geo-sequestration trapping mechanisms

As soon as the supercritical CO_2 is injected into the geological storage sites, most of the injected CO_2 migrates laterally and vertically with a risk of leaking toward the surface because of the buoyancy forces (i.e., the density differences between the formation water and the injected supercritical CO_2). This CO_2 leakage risk can be minimised by various physicochemical trapping mechanisms including structural trapping (Iglauer et al., 2015b), residual trapping (Iglauer et al., 2011), dissolution trapping (Iglauer, 2011), and mineral trapping (Gaus, 2010). These trapping mechanisms have different time scales (Figure 2-10). These four trapping mechanisms are described in detail in the following sections.

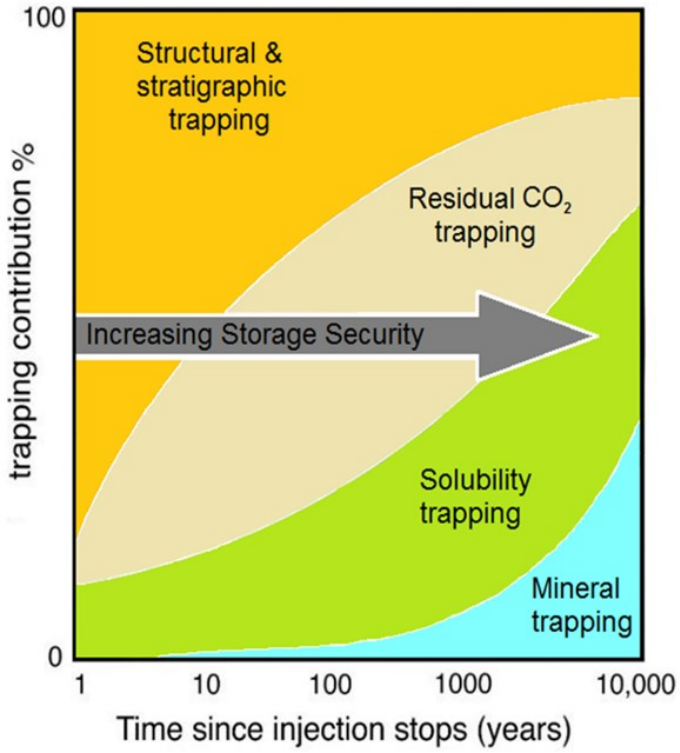

Figure 2-10 The post-injection time scale associated with different trapping mechanisms (Metz et al., 2005).

2.6.1 Structural trapping

Structural/hydrodynamic trapping represents a primary and physical trapping mechanism where the CO_2 is trapped below impermeable (or very low permeability) caprock such as clay, shale, tight carbonates, and mudrock (Iglauer et al., 2015b). CO_2 is often trapped below the caprock owing to the higher capillary forces associated with these very low-permeability seals compared to the buoyancy forces (Hesse et al., 2008). Structural trapping has an important role in any geological storage formation by preventing the CO_2 from migrating upward during the time required to the other storage mechanisms to start to apply (Bachu et al., 1994a).

The efficiency of structural trapping is affected by various parameters, such as interfacial tension, caprock wettability, and caprock properties (Iglauer et al., 2015b; Chiquet et al., 2007; Broseta et al., 2012).

2.6.2 Residual trapping

Residual trapping, also known as capillary trapping, is a major trapping mechanism of CO_2-geosequestration, which can rapidly store large amounts of CO_2 (Juanes et al., 2006; Kumar et al., 2005; Hesse et al., 2008; Pentland et al., 2011). The residual phase is formed when a particular (non-wetting) phase is displaced from the rock pore centre by another immiscible (wetting) phase. Then, a significant amount of CO_2 is trapped in the small pore spaces owing to capillary forces. The capacity of residual trapping is affected by various factors, including characteristics of the residual phase saturation, initial gas saturation, wettability, pore geometry, hysteresis and interfacial tension (Suekane et al., 2008; Iglauer et al., 2011; Chalbaud et al., 2009; Al-Menhali et al., 2015).

2.6.3 Solubility trapping

Solubility/dissolution trapping refers to the dissolution of injected CO_2 into the formation water (Iglauer, 2011). This dissolution of CO_2 in water results in high-density CO_2-enriched brine, which permanently sinks in the formation. The mass transfer in the solubility trapping is a function of the CO_2-water interface area and a larger CO_2-water contact area leads to increasing the amount of CO_2 dissolved in water (Doughty, 2010; Kumar et al., 2005). In addition, solubility trapping is influenced by various factors, such as the reservoir temperature, reservoir pressure, and formation water salinity (Metz et al., 2005). Dissolution trapping is a slow process, ranging from 100 to 1000 years (Emami-Meybodi et al., 2015).

2.6.4 Mineral trapping

Mineral trapping results from the reaction of CO_2 with the reservoir minerals, which is stored in the reservoir in form of minerals (Xu et al., 2005). Mineral trapping is considered an attractive trapping mechanism because it can permanently store the CO_2 (Gaus, 2010). Ortoleva et al. (1998) summarised the chemical reactions associated with the mineral trapping mechanism. First, the weak carbonic acid is produced from dissolving CO_2 in water:

$$CO_2\ (g) + H_2O = H_2CO_3 \qquad (2.20)$$

Then, the bicarbonate ion is formed by rapid carbonic acid dissociation:

$$H_2CO_3 = H^+ + HCO_3^- \quad (2.21)$$

Increasing acidity leads to inducing the formation minerals dissolution, which results in complexing of the bicarbonate ion with the dissolved cations:

$$Ca^{2+} + HCO_3^- = CaHCO_3^+ \quad (2.22)$$

Then, a carbonate mineral is precipitated after the reaction between the species of dissolved bicarbonate and divalent cations. This reaction could result in creating Fe(II), Mg, and Ca carbonates, which represents the mineral trapping (Gunter et al., 1997).

$$HCO_3^- + Ca^{2+} = CaCO_3(s) + H^+ \quad (2.23)$$

$$HCO_3^- + Mg^{2+} = MgCO_3(s) + H^+ \quad (2.24)$$

$$HCO_3^- + Fe^{2+} = FeCO_3(s) + H^+ \quad (2.25)$$

2.7 Previous simulation studies on the effect of wettability on CO_2 storage

Although various experimental studies have demonstrated (at the lab scale ranging from mm to cm) that wettability affects structural and residual trapping capacities (e.g., Iglauer et al., 2011; Iglauer et al., 2015; Espinoza and Santamarina, 2010; Farokhpoor et al., 2013), little attention has been placed on the effect of wettability on reservoir-scale processes and associated CO_2 geo-sequestration capacity predictions. Importantly, various parameters (e.g., hysteresis, residual water saturation, residual gas saturation, relative permeability and the capillary pressure) depend on wettability (Anderson, 1987a, b; Craig, 1993; Jackson et al., 2005; Morrow, 1990). This section, thus, introduces a short summary of the previous simulation studies performed on the effect of wettability and wettability dependent parameters on CO_2 geo-sequestration capacity.

First, it is important to mention that the first real research studies about the use of underground formations for storing CO_2 were completed at the beginning of the last decade in the nineteenth century (Holloway and Savage, 1993). After that, a wide

range of studies was conducted to develop the CO_2 geo-sequestration technology. There are different simulation models developed to study the effect of different rock and fluid properties on the CO_2 storage and movements.

Ghanbari et al. (2006) developed a three-dimensional homogeneous model to simulate CO_2 storage in a saline aquifer for 470 years after 30 years of CO_2 injection using the GEM-CMG simulator (Computer Modelling Group). The dimensions of the developed model were (8 km x 8 km x 200 m) and the number of grid blocks was (35 x 35 x 25) in X, Y and Z directions, respectively. The study was aimed at estimating the key parameters that affect the hydrodynamic and solubility trapping mechanisms by evaluating the effect of different parameters including residual gas saturation and residual water saturation. This study compared the ability of each case to increase the capacity of hydrodynamic and solubility trapping mechanisms. The results of this study showed that residual gas saturation increase leads to increasing the amount of immobilised CO_2 while reducing the solubility trapping capacity. In addition, this study concluded that higher residual water saturation results in a higher solubility trapping capacity.

Another simulation of CO_2 injection in deep geological formations was performed by Ukaegbu et al. (2009) using GEM-CMG software. The main focus of this study was on evaluating the effect of various reservoir conditions on the CO_2 distribution between different phases and the effect of gas relative permeability curve hysteresis, residual water, and gas saturation on the amount of CO_2 dissolved in brine. They concluded that hysteresis in the gas relative permeability curve affects the amount of CO_2 dissolved. In addition, they found that increasing the residual gas saturation leads to increasing the amount of immobile CO_2 while increasing irreducible water saturation leads to increasing the amount of CO_2 dissolved.

Ide et al. (2007) used the Eclipse simulator to simulate CO_2 geo-sequestration in deep saline aquifers. They studied the effect of capillary forces and capillary pressure on CO_2 storage capacity. This study concluded that including the capillary pressure in the reservoir simulation model leads to increasing the CO_2 trapping capacity.

Mo and Akervoll (2005) presented a reservoir simulation model using black-oil reservoir software to simulate long-term CO_2 sequestration in a shallow saline aquifer. This study focused on the effect of wettability-dependent parameters (i.e., capillary

pressure, residual gas saturation, and irreducible water saturation) on CO_2 distribution in reservoirs. This study indicated that both capillary pressure and irreducible water saturation have a small effect on CO_2 distribution. However, they concluded that the capillary trapping capacity is highly affected by residual gas saturation.

Doughty (2007) developed a numerical simulation model to simulate a CO_2 geo-sequestration process using the TOUGH2 simulator to study the effect of using hysteretic curves on the residual CO_2 trapping. She found that the use of hysteretic curves has a significant importance in increasing the accuracy of capturing CO_2 plume behaviour.

Kumar et al. (2005) simulated a CO_2 storage process in a saline aquifer using CMG-GEM to study the effect of residual gas saturation, as well as other different parameters (e.g., reservoir permeability, the ratio of vertical to horizontal permeability, aquifer temperature, permeability heterogeneity, mineralisation, and aquifer dip angle) on CO_2 storage. They found that residual gas saturation affects the CO_2 storage process and concluded that increasing residual gas saturation leads to decreasing the gas dissolution in water and gas migration while leading to an increase in the amount of residually trapped CO_2.

Sifuentes et al. (2009) presented a sensitivity analysis study using a reservoir simulation model to study the effect of residual gas saturation in addition to other physical properties (e.g., horizontal permeability and permeability heterogeneity) on the CO_2 storage efficiency in aquifers. The simulations were performed using the compositional simulator (Eclipse software). Sifuentes et al. (2009) showed that residual gas saturation affects the residual trapping capacity and that increasing residual gas saturation leads to increasing the amount of residually trapped CO_2.

Juanes et al. (2006) presented a reservoir simulation model to evaluate the effect of relative permeability hysteresis on the CO_2 storage process using the Eclipse 100 simulator. They found that the use of relative permeability hysteresis curves increases the accuracy of CO_2 geo-sequestration simulation outcomes.

Chalbaud et al. (2007) studied the effect of wettability on the CO_2 storage in aquifers by using micromodel experiments in a laboratory and a pore network model as a theoretical part. They simulated the CO_2 storage in a core scale without involving the actual reservoir heterogeneities.

Krevor et al. (2015) presented a simulation model to study the effect of wettability on the capillary trapping efficiency. They compared only two wettability conditions: water-wet and mixed-wet conditions. They found that the water-wet rocks have a higher capacity of capillary trapping compared to mixed-wet rocks.

Iglauer et al. (2015) presented a comprehensive review of the measurements of CO_2 wettability and its importance in CO_2 geo-sequestration. This study provided an example of the reservoir simulation model to study the effect of wettability CO_2 trapping mechanisms by using the MoRes simulator. They simulated only two wettability scenarios: water-wet and CO_2-wet. They found that wettability affects the amount of mobile and trapped CO_2.

In this thesis, the effect of CO_2-rock-brine wettability on CO_2 storage efficiency has been investigated by performing multiphase flow reservoir simulations on hectometre-scale reservoirs. Here, and for the first time, five wettability conditions (i.e., strongly CO_2 wet, weakly CO_2-wet, intermediate-wet, weakly water-wet, and strongly water-wet) have been simulated by developing five sets of relative permeability and capillary pressure curves (including hysteresis). The wettability effect has been investigated for both homogeneous and heterogeneous reservoirs and for different injection configurations (horizontal and vertical injection well). Further, and again for the first time, the impact of wettability heterogeneity on the effectiveness of CO_2 storage process has been demonstrated. The effect of other important parameters such as reservoir salinity, reservoir temperature, CO_2 injection scenario, injection well configuration on CO_2 geo-sequestration efficiency has also been studied.

Chapter 3 Influence of CO_2-Wettability on CO_2 Migration and Trapping Capacity in Deep Saline Aquifers

3.1 Introduction

CO_2 capture and storage (CCS) is considered an one effective method of mitigating greenhouse gas (GHG) emissions into the atmosphere by collecting CO_2 from large point sources and injecting it into deep geological formations (Pruess et al., 2003; Holloway, 2005). Storage sites, however, need to be screened for storage effectiveness, with prospective targets including unminable coal beds, deep saline aquifers and depleted hydrocarbon reservoirs (Metz et al., 2005; Iglauer, 2012; Juanes et al., 2006; Bachu, 2000; Bickle, 2009; Sakurovs and Lavrencic, 2011). Among all these types of CO_2 storage sites, deep saline aquifers are considered more suitable, because they have the largest CO_2 storage capacity and the widest geographical spread (Lackner, 2003; Bachu, 2000). For safety and efficiency reasons, CO_2 is injected at depths greater than 800 m, so that CO_2 remains in a supercritical (sc) state (Pentland et al., 2011; Hesse et al., 2008; Metz et al., 2005; Pruess et al., 2003). However, $scCO_2$ - although denser than CO_2 gas - is buoyant compared to formation water and migrates upwards; this migration can be minimized and CO_2 can be prevented from escaping to the atmosphere by four main trapping mechanisms: structural (Hesse et al., 2008; Naylor et al., 2011; Iglauer et al., 2015a), residual (Kumar et al., 2005; Pentland et al., 2011; Iglauer et al., 2011), dissolution (Lindeberg and Wessel-Berg, 1997; Spycher et al., 2003; Iglauer, 2011), and mineral (Bachu et al., 1994b; Xu et al., 2004; Gaus, 2010).

Many factors affect the efficiency and capacity of the main CO_2 trapping mechanisms: temperature (Ofori and Engler, 2011), vertical to horizontal permeability ratio (Basbug et al., 2005), cap rock properties (Iglauer et al., 2015a), [13] fault-seal behaviour (Bretan et al., 2011; Yielding et al., 2011), or reservoir heterogeneity (Gershenzon et al., 2015). One factor, which has received little attention, is the CO_2-wettability of the rock (Iglauer et al., 2015b; Vialle et al., 2016); we show here that CO_2-wettability has a dramatic impact on storage capacities, CO_2 plume migration patterns and CO_2 containment security. It is also important to note that CO_2-rock wettability can vary tremendously. Indeed, water contact angles between 0° (strongly water-wet) and 170°

(strongly CO_2-wet) have been measured, where CO_2-wettability mainly depends on the surface chemistry, and to a lesser extent on temperature, pressure and brine composition (Chiquet et al., 2007; Broseta et al., 2012; Iglauer et al., 2012; McCaughan et al., 2013; Saraji et al., 2013; Iglauer et al., 2014; Iglauer et al., 2015b; Iglauer et al., 2015a; Chen et al., 2015a; Javanbakht et al., 2015; Sarmadivaleh et al., 2015; Al-Yaseri et al., 2016; Arif et al., 2016b).

Wettability, as it has been previously shown in laboratory experiments (at the mm to cm scale), has a significant effect on residual trapping (Iglauer et al., 2011; Andrew et al., 2013; Chaudhary et al., 2013; Rahman et al., 2016) and structural trapping (Naylor et al., 2011; Iglauer et al., 2015a). However, despite this laboratory-scale evidence, the effect of wettability on reservoir scale processes and associated storage capacity and containment security predictions has received little attention (Iglauer et al., 2015b) and generally, though the wettability is incorporated in the pilot projects modelling via relative permeability curves and multiphase flow, the values are poorly constrained.

In this chapter, we investigate the influence of CO_2 wettability of rocks on CO_2 plume migration, CO_2 mobility and the capacity of residual and solubility trapping and demonstrate its key importance. For this purpose we performed multiphase flow reservoir simulations on a homogeneous hectometre scale formation using five relative permeability curves (including hysteresis) that represent five characteristic wettability scenarios from strongly water-wet to strongly CO_2-wet.

3.2 Methodology

3.2.1 Numerical model

We built a 3D homogeneous reservoir-scale model (Figure 3-1) using the nonisothermal multicomponent multiphase flow simulator TOUGH2 (Pruess et al., 1999) with the fluid property module ECO2M to model the thermodynamic and thermophysical properties of the H_2O-NaCl-CO_2 mixtures that includes super- and sub-critical conditions, as well as phase changes between liquid and gaseous CO_2 (Pruess, 2011). ECO2M is a tabular EOS and it depends on Altunin's correlations (Altunin, 1975) to compute the molar volumes of CO_2 (including the CO_2 dissolved

in brine). The amount of dissolved CO_2 was used to assess dissolution trapping (Lindeberg and Wessel-Berg, 1997; Spycher et al., 2003; Iglauer, 2011). The aquifer characteristics are summarized in Table 3-1 (Jahangiri and Zhang, 2011; Basbug et al., 2005); the top of the aquifer is at 800 m depth. It is overlayed by a lower permeability unit (10^{-6} D compared to 1 D for that of the reservoir) typical of mudstones (Dewhurst et al., 1999; Yang and Aplin, 2007), and is modelled as a water-wet formation, for all wettability scenarios considered in this chapter (including the CO_2-wet models): thus this unit constitutes a barrier preventing the CO_2 from migrating to the surface. Reservoir pressure and temperature were set to 8 MPa (at 800 m depth) and 313 K (40^0 C), respectively. The pressure followed the hydrostatic gradient (10 MPa/km) (Dake, 2007), while temperature conditions were isothermal. Dirichlet boundary conditions for pressure (i.e. constant pressure) were assigned on the outer boundary grid cells by applying a large volume multiplier (10000) (Nghiem et al., 2009).

CO_2 was injected into the reservoir at a constant rate of 3.171 kg/sec (100,000 tCO_2/ yr) for all modelled scenarios; this is an injection rate similar to that of the Ordos CCS demonstration project in China (Xiuzhang, 2014) and Tomakomai CCS demonstration project in Japan (Tanaka et al., 2014). CO_2 was injected at a depth of 1150m (i.e. near the bottom of the reservoir and at the centre of the model) over a 1 year period (i.e. a total of 100000 tons of CO_2 were injected). Subsequently the CO_2 injection well was shut down and the behaviour of the CO_2 plume was simulated for the following 10 year period ("storage period"). Five different wettability scenarios were analysed, namely strongly water-wet, weakly water-wet, intermediate-wet, weakly CO_2-wet and strongly CO_2-wet with an assumed contact angle (Θ) of (0^o, 70^o, 110^o, 130^o, and 170^o), respectively (Iglauer et al., 2015b; Arif et al., 2016b). Note that all wettability states are physically possible and they may prevail in a specific storage reservoir, as mentioned in the introduction.

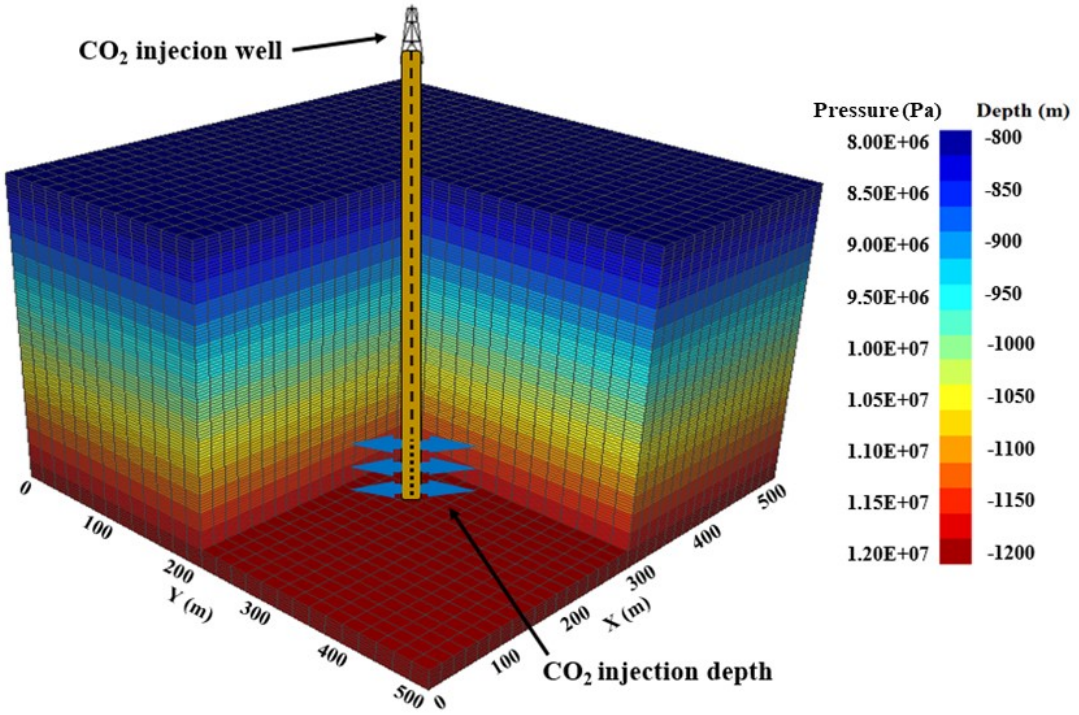

Figure 3-1 A sketch of the 3-D model including location of the injection well, model dimensions, and initial pressure.

Table 3-1 Reservoir model characteristics

Property	**Value**
Length	500 m
Width	500 m
Thickness	400 m
Cell number	35 x 27 x 100 (94500 cells in total)
Top depth of the reservoir	-800 m
Bottom depth of the reservoir	-1200 m
Reservoir temperature (isothermal)	313 K(40^0 C)
Initial pressure (at depth -800 m)	8 MPa
Initial pressure (at depth -1200 m)	12 MPa
Salinity	15% NaCl by weight
Horizontal permeability	1000 mD

Vertical to horizontal permeability ratio	0.1
Top seal permeability	10^{-3} mD
Porosity	0.25
Initial water saturation	100%

3.2.2 Wettability simulation

CO_2-wettability is an atomistic phenomenon as it is determined by intermolecular forces between CO_2, brine and rock (Liu et al., 2010; Iglauer et al., 2012; McCaughan et al., 2013; Javanbakht et al., 2015; Chen et al., 2015a). Thus, to perform hectometre-scale reservoir simulations, an upscaling mechanism is required; here we directly implement the effect of wettability into the relative permeability and capillary pressure curves (Anderson, 1987b; McCaffery and Bennion, 1974; Levine et al., 2014; Krevor et al., 2012; Anderson, 1987a; Morrow, 1976).

Specifically, we use McCaffery and Bennion's (1974) relative permeability curves to construct the curves for the 5 wettability scenarios investigated in this study and adjusted them based on Craig's criteria (Craig, 1993). This procedure consists in an adjustment of the values of end point saturations, water saturations where CO_2 and water relative permeabilities (k_{rg} and k_{rw}) are equal, and relative permeabilities at water floodout (i.e. the condition when the rock reached its maximum water saturation). According to Craig's criteria, and for a reservoir permeability of 1000 mD, the residual water saturation (S_{wr}) should be less than 15% in strongly CO_2-wet rocks, and should range between 20%-50% in strongly water-wet rocks. In addition, the water saturation where k_{rg} and k_{rw} are equal should be higher than 50% in a strongly water-wet reservoir, while it should be less than 50% in a strongly CO_2-wet reservoir. Moreover, the k_{rw} during the storage period should be less than 30% in the strongly water-wet formation, and it should range between 50%-100% in the strongly CO_2-wet reservoir. All above conditions were applied during construction of the relative permeability curves used in this study, which are displayed in (Figure 3-2). The curves were then fitted with the Van Genuchten-Mualem model (Van Genuchten, 1980; Mualem, 1976) for implementation into the computer code:

$$k_{rw} = \sqrt{S^*}\left\{1-\left(1-[S^*]^{1/\lambda}\right)^{\lambda}\right\}^2 \quad \text{if} \quad S_w < S_{ws} \qquad (3.1)$$

$$k_{rw} = 1 \quad \text{if} \quad S_w = 1 \tag{3.2}$$

$$k_{rg} = 1 - k_{rw} \quad \text{if} \quad S_{gr} = 0 \tag{3.3}$$

$$k_{rg} = \left(1 - \hat{S}\right)^2 \left(1 - \hat{S}^2\right) \quad \text{if} \quad S_{gr} > 0 \tag{3.4}$$

$$S^* = (S_w - S_{wr})/(S_{ws} - S_{wr}),$$
$$\hat{S} = (S_w - S_{wr})/(1 - S_{wr} - S_{gr}) \tag{3.5}$$

where:

k_{rg} = relative permeability for gas, k_{rw} = relative permeability for water

S_{gr} = residual gas saturation, S_w = water saturation

S_{ws} = saturated (maximum) water saturation (= 1), S_{wr} = residual water saturation.

λ = fitting parameter (pore size distribution index).

Initially, k_{rw} is set to 1 and k_{rg} to 0, which corresponds to full (100%) water saturation. During CO_2 injection (dashed black lines in Figure 3-2), k_{rw} reduces gradually, while k_{rg} increases until it reaches a maximum at the irreducible water saturation (S_{wr}). During the storage period (CO_2 injection has ceased, represented by red lines in (Figure 3-2), k_{rg} reduces and k_{rw} increases until residual gas saturation (S_{gr}) is reached. Note that the endpoint saturations (S_{wr}, S_{gr}) depend on wettability (Anderson, 1987b; Craig, 1993; Iglauer et al., 2011; Andrew et al., 2013; Chaudhary et al., 2013; Rahman et al., 2016). Moreover, lower water-wettability shifts the k_{rw} curve upwards, and the k_{rw}-k_{rg} cross-over point moves towards the left (i.e. to a lower water saturation value) (Craig, 1993). Furthermore, note that S_{gr} is also a function of the initial CO_2 saturation (Pentland et al., 2011; Krevor et al., 2011; Krevor et al., 2015) and porosity (Iglauer et al., 2011).

Figure 3-3 presents the capilarry pressure curves used in this study for the five different wettability scenarios. These curves has been developed by referring on previous studies (Anderson, 1987a; Morrow, 1976), (which look at the wettability-capillary pressure relationship) and by using the Van Genuchten-Mualem model (Van Genuchten, 1980; Mualem, 1976):

$$P_{cap} = P_0 \left([S^*]^{-1/\lambda} - 1\right)^{1-\lambda} \tag{3.6}$$

$$S^* = (S_w - S_{wr})/(S_{ws} - S_{wr}) \quad (3.7)$$

where:

P_{cap} = CO_2-water capillary pressure, P_o = capillary pressure scaling factor, S_{ws} = maximum (saturated) water saturation, S_{wr} = residual water saturation, λ = pore size distribution index.

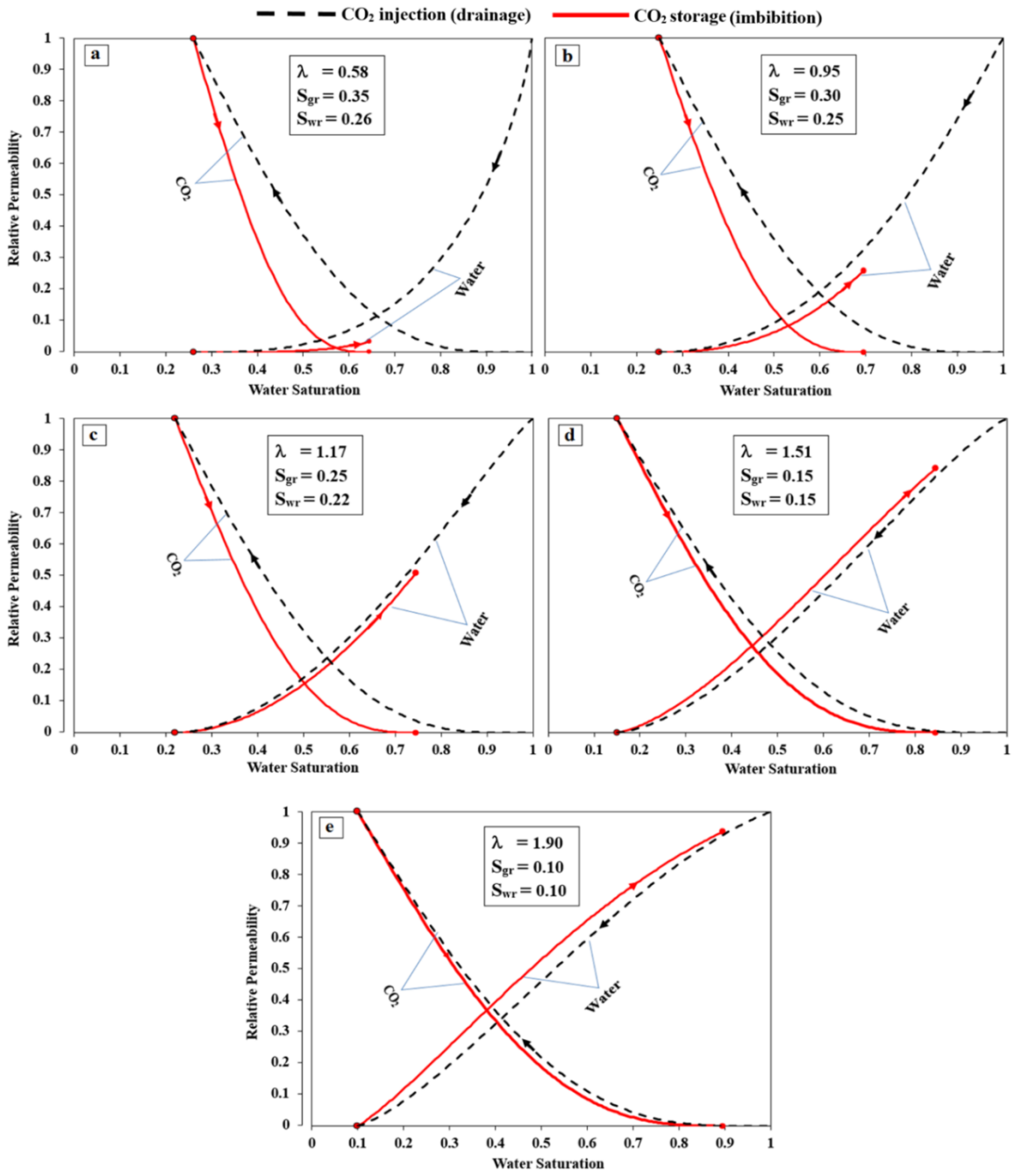

Figure 3-2 Relative permeability curves for the five different rock wettabilities investigated: a) strongly water-wet; b) weakly water-wet; c) intermediate-wet; d) weakly CO_2-wet; e) strongly CO_2-wet. See section 3.2.2 for the construction of these curves.

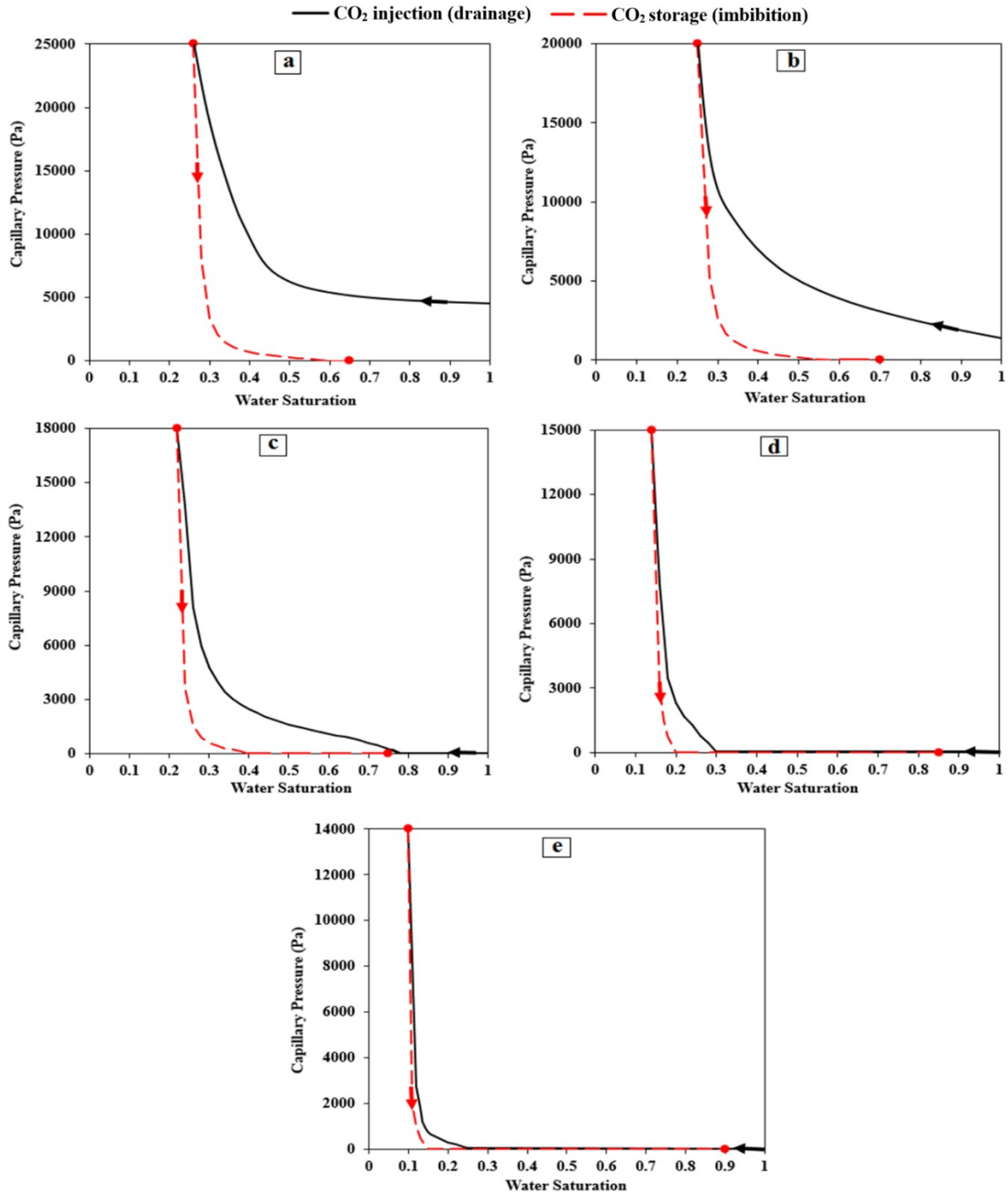

Figure 3-3 Capillary pressure curves for the five different rock wettabilities investigated: a) strongly water-wet; b) weakly water-wet; c) intermediate-wet; d) weakly CO_2-wet; e) strongly CO_2-wet. See section 3.2.2 for the construction of these curves.

3.3 Results and discussion

3.3.1 Influence of wettability on CO_2 plume migration and shape

Clearly wettability has a significant influence on the CO_2 migration pattern. (Figure 3-4) displays 3D views of the CO_2 plume for the five wettability scenarios described above and at various times after the end of the injection. The CO_2 plume moves upwards much more rapidly in the strongly CO_2-wet rock scenario, while it is best retained near the injection well in the strongly water-wet reservoir; this is quantified in Table 3-2, where the depth reached by the (free) CO_2 plume, as well as the total CO_2 vertical migration distance, are reported. Furthermore, rock wettability has a drastic impact on the shape of the CO_2 plume; while the plume is much more compact and "raindrop-like" in a water-wet reservoir, it has a (vertically) elongated "candle-like" shape in the CO_2-wet reservoir (Figure 3-4).

The underlying reason why the CO_2 plume moves upwards much more rapidly in strongly CO_2-wet rock is because of the wettability influence on relative permeability and capillary pressure on dual phase systems. Wettability is also the reason why the spreading patterns are different in CO_2-wet and water-wet reservoirs. Recall that the endpoint saturations (S_{wr}, S_{gr}) depend on wettability (Anderson, 1987b; Craig, 1993; Iglauer et al., 2011; Andrew et al., 2013; Chaudhary et al., 2013; Rahman et al., 2016) A CO_2 migration and plume extension are highly dependent on S_{gr} (Metz et al., 2005; Kumar et al., 2005; Doughty, 2010), CO_2 migration rate increases and the plume expands spatially with smaller S_{gr} values. (Figure 3-2), which shows the variation of S_{gr} with wettability, that the lowest S_{gr} (10%) is associated with the strongly CO_2-wet condition, while the highest S_{gr} (35%) is found in the strongly water-wet reservoir. We conclude that CO_2-wettability dramatically affects CO_2 plume migration both in time and space.

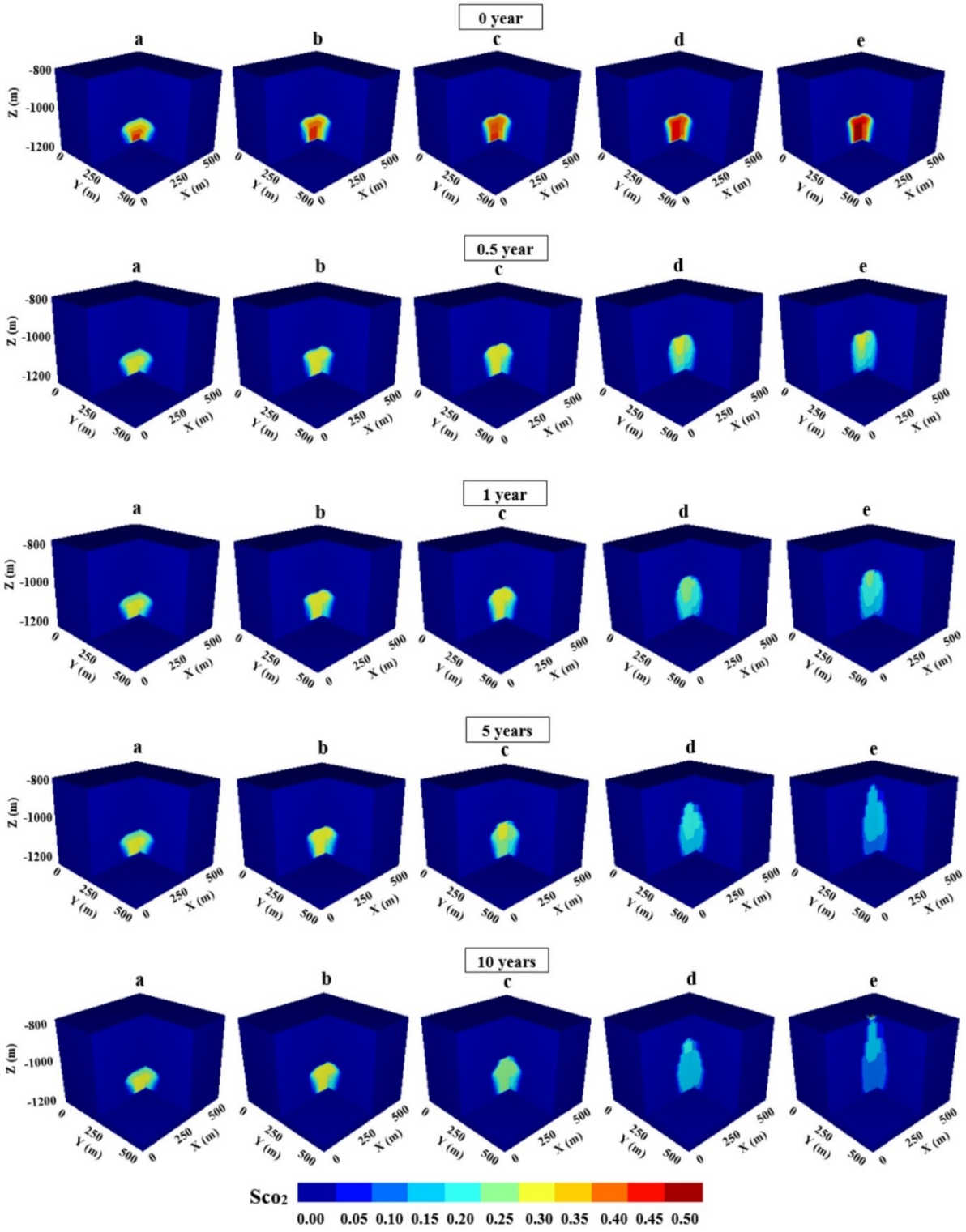

Figure 3-4 3D views of the CO_2 plume as a function of storage time (i.e times since the stop of injection) and wettability: a) strongly water-wet; b) weakly water-wet; c) intermediate-wet; d) weakly CO_2-wet; e) strongly CO_2-wet. Z= model height; X, Y= model length and width.

Table 3-2 Depth[a] reached and vertical migration distance of CO_2 plume after the end of the storage period (10 years) for the five different wettability scenarios investigated

Wettability	Depth reached by the free CO_2 plume (m)	Vertical migration distance of the free CO_2 plume (m)[b]
Strongly water-wet	-1034	116
Weakly water-wet	-1014	136
Intermediate-wet	-978	172
Weakly CO_2-wet	-889	261
Strongly CO_2-wet	-800[c]	350

[a]CO_2 injection depth was at (-1150 m).

[b]CO_2 plume migration distance measured from the top of the perforated interval.

cIn the case of the strongly CO_2-wet reservoir, CO_2 reached the top of the model (-800 m) after only 8 years; CO_2 then flowed laterally beneath the caprock.

3.3.2 Influence of wettability on storage mechanisms

We further analyse the impact of wettability on the CO_2 storage mechanisms by distinguishing (at the end of the 10 year storage period) and quantifying the amount of dissolved (in brine) CO_2, mobile CO_2 and residual CO_2. Residual CO_2 is CO_2 that is entrapped in the pore space of the rock by capillary forces (Iglauer et al., 2011; Andrew et al., 2013; Chaudhary et al., 2013; Rahman et al., 2016) and that has thus been immobilized.

The percentage of trapped CO_2, either by dissolution or by residual trapping and of mobile (free) CO_2 during the storage period is displayed in (Figure 3-5) for all wettability cases; corresponding percentages are reported in Table 3-3 for the end of the storage period (i.e. after 10 years). Generally for all wettability cases, the percentage of trapped CO_2, either by dissolution trapping or residual trapping, increased over time during the storage period, and consequently the amount of free scCO_2 decreased (Figure 3-5), which is consistent with previous studies (Iglauer et al.,

2015b; Kumar et al., 2005; Suekane et al., 2008; Qi et al., 2009; Gershenzon et al., 2015).

In the case of a strongly water-wet rock, most (99.5%) of the CO_2 is already trapped at the beginning of the storage period, either by dissolution (~18%) or by residual trapping (~81%). This is due to the relatively small amount of CO_2 injected and the high residual CO_2 saturation (S_{gr} = 35%) in the strongly water-wet rock compared with lower residual CO_2 saturation in the less water-wet scenarios (reducing to S_{gr} = 10% in the strongly CO_2-wet case (see Figure 3-2)); thus the CO_2 plume in the water-wet rock appears stagnant in Figure 3-4 (changes in dissolved CO_2 are insignificant). With increasing CO_2-wettability the amount of residual CO_2 trapping dropped dramatically, from ~80% in case of strongly water-wet rock to ~50% in case of strongly CO_2-wet rock, 10 years after the injection has stopped. This is due to the lower capillary forces in CO_2-wet rock and the resulting lower S_{gr} (Chaudhary et al., 2013; Rahman et al., 2016). Recall that S_{gr} strongly depends on the wettability (Anderson, 1987b; Craig, 1993; Iglauer et al., 2011; Andrew et al., 2013; Chaudhary et al., 2013; Rahman et al., 2016), see Figure 3-2. Consequently, residual trapping capacities strongly depend on wettability as wettability strongly impacts S_{gr} and therefore the overall residual CO_2 saturation.

On the contrary, dissolution trapping was more efficient in strongly CO_2-wet rock, with ~18 % for strongly water-wet rock compared to ~29% for strongly CO_2-wet rock after 10 years storage time. It is important to mention here that this difference in dissolution trapping between CO_2-wet and water-wet reservoirs is because the CO_2 plume moves faster through the CO_2-wet reservoir and spreads out more. The more the plume spreads , however, the larger the CO_2-brine interface becomes. And a larger CO_2-brine interface leads to more dissolution trapping (Metz et al., 2005; Kumar et al., 2005; Doughty, 2010).

Thus, our results show that there is a highly significant impact of wettability on the ratio of mobile to residual CO_2, and a significant effect on dissolution trapping.

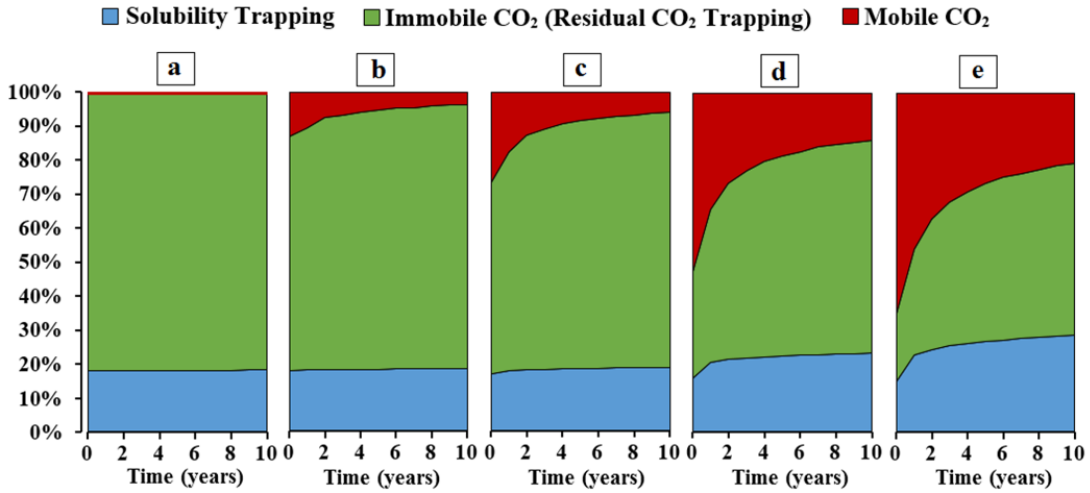

Figure 3-5 Percentage of free and trapped CO_2 for the five different rock wettabilities investigated (dissolution trapping is in blue, residual trapping is in green and mobile CO_2 is in red): a) strongly water-wet; b) weakly water-wet; c) intermediate-wet; d) weakly CO_2-wet; e) strongly CO_2-wet. Time = 0 is the beginning of the storage period.

Table 3-3 Percentage of free and trapped CO_2 at the end of the storage period (10 years) for the five different wettabilities investigated

Wettability	**Mobile CO_2 %**	**Solubility trapped CO_2 %**	**Residually trapped CO_2 %**
Strongly water-wet	0.5	18.3	81.2
Weakly water-wet	3.9	18.5	77.6
Intermediate-wet	6.0	18.7	75.3
Weakly CO_2-wet	13.8	23.2	63.0
Strongly CO_2-wet	20.7	28.6	50.7

3.4 Conclusions

CO_2-wettability of rocks can vary tremendously, from strongly water-wet to strongly CO_2-wet (cp. the recent review by (Iglauer et al., 2015b) and the reference list in the introduction of this study). Such wettability variation has been previously shown, in laboratory experiments, to strongly influence residual trapping (Iglauer et al., 2011;

Andrew et al., 2013; Chaudhary et al., 2013; Rahman et al., 2016) and structural trapping (Naylor et al., 2011; Iglauer et al., 2015a).

Here, for the first time, we systematically analysed the effect of rock wettability on the CO_2 plume behaviour in an idealized reservoir and computed the amount of mobile and trapped CO_2 (by both residual and solubility trapping mechanisms) at the hectometre-scale via reservoir simulations.

Our simulations clearly indicate that CO_2 is best retained in water-wet rock, while CO_2-wet reservoirs are relatively much more permeable to CO_2. Furthermore, the shape of the CO_2 plume is also strongly affected by wettability, the plume is much more compact in case of water-wet rock, while it is vertically elongated in CO_2-wet rock. Moreover, in our example case study over a 10 year storage period, the amount of residually trapped CO_2 is significantly higher in water-wet rock. On the contrary, dissolution trapping is more effective in CO_2-wet rock.

In summary, wettability significantly changes migration patterns and storage capacities, which is directly relevant to CO_2 geo-storage projects. Moreover, we conclude that strongly water-wet reservoirs are preferable CO_2 sinks due to their higher storage capacities and superior containment security. This result has important implications for designing geoengineering solutions aiming at increasing CO_2 storage especially in situations where an efficient and continuous seal is absent (e.g. the South West Hub project in Western Australia (Stalker et al., 2013)). Recent laboratory experiments indeed show that intermediate-wet and CO_2-wet reservoirs can be treated (e.g. with silica nanofluid (Al-Anssari et al., 2016)) to render them strongly water-wet.

Chapter 4 Impact of Reservoir Wettability and Heterogeneity on CO_2-Plume Migration and Trapping Capacity

4.1 Introduction

Capture and geological storage of Carbon dioxide (CCS) is considered one of the most promising technologies to mitigate greenhouse gas emissions into the atmosphere; CO_2 is captured from large CO_2 stationary sources and injected into deep geological formations (Pruess et al., 2003). There are three main sites for CO_2 storage, namely unminable coal beds, saline aquifers, and depleted hydrocarbon reservoirs (Metz et al., 2005). Among these storage sites, saline aquifers have the largest CO_2 storage capacity so they are considered the best storage sites (Lackner, 2003). However, economic feasibility and particularly safety of these CO_2 sequestration sites need to be insured (Metz et al., 2005; Gershenzon et al., 2015). Typically, CO_2 is injected in a dense supercritical ($scCO_2$) state, at a minimum aquifer depth of 800 m to maximise storage efficiency (Holloway and Savage, 1993; Pentland et al., 2011; Metz et al., 2005; Pruess et al., 2003). However, $scCO_2$ has a lower density than that of brine, and it will thus migrate upwards due to the buoyancy forces (Dai et al., 2014; Flett et al., 2007; Hassanzadeh et al., 2009). This CO_2 plume upward migration can be mitigated by four trapping mechanisms which have different timescales (i.e. different time lengths over which the storage mechanisms occurred). The first trapping mechanism is the structural trapping which is represented by the caprock (or seal) (Hesse et al., 2008; Naylor et al., 2011; Iglauer et al., 2015a; Gershenzon et al., 2015). The second trapping mechanism is the residual trapping mechanism (Kumar et al., 2005; Pentland et al., 2011; Iglauer et al., 2011). The third trapping mechanism is the dissolution trapping (Lindeberg and Wessel-Berg, 1997; Pruess and Garcia, 2002; Bachu and Adams, 2003; Spycher et al., 2003; Iglauer, 2011). This is a slow process (on the timescale of 100's to 1000's years) and it has been shown that it can be accelerated by convective dissolution or CO_2- brine mixing at the surface, wellbore, or in the subsurface (Emami-Meybodi et al., 2015). The last trapping mechanism is the mineral trapping (Bachu et al., 1994b; Xu et al., 2004; Gaus, 2010). The injected CO_2 can be permanently stored in the aquifer as the result of chemical reactions between the carbonic acid resulted from CO_2 dissolution in the brine process and the minerals

existing in the aquifer rocks [e.g. (Xu et al., 2003; Xu et al., 2005; Flett et al., 2007). In this study, we do not consider the mineral trapping mechanism, as it is a much slower process than the first three [e.g. (Xu et al., 2004; Metz et al., 2005; Gaus, 2010). Several studies have shown that geological heterogeneities (i.e. structural or stratigraphic heterogeneity, permeability and porosity distribution or differences in mineralogy) have a significant impact on the behaviour and vertical and horizontal movement of the CO_2 plume (Doughty and Pruess, 2004; Hovorka et al., 2004; Obi and Blunt, 2006; Bryant et al., 2006; Flett et al., 2007; Ide et al., 2007; Saadatpoor et al., 2009; Zhou et al., 2010; Hesse and Woods, 2010; Green and Ennis-King, 2010; Doughty, 2010; Krevor et al., 2015; Li and Benson, 2015) and consequently on the storage efficiency for the different storage mechanisms (Ambrose et al., 2008; Doughty, 2010; Han et al., 2010; Hesse and Woods, 2010; Green and Ennis-King, 2010; Gershenzon et al., 2015; Krevor et al., 2016). However, one parameter, reservoir wettabilty, has received little attention in CO_2 storage modelling, although it is expermentally clear that it strongly affects structural (Iglauer et al., 2015a) and residual trapping (Chaudhary et al., 2013; Rahman et al., 2016; Al-Menhali et al., 2016). In addition, previous simulation works presented by Krevor et al. [2015] (Krevor et al., 2015) and Juanes et al. [2006] (Juanes et al., 2006) showed that wettability and hysteresis in the capillary curves do affect the efficiency of capillary trapping; they compared two wettability scenarios, mixed-wet rocks and water-wet rocks, and concluded that mix-wet rocks have a lower capillary trapping capacity compared to water-wet rocks. Furthermore, it has been shown that rock wettability strongly affects the relative permeability curves (Owens and Archer, 1971; McCaffery and Bennion, 1974; Heiba et al., 1983; Anderson, 1987b; Krevor et al., 2012; Levine et al., 2014), capillary pressure curves (Anderson, 1987a; Batycky et al., 1981; Heiba et al., 1983; Melrose, 1965; Morrow, 1976) and the phase distribution within the rocks pore space (Morrow, 1990) and so, the CO_2-water displacement mechanisms (Morrow, 1990).

These different wettability conditions are the result of various geological and chemical factors including surface chemistry (e.g. organic content (Iglauer et al., 2015a; Iglauer et al., 2015b)), reservoir pressure (pressure increase leads to reduction in water wettability (Al-Yaseri et al., 2016; Arif et al., 2016a; Arif et al., 2016b; Chiquet et al., 2007; Broseta et al., 2012)), reservoir temperature (a higher temperature results in

higher water-wettability on mica or quartz (Broseta et al., 2012; Al-Yaseri et al., 2016; Arif et al., 2016a; Arif et al., 2016b)), salinity and ion type (increasing salinity leads to increasing CO_2 wettability (Al-Yaseri et al., 2016; Arif et al., 2016b; Chiquet et al., 2007; Espinoza and Santamarina, 2010; Wang et al., 2012)). It is thus of key importance to quantify the effect of wettability on storage capacities.

Thus, in this chapter, we developed 3D reservoir simulation models to predict storage capacities (i.e. residual trapping and dissolution trapping), mobile CO_2 capacity and CO_2 plume migration patterns for five different wettability conditions (strongly water-wet, weakly water-wet, intermediate-wet, weakly CO_2-wet, and strongly CO_2-wet). Furthermore, we investigate how reservoir heterogeneity interacts with these processes by comparing a set of simulations using a homogeneous distribution of permeability and porosity values with a set of simulations using heterogeneous distributions.

4.2 Methodology

4.2.1 Reservoir model

We used the nonisothermal multicomponent multiphase flow simulator TOUGH2 (Pruess et al., 1999) for simulating CO_2 migration in a storage reservoir. The thermophysical properties of the H2O-NaCl-CO_2 mixtures (including super-and sub-critical CO_2 conditions) and phase changes between liquid and gaseous CO_2 were modelled with the tabular equation of state (EOS) ECO2M (Pruess, 2011).

The aquifer dimensions were 400 m × 800 m with a thickness of 85 m, which was equivalent to 24 × 48 × 85 cells (97920 cells in total). The pressure at 1500 m depth (the top of the aquifer) was 15 MPa and a hydrostatic pressure gradient of 10 MPa/km was applied (Dake, 2007) [Dake, 2007], while temperature was kept constant at 333 K (i.e. isothermal conditions were applied). A constant pressure boundary condition (i.e. Dirichlet boundary conditions) was applied by multiplying the volume of the outer boundary cells, on the sides and bottom of the reservoir, by a large factor of 10^8 (Mo et al., 2005; Nghiem et al., 2009). The aquifer was initially fully saturated with water (S_{wi} = 100%) with a salinity of 15% (by weight). Porosity and permeability were kept constant throughout the reservoir for the set of simulations modelling a homogeneous

scenario. Porosity was set at 0.17. Anisotropy in permeability was introduced by taking a vertical-to-horizontal ratio of 0.1, with a value of 355 mD in the horizontal direction. The top of the reservoir (at 1500 m depth) was overlaid by a seal: it was simulated by reducing the ratio of vertical-to-horizontal permeability from 0.1 in the storage reservoir to 0.0001 at the top boundary of the reservoir in order to create a barrier preventing the CO_2 from leaking out of the reservoir. This model is called 'homogeneous model' in the following paragraphs.

In order to assess the impact on aquifer heterogeneity, we used the porosity and permeability data from the tenth SPE comparative solution project (Christie and Blunt, 2001), (Figure 4-1 and Figure 4-2). The values of porosity and horizontal permeability used in the homogeneous model are average values of these SPE data values. This model is called 'heterogeneous model' in the following paragraphs.

Five different wettability scenarios (see section 4.2.2 for implementation details) were then evaluated both for the homogenous and heterogeneous models.

Furthermore, we tested the impact of CO_2 injection rate by using five different injection rates of 10000 t/year, 15000 t/year, 20000 t/year, 25000 t/year and 30000 t/year; these injection rates were similar to those found in various CO_2 pilot projects: (e.g. 30000 t/year in the CO_2SINK in Ketzin, Germany) (Forster et al., 2006; Prevedel et al., 2009), 7000 ton/ year and 15000 t/year in the Nagaoka pilot project in Japan (Mito et al., 2008; Xue et al., 2006)).

$ScCO_2$ was injected at a depth of 1570 m at the centre of the model (in the XY plane) (Figure 4-1). The injection period (1 year) was followed by a 10 year shut-off period (representing the storage period).

The CO_2 migration behaviour and the amount of residually and solubility trapped CO_2 were computed as a function of the amount of injected CO_2, storage time, reservoir heterogeneity, and most importantly, reservoir wettability.

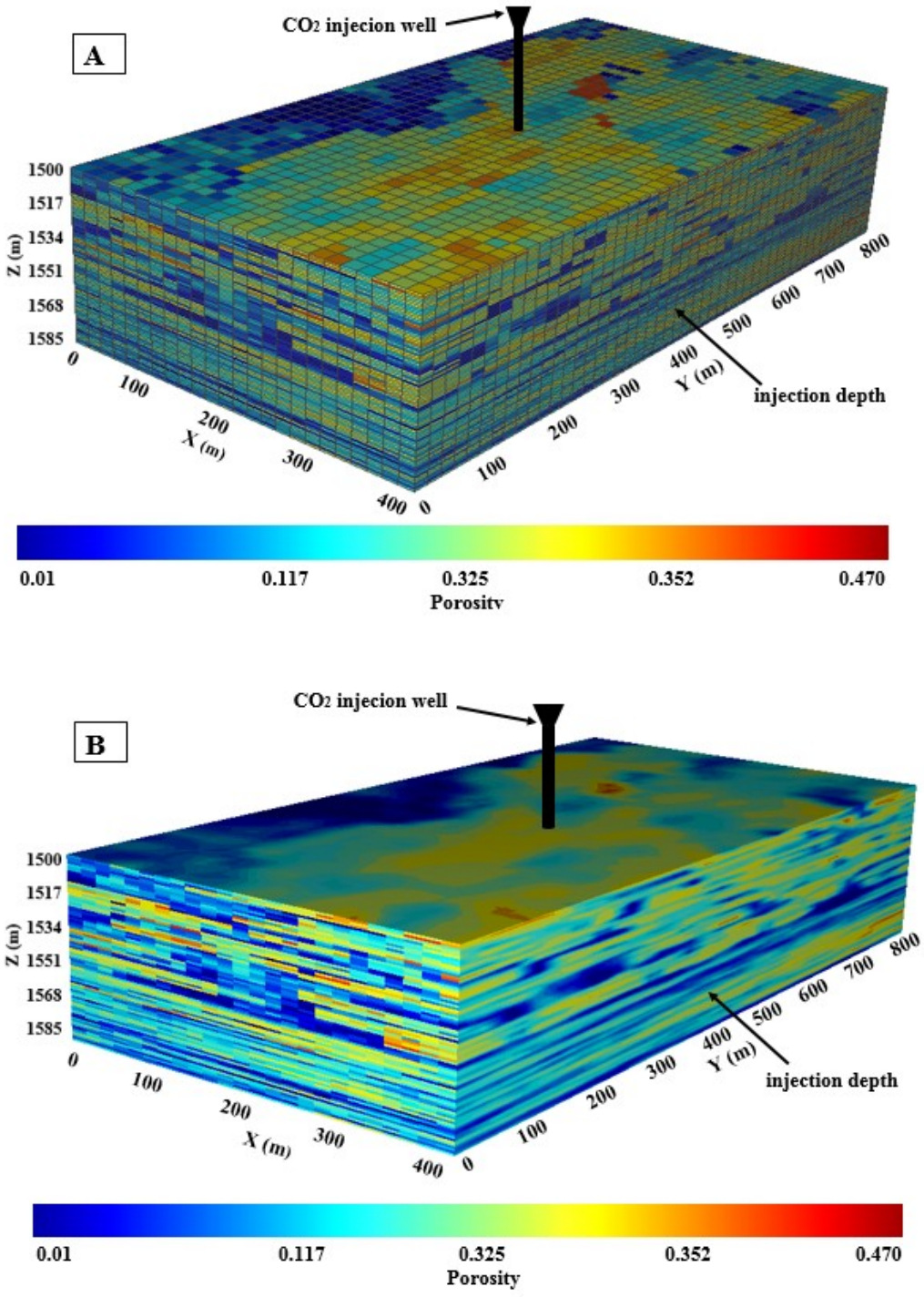

Figure 4-1 Representation of the 3-D model showing the aquifer porosity distribution and including the location of the injection well and model dimensions: A) with grid blocks view; B) compact view without grid blocks.

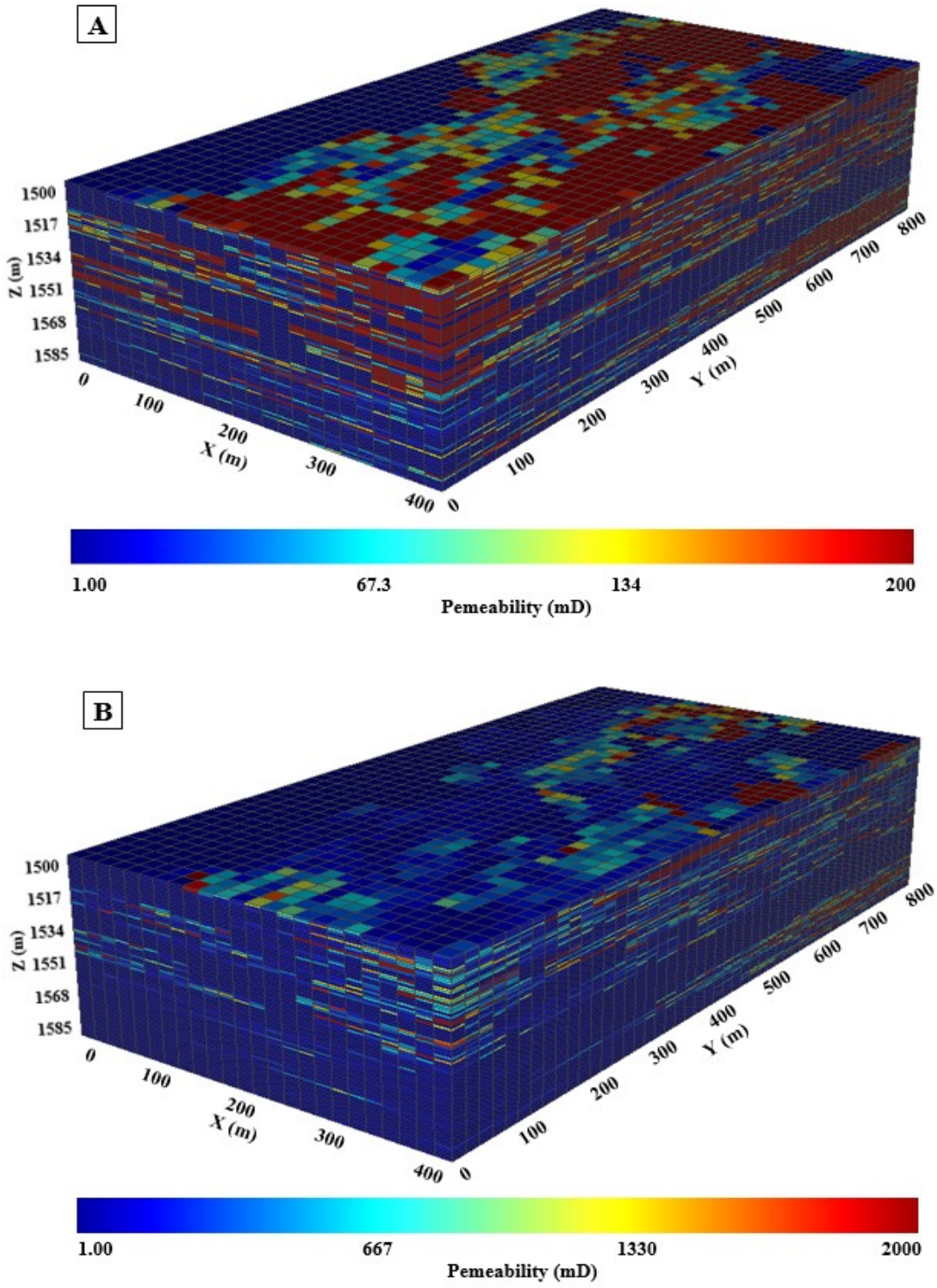

Figure 4-2 Representation of the 3-D model showing the aquifer horizontal permeability distribution for two different maximum permeability scale for permeability visualizing: A) for maximum permeability = 200 mD; B) for maximum permeability= 2000 mD.

4.2.2 Implementation of Reservoir Wettability

In order to simulate the different wettability conditions, we used the corresponding characteristics capillary pressure and relative permeability curves for each wettability condition from strongly water-wet to strongly CO_2-wet. Indeed, it has been shown that the outcome of CO_2 storage simulation results is highly affected by the choice of the characteristics curves (Doughty, 2007; Juanes et al., 2006). In this study, these curves were constructed based on earlier work on relative permeability (Owens and Archer, 1971; McCaffery and Bennion, 1974; Heiba et al., 1983; Anderson, 1987b; Krevor et al., 2012; Levine et al., 2014), capillary pressure (Anderson, 1987a; Batycky et al., 1981; Heiba et al., 1983; Melrose, 1965; Morrow, 1976) and associated residual water- and CO_2-saturations (Anderson, 1987b; Craig, 1993; Iglauer et al., 2011; Andrew et al., 2013; Chaudhary et al., 2013; Pentland et al., 2011; Rahman et al., 2016). Importantly, both residual water saturation and residual gas saturation (Swr and Sgr, respectively) depend on reservoir wettability (Anderson, 1987a; Anderson, 1987b; Craig, 1993; Iglauer et al., 2011; Andrew et al., 2013; Chaudhary et al., 2013; Rahman et al., 2016).

Specifically, for the construction of the relative permeability curves, we used McCaffery and Bennion's data (1974). We used Didger software (Golden Software Inc, 2013, Colorado) to digitize these curves and obtain data for the relative permeability values as a function of water saturation; we adjusted these curves using Craig's rules of thumb (Craig, 1993) (Table 4-1). Hence we took S_{wr} less than 15% for CO_2-wet rocks and more than 25 % for water-wet rocks. Furthermore, the water saturation (S_w) at which the relative permeability of CO_2 (k_{rg}) and that of water (k_{rw}) are equal was taken greater than 50% for strongly water-wet systems and lower than 50% for strongly CO_2-wet systems. Finally, during the storage period, k_{rw} at the maximum water saturation must be less than 30% in the strongly water-wet rocks, while it must be between 50% and 100% in the strongly CO_2-wet rocks. These curves were then fitted using the Van Genuchten-Mualem model described by equations 1 to 5 (Van Genuchten, 1980; Mualem, 1976) and fed into the simulator.

$$k_{rw} = \sqrt{S^*}\left\{1 - \left(1 - [S^*]^{1/\lambda}\right)^{\lambda}\right\}^2 \quad \text{if} \quad S_w < S_{ws} \tag{4.1}$$

$$k_{rw} = 1 \quad \text{if} \quad S_w \geq S_{ws} \tag{4.2}$$

$$k_{rg} = 1 - k_{rw} \quad \text{if} \quad S_{gr} = 0 \tag{4.3}$$

$$k_{rg} = \left(1 - \hat{S}\right)^2 \left(1 - \hat{S}^2\right) \quad \text{if} \quad S_{gr} > 0 \tag{4.4}$$

$$S^* = (S_w - S_{wr})/(S_{ws} - S_{wr}),$$
$$\hat{S} = (S_w - S_{wr})/(1 - S_{wr} - S_{gr}) \tag{4.5}$$

with the restriction $0 \leq k_{rw}, k_{rg} \leq 1$

where:

k_{rg} = gas relative permeability, k_{rw} = water relative permeability,

S_{gr} = residual saturation for gas, S_w = water saturation,

S_{ws} = maximum water saturation (= 1), S_{wr} = residual saturation for water,

λ = pore size distribution index (fitting parameter).

Initially the aquifer is fully saturated with brine ($S_w = 1$), thus $k_{rg} = 0$ and $k_{rw} = 1$ (right upper corner in the five plots of Figure 4-3). During CO_2 injection, S_w decreases from 1 to S_{wr} (black lines of Figure 4-3), and k_{rw} decreases steadily until reaching zero at S_{wr}, while k_{rg} increases until its maximum is reached at S_{wr}. During the storage period (which corresponds to water imbibition, represented by the red lines in Figure 4-3), k_{rg} will reduce again gradually to zero (residual CO_2 trapping), and k_{rw} increases again until it reaches its secondary maximum at S_{gr}.

The five capillary pressure curves used in this study (which correspond to the five wettability scenarios) are plotted in Figure 4-4. The curves for the strongly water-wet rock are based on the capillary pressure measurements on Berea sandstone provided by Pini et al. [2012, 2013] (Pini et al., 2012; Pini et al., 2013). The other curves were then adjusted according to previous studies of capillary pressure curves that studied the effect of wettability on the capillary pressure curves (i.e. (Anderson, 1987a; Batycky et al., 1981; Heiba et al., 1983; Melrose, 1965; Morrow, 1976)), as explained above. Table 4-2 presents the data used for the construction of capillary pressure curves for the different wettabilities.

The positive parts of these curves were implemented into the simulations, according to the current capabilities of the software, via the Van Genuchten-Mualem model (Van Genuchten, 1980; Mualem, 1976):

$$P_{cap} = P_0 \left([S^*]^{-1/\lambda} - 1\right)^{1-\lambda} \tag{4.6}$$

with the restriction $0 \leq P_{cap} \leq P_{max}$

and, $S^* = (S_w - S_{wr})/(S_{ws} - S_{wr})$ (4.7)

where:

P_{cap} = CO_2-water capillary pressure, Po = capillary pressure scaling factor,

S_{ws} = maximum (saturated) water saturation, S_{wr} = residual water saturation,

λ = pore size distribution index.

The Leverett J-function (Leverett, 1941) was then used to scale Pc with the spatially varying porosity and permeability values:

$$J(S_w) = \frac{P_c}{\sigma \cos\theta}\sqrt{\frac{k}{\phi}} \quad (4.8)$$

where:

J = dimensionless capillary pressure, S_w = water saturation, Pc = capillary pressure,

k = permeability, ϕ = porosity, σ = surface tension, θ = contact angle.

Table 4-1 Parameters used for implementing the relative permeability curves into the model

Wettability scenario	CO_2 injection process			CO_2 storage process		
	S_{gr}	S_{wr}	λ	S_{gr}	S_{wr}	λ
Strongly water-wet	0	0.26	0.78	0.35	0.26	0.58
Weakly water-wet	0	0.25	1.05	0.30	0.25	0.95
Intermediate-wet	0	0.22	1.22	0.25	0.22	1.17
Weakly CO_2-wet	0	0.15	1.41	0.15	0.15	1.51
Strongly CO_2-wet	0	0.1	1.7	0.1	0.1	1.9

Table 4-2 Parameters used for implementing the capillary pressure curves for the five different wettability scenarios into the TOUGH2 simulator

Wettability	CO_2 injection process				CO_2 storage process			
	S_{wr}	λ	P_0 [Pa]	P_{max} [Pa]	S_{wr}	λ	P_0 [Pa]	P_{max} [Pa]
Strongly water-wet	0.259	0.7	1500	25000	0.259	0.51	1000	25000
Weakly water-wet	0.249	0.7	1500	20000	0.249	0.51	1000	20000
Intermediate-wet	0.219	0.7	1500	18000	0.219	0.51	1000	18000
Weakly CO_2-wet	0.149	0.7	1500	15000	0.149	0.51	1000	15000
Strongly CO_2-wet	0.099	0.7	1500	14000	0.099	0.51	1000	14000

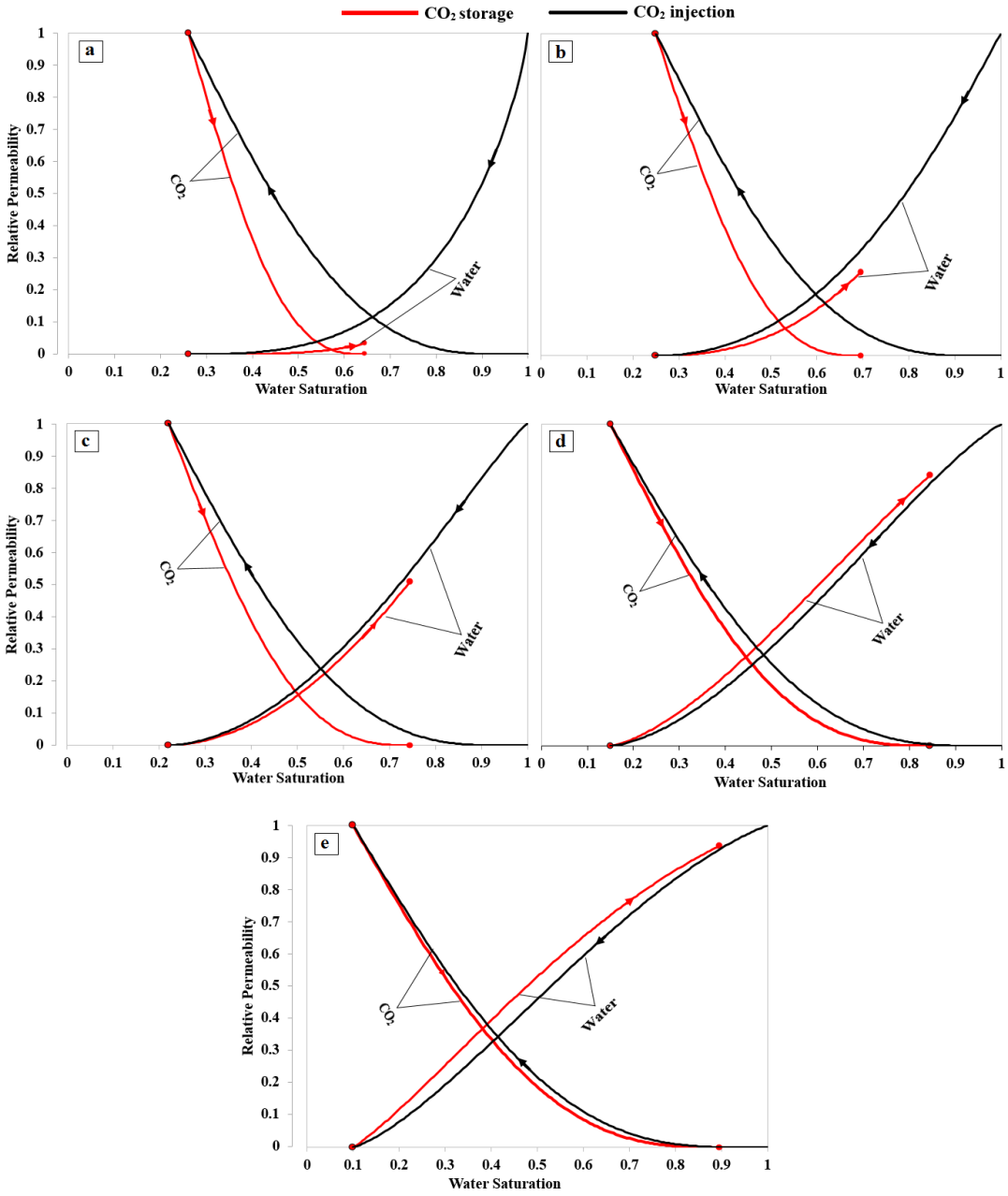

Figure 4-3 Relative permeability curves for the five different rock wettabilities investigated: a) strongly water-wet; b) weakly water-wet; c) intermediate-wet; d) weakly CO_2-wet; e) strongly CO_2-wet.

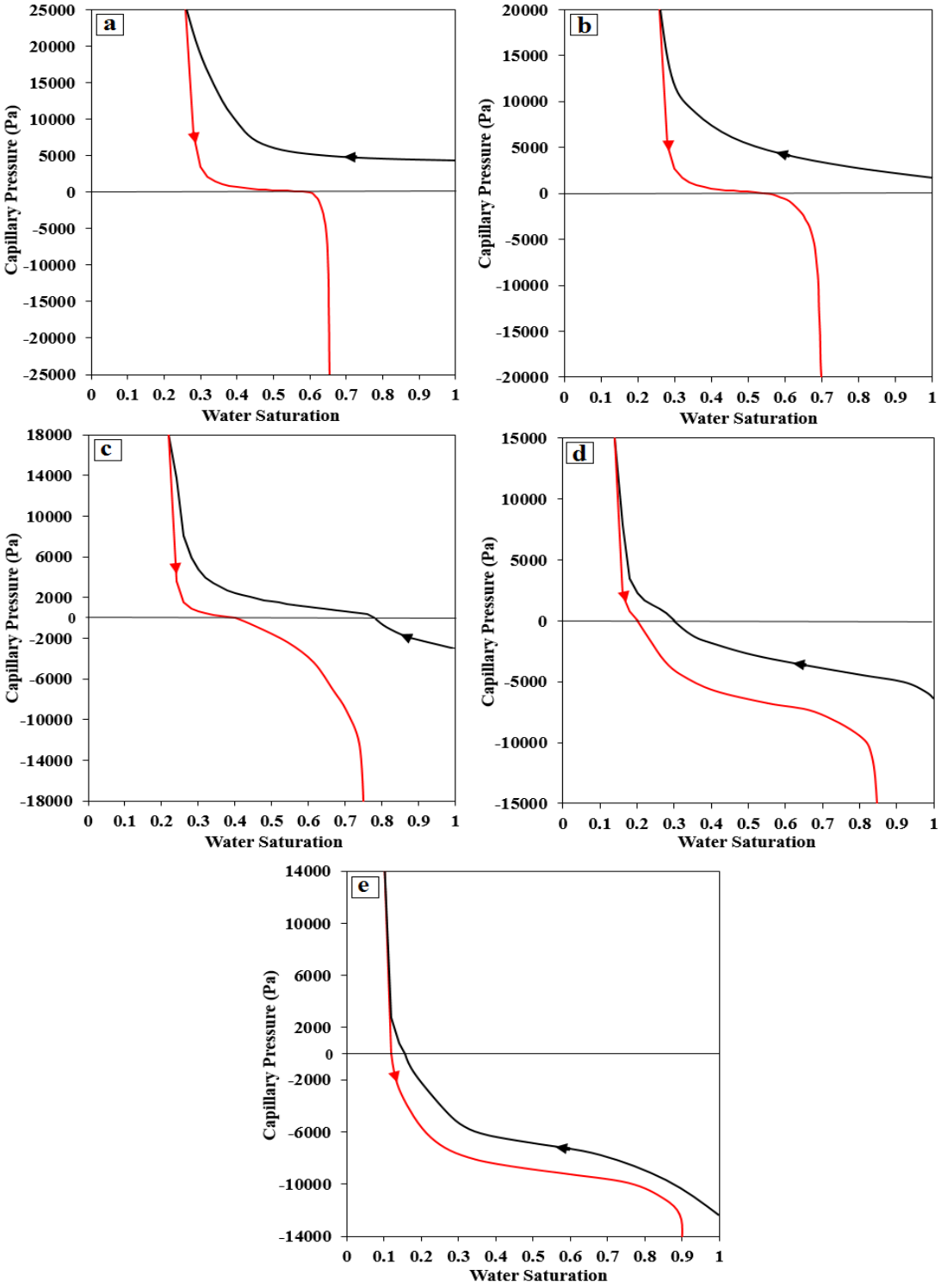

Figure 4-4 Capillary pressure curves for the five different rock wettabilities investigated: a) strongly water-wet; b) weakly water-wet; c) intermediate-wet; d) weakly CO_2-wet; e) strongly CO_2-wet. Only the positive parts of these curves were implemented into the simulations, according to the current software capabilities.

4.3 Results and discussion

4.3.1 Impact of wettability on CO_2 storage in a heterogeneous reservoir

4.3.1.1 Impact of the reservoir wettability on the CO_2-plume migration

It is well established that the CO_2-plume migrates upwards because of the density differences between the injected supercritical CO_2 and the aquifer brine (Dai et al., 2014; Flett et al., 2007; Hassanzadeh et al., 2009).

The set of simulations we have performed shows furthermore that wettability affects this CO_2 plume upward migration (Figure 4-5 to Figure 4-7). CO_2 migrates upward furthest in the strongly CO_2-wet rock (scw), while it is best retained in the strongly water-wet rock (sww) (e.g. the vertical migration distances are scw =32 m and sww =17 m, scw =33 m and sww =18 m, scw =34 m and sww =19 m, scw =34 m and sww =19 m, scw =35 m and sww =20 m, at the end of storage period and after injecting for 1 a period of year 10,000 tCO_2, 15,000 tCO_2, 20,000 tCO_2, 25,000 tCO_2 and 30,000 tCO_2, respectively (Figure 4-8)). The CO_2 plume migration distance for the weakly water-wet, intermediate-wet and weakly CO_2-wet ranges between these two above extreme cases (Figure 4-8). In summary the migration distance increases steadily with increasing the CO_2 wettability of the rocks. Our results are in agreement with previous simulations studies which showed that the CO_2 plume migration distance increases with decreasing the amount of the residual CO_2 saturation (Metz et al., 2005; Kumar et al., 2005; Doughty, 2010).

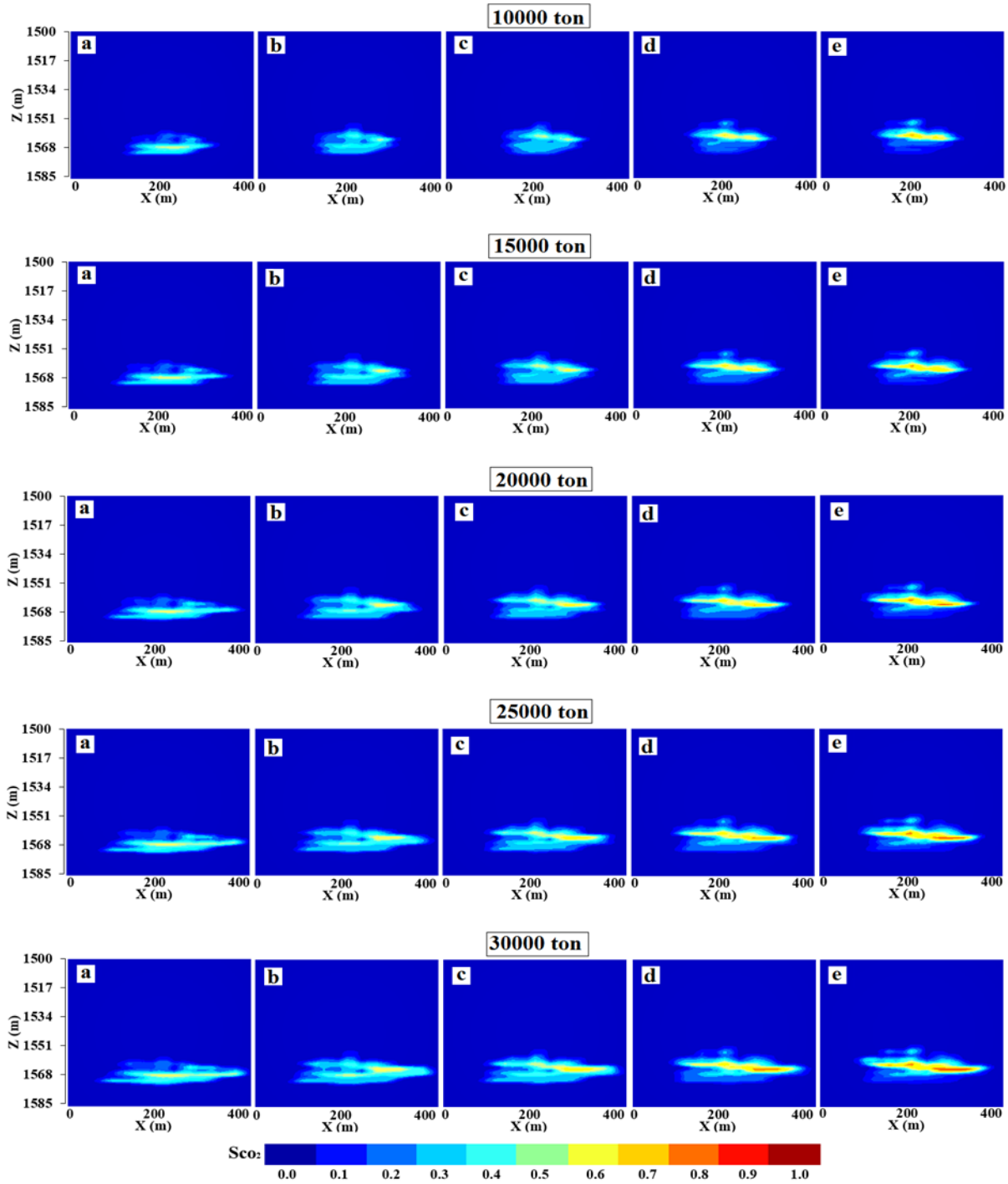

Figure 4-5 2D vertical cross-sections through the middle of the storage heterogeneous aquifer. CO_2 is injected at a depth of 1570 m. The CO_2 plume shape and height in the aquifer are shown for different amount of CO_2 injected after 1 years of storage period for the five different rock wettability cases investigated: a) strongly water-wet; b) weakly water-wet; c) intermediate-wet; d) weakly CO_2-wet; e) strongly CO_2-wet. Z= model height; X= model length.

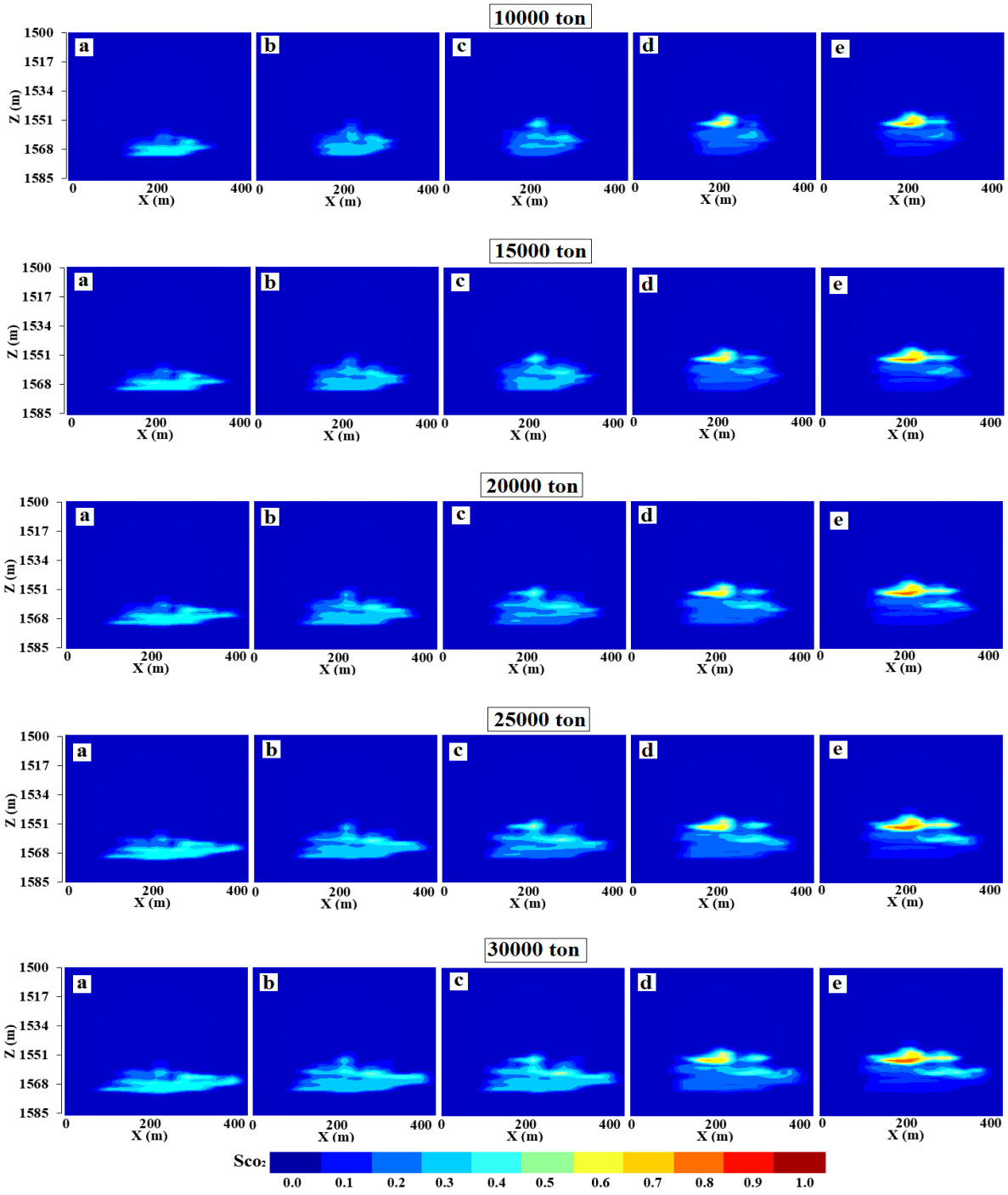

Figure 4-6 2D vertical cross-sections through the middle of the storage heterogeneous aquifer. CO_2 is injected at a depth of 1570 m. The CO_2 plume shape and height in the aquifer are shown for different amount of CO_2 injected after five years of storage period for the five different rock wettability cases investigated: a) strongly water-wet; b) weakly water-wet; c) intermediate-wet; d) weakly CO_2-wet; e) strongly CO_2-wet. Z= model height; X= model length.

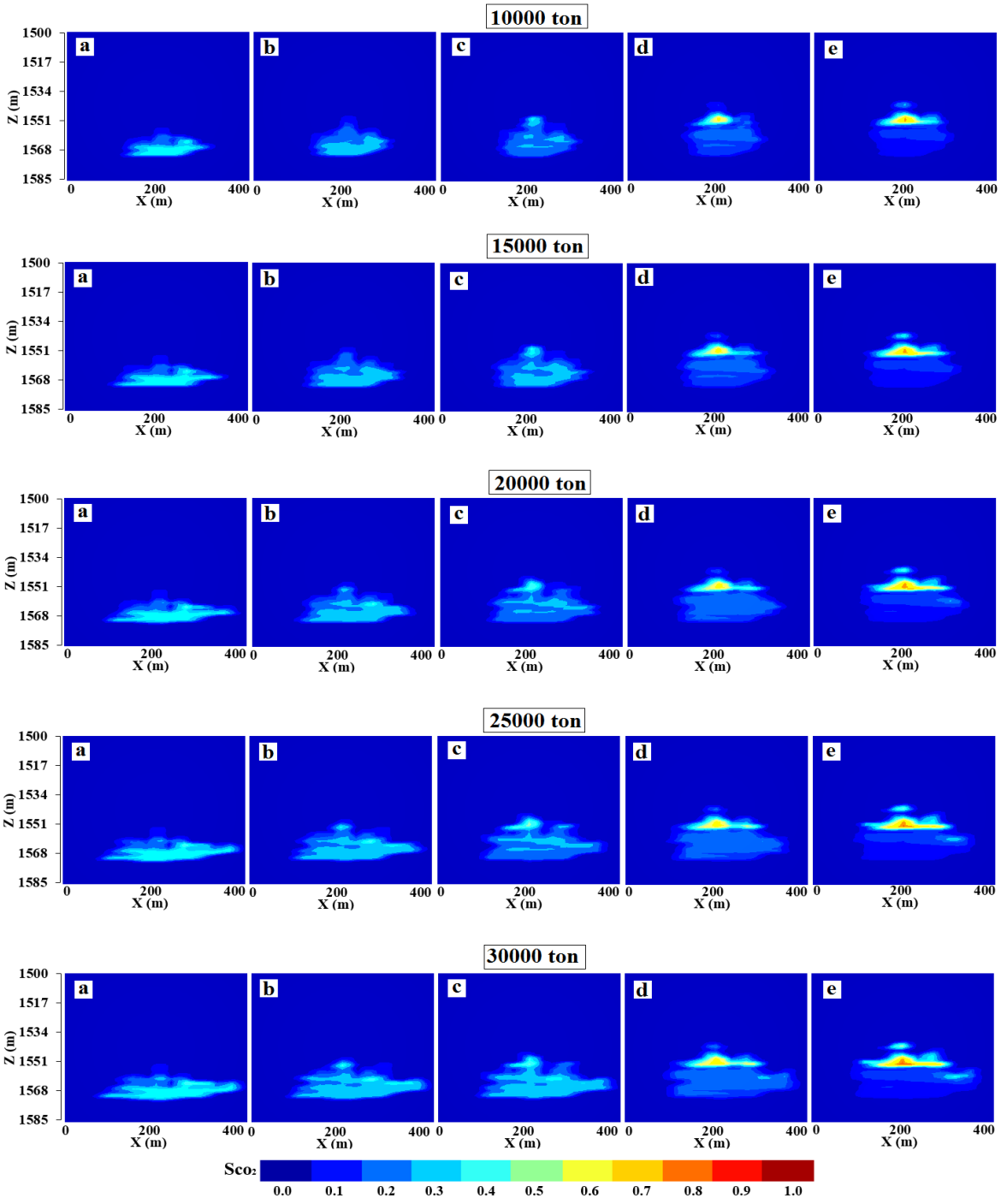

Figure 4-7 2D vertical cross-sections through the middle of the storage heterogeneous aquifer. CO_2 is injected at a depth of 1570 m. The CO_2 plume shape and height in the aquifer are shown for different amount of CO_2 injected at the end of storage period (10 years), for the five different rock wettability cases investigated: a) strongly water-wet; b) weakly water-wet; c) intermediate-wet; d) weakly CO_2-wet; e) strongly CO_2-wet. Z= model height; X= model length.

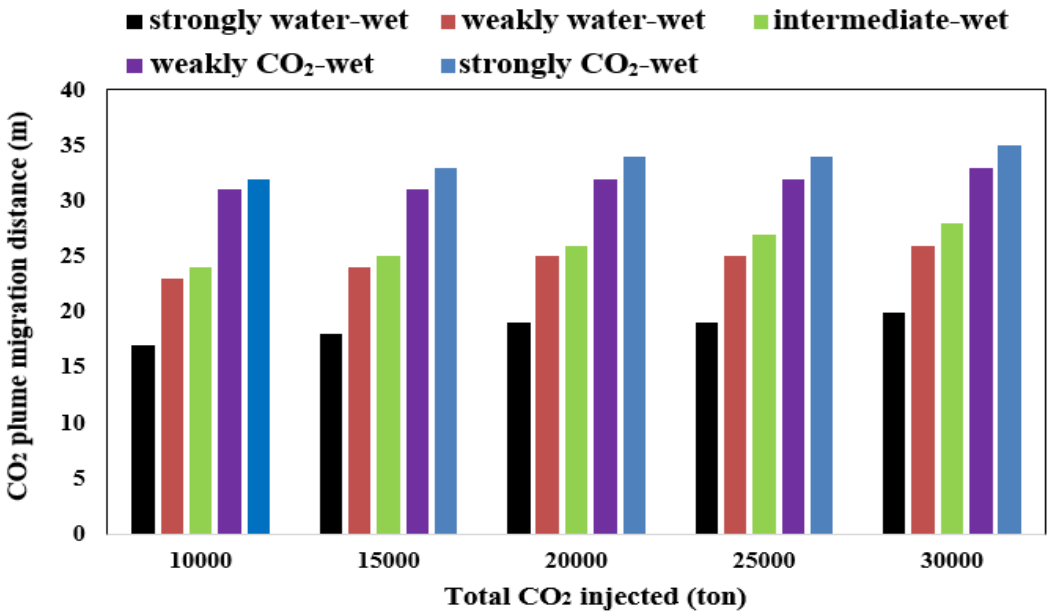

Figure 4-8 CO_2 plume vertical migration distance with different amounts of CO_2 injected, after 10 years of storage period and for the heterogeneous reservoir simulation case.

4.3.1.2 Impact of reservoir wettability on CO_2 trapping capacity

The highest CO_2 mobility (i.e. the amount of free or mobile CO_2) is found for the strongly CO_2-wet reservoir case: mobile CO_2 is 6425 ton, 9876 ton, 13496 ton, 17112 ton and 20761 ton for the five amounts of CO_2 injected, 10,000 tCO_2, 15,000 tCO_2, 20,000 tCO_2, 25,000 tCO_2 and 30,000 tCO_2, respectively (Figure 4-9). For the other wettability conditions, CO_2 mobility reduces with decreasing CO_2 wettability (i.e. when the reservoir becomes more water-wet) (Figure 4-9).

CO_2 trapped by dissolution in the aqueous phase is found to be a function of both reservoir wettability and of the amount of CO_2 injected. From Figure 4-10, it is clear that the amount of dissolved CO_2 increases with increasing CO_2-wettability and the amount of injected CO_2. For example, the amount of dissolved CO_2 at the end of the storage period in the strongly CO_2-wet reservoir (scw) and strongly water-wet reservoir (sww) was computed as follow: scw =2594 ton and sww =1702 ton, scw =3645 ton and sww =2437 ton, scw =4603 ton and sww =3108 ton, scw =5528 ton and sww =3823 ton, scw =6418 ton and sww =4520 ton, after injecting 10,000 tCO_2, 15,000 tCO_2, 20,000 tCO_2, 25,000 tCO_2 and 30,000 tCO_2, respectively (Figure 4-10). Previous simulations studies, which had not incorporated the effect of the wettability

(e.g. (Metz et al., 2005; Kumar et al., 2005; Doughty, 2010)), showed that solubility trapping increases with increasing CO_2 plume migration, which is consistent with our results as this study shows that more CO_2 migration is associated with a more CO_2-wet reservoir.

Residual trapping at the reservoir scale is also strongly influenced by the reservoir wettability. Several studies (Anderson, 1987a; Anderson, 1987b; Craig, 1993; Iglauer et al., 2011; Andrew et al., 2013; Chaudhary et al., 2013; Pentland et al., 2011; Rahman et al., 2016) demonstrated that the residual trapping for CO_2 is influenced by residual CO_2 saturation; residual CO_2 saturation is incorporated in our reservoir modelling scenarios via the relative permeability and capillary pressure curves we constructed. Clearly, the results show that residually trapped CO_2 increases with decreasing CO_2 wettability and that the residually trapped CO_2 in the strongly CO_2-wet reservoirs (scw) is less than that in the strongly water-wet (sww) (e.g. scw =981 ton and sww =7154 ton, scw =1479 ton and sww =10595 ton, scw =1901 ton and sww =13654 ton, scw = 2360 ton, and sww =15770 ton, scw =2821 to and sww =18238 ton, at the end of storage period and after injecting 10,000 tCO_2, 15,000 tCO_2, 20,000 tCO_2, 25,000 tCO_2 and 30,000 tCO_2, respectively (Figure 4-11)). These results are consistent with previous simulation studies (e.g. (Krevor et al., 2015; Juanes et al., 2006)) that have shown that mixed-wet rocks have a lower residual trapping capacity when compared to water-wet rocks.

In summary, our results show that reservoir wettability has a strong effect on CO_2 mobility and on residual and dissolution trapping capacities.

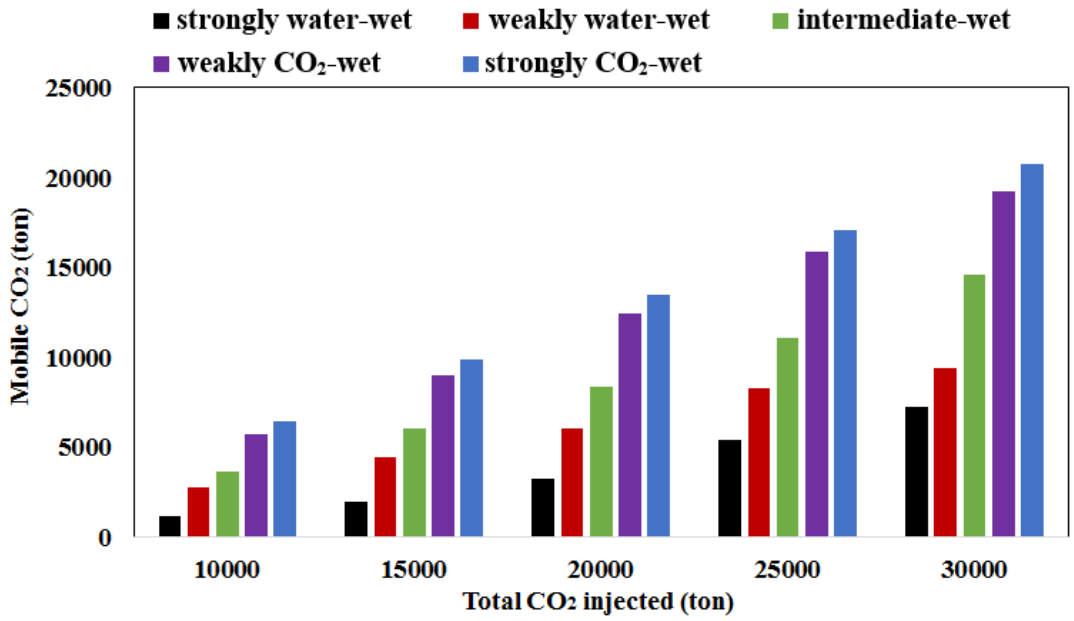

Figure 4-9 Amount of mobile CO_2 as a function of total amount of injected CO_2 and as a function of rock wettability, at the end of storage period (10 years). In all cases, CO_2 was injected for 1 year.

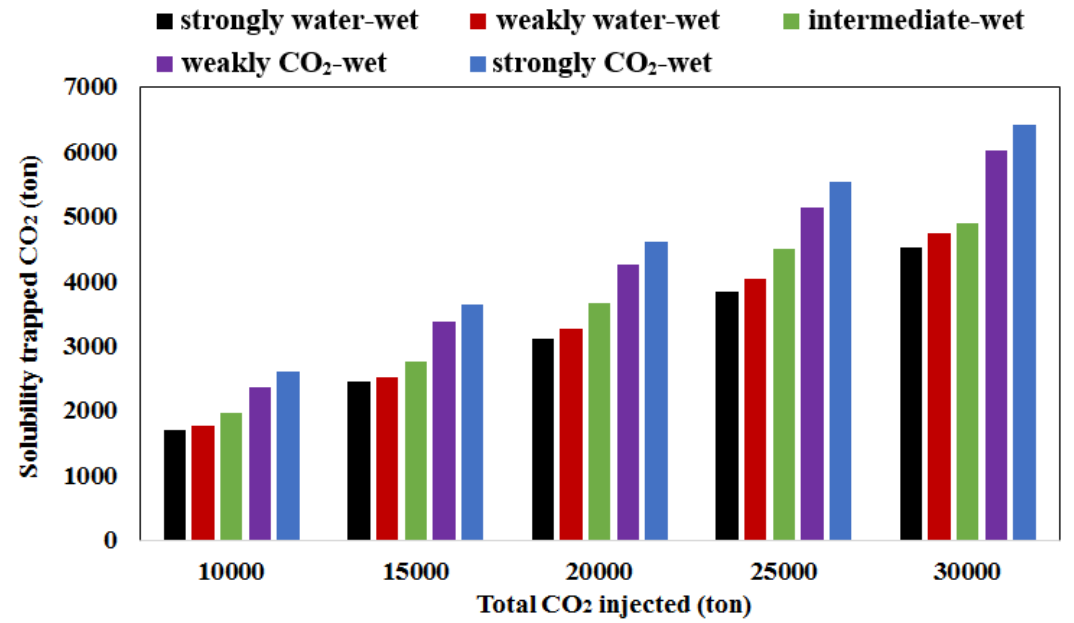

Figure 4-10 Amount of CO_2 tapped by solubility as a function of total amount of injected CO_2 and rock wettability, at the end of storage period (10 years). In all cases, CO_2 was injected for 1 year.

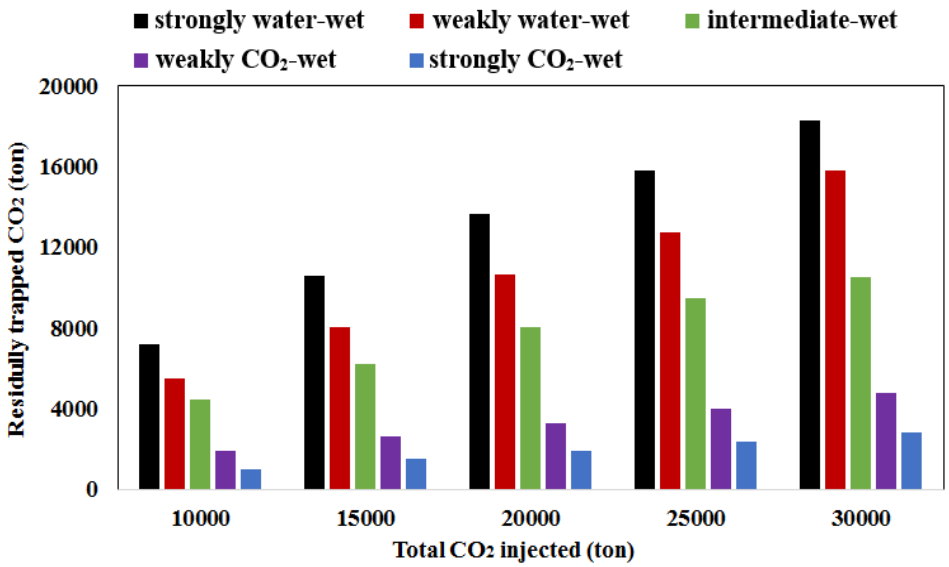

Figure 4-11 Amount of residually trapped CO_2 as a function of total amount of injected CO_2 and rock wettability, at the end of storage period (10 years). In all cases, CO_2 was injected for 1 year.

4.3.2 Impact of heterogeneity on CO_2 storage as a function of rock wettability

Many studies have shown that reservoir heterogeneity has a significant impact on CO_2 plume migration and on trapping capacities (e.g. (Doughty, 2010; Hovorka et al., 2004; Obi and Blunt, 2006; Bryant et al., 2006; Flett et al., 2007; Ide et al., 2007; Saadatpoor et al., 2009; Zhou et al., 2010; Hesse and Woods, 2010; Green and Ennis-King, 2010; Ambrose et al., 2008; Han et al., 2010; Gershenzon et al., 2015)). However, the combined effect of heterogeneity and wettability has received little attention. We thus compare the results obtained for the case of a heterogeneous reservoir, presented above, with those obtained for the case of a homogeneous reservoir.

4.3.2.1 Impact of reservoir heterogeneity on CO_2-plume flow behaviour

For all wettability conditions analysed, the CO_2-plume vertical migration distance is larger in the homogeneous reservoir than in the heterogeneous reservoir (Figure 4-12 and Table 4-3). The highest migration distance, obtained for both the homogeneous and heterogeneous cases for the strongly CO_2-wet reservoir, was computed to be 70 m for the homogeneous scenario but only half of that (35 m) for the heterogeneous scenario, at the end of storage period and after injecting 30,000 ton of CO_2 (Table 4-3). Similarly, for the strongly water-wet reservoir case, the highest migration distance was computed to be 64 m for the homogeneous scenario but only 20 m for the

heterogeneous scenario, at the end of storage period and after injecting 30,000 ton of CO_2 (Table 4-3). For all other wettability conditions and for all amounts of CO_2 injected, the CO_2 plume migration distance in the homogeneous model is approximately two times more than that computed for the heterogeneous model (Figure 4-12 and Table 4-3). However, although the reservoir heterogeneity reduces the vertical CO_2 plume migration, it enhanced the lateral movements of the CO_2 in the aquifer, as shown, previously, in Figure 4-5 to Figure 4-7.

In summary, our results show that the reservoir heterogeneity has a significant impact on the CO_2 plume flow behaviour.

Table 4-3 CO_2 plume vertical migration distance with different amount of injected CO_2, for the homogeneous and heterogeneous reservoir scenarios, at the end of the storage period (10 years) and for the five investigated wettability conditions

heterogeneity model	Total injected CO_2 (ton)	Strongly water -wet	weakly water-wet	Intermediate-wet	weakly CO_2-wet	strongly CO_2-wet
CO_2 plume vertical migration distance in heterogeneous model	10000	17	23	24	31	32
	15000	18	24	25	31	33
	20000	19	25	26	32	34
	25000	19	25	27	32	34
	30000	20	26	28	33	35
CO_2 plume vertical migration distance in homogeneous model	10000	45	50	58	65	70
	15000	53	55	62	67	70
	20000	58	59	64	70	70
	25000	61	63	66	70	70
	30000	64	66	68	70	70

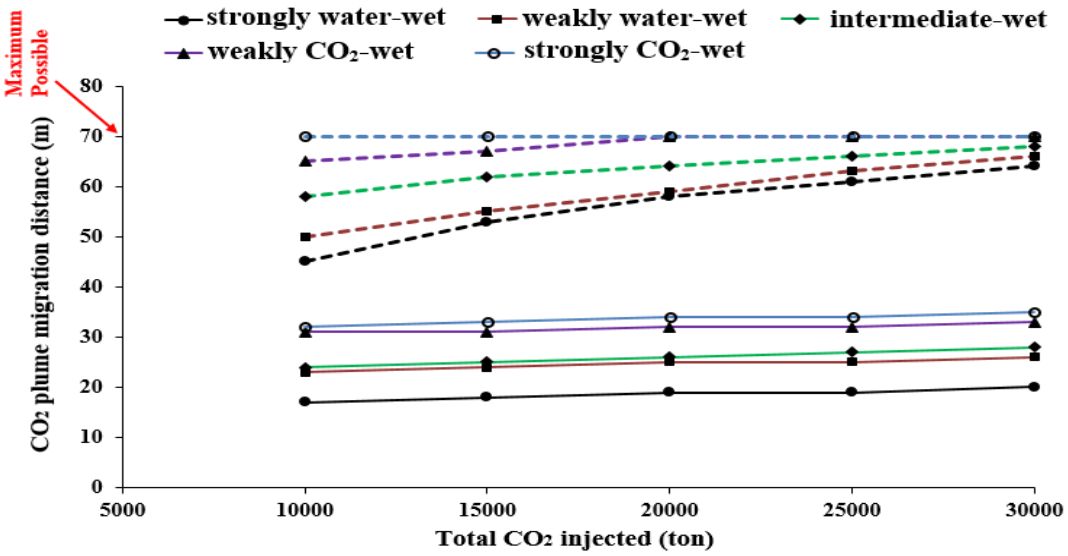

Figure 4-12 CO_2 plume vertical migration distance with different amount of injected CO_2, for the homogeneous (dashed line) and heterogeneous (solid line) reservoir scenarios, at the end of storage period (10 years) and for the five investigated wettability conditions.

4.3.2.2 Impact of the reservoir heterogeneity on CO_2 trapping capacity

Although the general impact of wettability on the trapping mechanisms is the same for both homogeneous and heterogeneous reservoir (i.e. more mobile, more solubility trapped CO_2 and less residually trapped CO_2 in the more CO_2-wet reservoirs), there is a significant difference between the heterogeneous and homogeneous reservoir both in time and in space, as illustrated in Figure 4-13 and Figure 4-14 and Table 4-4. Our simulation results show that more mobile CO_2 (the majority of this mobility following a horizontal movement not a vertical migration) is computed for the heterogeneous reservoir than for the homogeneous reservoir model, for all wettability conditions. We indeed mentioned in the previous sections that, although the heterogeneity inhibited the vertical migration of CO_2 plume, it enhanced the lateral CO_2 flow.

Moreover, our results show that reservoir heterogeneity decreases the percentage of residually trapped CO_2, which is consistent with Han et al.'s [2010] work; these authors concluded that increasing permeability heterogeneities resulted in decreasing the amount of residually trapped CO_2. Our simulations show that heterogeneity also decreases the percentage of dissolved CO_2 (Figure 4-13 and Figure 4-14 and Table 4-

4). It is important to mention here that the amount of dissolved CO_2 is essentially a function of CO_2 plume migration (Metz et al., 2005; Kumar et al., 2005; Doughty, 2010) due to the fact that permeability heterogeneity (or permeability barrier) reduces the vertical plume migration: we observe that the percentage of dissolved CO_2 decreases for all wettability scenarios (Table 4-4).

We thus conclude that even though the general trends of the effect of wettability on CO_2 storage capacities (i.e. that the more water-wet the reservoir, the less CO_2 is mobile, the less CO_2 is solubility trapped and the more CO_2 is residually trapped) is the same for both, the homogeneous and the heterogeneous scenarios, the absolute values are quite different. Hence, not taking into account heterogeneities in the porosity and permeability distributions can lead to erroneous estimates of CO_2 storage capacities.

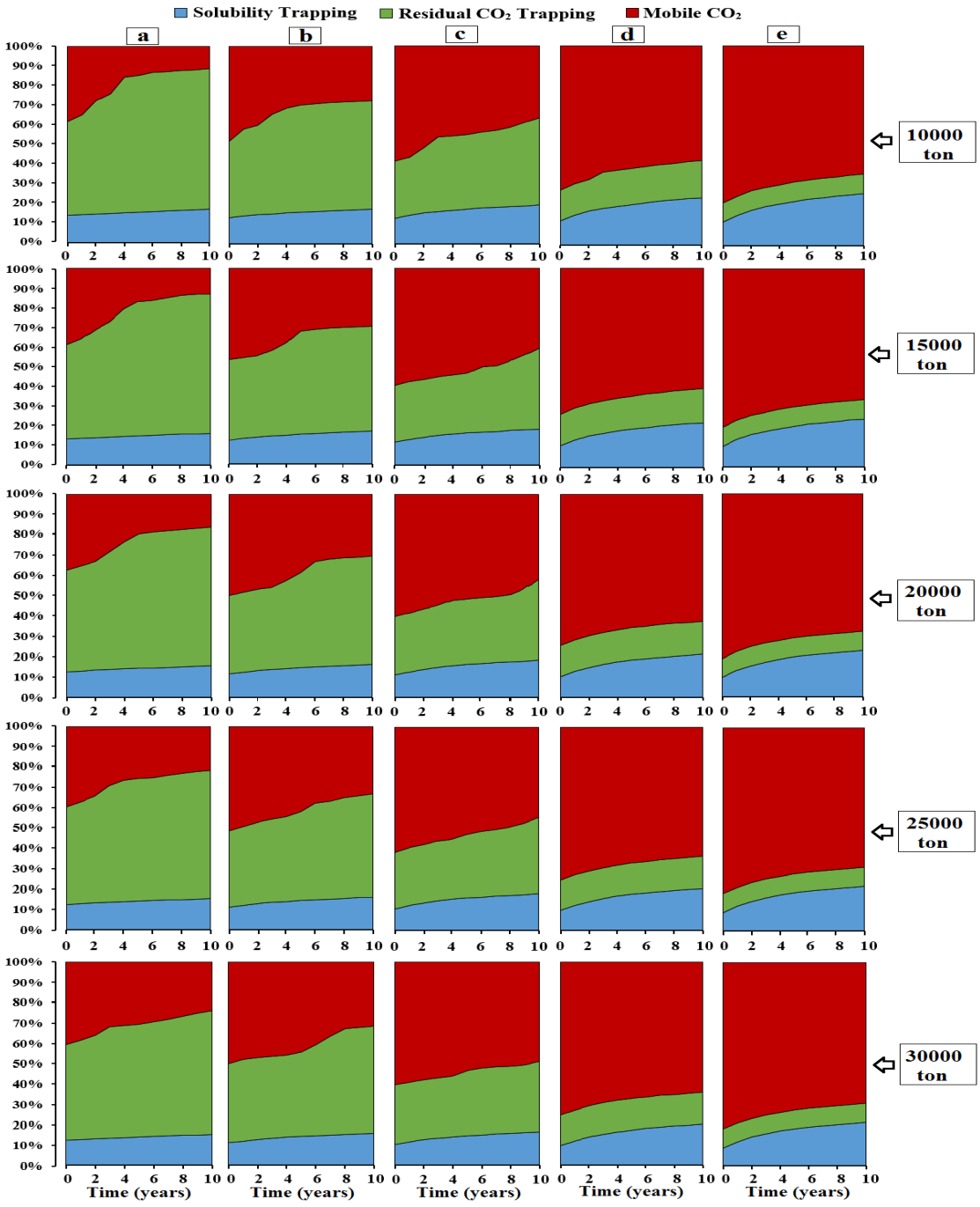

Figure 4-13 Percentage of trapped and free CO_2 (dissolution trapping is in blue, residual trapping in green and mobile CO_2 is in red) as a function of amount of injected CO_2 and storage time, for the case of the heterogeneous aquifer and for the five different rock wettabilities investigated: a) strongly water-wet; b) weakly water-wet; c) intermediate-wet; d) weakly CO_2-wet; e) strongly CO_2-wet.

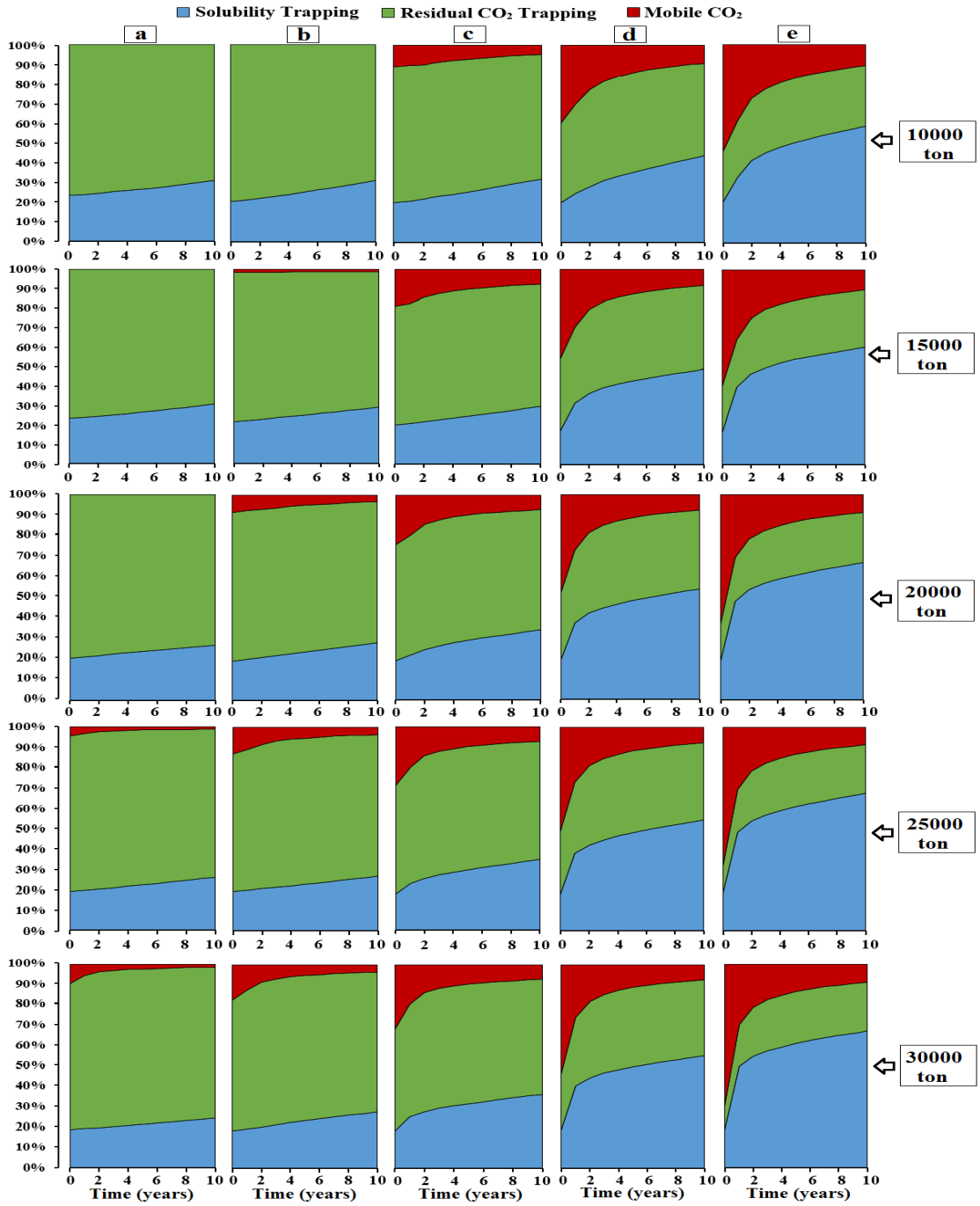

Figure 4-14 Percentage of trapped and free CO_2 (dissolution trapping is in blue, residual trapping in green and mobile CO_2 is in red) as a function of amount of injected CO_2 and storage time, for the case of the homogeneous aquifer and for the five different rock wettabilities investigated: a) strongly water-wet; b) weakly water-wet; c) intermediate-wet; d) weakly CO_2-wet; e) strongly CO_2-wet.

Table 4-4 Amount of mobile and trapped CO_2 computed at the end of the storage period (10 years) with different amount of CO_2 injected during the injection period,in both heterogeneous and homogenous reservoir models and for the five different wettabilities investigated.

Wettability	Trapping mechanism (ton)	Total injected CO_2 in heterogeneous reservoir (ton)					Total injected CO_2 in homogeneous reservoir (ton)				
		10000	15000	20000	25000	30000	10000	15000	20000	25000	30000
Strongly water-wet	solubility trapped CO_2	1702	2437	3108	3823	4520	2685	3627	5358	6481	7328
	residually trapped CO_2	7154	10595	13654	15770	18238	7315	11373	14642	18207	22165
	mobile CO_2	1144	1968	3238	5407	7242	0	0	0	312	507
Weakly water-wet	solubility trapped CO_2	1775	2517	3254	4040	4742	3117	4354	5600	6744	8362
	residually trapped CO_2	5483	8054	10666	12703	15819	6883	10472	13714	17387	20608
	mobile CO_2	2742	4429	6080	8257	9439	0	174	686	869	1030
Intermediate-wet	solubility trapped CO_2	1971	2745	3655	4492	4884	3224	4426	6844	8712	10940
	residually trapped CO_2	4410	6231	8006	9429	10520	6328	9434	11738	14532	17005
	mobile CO_2	3619	6024	8339	11079	14596	448	1140	1418	1756	2055
Weakly CO_2-wet	solubility trapped CO_2	2360	3372	4248	5133	6009	4389	7345	10787	13634	16608
	residually trapped CO_2	1879	2584	3273	3995	4779	4702	6415	7720	9472	11222
	mobile CO_2	5761	9044	12479	15872	19212	909	1240	1493	1894	2170
Strongly CO_2-wet	solubility trapped CO_2	2594	3645	4603	5528	6418	5913	9058	13341	16911	20155
	residually trapped CO_2	981	1479	1901	2360	2821	3028	4402	4896	5948	7239
	mobile CO_2	6425	9876	13496	17112	20761	1059	1540	1763	2141	2606

4.4 Conclusions

Reservoir wettability can vary widely from strongly water-wet (0° contact angle) to strongly CO_2-wet (170° contact angle) (Dickson et al., 2006; Chiquet et al., 2007; Yang et al., 2008b; Espinoza and Santamarina, 2010; Bikkina, 2011; Kaveh et al., 2011; Wang et al., 2012; Iglauer et al., 2012; Iglauer et al., 2014; Iglauer et al., 2015a; Iglauer et al., 2015b; Chaudhary et al., 2015; Chen et al., 2015a; Sarmadivaleh et al., 2015; Arif et al., 2016a; Arif et al., 2016b). However, the effect of rock wettability on CO_2 storage capacity and containment security has received only little attention (Iglauer et al. 2015a), and no data is available for the combined effect of wettability and reservoir permeability heterogeneity.

In this study, we simulated the CO_2 plume migration and associated CO_2 trapping mechanisms for both a homogeneous and a heterogeneous reservoir. The effect of the amount of CO_2 injected was also investigated. Our results show that a strongly water-wet reservoir has the lowest CO_2 plume migration, with the lowest percentage of mobile CO_2, lowest percentage of CO_2 dissolved in water, and the highest percentage of residually trapped CO_2, independently of the injection rate of CO_2. This observation is valid for both the homogenous and heterogeneous cases but the magnitude of these observations varies both in time and in space between the two cases. Importantly, our results of the impact of wettability on residual trapping (same as capillary trapping) is in line with previous simulation studies (e.g. (Krevor et al., 2015; Juanes et al., 2006)) which concluded that mixed-wet rocks have a lower residual trapping capacity when compared to water-wet rocks. The CO_2 plume spreads more laterally in the heterogeneous reservoir while it has more vertical migration in the homogeneous reservoir. This is due to the fact that the CO_2 plume is prevented to move upwards driven by buoyancy forces because of the presence of lower permeability zones that decrease vertical CO_2 flow velocities. This leads to more mobile CO_2 and less solubility and residually trapped CO_2, consistent with literature data from previous simulation studies which investigated the effect of reservoir heterogeneity, without incorporating the effect of reservoir wettability, (i.e. (Doughty, 2010; Doughty and Myer, 2009; Hovorka et al., 2004; Obi and Blunt, 2006; Bryant et al., 2006; Flett et al., 2007; Zhou et al., 2010; Hesse and Woods, 2010; Han et al., 2010)).

In summary, we conclude that reservoir wettability has a critical impact on the CO_2 plume migration and trapping capacities, with water-wet reservoirs being preferable

CO_2 sinks. Furthermore, simulations, classically performed with homogeneous reservoir properties (e.g. porosity and permeability) may give correct general behaviour of the CO_2 plume in the subsurface (for example that the CO_2 plume vertical migration distance increases with increasing the CO_2 wettability (i.e. when the reservoir becomes more CO_2-wet) for both of homogeneous and heterogeneous models) but the magnitude of these observations may be inaccurate both in time and in space for the real reservoir, for which rock properties are heterogeneous. We conclude that both reservoir wettability and rock properties heterogeneities such as porosity and permeability need to be accurately reflected in CCS reservoir simulations in order to reliably assess CO_2 storage capacities and containment security.

Chapter 5 Influence of Injection Well Configuration and Rock Wettability on CO_2 Plume Behaviour and CO_2 Trapping Capacity in Heterogeneous Reservoirs

5.1 Introduction

The main reason of Earth's climate changes has been identified as due to greenhouse gas emission and carbon dioxide (CO_2) is the major component of this emission (Houghton et al., 2001; Zhang, 2016). The geological sequestration of CO_2 is considered one of the most effective methods to mitigate greenhouse gas emission by collecting it from power plants, refineries, and other industrial resources and injecting it into a deep underground geological formation (Pruess et al., 2003). The CO_2 can be stored underground in different trapping sites (i.e. unminable coal beds, saline aquifers, and depleted hydrocarbon reservoirs (Metz et al., 2005; Xie and Economides, 2009; Zhang et al., 2016b)). The injected CO_2 migrates upward towards the surface due to the density differences between the brine and CO_2 (Dai et al., 2014; Flett et al., 2007; Hassanzadeh et al., 2009). This vertical CO_2 migration (i.e. CO_2 leakage) is considered the most significant risk involved in CO_2 injection (Deel et al., 2007; Li and Liu, 2016). Such CO_2 leakage can result in various risks (i.e. humans and animals health risks, ecosystems damage, underground sources of drinking water contamination, and safety and environmental risks (Humez et al., 2013; Smyth et al., 2009; Kharaka et al., 2009; Kharaka et al., 2013; Oldenburg, 2008)). This CO_2 leakage risk can be reduced by four different trapping mechanisms. In the first one, a significant ratio of the CO_2 will be trapped in the high porosity and permeability zones of the target reservoir and prevented to move further by seal beds of the cap rocks or by low permeability reservoir layers: this trapping mechanism is called the structural trapping (Hesse et al., 2008; Naylor et al., 2011; Iglauer et al., 2015b; Gershenzon et al., 2015). The second trapping mechanism is related to the hysteresis of capillary pressure and relative permeability curves and is called residual trapping mechanism (Kumar et al., 2005; Pentland et al., 2011; Iglauer et al., 2011). The third trapping mechanism deals with the amount of CO_2 that will be trapped in the form of dissolved CO_2 in the aqueous phase: it is called solubility trapping (Lindeberg and Wessel-Berg,

1997; Spycher et al., 2003; Iglauer, 2011) and is highly dependent on the CO_2-water interface area (Metz et al., 2005; Kumar et al., 2005; Doughty, 2010). The fourth trapping mechanism, and that can take place over the longest time scale (could reach for thousands of years) is the mineral trapping where the CO_2 can be permanently trapped in the aquifer as carbonate minerals, as a result of CO_2/brine/mineral interactions (Bachu et al., 1994b; Xu et al., 2004; Gaus, 2010; Flett et al., 2007; Metz et al., 2005).

The storage efficiency of saline aquifers can be enhanced either by the accurate evaluation of the geological factors affecting the CO_2 storage process (e.g. caprock properties, porosity and permeability heterogeneity, permeability anisotropy (K_v/K_h)), or by optimising the CO_2 injection process (i.e. the type of injection scenario that includes continues CO_2 injection, water alternate gas (WAG) and, possibly, as we will explain in this study, injection well configuration (vertical or horizontal wells)). In this context, previous studies show that there are various geological factors that have been identified as significant in affecting the CO_2 storage processes including properties of cap rocks (Iglauer et al., 2015a) and vertical to horizontal permeability ratio (K_v/K_h) (Kumar et al., 2005; Basbug et al., 2005; Hassanzadeh et al., 2009). Furthermore, some initial and boundary conditions of the injection sites have an important impact on the safety of CO_2 storage mechanism which are: injection site temperature (Kumar et al., 2005; Bennion and Bachu, 2006; Ofori and Engler, 2011), and injection depth (Zeidouni et al., 2015). In addition, CO_2 injection scenario, such as using a WAG scenario compared to a traditional pure CO_2 injection, is also considered as an important factor that enhances the storage capacity by increasing the efficiency of residual (Juanes et al., 2006) and dissolution (Hassanzadeh et al., 2009; Leonenko and Keith, 2008; Vivek and Kumar, 2016)) CO_2 trappings. Moreover, the geological heterogeneity (i.e. porosity and permeability heterogeneity) had been shown previously as an important effecting factor on the CO_2 storage efficiency (Hovorka et al., 2004; Flett et al., 2007; Hesse and Woods, 2010; Green and Ennis-King, 2010; Song et al., 2014a; Gershenzon et al., 2015; Gershenzon et al., 2016). In addition, the top-surface morphology has been well investigated in literature as an affecting factor on CO_2 storage capacity (Nilsen et al., 2012; Shariatipour et al., 2016; Syversveen et al., 2012). Furthermore and importantly, reservoir wettability, from laboratory investigations (mm to cm scale), has been found to be an important rock parameter that has a significant impact on residual trapping (cp. Iglauer et al., 2011 and Andrew

et al., 2013 versus Chaudhary et al., 2013 and Rahman et al., 2016) and structural trapping (cp. Naylor et al., 2011 versus Iglauer et al., 2015). Furthermore, a recent 3D multi-phase flow simulation study by Al-Khdheeawi et al., (2017c) showed that wettability affects the CO_2 storage capacity. The impact of CO_2 injection well type has been well investigated for Enhanced Oil Recovery (EOR) and it has been found that the use of horizontal wells leads to improve the productivity and the injectivity because a horizontal well provide a larger flow area than a vertical well, for the same reservoir volume (Kossack et al., 1987; Reiss, 1987; Macdonald, 1988; Joshi, 1988; Joshi, 2003; Babu and Odeh, 1989; Hardman, 1989; Murphy, 1990; Economides et al., 1991; Thomas, 2008). However, the impact of injection well configuration on the CO_2 plume behaviour and on the efficiency of CO_2 trapping mechanisms has not been addressed in detail previously.

In this chapter, we have assessed how to reduce the CO_2 leakage risk by investigating the impact of the CO_2 injection well configuration (vertical versus horizontal) and rock wettability on the CO_2 plume behaviour, its vertical migration and on CO_2 storage capacities (mobile CO_2, residually trapped CO_2 and solubility trapped CO_2). For that purpose, we developed 3D multiphase flow simulations in a heterogeneous reservoir using five different rock wettability conditions and four injection well scenarios: one vertical well, two vertical wells, four vertical wells and one horizontal well.

5.2 Methodology

5.2.1 Numerical simulation models

Four sets of simulation models for a heterogeneous saline aquifer have been developed in this study in order to investigate the influence of the CO_2 injection well configuration and rock wettability on the CO_2 plume movements, shape and vertical migration and on the capacity of mobile and trapped CO_2. These four sets are performed in the same heterogeneous geological model: three use different vertical wells scenarios (i.e. one well (scenario V1), two wells (scenario V2), and 4 wells (scenario V4)) and the fourth one uses one horizontal well (scenario H). These four sets of simulation models have each five scenarios representing five different rock wettability conditions, which are: strongly water-wet, weakly water-wet, intermediate-

wet, weakly CO_2-wet and strongly CO_2-wet. The nonisothermal multicomponent multiphase flow simulator TOUGH2 (Pruess et al., 1999) with the tabular equation of state (EOS) ECO2M which has been used to simulate the thermodynamic and thermophysical properties of the H_2O-NaCl-CO_2 mixtures including the super- and sub-critical conditions, along with phase changes between liquid and gaseous CO_2 (Pruess, 2011). ECO2M EOS uses the Altunin's correlations (1975) to compute the molar volumes of CO_2 (i.e. supercritical CO_2, gaseous CO_2, and CO_2 dissolved in water as liquid). The model dimensions were 1600 m × 1200 m with a thickness of 700 m. The model has 37 × 33 × 80 cells (97680 cells in total). The pressure at the top of the aquifer (800 m) is 8 MPa and at the bottom of the aquifer (1500 m) is 15 MPa following the hydrostatic pressure gradient (10 MPa/km) (Dake, 2007), (Figure 5-1). The top of the reservoir was sealed by reducing the vertical to horizontal permeability ratio (k_v/k_h) from 0.1 in the storage reservoir to 10^{-4} in the top layer of the reservoir, so that a barrier prevents the CO_2 from leaking to the surface. Isothermal conditions have been applied for the reservoir model and temperature was set at 333 K. The volume of the outer boundary cells of the model has been multiplied by a large volume factor of 10^8 to simulate a constant pressure boundary condition (Mo et al., 2005; Nghiem et al., 2009). Initially the reservoir was fully saturated with brine (S_{wi} = 100%) with a salinity of 15% (by weight). The model characteristics, initial and boundary conditions described above are the same for all sets of simulations, dealing with horizontal and vertical configurations of the injection well. Generally, horizontal wells are different from vertical wells by the length of the well-reservoir contact area: horizontal wells provide a larger well-reservoir contact area (Joshi, 1991), which in our model example was around 600 m (Figure 5-2). Thus, we have used different scenarios of vertical well configurations (i.e. one, two, and four vertical injection wells) in order to increase the well-reservoir contact area in the vertical well configurations. These vertical wells have been distributed in the center of the model and separated by a distance of 300 m for the two vertical wells scenario and 200 m for the four vertical wells scenario. We used geometric scaling to implement the porosity and permeability data to the heterogeneous aquifer model (97680 cells) of the tenth SPE comparative solution project (1.122 million cells; Christie and Blunt 2001), which was initially built for the PUNQ project (Floris et al., 1999), (Figure 5-3). The geometric scaling has been used to distribute the porosity and permeability. The used 10th SPE comparative solution project is considered a highly complex geological

model consisting of two formations. The top 35 layers represent the Tarbert formation, which is a prograding near shore environment with a smooth variation in the permeability. The bottom 50 layers represent the Upper-Ness formation which, is a highly heterogeneous fluvial with many channel structures. The porosity was strongly correlated to the permeability during this very complex geological model (Christie and Blunt 2001).

CO_2 was injected into the reservoir at a constant injection rate of 1,000,000 tons CO_2/yr for both the horizontal and vertical modelled cases; this rate is similar to the maximum CO_2 injection rate that was used in the Sleipner CO_2 storage project in Norway (Leung et al., 2014; Torp and Gale, 2004), and in the Quest CCS project in Canada (Bourne et al., 2014). CO_2 was injected at a depth of 1373 m and at the center of the model (Y = 600), for both the horizontal and vertical wells and for all wettability conditions; this injection lasted a period of 2 years (i.e. a total of 2 Mton of CO_2 are injected). This 2 years injection period was followed by a 200 years shut-off injection period to simulate the storage period in the reservoir. The plume behaviour was simulated during the storage period for all injection well configurations and for the 5 wettability conditions. In addition, the amount of mobile CO_2, residually trapped CO_2 and solubility trapped CO_2 were computed as a function of time for both horizontal and vertical injection wells configuration and for all the wettability scenarios. The results obtained from the horizontal well and vertical well models were compared in order to investigate the impact of injection well configuration and rock wettability on CO_2 storage efficiency in a heterogeneous reservoir.

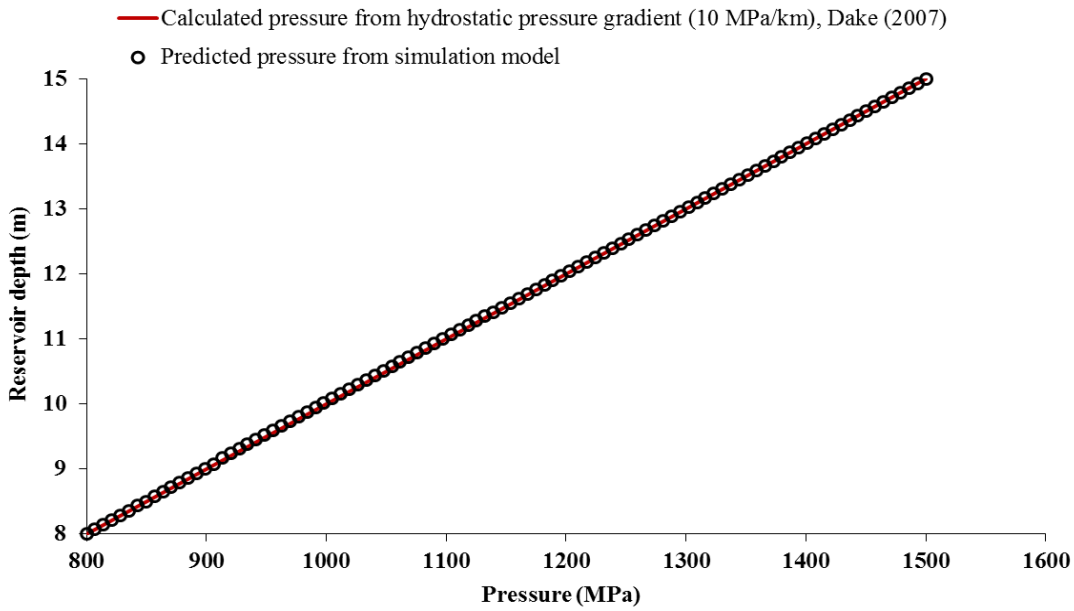

Figure 5-1 Representation of model validation by comparing the predicted and calculated initial reservoir pressure.

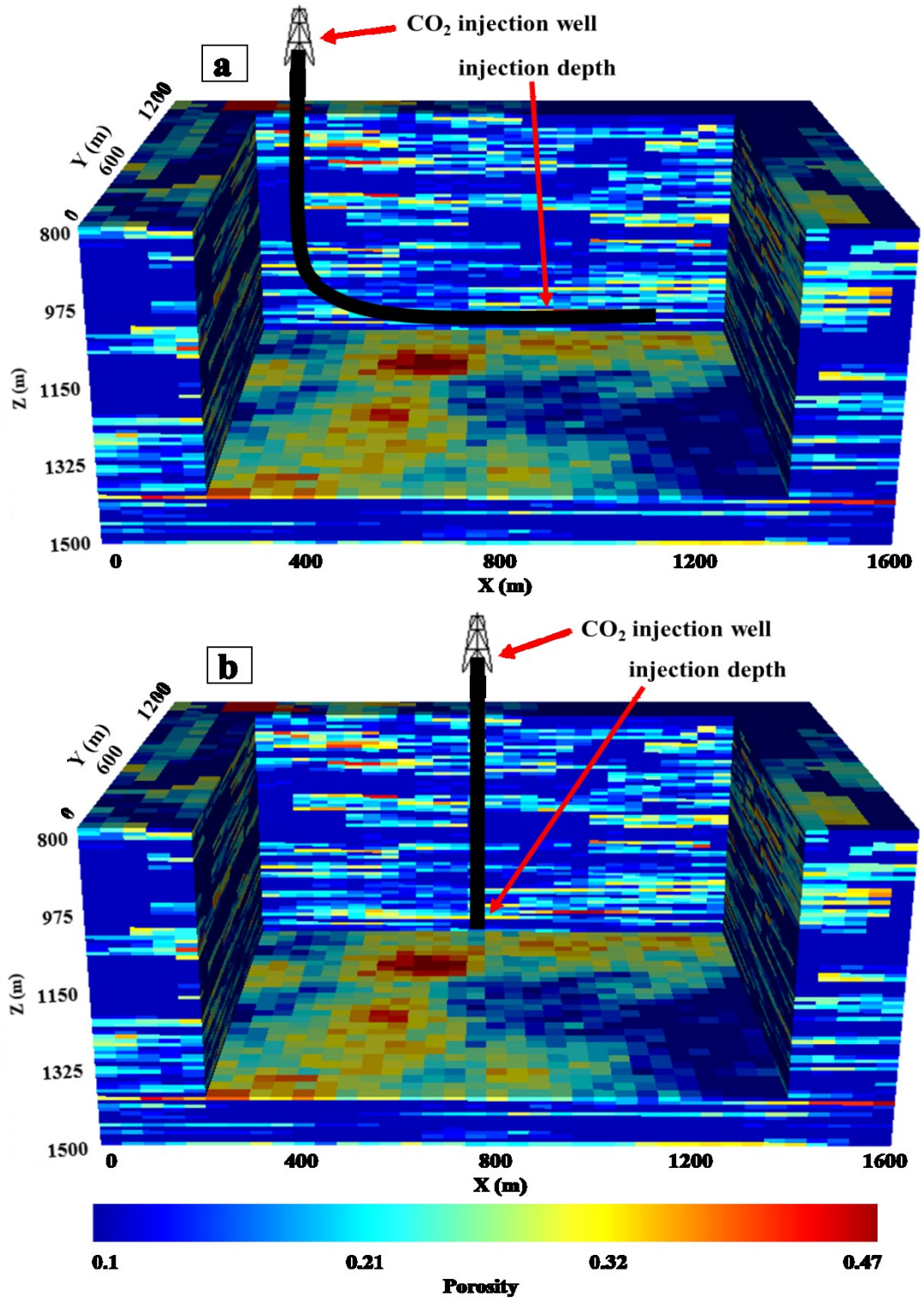

Figure 5-2 Representation of the 3-D model showing injection wells locations with porosity distribution for the reservoir and model dimensions: A) horizontal well; B) single vertical well.

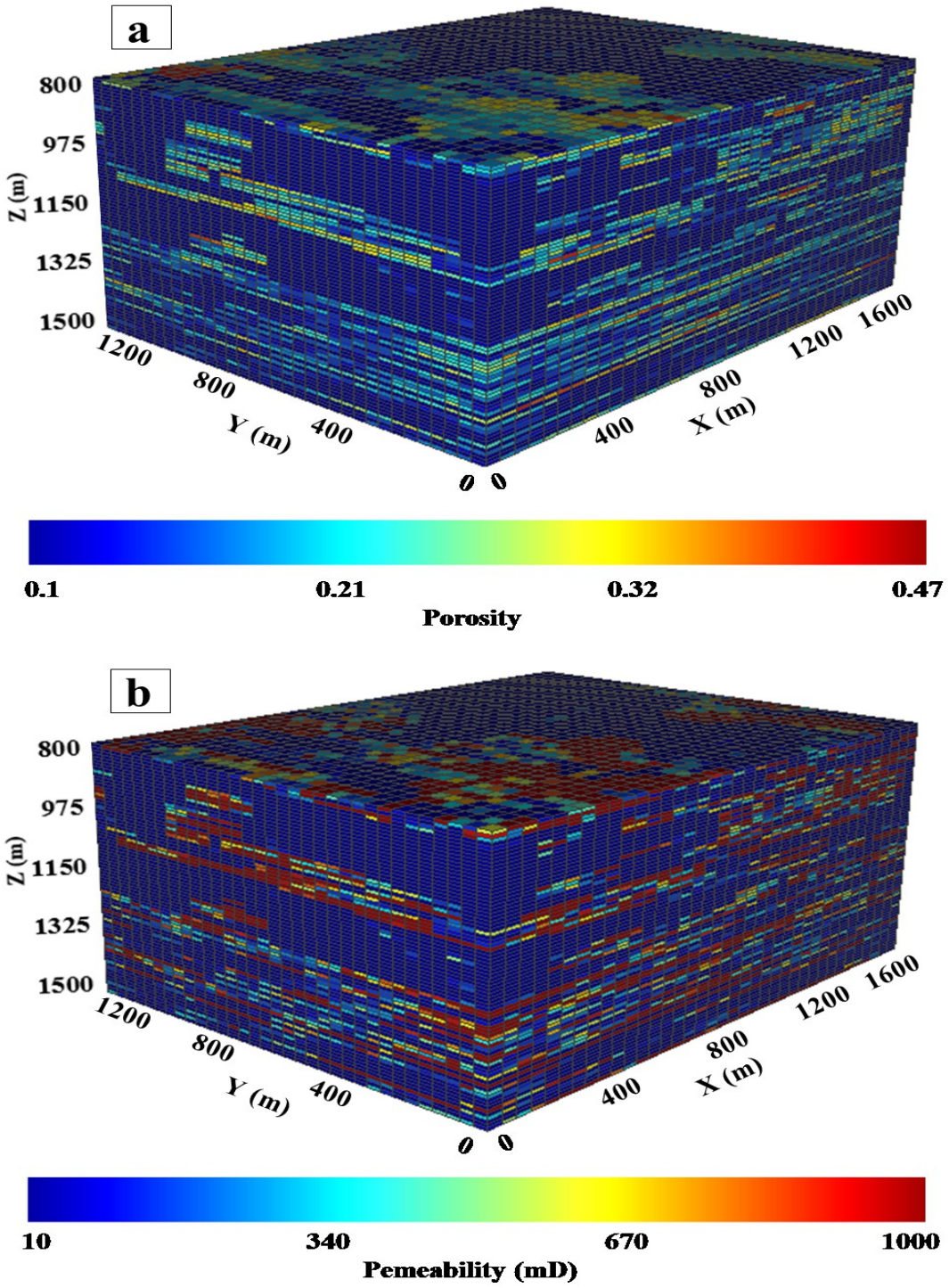

Figure 5-3 Representation of the 3-D model showing the reservoir porosity and permeability heterogeneity with model dimensions: A) porosity distribution; B) permeability distribution.

5.2.2 Simulation of different rock wettability scenarios

We have used 5 different rock wettability conditions for all well configuration models (i.e. vertical wells and horizontal well models): strongly water-wet, weakly water-wet, intermediate-wet, weakly CO_2-wet and strongly CO_2-wet. These different wettabilities have been simulated by using five different pairs of relative permeability and capillary curves for all models of horizontal and vertical injection wells, as previously performed in Al-Khdheeawi et al., (2017). McCaffery and Bennison's (1974) relative permeability curves have been used with an accurate modification according to Craig's rules of thumb (Craig, 1993) and comparison with previous studies which showed the effect of wettability on the relative permeability curves (i.e. Owens and Archer, 1971; Heiba et al. 1983; Anderson, 1987b; Krevor et al., 2012; Levine et al., 2014) to fit the various wettability conditions (Figure 5-4). These adjusted curves have been implemented into the developed reservoir simulation models by using the Van Genuchten-Mualem model (Van Genuchten, 1980; Mualem, 1976) summarized by the following set of correlations:

$$k_{rw} = \sqrt{S^*}\left\{1-\left(1-[S^*]^{1/\lambda}\right)^{\lambda}\right\}^2 \quad \text{if} \quad S_w < S_{ws} \tag{5.1}$$

$$k_{rw} = 1 \quad \text{if} \quad S_w \geq S_{ws} \tag{5.2}$$

$$k_{rg} = 1 - k_{rw} \quad \text{if} \quad S_{gr} = 0 \tag{5.3}$$

$$k_{rg} = \left(1-\hat{S}\right)^2\left(1-\hat{S}^2\right) \quad \text{if} \quad S_{gr} > 0 \tag{5.4}$$

$$S^* = (S_w - S_{wr})/(S_{ws} - S_{wr}),$$
$$\hat{S} = (S_w - S_{wr})/(1 - S_{wr} - S_{gr}) \tag{5.5}$$

where:

k_{rg} = gas relative permeability, k_{rw} = water relative permeability,

S_{gr} = residual saturation for gas, S_w = water saturation,

S_{ws} = maximum water saturation (= 1), S_{wr} = residual saturation for water,

λ = pore size distribution index (fitting parameter).

In addition, Pini's et al., (2012, 2013) capillary pressure curves for strongly water-wet Berea sandstone have been used and adjusted for the other wettability conditions by using the criteria of (Anderson, 1987a; Batycky et al., 1981; Heiba et al., 1983; Melrose, 1965; Morrow, 1976) that explains the impact of wettability on capillary

pressure curves (Figure 5-5). These adjusted curves have been implemented into the simulation models by using Van Genuchten-Mualem capillary pressure model (Van Genuchten, 1980; Mualem, 1976) which can be summarized by the following correlations:

$$\left(P_{cap}\right) = P_0 \left([S^*]^{-1/\lambda} - 1\right)^{1-\lambda} \quad (5.6)$$

with the restriction $0 \leq P_{cap} \leq P_{max}$

and, $S^* = (S_w - S_{wr})/(S_{ws} - S_{wr})$ (5.7)

where:

P_{cap} = rock capillary pressure (Pa), P_0 = pressure scaling parameter (Pa),

S_{ws} = maximum water saturation, S_{wr} = residual saturation for water,

λ = pore size distribution index.

Importantly, the impact of porosity and permeability heterogeneity, for each grid block, on the capillary pressure has been implemented by using the scaling Leverett J-function (Leverett, 1941):

$$J(S_w) = \frac{P_c}{\sigma \cos \Theta} \sqrt{\frac{k}{\phi}} \quad (5.8)$$

where:

s_w = water saturation, P_c = capillary pressure (Pa), k = permeability (m^2, mD),

ϕ = porosity, σ = surface tension (N/m), Θ = contact angle (^{o}).

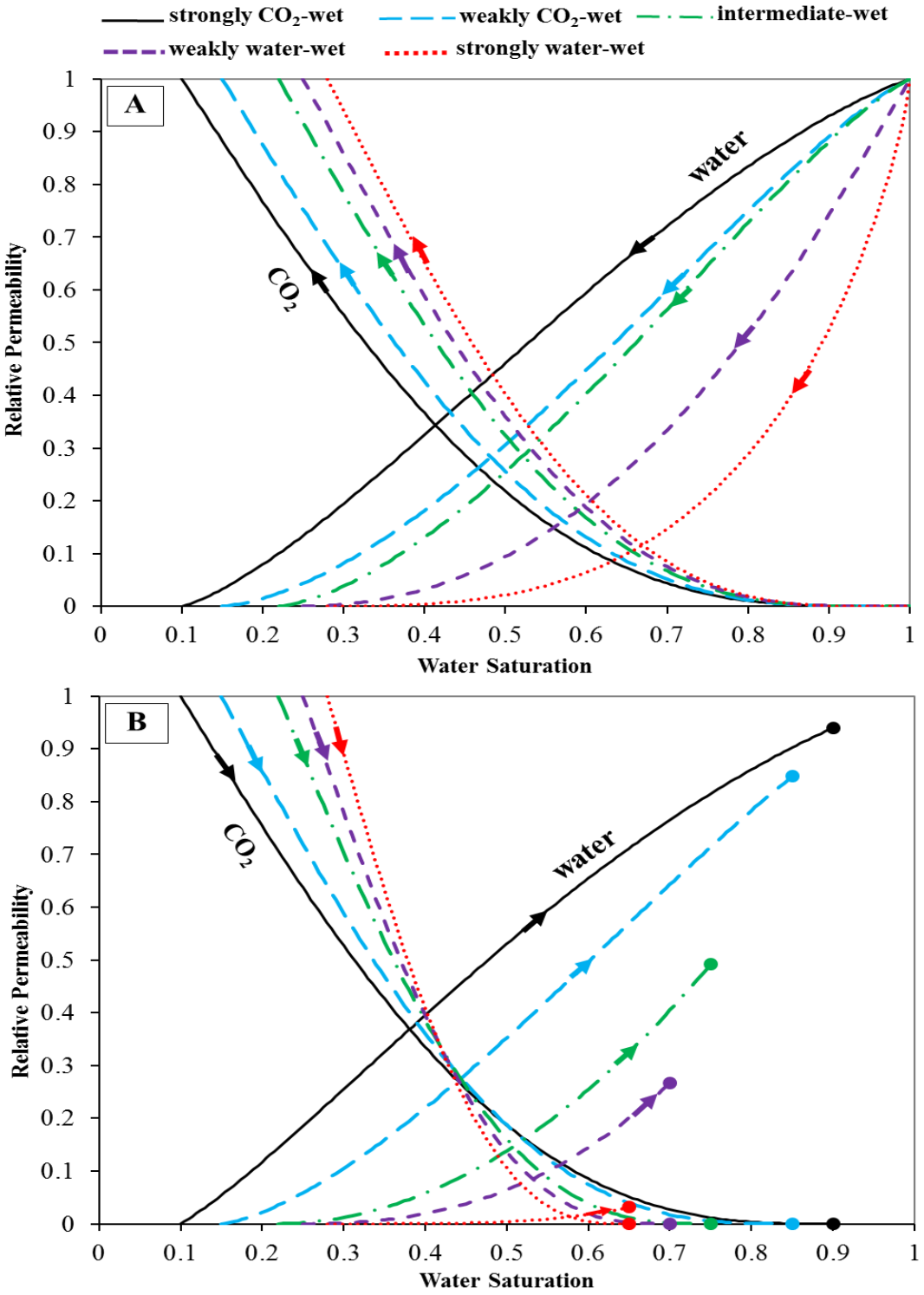

Figure 5-4 Relative permeability curves used for both injection well configurations (vertical and horizontal well) for 5 different rock wettability scenarios: A) CO_2 injection process (drainage); B) CO_2 storage process (imbibition).

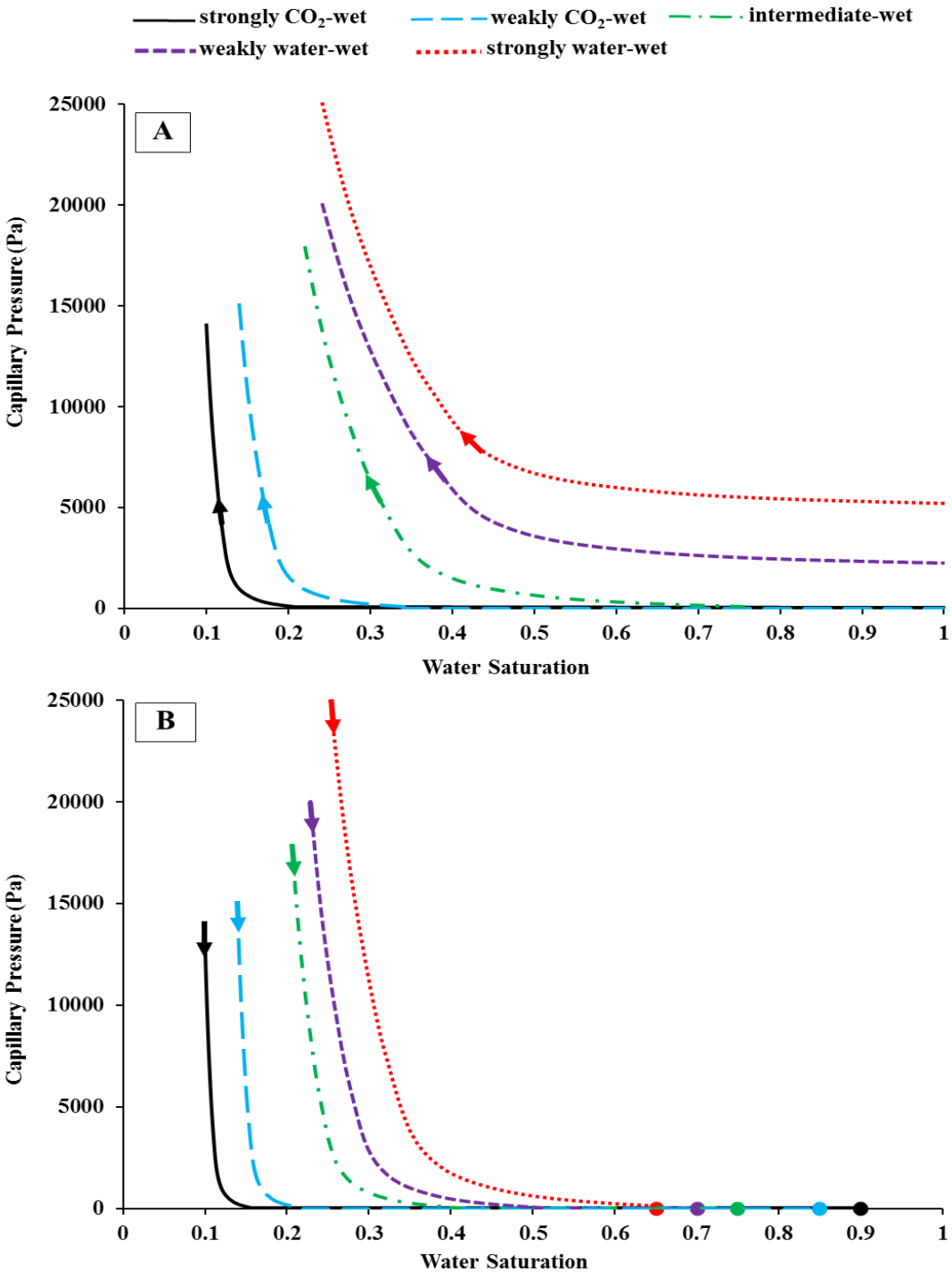

Figure 5-5 Capillary pressure curves used for both injection well configurations (vertical and horizontal well) models for 5 different rock wettability scenarios: A) CO_2 injection process (drainage); B) CO_2 storage process (imbibition).

Initially, at the beginning of the injection period, the reservoir is fully saturated with water (S_w =100%, S_g =0) so at the start of the CO_2 injection process k_{rw} = 1 and k_{rg} = 0 (Figure 5-4A, top right). Then during the progress of the CO_2 injection, k_{rw} decreases gradually until it reaches its minimum value k_{rw} = 0 at the residual water saturation (S_{wr}) (as represented by the arrows on the 5 curves related to water relative permeability, Figure 5-4A). Simultaneously, k_{rg} increases from zero at the residual gas saturation (S_{gr}) to one at the residual water saturation (S_{wr}). For the storage period, (Figure 5-4B), k_{rg} decreases from one at S_{wr} to zero at S_{gr} and k_{rw} increases from zero at S_{gr} until it reaches its maximum value (according to the specified wettability condition at S_{wr} Craig (1993)). Here it is important to mention that both S_{wr} and S_{gr} are a function of wettability and that strongly water-wet rocks have the highest S_{wr} and S_{gr} values (0.26 and 0.35, respectively), while strongly CO_2-wet rocks have the lowest S_{wr} and S_{gr} values (0.1 and 0.1, respectively) (Anderson 1987a, b; Craig, 1993; Iglauer et al., 2011; Pentland et al., 2011; Krevor et al., 2012; Chaudhary et al., 2013; Akbarabadi and Piri, 2013; Ruprecht et al., 2014; Rahman et al., 2016; Al-Menhali et al., 2016; Al-Khdheeawi et al., 2017). Furthermore, the water saturation (S_w) at which k_{rw} and k_{rg} are equal should be less than 0.5 in the water-wet rock curves, and more than 0.5 in the CO_2-wet rock curves, according to Craig (1993). For capillary pressures (Figure 5-5), the capillary pressure curves also start from the lowest capillary pressure values at the beginning of the injection period until reaching the maximum capillary pressure values, for each wettability case, at S_{wr} (Figure 5-5A). Then, during the storage period, capillary pressure values reduces again until they reache zero at S_{gr}, for all wettability conditions (Figure 5-5B) (Anderson, 1987a; Pentland et al., 2011; Pini et al., 2012, 2013; Krevor et al., 2015, 2016).

5.3 Results and discussion

5.3.1 Influence of CO_2 injection well configuration and rock wettability on CO_2 plume behaviour

By comparing the shape of the plume, at a given time after the end of the injection period and for a given rock wettability, for the three vertical well scenarios (i.e. one well, two wells, and 4 wells) (Figure 5-6 to Figure 5-8), respectively, and for the horizontal one (Figure 5-9), it is clear that the injection well configuration and rock

wettability have a significant impact on the CO_2 plume behaviour (i.e. its shape, its vertical and horizontal migration). For all rocks wettability scenarios, the CO_2 plume for all vertical well configurations (scenarios V1, V2 and V4), reached a shallower depth (i.e. closer to the top of the reservoir) than for the horizontal well configuration (scenario H); also, for all injection well configurations, the more CO_2-wet rock has the shallower CO_2 plume depth than the more water-wet rock, as reported in Table 5-1 and Figure 5-10 (e.g. V1 = 1217 m, V2 = 1221 m, V4 = 1226 m and H = 1246 m for the strongly water-wet reservoir, while scenarios V1, V2, and V3 = 800 m (i.e. the top depth of the model) and H = 955 m for the strongly CO_2-wet reservoir, at the end of the storage period of 200 years). Moreover, the total migration distance of the CO_2 plume (the distance between the lowest depth and the highest depth reached by the CO_2 plume) in all vertical well models was higher than in the horizontal well model, for all different rock wettability reservoir cases; also, for all injection well configurations, the total CO_2 plume migration distance is higher in the more CO_2-wet rock than in the more water-wet rock, as reported in Table 5-1 and Figure 5-11 (e.g. V1 = 156 m, V2 = 152 m, V4 = 147 m and H = 127 m for the strongly water-wet, while scenarios V1, V2, and V3 = 573 m and H = 418 m for the strongly CO_2-wet, at the end of storage period). Importantly, the CO_2 plume has a higher vertical migration distance in the vertical well configurations than in the horizontal well configuration, because the horizontal well has a larger contact area than the vertical well. Thus, for the horizontal well, the CO_2 lateral movement will be higher than its vertical migration, which is beneficial for controlling CO_2 upward migration. Furthermore, CO_2 plume migration is highly affected by the residual gas saturation (S_{gr}) and increasing S_{gr} leads to a reduction in vertical CO_2 migration (Metz et al., 2005; Doughty, 2010). S_{gr} is in turn a function of reservoir wettability (i.e. S_{gr} reduced from 0.35 in strongly water-wet rocks to 0.1 in strongly CO_2-wet rocks, Figure 5-4) (Anderson 1987a, b; Craig, 1993; Iglauer et al., 2011; Pentland et al., 2011; Krevor et al., 2012; Chaudhary et al., 2013; Akbarabadi and Piri, 2013; Ruprecht et al., 2014; Rahman et al., 2016; Al-Menhali et al., 2016; Al-Khdheeawi et al., 2017).

In summary, the results demonstrate that injection well configuration and rock wettability have a significant impact on the CO_2 plume behaviour. Our results indicate that the use of horizontal well technology, for all rock wettability conditions, or the

more water-wet reservoirs, for both well configurations, will reduce the vertical CO_2 plume migration, which implies an improved CO_2 storage process.

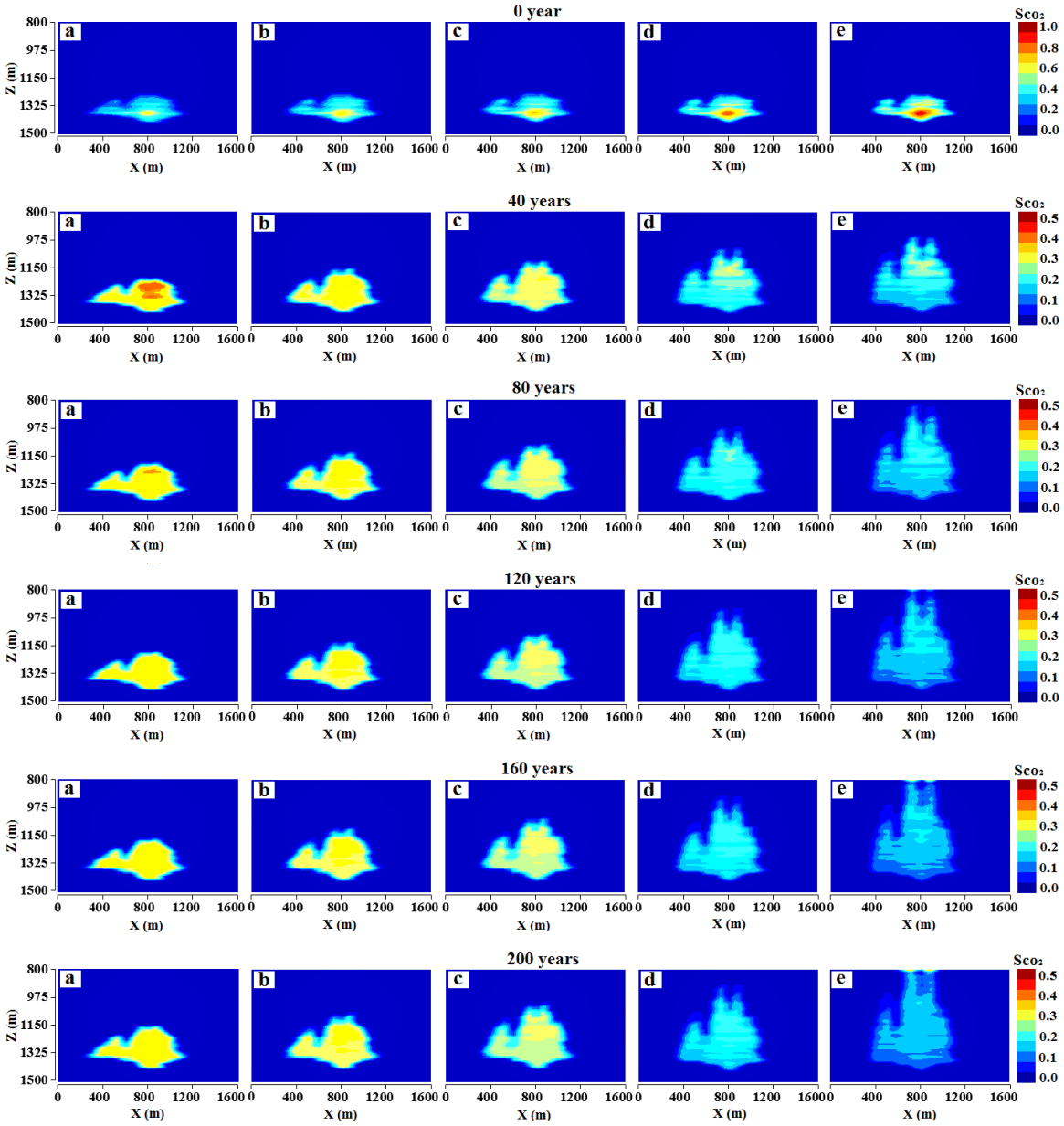

Figure 5-6 2D vertical cross-sections through the centre of the storage reservoir. CO_2 is injected at a depth of (1373 m) through a one vertical well. The CO_2 plume shape and height in the reservoir are shown for 5 different rock wettability types: a) strongly water-wet; b) weakly water-wet; c) intermediate-wet; d) weakly CO_2-wet; e) strongly CO_2-wet. 2 Mt of CO_2 was injected in total.

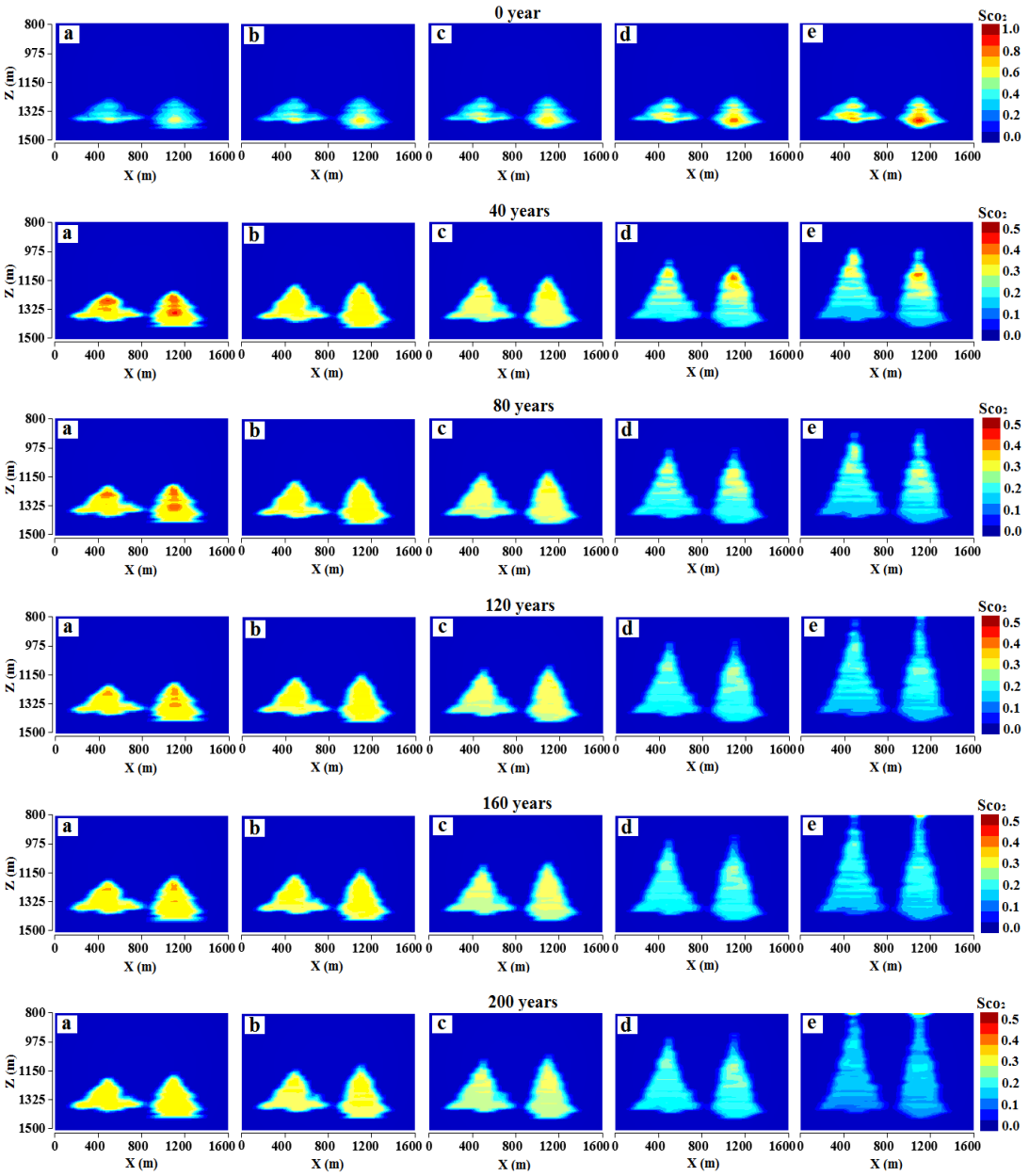

Figure 5-7 2D vertical cross-sections through the centre of the storage reservoir. CO_2 is injected at a depth of (1373 m) through the a two vertical wells. The CO_2 plume shape and height in the reservoir are shown for 5 different rock wettability types: a) strongly water-wet; b) weakly water-wet; c) intermediate-wet; d) weakly CO_2-wet; e) strongly CO_2-wet. 2 Mt of CO_2 was injected in total.

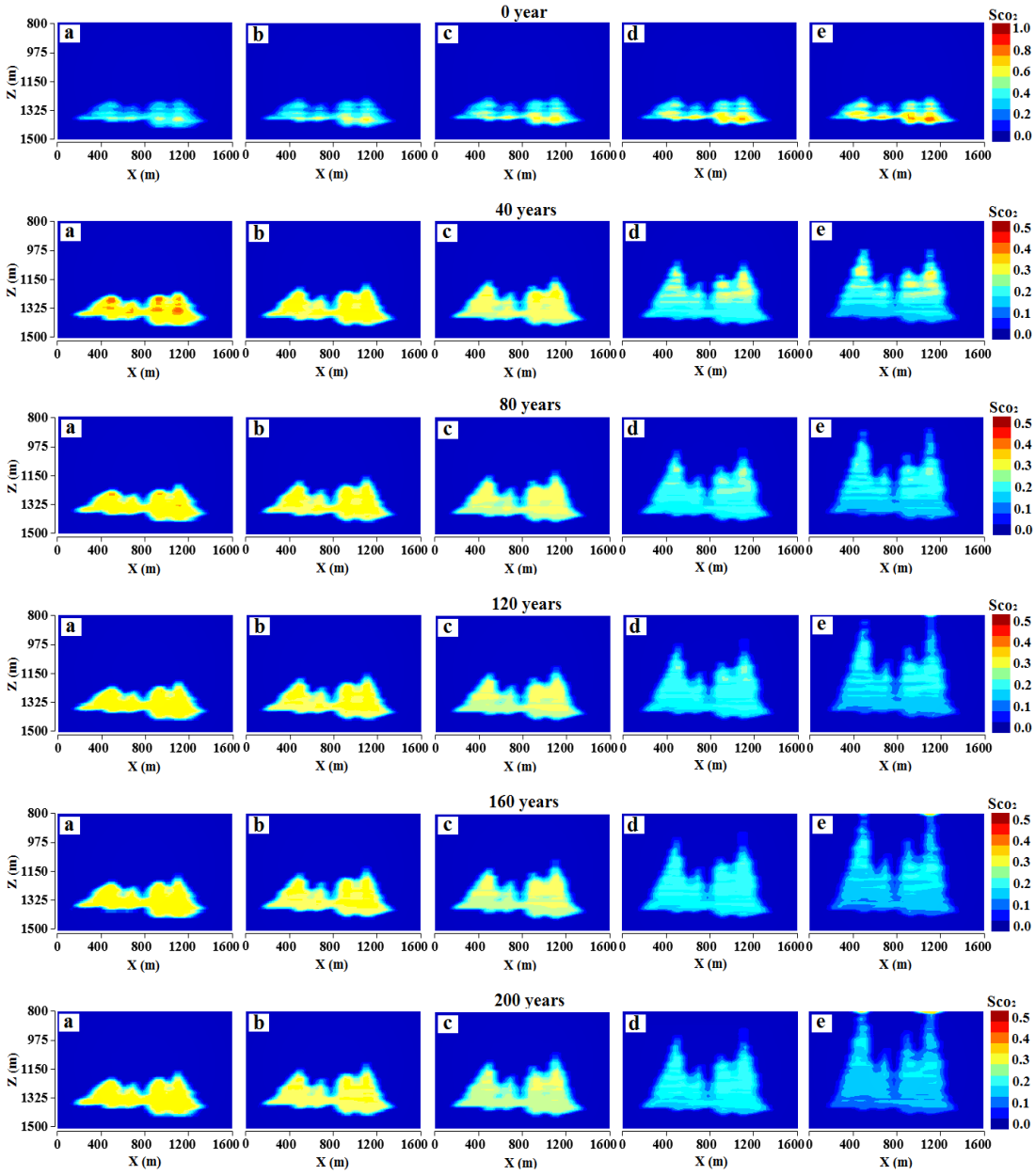

Figure 5-8 2D vertical cross-sections through the centre of the storage reservoir. CO_2 is injected at a depth of (1373 m) through a four vertical wells. The CO_2 plume shape and height in the reservoir are shown for 5 different rock wettability types: a) strongly water-wet; b) weakly water-wet; c) intermediate-wet; d) weakly CO_2-wet; e) strongly CO_2-wet. 2 Mt of CO_2 was injected in total.

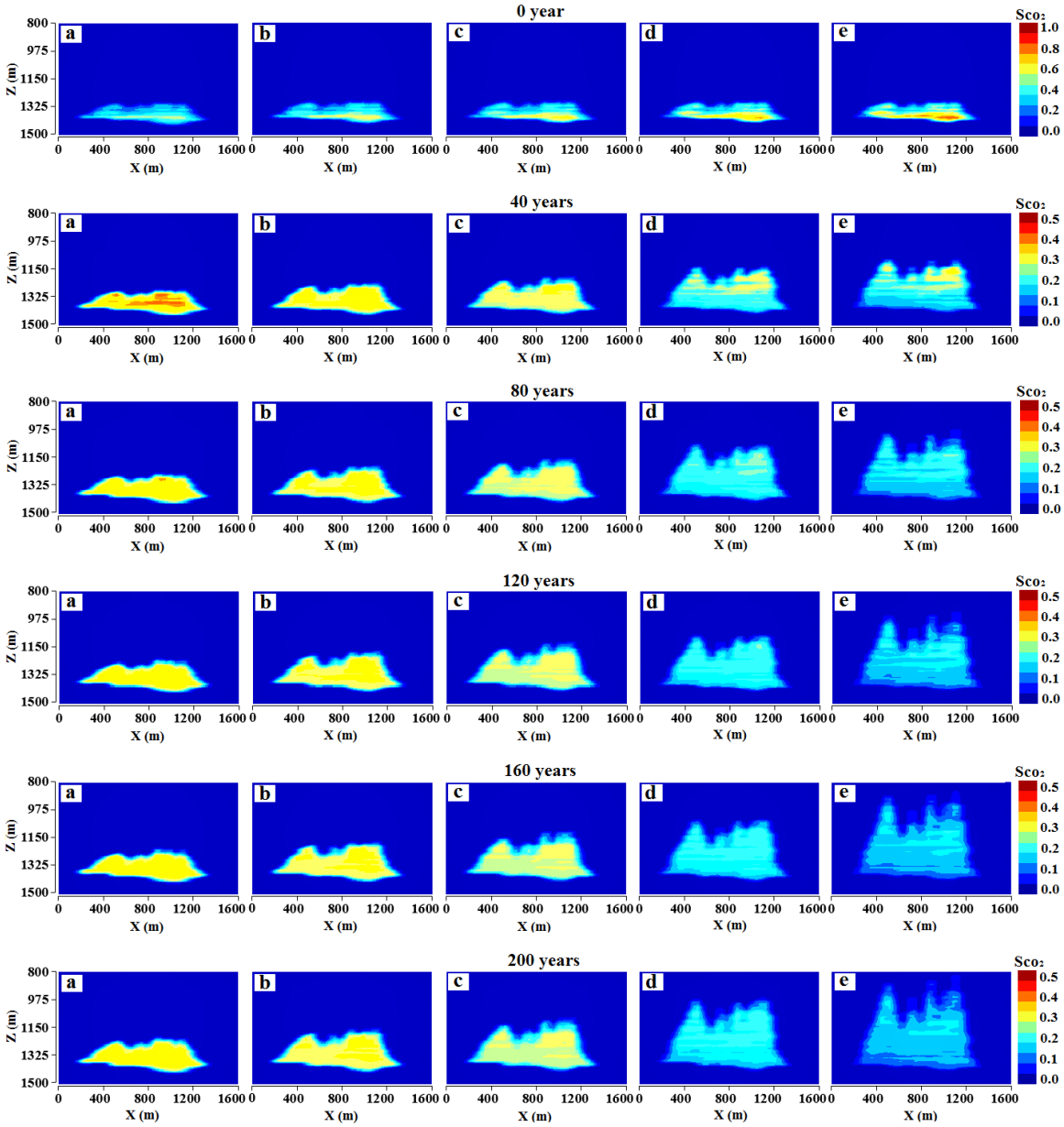

Figure 5-9 2D vertical cross-sections through the centre of the storage reservoir. CO_2 is injected at a depth of (1373 m) through a horizontal well. The CO_2 plume shape and height in the reservoir are shown for 5 different rock wettability types: a) strongly water-wet; b) weakly water-wet; c) intermediate-wet; d) weakly CO_2-wet; e) strongly CO_2- wet. 2 Mt of CO_2 was injected in total.

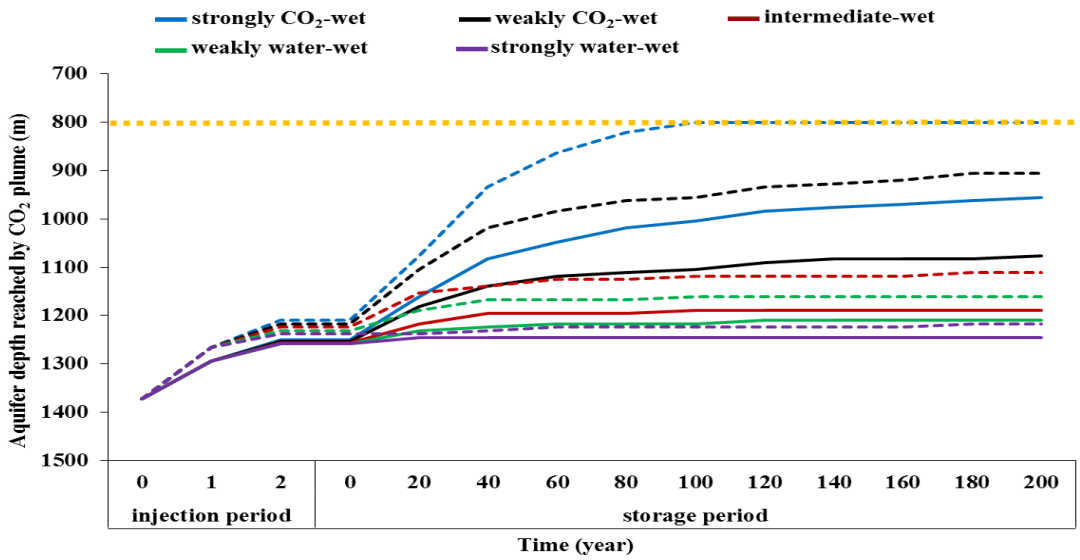

Figure 5-10 Aquifer (reservoir) depth reached by CO_2 plume as a function of injection well configuration (dashed line represents vertical well (i.e. one vertical well) and solid line represents horizontal well) and injection and storage time for different rock wettability reservoirs. The square dot yellow (horizontal) line represents the caprock seal depth at the top of the reservoir. For the two and four vertical well scenarios the CO_2 plume depths reached are very similar. Thus, here we have presented only the one vertical well scenario for simplicity.

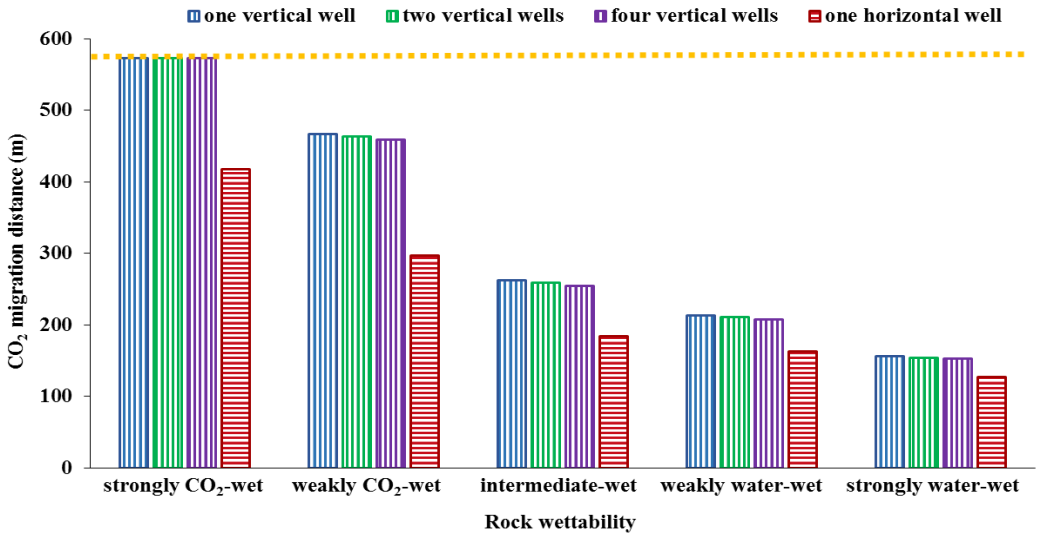

Figure 5-11 CO_2 plume migration distance as a function of injection well configuration and rock wettability at the end of storage period (200 years). The dashed yellow (horizontal) line represents the maximum possible migration distance (i.e. CO_2 reaches the caprock seal at the top of the reservoir).

Table 5-1 Depth[a] reached and vertical migration distance of CO_2 plume after the end of the storage period (200 years) for the vertical wells and horizontal well in different rock wettability scenarios

CO_2 plume depth and migration distance	well configuration	strongly CO_2-wet[b]	weakly CO_2-wet	Intermediate-wet	weakly water-wet	strongly water-wet
Depth reached by CO_2 plume (m)	one vertical well	800	906	1111	1160	1217
	two vertical wells	800	915	1120	1167	1221
	four vertical wells	800	927	1132	1175	1226
	one horizontal well	955	1076	1189	1210	1246
Vertical CO_2 plume migration distance (m)	one vertical well	573	467	262	213	156
	two vertical wells	573	458	253	206	152
	four vertical wells	573	446	241	198	147
	one horizontal well	418	297	184	163	127
Percentage of vertical migration distance to the maximum possible migration distance (%)	one vertical well	100	82	46	37	27
	two vertical wells	100	81	45	37	27
	four vertical wells	100	80	45	36	27
	one horizontal well	73	52	32	28	22

[a]CO_2 injection depth is at (1373 m).

[b]In the scenario of the vertical well in the strongly CO_2-wet rock, CO_2 plume reached the caprock seal at the top of the reservoir (800 m) after only 100 years of storage period; CO_2 then flowed laterally beneath the caprock.

5.3.2 Influence of CO_2 injection well configuration and rock wettability on trapping mechanisms

For each wettability case, Figure 5-12 to Figure 5-14 and Table 5-2 report and compare the amount of mobile, solubility trapped and residually trapped CO_2, for each of the two configurations of the wells. Firstly, the results show that use of vertical wells will lead to a greater amount of free CO_2 (mobile CO_2) at the end of the storage period than that when a horizontal well was used, for all rock wettability conditions; also the results show that the more CO_2-wet rock has more CO_2 mobility, for both vertical and horizontal well configurations (e.g., the total amount of mobile CO_2 at the end of the storage period (after 200 years), V1 = 129 kton, V2 = 127 kton, V4 = 126 kton, and H = 94 kton for the strongly water-wet reservoir, while V1 = 809 kton, V2 = 801 kton, V4 = 791 kton, and H = 724 kton for the strongly CO_2-wet reservoir (Figure 5-12)). In addition, the results demonstrate that the use of vertical wells will result in more solubility trapped CO_2 than that obtained with a horizontal injection well; also the more CO_2-wet rock has more solubility trapped CO_2 than that in the more water-wet rock (e.g., the total amount of solubility trapped CO_2 at the end of the storage period (after 200 years), V1 = 271 kton, V2 = 269 kton, V4 = 268 kton, and H = 253 kton for the strongly water-wet reservoir, while V1 = 558 kton, V2 = 556 kton, V4 = 555 kton, and H = 513 kton for the strongly CO_2-wet reservoir (Figure 5-13)). Importantly, the amount of trapped CO_2 increases with increasing plume migration as a result of increasing the brine-CO_2 contact area (Doughty, 2010). Thus, both vertical wells configurations combined with the more CO_2-wet rocks have the highest CO_2 plume migration distance, and consequently higher solubility trapping capacity.

Finally, the results show that the use of horizontal well is associated with more residually trapped CO_2 than in the case of the vertical injection wells, for all wettability conditions; also the results show that the residually trapped CO_2 reduces with increasing the CO_2 wettability of the rock, for both of the injection well configurations (e.g., the total amount of residually trapped CO_2 at the end of the storage period (after 200 years), V1 = 1600 kton, V2 = 1604 kton, V4 = 1606 kton, and H = 1653 kton for the strongly water-wet revervoir, while V1 = 633 kton, V2 = 643 kton, V4 = 654 kton, and H = 763 kton for the strongly CO_2-wet reservoir; Figure 5-14). Importantly, residual trapping is a function of S_{gr} and increasing S_{gr} leads to improve the residual

trapping. Recall, strongly water-wet rocks have the highest S_{gr} value (0.35), while strongly CO_2-wet rocks have the lowest S_{gr} value (0.1) (Anderson 1987a, b; Craig, 1993; Iglauer et al., 2011; Andrew et al., 2013; Chaudhary et al., 2013; Rahman et al., 2016), FiguresFigure 5-4 andFigure 5-5. Thus, residual trapping increases with increasing water-wettability. These results, related to the influence of wettability on residual trapping of CO_2, are in line with previous experimental studies (cp. Iglauer et al., 2011 and Andrew et al., 2013 versus Chaudhary et al., 2013 and Rahman et al., 2016). In summary, our simulation results conclude that the injection well configuration and rock wettability has an important impact on the amounts of mobile and trapped CO_2 and the use of horizontal well and the more water-wet rock will enhance the CO_2 storage process.

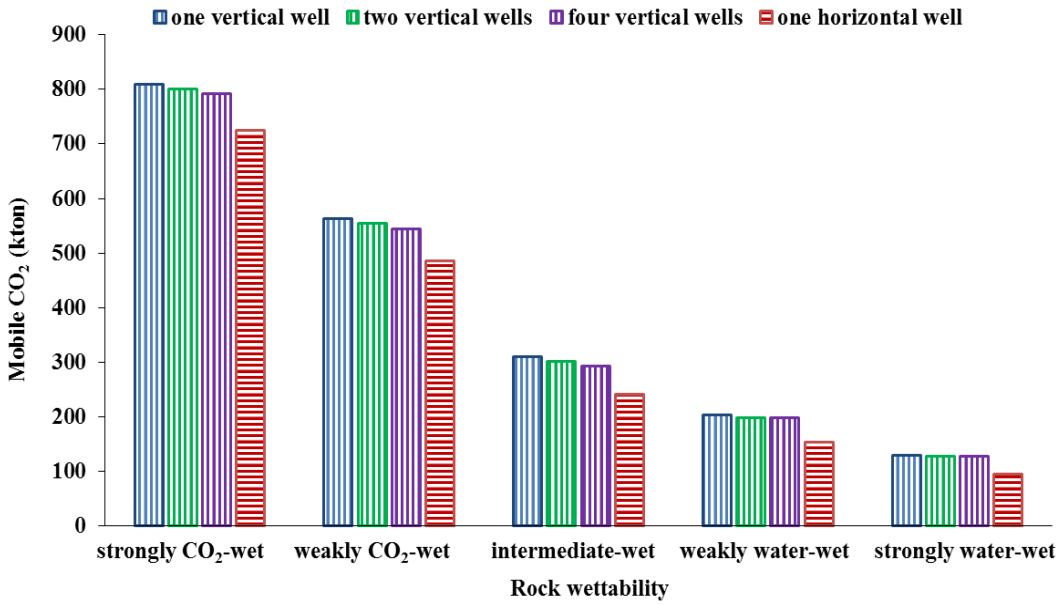

Figure 5-12 Total amount of mobile CO_2 (in thousand tons) as a function of injection well configuration and rock wettability at the end of storage period (200 years). 2 Mt of CO_2 was injected in total.

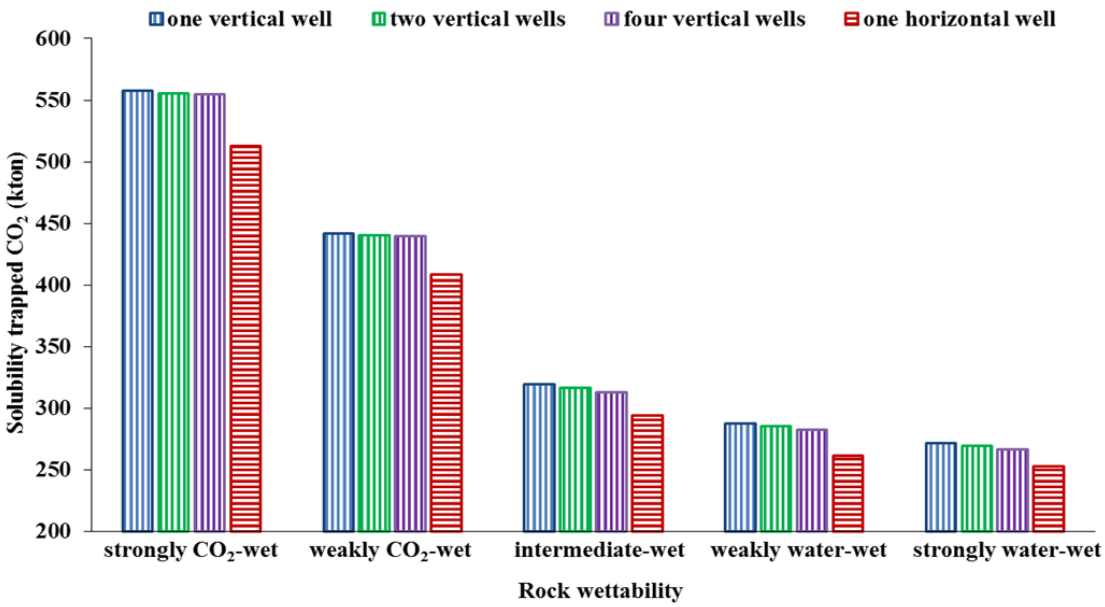

Figure 5-13 Total amount of solubility trapped CO_2 (in thousand tons) as a function of injection well configuration and rock wettability at the end of storage period (200 years). 2 Mt of CO_2 was injected in total.

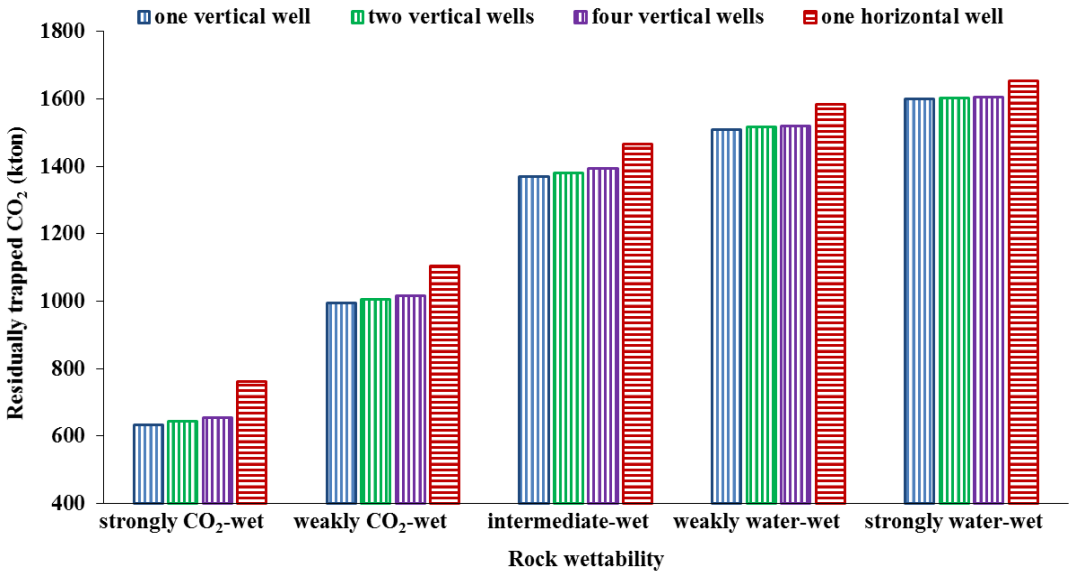

Figure 5-14 Total amount of residually trapped CO_2 (in thousand tons) as a function of injection well configuration and rock wettability at the end of storage period (200 years). 2 Mt of CO_2 was injected in total.

Table 5-2 CO_2 mobility and capacity of trapping mechanisms for horizontal and vertical wells in different rock wettability scenarios at the end of storage period (200 years). For all wettability scenarios and in all injection well configurations (vertical and horizontal) 2 Mt of CO_2 was injected in total

Amount and percentage of mobile and trapped CO_2		well configuration	strongly CO_2-wet	weakly CO_2-wet	Intermediate-wet	weakly water-wet	strongly water-wet
Total amount of mobile and trapped CO_2 (Thousand tons)	Mobile	one vertical	809	563	310	203	129
		two vertical	801	554	301	199	127
		four vertical	791	543	293	198	127
		one horizontal	724	486	240	153	94
	Solubility trapped	one vertical	558	441	320	287	271
		two vertical	556	441	317	285	269
		four vertical	555	440	312	282	266
		one horizontal	513	408	294	262	253
	Residually trapped	one vertical	633	996	1370	1510	1600
		two vertical	643	1005	1382	1516	1604
		four vertical	654	1017	1395	1520	1607
		one horizontal	763	1106	1466	1585	1653
Percentage of mobile and trapped CO_2 to the total injected CO_2 (%)	Mobile	one vertical	40	28	15	10	6
		two vertical	40	28	15	10	6
		four vertical	40	27	15	10	6
		one horizontal	36	24	12	8	5
	Solubility trapped	one vertical	28	22	16	14	14
		two vertical	28	22	16	14	13
		four vertical	28	22	16	14	13
		one horizontal	26	21	15	13	12
	Residually trapped	one vertical	32	50	69	76	80
		two vertical	32	50	69	76	81
		four vertical	32	51	69	76	81
		one horizontal	38	55	73	79	83

5.4 Conclusions

CO_2 capture and storage (CCS) is highly affected by various factors (e.g. caprock properties, permeability anisotropy, aquifer temperature, aquifer depth, CO_2 injection scenarios, porosity and permeability heterogeneity (cp. the reference for each factor in section 5.1 of this chapter). Other possible affecting factor, which has not received a sufficient attention, is the injection well configuration. Even though the use of horizontal well type has been addressed as an important factor to enhance the oil productivity from the oil reservoirs (Kossack et al., 1987; Reiss, 1987; Macdonald, 1988; Joshi, 1988, 2003; Babu and Odeh, 1989; Hardman, 1989; Murphy, 1990; Economides et al., 1991; Thomas, 2008), its impact on the efficiency of CO_2 storage process in saline aquifers has not been addressed.

Thus, for the first time, we have developed two sets of 3D heterogeneous reservoir simulation models to demonstrate the impact of the injection well configuration, horizontal versus three different vertical injection well scenarios (i.e. one, two and four vertical wells), on the CO_2 plume behaviour and CO_2 storage capacities for a wide range of rock wettabilities.

Our simulation results clearly indicate that, at the end of the 200 years storage period, the CO_2 injection well configuration has a significant impact on the CO_2 plume behaviour and storage capacities. A horizontal well, for all wettability conditions, reduced the CO_2 plume vertical mobility and the amount of the solubility trapped CO_2, while it increased the amount of residually trapped CO_2. Furthermore, our simulation results show that water-wet rocks improved the CO_2 storage capacities for both well configurations. Importantly, our results about the impact of rock wettability on the CO_2 storage capacities are consistent with our previous simulation study in a homogeneous reservoir (Al-Khdheeawi et al., 2017) and previous experimental studies (cp. Iglauer et al., 2011; Andrew et al., 2013; Chaudhary et al., 2013; Rahman et al., 2016).

We conclude that technically the use of a horizontal well and geologically the more water-wet rock will significantly improve CO_2 storage capacity and reduce vertical CO_2 plume migration thus de-risking CO_2-projects.

This study has also important implications for reducing the cost associated with of CO_2 geo-sequestration. Joshi (2003) presented a study about the economic benefits of horizontal wells, which showed that the cost of drilling a horizontal well is 1.5 to 2.5

times higher than drilling one vertical well. However, we have found here that using one horizontal well leads to higher CO_2 storage capacities when compared to even 4 vertical wells.

Chapter 6 Effect of Wettability Heterogeneity and Reservoir Temperature on CO_2 Storage Efficiency in Deep Saline Aquifers

6.1 Introduction

CO_2 emissions, from large stationary points and different industrial activities, represent the majority of greenhouse gas emissions (Houghton et al., 2001; Zhang, 2016). To mitigate these emissions, Carbon Capture and Storage (CCS) is the most effective strategy by capturing and injecting the CO_2 into deep geological formations for long-term storage (Pruess et al., 2003; Lebedev et al., 2017; Oldenburg and Unger, 2003). These geological formations include depleted oil and gas reservoirs (Honari et al., 2016), unmineable coal seams (Shi and Durucan, 2005; Zhang et al., 2016b), and deep saline aquifers (DePaolo et al., 2007). Out of all these possible storage formations, deep saline aquifers are the most preferable as they have the highest storage capacity (Lackner, 2003). However, due to the density contrast between aquifer water and the injected CO_2, the low-density CO_2 migrates upwards and can potentially leak through wells, cap rock, and geological fault systems back towards the surface (Li and Liu, 2016; Vialle et al., 2016). There are various physical and chemical trapping mechanisms that can reduce or prevent this CO_2 migration; including structural trapping (Iglauer et al., 2015a; Naylor et al., 2011; Nilsen et al., 2012), residual trapping (Baz et al., 2016; Ide et al., 2007; Iglauer et al., 2011; Krevor et al., 2015; Pentland et al., 2011; Ruprecht et al., 2014; Suekane et al., 2008), dissolution trapping (Bachu and Adams, 2003; Emami-Meybodi et al., 2015; Iglauer, 2011; Lindeberg and Wessel-Berg, 1997; Mito et al., 2008; Pruess and Garcia, 2002; Spycher et al., 2003; Suekane et al., 2008) and mineral trapping (Bachu et al., 1994b; Gaus, 2010; Metz et al., 2005; Mito et al., 2008; Xu et al., 2003; Xu et al., 2004; Xu et al., 2005).

Various site characteristics can affect the efficiency of these trapping mechanisms, including injection well configuration (Al-Khdheeawi et al., 2017d), caprock properties (Iglauer et al., 2015a), aquifer brine salinity (Al-Khdheeawi et al., 2017a; Al-Khdheeawi et al., 2018) or porosity and permeability heterogeneity (Al-Khdheeawi

et al., 2017b; Ambrose et al., 2008; Doughty and Pruess, 2004; Doughty and Myer, 2009; Flett et al., 2007; Gershenzon et al., 2015; Gershenzon et al., 2016; Gershenzon et al., 2017; Green and Ennis-King, 2010; Han et al., 2010; Hesse and Woods, 2010; Hovorka et al., 2004; Obi and Blunt, 2006; Saadatpoor et al., 2009; Zhou et al., 2010). In addition, it has been established that reservoir wettability has a significant impact on CO_2 plume migration and trapping mechanisms, and that water-wet rocks are preferable CO_2 sinks due to their slower vertical CO_2 migration and enhanced residual trapping capacity (Al-Khdheeawi et al., 2017c; Al-Khdheeawi et al., 2017e; Al-Khdheeawi et al., 2017b; Iglauer et al., 2015a; Iglauer et al., 2015b; Iglauer, 2017; Krevor et al., 2015; Rahman et al., 2016).

However, in previous studies homogeneous wettability was assumed; and most studies assumed strongly water-wet conditions although this is a very unlikely scenario (Iglauer, 2017). Furthermore, it is well established that reservoir wettability is distributed heterogeneously at various length scales (from the microscale to the macroscale; (Aspenes et al., 2003; Chaouche et al., 1994; Graue et al., 2002; Masalmeh, 2002; Morrow et al., 1986; Spinler et al., 2002; Standnes and Austad, 2000; Vizika and Duquerroix, 1997).

Multiple factors are responsible for this, ranging from adsorption of organics, pore-surface roughness heterogeneity, grain size heterogeneity, chemical heterogeneity of the mineral surface, differences in surface chemistry, reservoir permeability heterogeneities and associated reservoir fluid movements, or depth in the reservoir (Crocker and Marchin, 1988; Drelich and Miller, 1994; Gaydos and Neumann, 1987; Iglauer et al., 2015a; Iglauer et al., 2015b; Iglauer, 2017; Jafari and Jung, 2016; Laroche et al., 1999; Li, 1996; Lin et al., 1993; Morrow et al., 1986; Saghafi et al., 2014; Van Lingen et al., 1996; Vizika and Duquerroix, 1997). It is also well established that wettability heterogeneity has a significant influence on the fluid displacement mechanisms and phase distributions in gas injection processes (Laroche et al., 1999; Anderson, 1986c; Anderson, 1987a; Anderson, 1987b; Chang et al., 1997; Morrow, 1990; Bertin et al., 1998; Blunt, 1997; Kiriakidis et al., 1993).

There is thus a serious gap in knowledge with respect to how wettability heterogeneity influences the CO_2 storage efficiency . Furthermore, the impact of reservoir temperature on CO_2 storage efficiency has not been examined systematically.

Here we thus investigate the effect of wettability heterogeneity (at isothermal and non-isothermal conditions) and reservoir temperature on vertical CO_2 plume migration and dissolution and residual trapping storage capacities.

6.2 Methodology

6.2.1 Numerical model: underlying theory

We developed a 3D heterogeneous porosity and permeability reservoir model using a nonisothermal multicomponent multiphase flow simulator (TOUGH2; Pruess et al., 1999) and the ECO2M equation of state (Pruess, 2011) to predict the thermodynamic and thermophysical properties of the H_2O-NaCl-CO_2 mixtures including super-and sub-critical CO_2 phases, and CO_2 phase changes. The mass and energy balances describing the fluid and heat flow in these (multiphase and multicomponent) systems are given by:

$$\frac{d}{dt}\int_{V_n} M^k \, dV_n = \int_{\Gamma_n} F^k \bullet n d\Gamma_n + \int_{V_n} Q^k \, dV_n \tag{6.1}$$

where:

V_n is an arbitrary sub-domain which is bounded by the closed surface Γ_n, M is the mass or energy per volume, k (= 1 to n) is a labeling factor representing different mass components (e.g. water, CO_2, air, solutes...etc.), F is the mass or heat flux, Q is the sink (source) term, $\boldsymbol{n}$ is the normal vector on surface element $d\Gamma_n$, pointing inward into V_n.

In addition, mass accumulation can be computed in TOUGH2 using the following formula:

$$M^k = \phi \sum_{\psi} S_\psi \, \rho_\psi \, X_\psi^k \tag{6.2}$$

where:

ϕ is rock porosity, ψ identifies fluid phase, S_ψ is the saturation of phase ψ, ρ_ψ is the density of phase ψ, and X_ψ^k is the mass fraction of component k in phase ψ.

The individual phase mass flux, which can be used to compute the cumulative mass flux, can be predicted via the multiphase version of Darcy's law:

$$F_\psi = \rho_\psi u_\psi = -k \frac{k_{r\psi} \rho_\psi}{\mu_\psi} (\nabla P_\psi - \rho_\psi g) \quad (6.3)$$

where:

F_ψ = individual phase mass flux, u_ψ = Darcy velocity of phase ψ,

k = absolute permeability, $k_{r\psi}$ = relative permeability of phase ψ,

μ_ψ = viscosity of phase ψ, P_ψ = pressure of phase ψ.

6.2.2 Model characteristics

The reservoir model had the dimensions: 1600 m length, 1200 m width and 700 m height (Figure 6-1); these were split in 37 × 33 × 80 cells (=97680 cells). For simulating a highly heterogeneous reservoir, the heterogeneous porosity and permeability data of the SPE comparative solution project (Christie and Blunt, 2001) were used (Figure 6-1). The ratio of vertical to horizontal permeability (k_v/k_h) for the storage reservoir was 0.1 and it was 10E-6 (10^{-6}) for the caprock (i.e. the top boundary of the model at 800 m depth) to prevent vertical flow at the top of the model (Al-Khdheeawi et al., 2017c; Al-Khdheeawi et al., 2017b). The model was initially fully saturated with water (water saturation = 100%) with an initial salinity of 15 wt% Nacl. The initial pressure at the top of the model at 800 m depth was 8 MPa. This initial pressure increased to 15 MPa at the bottom of the reservoir model at 1500 m depth following a pressure gradient of 10 MPa/km (Dake, 2007). Constant pressure boundary conditions were prescribed by expanding the volumes of the lateral outer boundary cells with a large volume modifier of 10E8 (10^8) for each outer boundary cell (Nghiem et al., 2010).

Two different reservoir temperature conditions were considered (i.e. non-isothermal and isothermal conditions) for both heterogeneous and homogeneous wettability scenarios. For the non-isothermal conditions, a geothermal gradient was applied using a vertical temperature gradient of 30 ^{0}C/km (Turcotte and Schubert, 2014; Grant and Bixley, 2011; Doughty et al., 2008) with a surface temperature of 25 ^{0}C. For the isothermal conditions, and in order to cover most temperatures of interest for subsurface CO_2 storage, a wide range of reservoir and CO_2 injection temperatures was tested (i.e. 303 K, 313 K, 323 K, 333 K, 343 K and 353 K) for both wettability

distribution scenarios. The dynamic pressure-temperature effects (Joule-Thompson) have been included in the reservoir model (Katz and Lee, 1990; Pruess, 2005; Oldenburg, 2007).

CO_2 was then injected at a depth of 1373 m at an injection rate of 1 Mt/year for a period of 10 years (i.e. the total amount of injected CO_2 was 10 Mton) with an injection temperature of 338 K for the non-isothermal scenario. Note that this injection rate is similar to that used in the Sleipner (Leung et al., 2014; Torp and Gale, 2004) and Quest (Bourne et al., 2014) CCS projects. A 500 year post-injection (storage) periods were then simulated, where the migration and behaviour of the CO_2 plume was examined, and the vertical CO_2 migration distance and dissolution and residual trapping capacities were predicted.

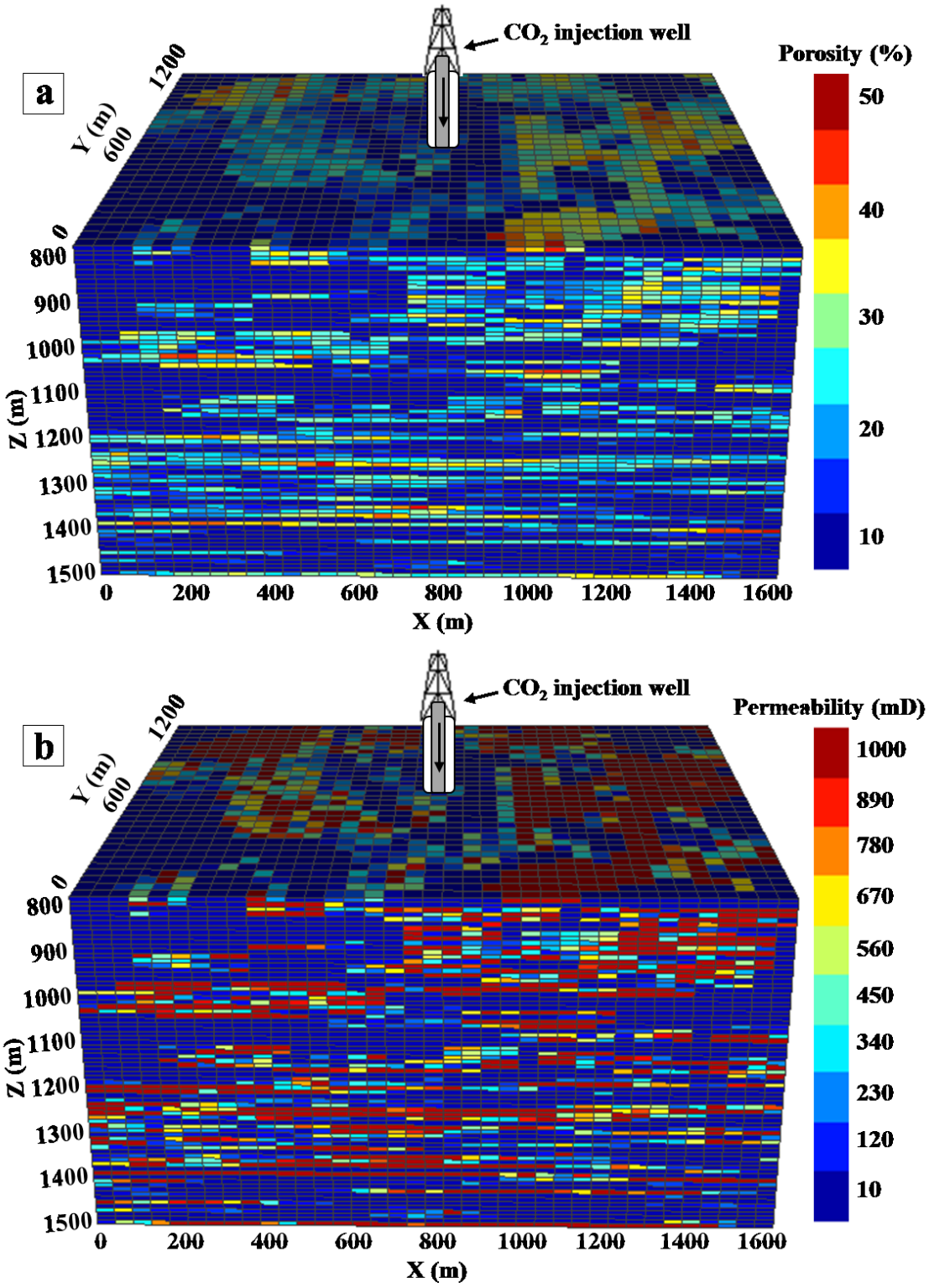

Figure 6-1 3D views of the heterogeneous reservoir model showing the location of the CO_2 injection well, model dimensions and a) heterogeneous porosity field; b) heterogeneous permeability field.

6.2.3 Simulation of homogeneous and heterogeneous wettability

It is clear that reservoir wettability can vary widely (Iglauer, 2017), and that wettability strongly influences relative permeabilities (Al-Khdheeawi et al., 2017c; Al-Khdheeawi et al., 2017d; Al-Khdheeawi et al., 2017b; Anderson, 1987b; Krevor et al., 2012; Levine et al., 2014; McCaffery and Bennion, 1974; Owens and Archer, 1971), capillary pressures (Al-Khdheeawi et al., 2017c; Al-Khdheeawi et al., 2017d; Al-Khdheeawi et al., 2017b; Anderson, 1987a; Batycky et al., 1981; Melrose, 1965; Morrow, 1976; Pini et al., 2013; Pini et al., 2012) and the associated residual gas and water saturations (Akbarabadi and Piri, 2013; Al-Menhali et al., 2016; Chaudhary et al., 2013; Craig, 1993; Iglauer et al., 2011; Pentland et al., 2011; Rahman et al., 2016; Ruprecht et al., 2014).

Wettability therefore strongly influences reservoir-scale fluid dynamics (Al-Khdheeawi et al., 2017c; Al-Khdheeawi et al., 2017e; Al-Khdheeawi et al., 2017b). We thus used our recently developed relative permeability and capillary pressure curves to simulate specific wettability scenarios (Al-Khdheeawi et al., 2017c; Al-Khdheeawi et al., 2017d; Al-Khdheeawi et al., 2017b). Note that our previous developed relative permeability and capillary pressure curves were built based on various experimental studies (e.g. Melrose, 1965; Owens and Archer, 1971; McCaffery and Bennion, 1974; Morrow, 1976; Batycky et al. 1981; Anderson, 1987a, 1987b; Craig, 1993; Pentland et al., 2011; Krevor et al., 2012; Pini et al., 2012; Pini et al., 2013; Levine et al., 2014). To mimic heterogeneous wettability, five wettabilities (i.e. strongly water-wet, weakly water-wet, intermediate-wet, weakly CO_2-wet and strongly CO_2-wet) were randomly assigned to different cells using a discrete probability distribution. To represent the deep saline aquifer, 5% of the rock was assigned strongly water-wet, 30% weakly water-wet, 45% intermediate-wet, 15% weakly CO_2-wet and 5 % strongly CO_2-wet (Figure 6-2). These distributions were chosen for two reasons: a) we have followed the more likely percentages in an actual saline aquifer (Iglauer et al. 2015a, b, 2017) and b) the weighted averages of the residual gas saturation and residual water saturation for this nonuniform wettability distribution are equal to that used in the homogenous wettability model (intermediate-wet), where $S_{gr} = 0.25$ and $S_{wr} = 0.22$ (Al-Khdheeawi et al., 2017c; Al-Khdheeawi et al., 2017d; Al-Khdheeawi et al., 2017b). Without any further studies available in literature, as regard any correlation between wettability distribution and other petrophysical or geological parameters (i.e. permeability, porosity and mineralogy) we

have used here a random distribution. Indeed, many previous studies, which discuss the wettability heterogeneity in oil reservoirs, used random distribution to represent the wettability heterogeneity in the reservoir (e.g. (Aspenes et al., 2003; Chaouche et al., 1994; Graue et al., 2002; Masalmeh, 2002; Morrow et al., 1986; Spinler et al., 2002; Standnes and Austad, 2000; Vizika and Duquerroix, 1997), this is thus the established approach which we follow here.

The weighted averages of residual gas saturation ($\bar{S}_{\mathrm{gr}}$) and residual water saturation ($\bar{S}_{\mathrm{wr}}$) in the heterogeneous wettability model were calculated using the above percentages of each wettability condition with our recently used values of residual gas and residual water saturation for the different wettability scenarios (Table 6-1; (Al-Khdheeawi et al., 2017c; Al-Khdheeawi et al., 2017d; Al-Khdheeawi et al., 2017b). Thus the weighted average of the residual gas saturation ($\bar{S}_{\mathrm{gr}}$) and residual water saturation ($\bar{S}_{\mathrm{wr}}$) for the heterogeneous wettability scenario have been calculated as follows:

$$\bar{S}_{\mathrm{gr}} = \sum_i P_i \; S_{gri}/100$$

$$\bar{S}_{\mathrm{gr}} = \begin{pmatrix} (P \times S_{gr})_{\text{strongly water-wet}} + (P \times S_{gr})_{\text{weakly water-wet}} \\ + (P \times S_{gr})_{\text{intermediate-wet}} + (P \times S_{gr})_{\text{weakly } CO_2\text{-wet}} \\ + (P \times S_{gr})_{\text{strongly } CO_2\text{-wet}} \end{pmatrix} /100 \quad (6.4)$$

And,

$$\bar{S}_{\mathrm{wr}} = \sum_i P_i \; S_{wri}/100$$

$$\bar{S}_{\mathrm{wr}} = \begin{pmatrix} (P \times S_{wr})_{\text{strongly water-wet}} + (P \times S_{wr})_{\text{weakly water-wet}} \\ + (P \times S_{wr})_{\text{intermediate-wet}} + (P \times S_{wr})_{\text{weakly } CO_2\text{-wet}} \\ + (P \times S_{wr})_{\text{strongly } CO_2\text{-wet}} \end{pmatrix} /100 \quad (6.5)$$

Where:

$\bar{S}_{\mathrm{gr}}$ is the weighted average of residual gas saturation for the heterogeneous wettability model, P_i is the wettability percentage of wettability scenario i in the heterogeneous model, i = different wettability scenarios from strongly water-wet to strongly CO_2-wet (5 cases), S_{gri} is the residual gas saturation for wettability scenario i, $\bar{S}_{wr}$ is the weighted average of residual water saturation for the heterogeneous wettability scenario, and S_{wri} is the residual water saturation for wettability scenario i.

Here, we are representing hysteresis by using different values for the parameters (i.e. λ, S_{gr} and S_{wr}) in equations (6-11) to simulate the relative permeability and capillary pressure curves for the CO_2 injection period (dashed lines) and post-injection period (solid lines; Figures Figure 6-3 andFigure 6-4) for the different wettability scenarios. These parameters (Tables 6-1 and 6-2) were imported into the TOUGH2 code using the Genuchten-Mualem model (Mualem, 1976; Van Genuchten, 1980; Equations 6-11 below) to implement the developed relative permeability and capillary pressure curves in the reservoir simulations. Note that the used approch for treating the hysteresis is not as rigorous as using a true hysteretic formulation (Doughty, 2007), but it is able to represent the CO_2 injection and post-injection periods for the different wettability scenarios adequeatly (Al-Khdheeawi et al., 2017b).

$$k_{rw} = \sqrt{S^*}\left\{1-\left(1-[S^*]^{1/\lambda}\right)^{\lambda}\right\}^2 \quad \text{if} \quad S_w < S_{ws} \tag{6.6}$$

$$k_{rw} = 1 \quad \text{if} \quad S_w \geq S_{ws} \tag{6.7}$$

$$k_{rg} = 1 - k_{rw} \quad \text{if} \quad S_{gr} = 0 \tag{6.8}$$

$$k_{rg} = \left(1-\hat{S}\right)^2\left(1-\hat{S}^2\right) \quad \text{if} \quad S_{gr} > 0 \tag{6.9}$$

$$\left(P_{cap}\right) = P_0\left([S^*]^{-1/\lambda}-1\right)^{1-\lambda} \tag{6.10}$$

$$S^* = (S_w - S_{wr})/(S_{ws} - S_{wr}),$$
$$\hat{S} = (S_w - S_{wr})/(1 - S_{wr} - S_{gr}) \tag{6.11}$$

where:

k_{rg} = gas relative permeability, k_{rw} = water relative permeability,

S_{gr} = residual saturation for gas, S_w = water saturation,

S_{ws} = saturated water saturation (= 1), S_{wr} = residual saturation for water

P_c = CO_2-water capillary pressure, P_o = capillary pressure scaling factor.

λ = pore size distribution index (fitting parameter),

In order to implement the effect of porosity and permeability heterogeneity on the capillary pressure curves for each gridblock we used the Leverett J-function (Leverett, 1941):

$$J(S_w) = \frac{P_c}{\sigma \cos \Theta} \sqrt{\frac{k}{\phi}} \quad (6.12)$$

where:

J = dimensionless capillary pressure, k = reservoir permeability,

ϕ = reservoir porosity, σ = CO_2-brine surface tension,

θ = CO_2-brine-rock contact angle.

Table 6-1 The values imported into the TOUGH2 code to implement the relative permeability curves for the different wettability scenarios (Al-Khdheeawi et al., 2017c; Al-Khdheeawi et al., 2017d; Al-Khdheeawi et al., 2017b)

Wettability scenario	CO_2 injection period			CO_2 post-injection period		
	S_{gr}	S_{wr}	λ	S_{gr}	S_{wr}	λ
Strongly water-wet	0	0.26	0.78	0.35	0.26	0.58
Weakly water-wet	0	0.25	1.05	0.30	0.25	0.95
Intermediate-wet	0	0.22	1.22	0.25	0.22	1.17
Weakly CO_2-wet	0	0.15	1.41	0.15	0.15	1.51
Strongly CO_2-wet	0	0.1	1.7	0.1	0.1	1.9

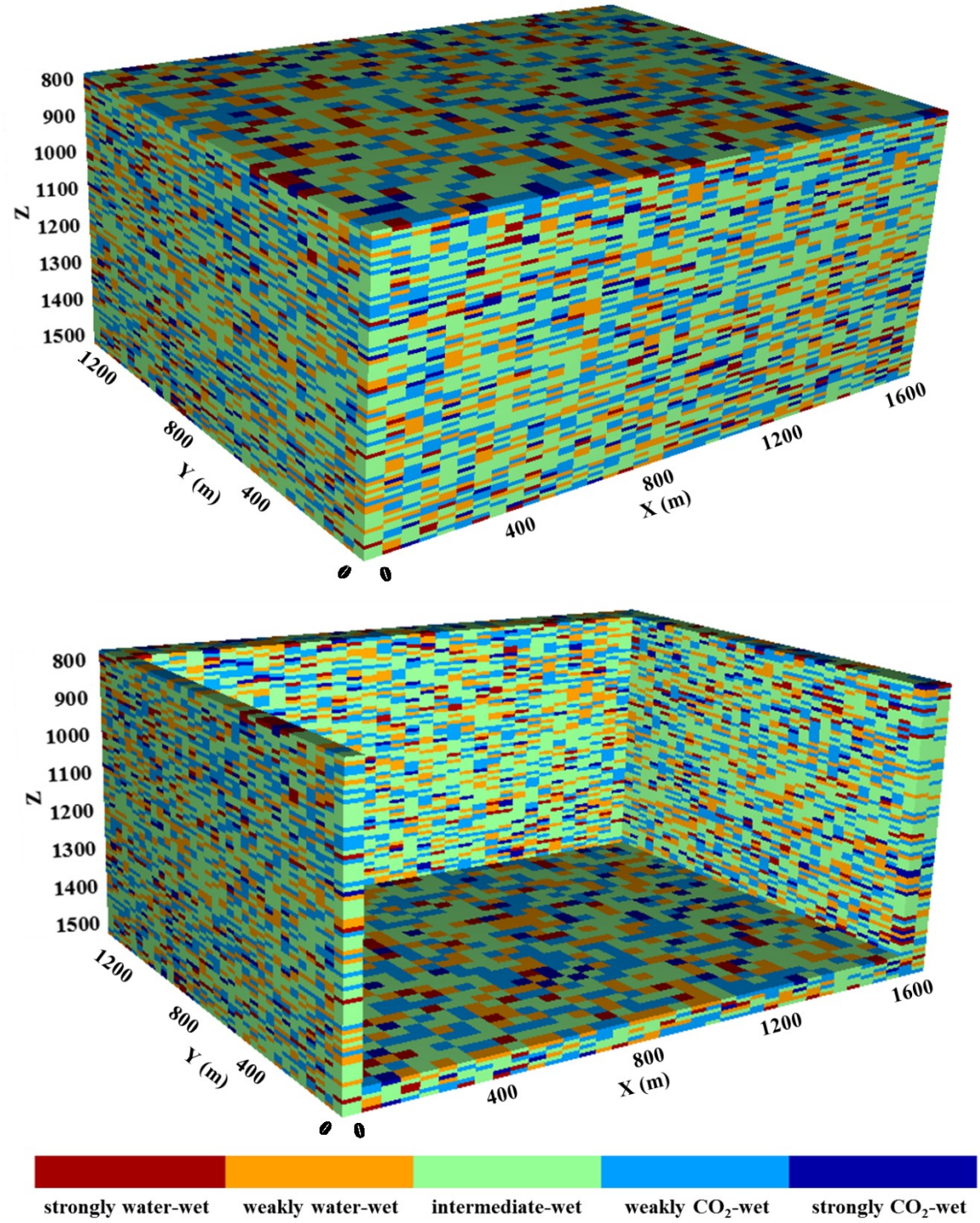

Figure 6-2 3-D views of the heterogeneous wettability model: 5% strongly water-wet; 30% weakly water-wet; 45% intermediate-wet; 15% weakly CO_2-wet; and 5 % strongly CO_2-wet was assigned.

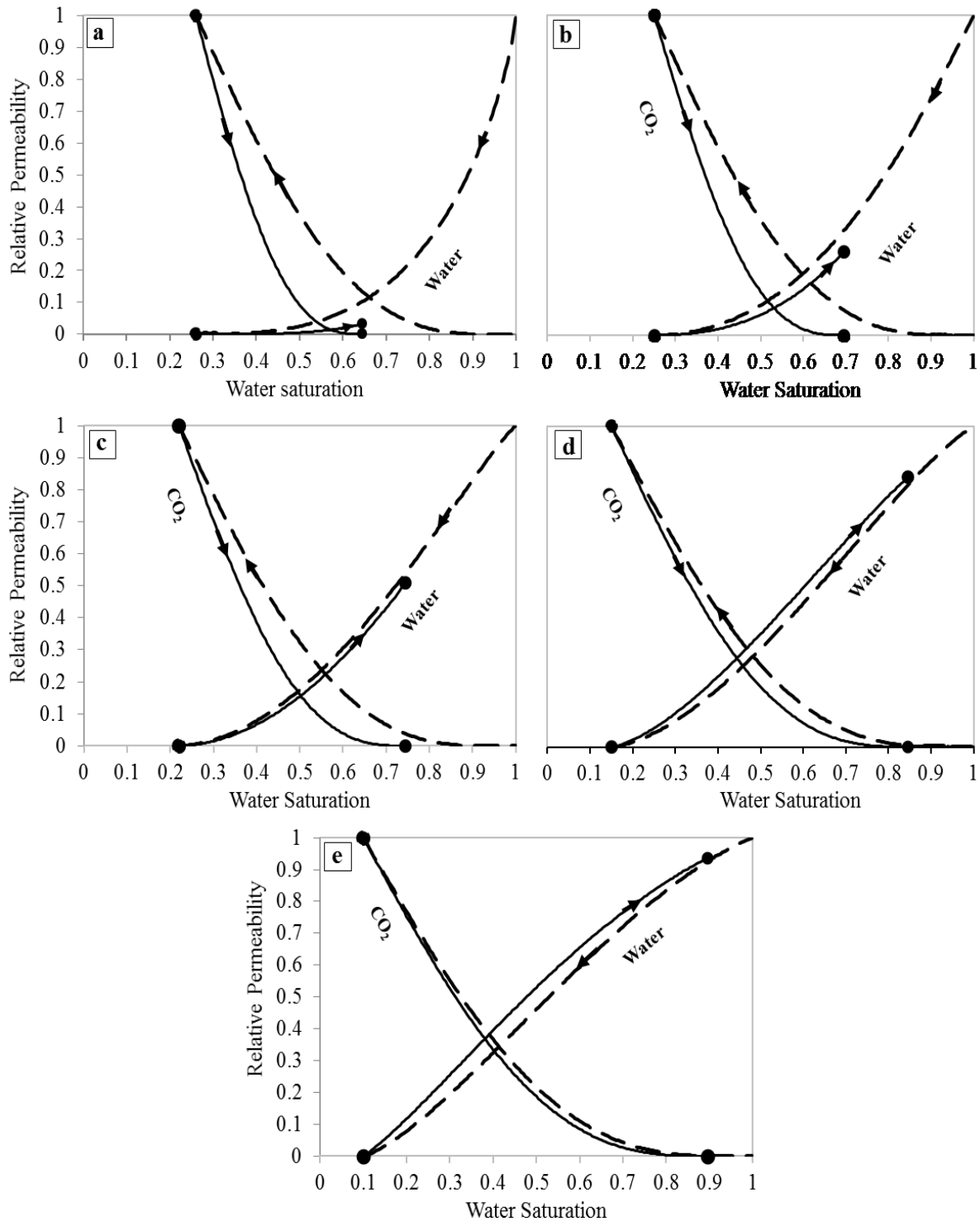

Figure 6-3 Relative permeability curves used for the five rock wettability conditions: (a) strongly water-wet; (b) weakly water-wet; (c) intermediate-wet; (d) weakly CO_2-wet; (e) strongly CO_2-wet (Al-Khdheeawi et al., 2017c; Al-Khdheeawi et al., 2017d; Al-Khdheeawi et al., 2017b). Dashed lines represent CO_2 injection period and solid lines represent post-injection (storage) period.

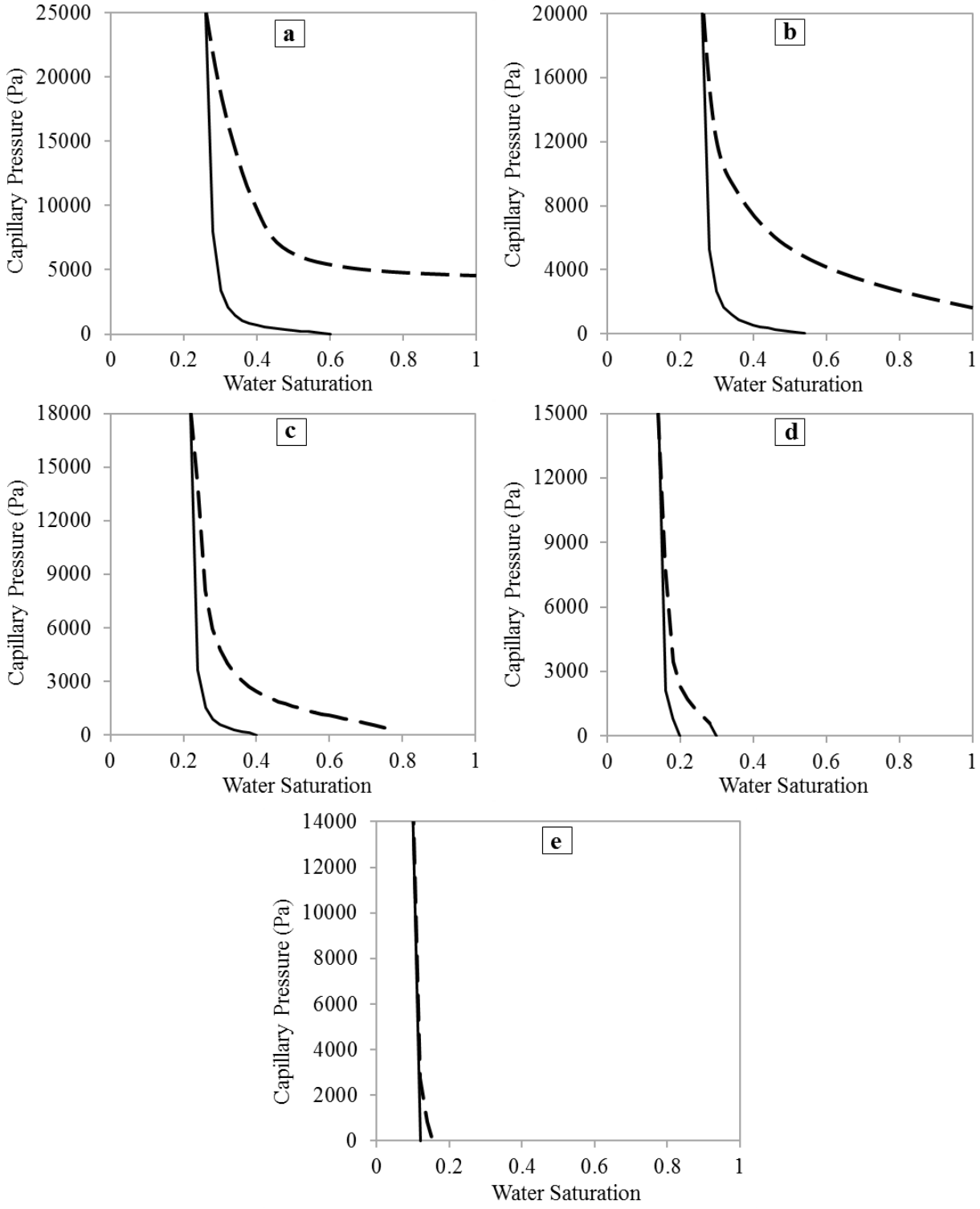

Figure 6-4 Capillary pressure curves used for the five rock wettability scenarios: (a) strongly water-wet; (b) weakly water-wet; (c) intermediate-wet; (d) weakly CO_2-wet; (e) strongly CO_2-wet (Al-Khdheeawi et al., 2017c; Al-Khdheeawi et al., 2017d; Al-Khdheeawi et al., 2017b). Dashed lines represent CO_2 injection period and solid lines represent post-injection (storage) period.

Table 6-2 The values imported into the TOUGH2 code to implement the capillary pressure curves for the different wettability scenarios (Al-Khdheeawi et al., 2017c; Al-Khdheeawi et al., 2017d; Al-Khdheeawi et al., 2017b)

Wettability	CO_2 injection period					CO_2 post-injection period				
	S_{wr}	S_{ws}	λ	P_0 [Pa]	P_{max} [Pa]	S_{wr}	S_{ws}	λ	P_0 [Pa]	P_{max} [Pa]
Strongly water-wet	0.259	1	0.7	1500	25000	0.259	0.6	0.51	1000	25000
Weakly water-wet	0.249	1	0.7	1500	20000	0.249	0.55	0.51	1000	20000
Intermediate -wet	0.219	0.8	0.7	1500	18000	0.219	0.4	0.51	1000	18000
Weakly CO_2-wet	0.149	0.3	0.7	1500	15000	0.149	0.2	0.51	1000	15000
Strongly CO_2-wet	0.099	0.15	0.7	1500	14000	0.099	0.1	0.51	1000	14000

6.3 Results and discussion

6.3.1 CO_2 migration analysis

6.3.1.1 Effect of wettability heterogeneity on CO_2 migration

It was previously shown that reservoir wettability has a significant impact on the vertical CO_2 plume migration and that CO_2 migration is highest in CO_2-wet rocks (Al-Khdheeawi et al., 2017c; Al-Khdheeawi et al., 2017d; Al-Khdheeawi et al., 2017b). Importantly, in these previous studies, only homogeneous wettability scenarios were investigated. However, it is well established that wettability is heterogeneously distributed in reservoirs (Aspenes et al., 2003; Chaouche et al., 1994; Graue et al., 2002; Masalmeh, 2002; Morrow et al., 1986; Spinler et al., 2002; Standnes and Austad, 2000; Vizika and Duquerroix, 1997). Hence, we investigated this effect and show that wettability heterogeneity leads to a significant increase in vertical CO_2 plume migration, which substantially affects residual and dissolution trapping as shown in

Figure 6-5 (for the non-isothermal scenario), and FiguresFigure 6-6 and Figure 6-7 (heterogeneous and homogeneous wettability cases, respectively; for the isothermal scenario). For both, non-isothermal and isothermal conditions tested, a heterogeneously wetted reservoir had fastest and highest vertical CO_2 plume migration (FiguresFigure 6-5 to Figure 6-8, and Table 6-3). For the non-isothermal scenario, the total vertical CO_2 migration distance at the end of the CO_2 post-injection period (500 years) was 573 m in case of the heterogeneously wetted reservoir, while it was only 464 m in the homogeneous wettability scenario (Figure 6-5 and Table 6-3). Also, for all isothermal temperatures tested (i.e. 303 K, 313 K, 323 K, 333 K, 343 K and 353 K), the heterogeneous wettability scenario had the fastest and highest vertical CO_2 migration (e.g. the total vertical CO_2 migration distance for the 303 K, isothermal temperature model was 375 m in case of heterogeneous wettability, while it was only 304 m in the homogeneous wettability scenario, at the end of the CO_2 post-injection period; Figure 6-8 and Table 6-3). We also noticed that, for non-isothermal conditions, the difference in the CO_2 upward migration rates (when comparing homogenous and heterogeneous wettability scenarios) is larger for higher temperatures.

In summary, our results indicate that spatial heterogeneities in wettability distribution lead to accelerated CO_2 upwards migration for both isothermal and non-isothermal conditions. Hence, simulations made with a homogeneous wettability distribution predicted a lower vertical migration distance than those assuming a heterogeneous wettability distribution.

Table 6-3 CO_2 plume statistics during the post-injection period (0-500 years) for the different reservoir temperature conditions (isothermal and non-isothermal) in both heterogeneous (HT) and homogeneous (HM) wettability scenarios

Reservoir temperature condition		Plume depth at the end of the injection period (m)		Shallowest depth reached by the CO_2 plume (m)		Time required to reach the shallowest plume depth (years)		Total migration distance (m)*	
		HT	HM	HT	HM	HT	HM	HT	HM
Non-Isothermal****		1049	1049	800	909	35***	500**	573	464
Isothermal	303 K	1196	1196	998	1069	500**	500**	375	304
	313 K	1168	1168	934	1033	500**	500**	439	340
	323 K	1118	1118	807	941	500**	500**	566	432
	333 K	1040	1040	800	821	100** *	500**	573	552
	343 K	941	941	800	800	30***	150***	573	573
	353 K	864	864	800	800	10***	50***	573	573

*The maximum possible vertical migration distance is 573 m, which represents the vertical distance between the CO_2 injection depth (1373 m) and the top seal of the reservoir (800 m).

** For the heterogeneous wettability at 303 K, 313 K and 323 K of the isothermal conditions, and for the homogeneous wettability at non- isothermal condition and 303 K, 313 K, 323 K and 333 K of the isothermal conditions the CO_2 plume did not reach the caprock depth (800 m) during the whole post injection period (0 to 500 years). Thus, the shallowest CO_2 plume depth is recorded at the end of the post-injection period (after 500 years).

*** For the heterogeneous wettability at non- isothermal condition and at 333K, 343 K and 353 K of the isothermal conditions, and for homogeneous wettability at 343 K and 353 K of the isothermal conditions the CO_2 plume reached the caprock (800 m depth) at various times during the post injection period.

**** The geothermal gradient: T (^{0}C) = 25 + 0.03 × depth (m).

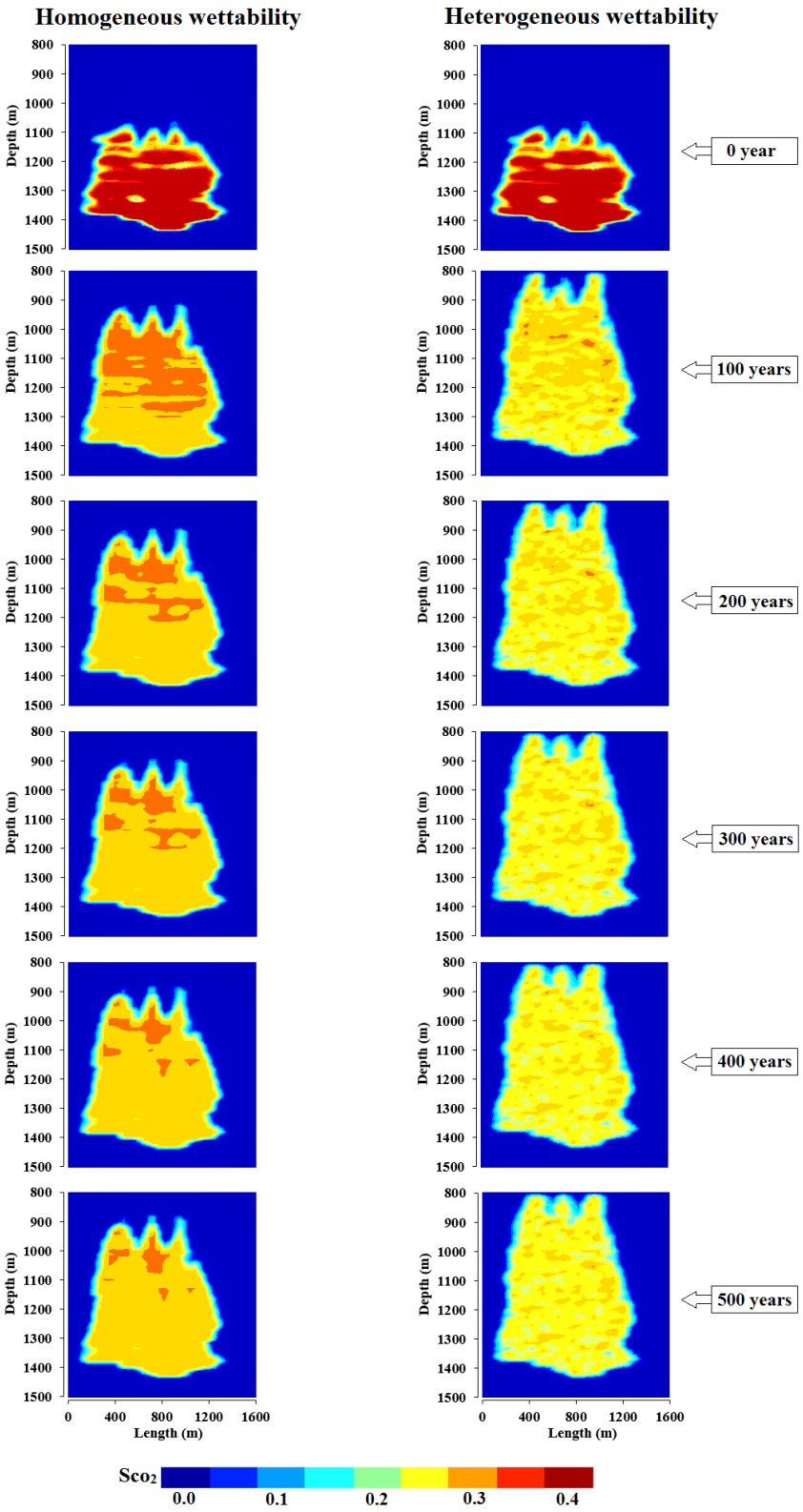

Figure 6-5 2D views through the center of the reservoir showing the CO_2 plume for the model with a vertical geothermal gradient (the non-isothermal conditions) as a function of wettability heterogeneity. Time = 0 year represents the end of the injection period.

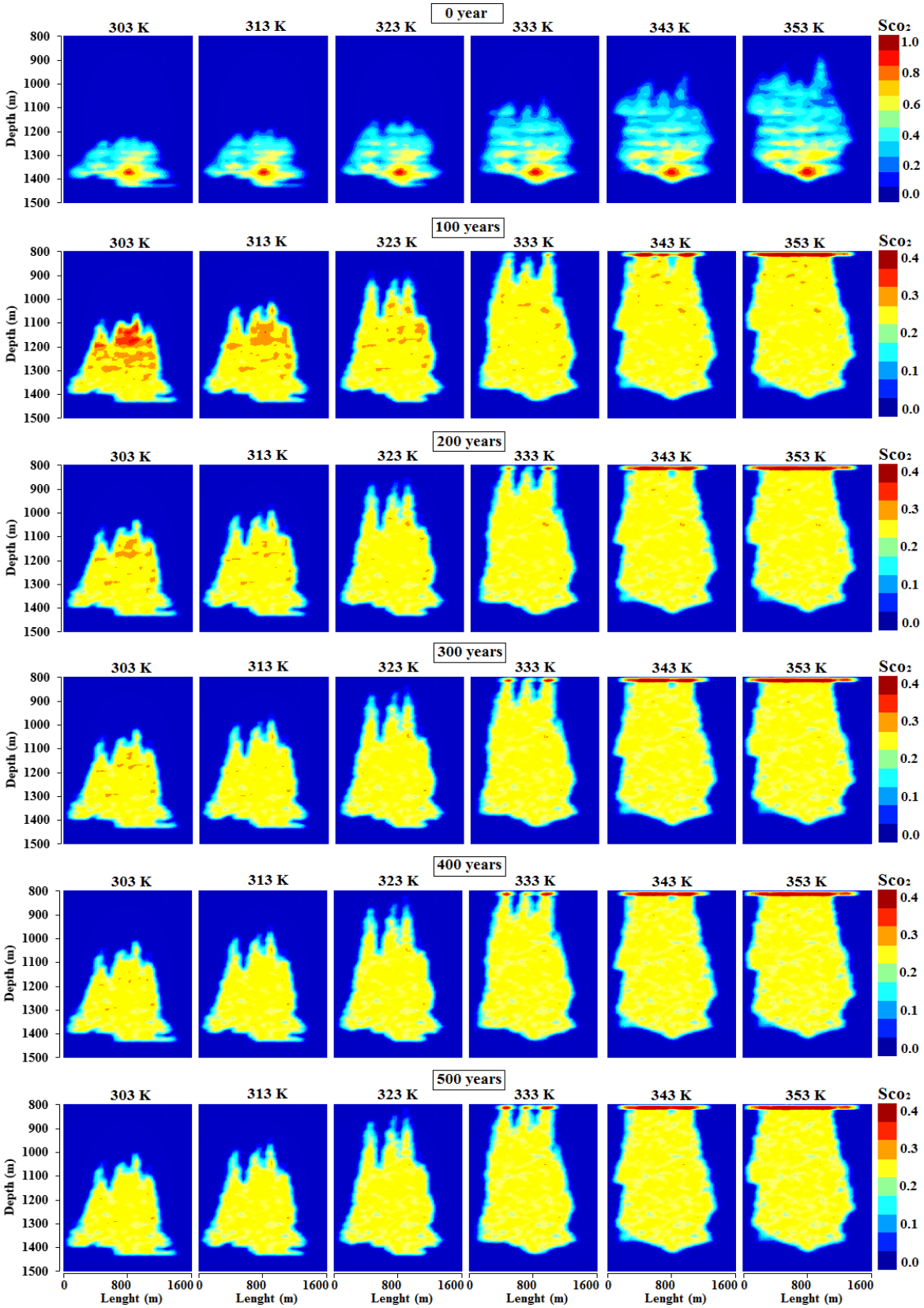

Figure 6-6 2D views through the center of the reservoir showing the CO_2 plume as a function of reservoir temperature and storage time (heterogeneous wettability. Time = 0 year represents the end of the injection period.

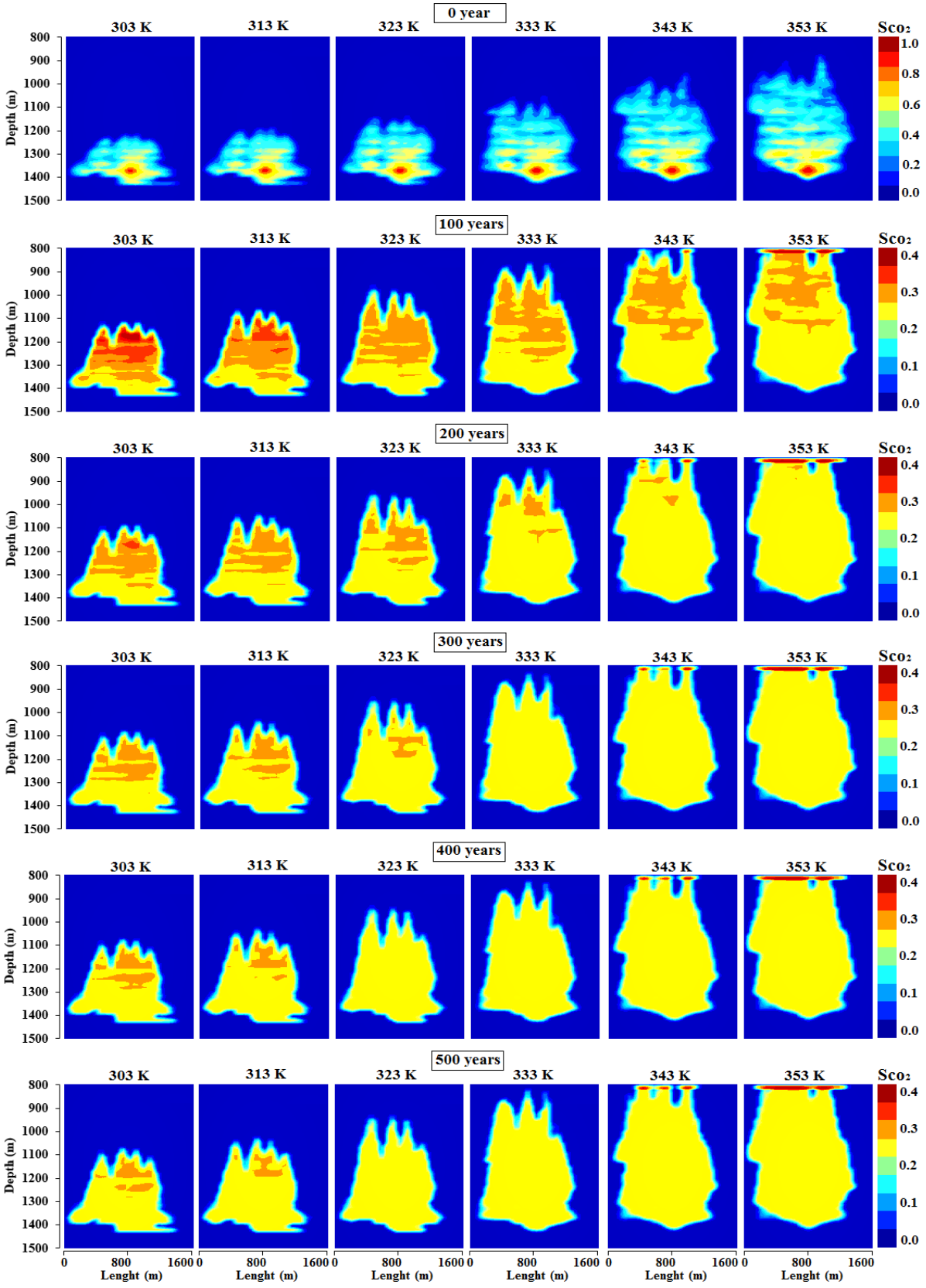

Figure 6-7 2D views through the center of the reservoir showing the CO_2 plume as a function of reservoir temperature and storage time (homogeneous wettability). Time = 0 year represents the end of the injection period.

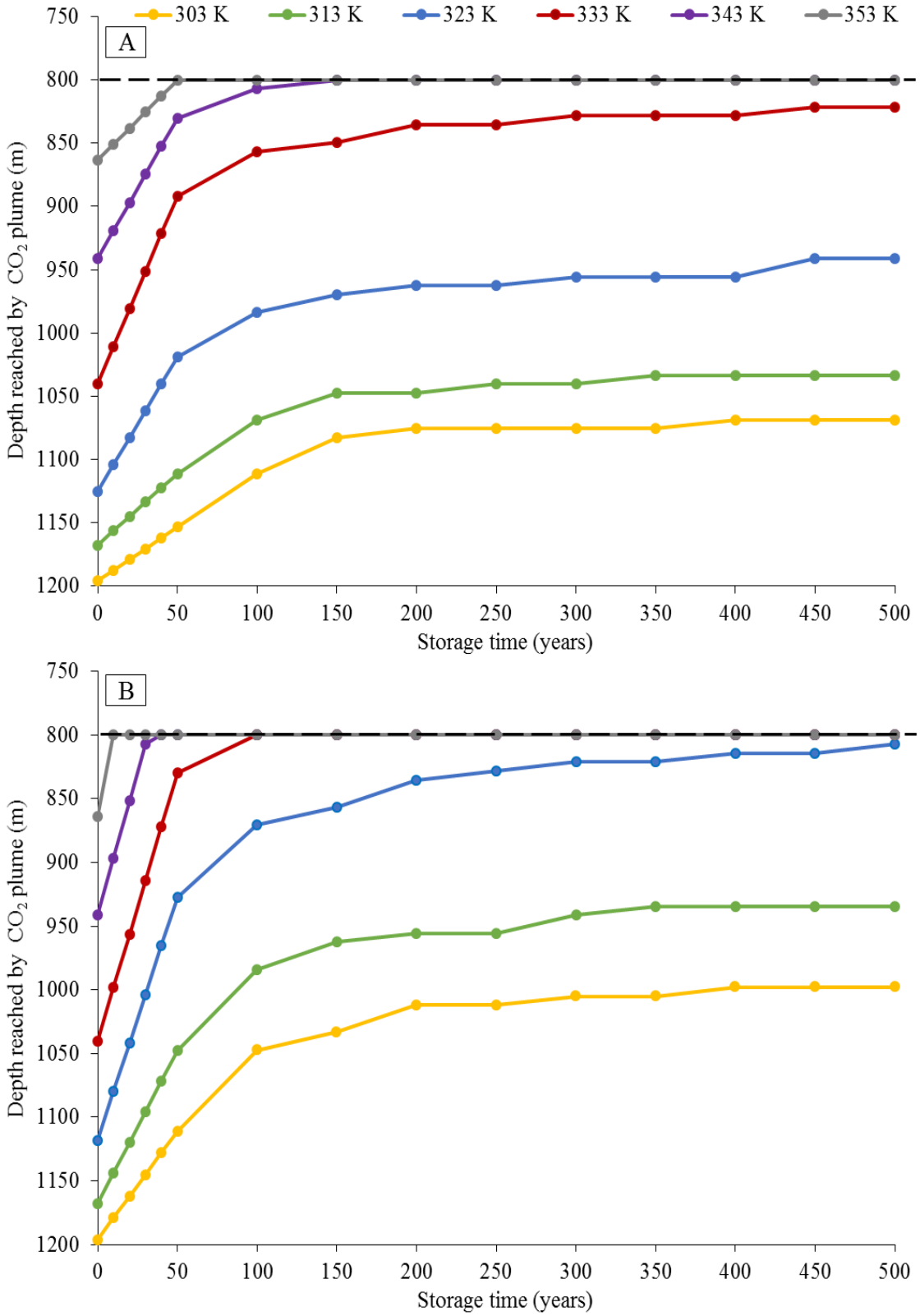

Figure 6-8 Depth reached by the CO_2 plume as a function of storage time and isothermal reservoir temperature; A) homogeneous wettability, B) heterogeneous wettability. The horizontal dashed (black) line shows the caprock seal.

6.3.1.2 Effect of reservoir temperature on CO_2 migration

Clearly, reservoir temperature has a significant impact on the vertical CO_2 migration (Figure 6-8). For both (homogeneous and heterogeneous) wettability scenarios, higher reservoir temperatures drastically accelerated the vertical CO_2 migration.

Specifically, the total post-injection time required for the CO_2 plume to reach the caprock seal depth (800 m) (i.e. the CO_2 plume migrates its maximum possible migration distance; 573 m) was 30 years for the heterogeneous wettability and 150 years for the homogeneous wettability case at 343 K, while it was only 10 years for the heterogeneous wettability and only 50 years for the homogeneous wettability at 353 K (Figure 6-8). Importantly, for all other reservoir temperatures, for both homogeneous and heterogeneous wettability scenarios, a higher reservoir temperatures accelerated the CO_2 plume migration (Figure 6-8 and Table 6-3).

We conclude that higher reservoir temperatures lead to accelerated CO_2 upwards movement.

6.3.2 Trapping capacity analysis

6.3.2.1 Effect of wettability heterogeneity on trapping capacity

Residual and dissolution trapping capacities, and the amount of mobile CO_2 were predicted for both wettability scenarios and for both reservoir temperature conditions investigated (non-isothermal, Figure 6-9, and isothermal, Figure 6-10). Heterogeneous wettability increased the amount of mobile CO_2, while it reduced residual trapping, but improved solubility trapping (Figure 6-9 for the non-isothermal conditions scenario, Figure 6-10 for the isothermal conditions scenario and Table 6-4). Note that the improved solubility trapping is caused by the increased CO_2 plume migration distance, which leads to more dissolved CO_2 as a result of the increased brine-CO_2 contact area (Doughty, 2010).

In summary, our results show that wettability heterogeneity reduces residual trapping, and increases CO_2 mobility and solubility trapping.

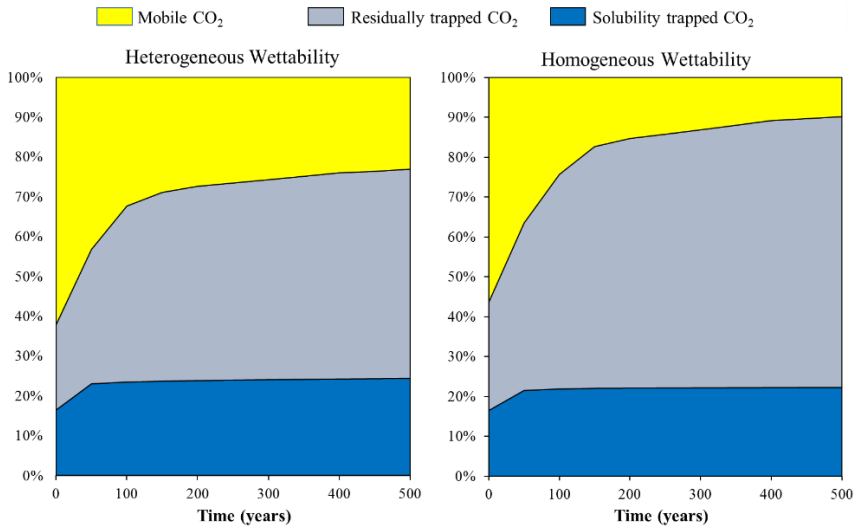

Figure 6-9 Percentages of mobile, residually trapped and solubility trapped CO_2 for the model with vertical geothermal gradient (the non-isothermal conditions) as a function of storage time and wettability heterogeneity. Clearly, wettability heterogeneity leads to increased CO_2 mobility and solubility trapping; while it leads to reduced residual trapping.

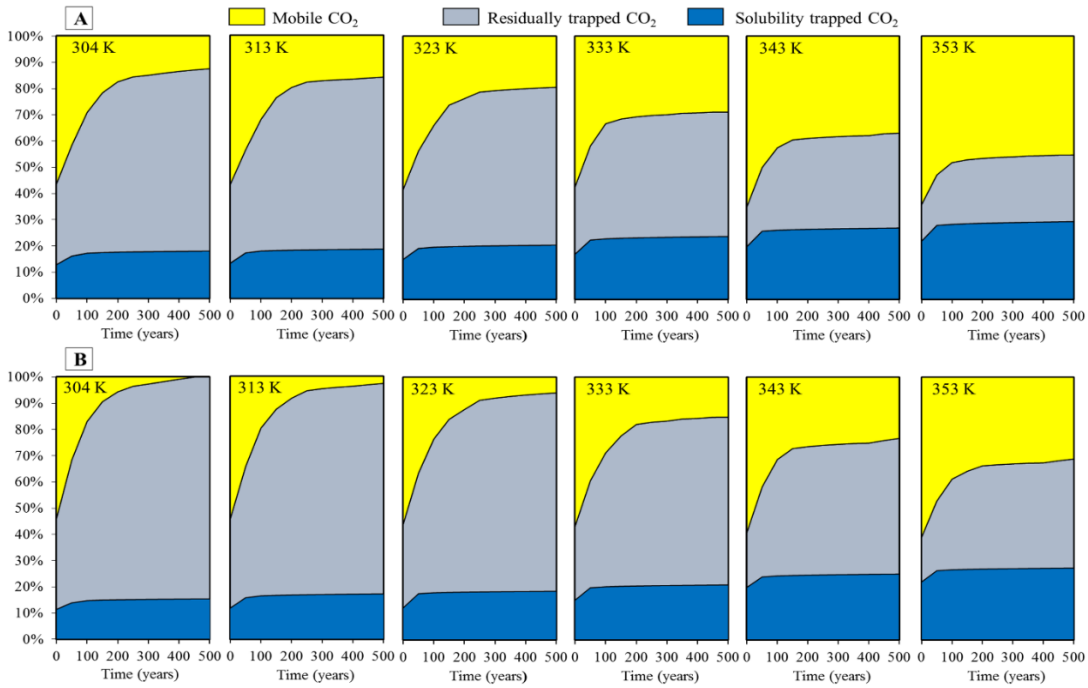

Figure 6-10 Percentages of mobile, residually trapped and solubility trapped CO_2 as a function of storage time, reservoir temperature and wettability heterogeneity; A) heterogeneous wettability scenario and B) homogeneous wettability scenario. Clearly, increasing wettability heterogeneity and increasing reservoir temperature lead to increasing CO_2 mobility and solubility trapping; while it reduces residual trapping.

Table 6-4 Ratio of CO_2 mobility and trapping capacity to the amount of total injected CO_2 (10 Mton) for the different reservoir temperature conditions in both heterogeneous (HT) and homogeneous (HM) wettability scenarios at the end of the post-injection period (500 years)

Ratio of CO_2 mobility and trapping capacities to the total injected CO_2 (10 Mton)	Wettability scenario	Isothermal Reservoir temperature (K)						Non-isothermal conditions
		303	313	323	333	343	353	
Residual trapping (%)	HT	70	65	60	47	36	25	53
	HM	85	80	75	64	52	42	68
dissolution trapping (%)	HT	18	19	21	24	27	30	24
	HM	15	17	19	21	25	27	22
Mobile (free) CO_2 (%)	HT	12	16	19	29	37	45	23
	HM	0	3	6	15	23	31	10

6.3.2.2 Effect of reservoir temperature on trapping capacity

Clearly, reservoir temperature highly affects CO_2 mobility and residual and dissolution trapping (Figure 6-10). Increasing reservoir temperature increased CO_2 mobility (for both, homogeneous and heterogeneous wettability; Figure 6-10 and Table 6-4). This is coupled with reduced residual trapping (e.g. the amount of residually trapped CO_2 decreased from 70% to 25% when the reservoir temperature was increased from 303 K to 353 K; in the heterogeneous-wet case model, after 500 years; but improved solubility trapping (e.g. the amount of solubility trapped CO_2 increased from 18% to 30% when the reservoir temperature increased from 303 K to 353 K; in the heterogeneous-wet model, after 500 years; Figure 6-10 and Table 6-4). These results are consistent with previous studies (e.g. Kumar et al., 2005; Ofori and Engler, 2011) which demonstrated that increasing reservoir temperature leads to increased CO_2 solubility trapping. It is important to note that the solubility of CO_2 in water decreases with increasing temperature (e.g. the mass fraction of CO_2 in the

aqueous phase decreases from 0.053 to 0.032 when the temperature increases from 303K to 353K at 80 bars; Doughty, 2010). However, the greater CO_2 plume migration distance (i.e. the larger CO_2-brine contact area) has also a large effect on CO_2 solubility (Doughty, 2010); so CO_2 solubility trapping increases with increasing reservoir temperature. Recall that our results show that higher reservoir temperatures leads to higher CO_2 plume migration. So this is overcompensates the thermodynamic effect.

In summary, we conclude that the reservoir temperature has an important impact on the amount of mobile and trapped CO_2, and lower temperatures are preferred.

6.4 Conclusions

It is well known that reservoir wettability is distributed heterogeneously at various length scales in a reservoir (Aspenes et al., 2003; Chaouche et al., 1994; Graue et al., 2002; Masalmeh, 2002; Morrow et al., 1986; Spinler et al., 2002; Standnes and Austad, 2000; Vizika and Duquerroix, 1997). Furthermore, it has been shown previously that such wettability heterogeneity has a significant impact on the displacement mechanisms and phase distributions in gas injection processes for oil recovery (Laroche et al., 1999; Anderson, 1986, 1987a, b; Chang et al., 1997; Morrow, 1990; Bertin et al., 1998; Blunt, 1997; Kiriakidis et al., 1993). However, the effect of wettability heterogeneity on CO_2 storage efficiency at isothermal and non-isothermal reservoir conditions has not been addressed. Moreover, reservoir temperature is another factor which has not received sufficient attention in this context.

Thus, we studied the effect of wettability heterogeneity and reservoir temperature on CO_2 plume migration and residual and solubility trapping. Our results clearly demonstrate that both increased wettability heterogeneity and increased reservoir temperature significantly increase the vertical CO_2 plume migration distance, CO_2 mobility and CO_2 dissolution trapping, but decrease residual trapping.

We thus conclude that wettability heterogeneity needs to be accurately modelled in reservoir-scale simulations in order to obtain reliable CO_2 storage predictions. Furthermore, we conclude that lower reservoir temperatures are preferential because they improve trapping capacity.

Chapter 7 Impact of Salinity on CO_2 Containment Security in Highly Heterogeneous Reservoirs

7.1 Introduction

Geological Carbon Storage is one of the most promising technologies to mitigate anthropogenic carbon emissions by capturing the CO_2 from large stationary sources and injecting it deep into geological formations. (Pruess et al., 2003). The brine-CO_2 density difference will then cause a vertical CO_2 migration towards the surface. This migration can be reduced and CO_2 can be inhibited from leaking to the atmosphere by four main trapping mechanisms, namely structural trapping, (i.e. caprock seal beds or permeability barrier units),(Hesse et al., 2008; Naylor et al., 2011; Iglauer et al., 2015a) residual trapping which depends on the capillary forces,(Pentland et al., 2011; Iglauer et al., 2011; Krevor et al., 2015; Rahman et al., 2016; Iglauer and Wülling, 2016) dissolution trapping (Lindeberg and Wessel-Berg, 1997; Spycher et al., 2003; Iglauer, 2011) which is affected by the CO_2-brine interfacial area,(Metz et al., 2005; Kumar et al., 2005; Doughty, 2010; Pentland et al., 2012) and mineral trapping,(Bachu et al., 1994b; Xu et al., 2004; Gaus, 2010) which depends on the chemical reactions between reservoir rock minerals and fluids and the injected CO_2 (Xu et al., 2003; Xu et al., 2005).

Many factors affect the CO_2 storage efficiency, e.g. reservoir heterogeneity,(Doughty and Pruess, 2004; Hovorka et al., 2004; Obi and Blunt, 2006; Bryant et al., 2006; Flett et al., 2007; Ide et al., 2007; Saadatpoor et al., 2009; Zhou et al., 2010; Ambrose et al., 2008; Han et al., 2010; Hesse and Woods, 2010; Green and Ennis-King, 2010; Gershenzon et al., 2015; Gershenzon et al., 2016) rock wettability, (Iglauer et al., 2015a; Iglauer et al., 2015b; Al-Khdheeawi et al., 2017c; Al-Khdheeawi et al., 2017b) injection well configuration,(Al-Khdheeawi et al., 2017d) the ratio of vertical to horizontal permeability,(Basbug et al., 2005) stratum dip angle,(Wang et al., 2016a; Wang et al., 2016b) key model parameters (i.e. outer boundary condition, reservoir size, and CO_2 effective permeability; Zhang et al., 2016a) cap rock properties, (Iglauer et al., 2015a) or aquifer depth and leakage-pathway (Zeidouni et al., 2015). However, although it is well established that brine salinity can vary widely between prospective

storage reservoirs (Morton and Land, 1987; Bachu and Bennion, 2008; Chalbaud et al., 2010; Al-Khdheeawi et al., 2017a), there is a knowledge gap in terms of how this can influence storage efficiency. Importantly, experimental data showed that water salinity has a significant impact on the water-CO_2-rock contact angle θ (i.e. rock wettability; Iglauer, 2017). For example, Arif *et al.* (Arif et al., 2016b) reported that increasing water salinity from 0 wt% (DI water) to 20 wt% leads to an increase in advancing contact angle by 16° (from 59° to 75°) and an increase in receding contact angle by 12° (from 54° to 66°) for a mica surface at 323 K and 15 MPa. Similarly, significant increases were measured for quartz (Al-Yaseri et al., 2016; Espinoza and Santamarina, 2010; Farokhpoor et al., 2013; Jung and Wan, 2012; Saraji et al., 2014; Wang et al., 2012; Broseta et al., 2012; Sarmadivaleh et al., 2015). This effect is caused by a better surface charge screening at higher salinities. Mechanistically, cations move to the negative surfaces charges and shield them, thus reducing the surface potential and surface polarity, which leads to a dewetting of the surface (Iglauer, 2017). Furthermore, salinity has a slight effect on water viscosity (e.g. Denny (Denny, 1993) reported that water viscosity slightly increased from 0.00065 Pa.s for freshwater to 0.00071 Pa.s for seawater, measured at 313 K). Moreover, several studies have shown that brine salinity has a significant impact on CO_2 solubility in the brine,(Rumpf et al., 1994; Duan and Sun, 2003; Spycher and Pruess, 2004; Iglauer, 2011; El-Maghraby et al., 2012) while its impact on CO_2 plume migration, CO_2 mobility and residually trapped CO_2 has not been addressed.

Thus, in this chapter, the effect of salinity (3-20 wt%) on CO_2 plume migration, CO_2 mobility and dissolution and residual trapping in a highly heterogeneous 3D reservoir are computationally examined.

7.2 Methodology

7.2.1 Modelling theory

To study the effect of brine salinity on the CO_2 geo-storage efficiency, a 3D heterogeneous reservoir scale model has been developed using the TOUGH2 simulator (i.e. a nonisothermal multicomponent multiphase flow simulator; Pruess et al., 1999) with the tabular equation of state ECO2M (Pruess, 2011). TOUGH2 and the ECO2M module describe thermodynamic and thermophysical properties (e.g.

viscosity, density and specific enthalpy) of H_2O–NaCl–CO_2 mixtures, as a function of temperature, pressure and salinity (i.e. composition), including super-and sub-critical CO_2 conditions, and CO_2 phase changes; Pruess, 2011). Furthermore, TOUGH2 solves the mass and energy balance equations which describe fluid and heat flow in multiphase and multicomponent systems, for $k = \boldsymbol{1}$ *to* $\boldsymbol{n}$ mass components, by the formula:

$$\frac{d}{dt}\int_{V_n} M^k \, dV_n = \int_{\Gamma_n} F^k \bullet n d\Gamma_n + \int_{V_n} Q^k \, dV_n \tag{7.1}$$

where:

V_n is an arbitrary sub-domain which is bounded by the closed surface Γ_n, M is the mass or energy per volume, k is the mass component labelling factor which represents different mass components (e.g. for water, CO_2, air, solutes...etc.), F is the mass or heat flux, Q is the sink and source term, and $\boldsymbol{n}$ is the surface element $d\Gamma_n$, a normal vector, pointing inward into V_n. Furthermore, TOUGH2 predicts the accumulation of mass based on the following formula:

$$M^k = \phi \sum_{\beta} S_\psi \, \rho_\psi \, X_\psi^k \tag{7.2}$$

where:

ψ is the number of fluid phases (i.e. liquid, gas, non-aqueous phase liquid), ϕ is the system porosity, S_ψ is the saturation of phase ψ, ρ_ψ is the density of phase ψ, and X_ψ^k is the mass fraction of component k in phase ψ. The cumulative mass and heat fluxes are calculated by summing up all individual fluxes, while the multiphase version of Darcy's law is used to compute these individual phase fluxes:

$$F_\psi = \rho_\psi u_\psi = -k \, \frac{k_{r\psi} \, \rho_\psi}{\mu_\psi} (\nabla P_\psi - \rho_\psi \mathrm{g}) \tag{7.3}$$

where:

F_ψ is the individual mass or heat flux, u_ψ is the Darcy velocity of phase ψ, k is the absolute permeability, $k_{r\psi}$ is the phase ψ relative permeability, $\boldsymbol{\mu}_\psi$ is the viscosity of phase ψ, and P_ψ is the pressure of phase ψ.

7.2.2 Model description and initialization

The dimensions of the heterogeneous reservoir model were 1600 m × 1200 m with a thickness of 700 m equivalent to a 37 × 33 × 80 grid (97680 cells in total) as shown in Figure 7-1. The initial water saturation in the reservoir was 100% at isothermal conditions (323 K), and initial pressure was 8 MPa at 800m depth. Pressure at 1500 m depth was 15 MPa assuming a pressure gradient of 10 MPa/km (Dake, 2007). The reservoir outer boundary cells were extended by multiplying their volume by 10^8 to simulate constant pressure boundary conditions (i.e. Dirichlet boundary conditions). (Mo et al., 2005; Nghiem et al., 2009). Porosity and permeability heterogeneity of the SPE comparative solution project (Christie and Blunt, 2001) were used for each grid block to simulate a representative highly heterogeneous reservoir (Figure 7-1). Specifically, porosity ranged from 10% to 47% and permeability ranged from 10 mD to 1000 mD. This comparative solution project was initially developed for the PUNQ project (Floris et al., 1999). The 10^{th} SPE model consists of two parts: The top part is prograding near shore environment, representing the Tarbert formation; and the bottom part is a fluvial reservoir with channel structures representing the Upper-Ness formation (Christie and Blunt, 2001). The vertical to horizontal permeability ratio (k_v/k_h) was reduced from 0.1 in the reservoir to (10^{-4}) at the top boundary of the reservoir to simulate a barrier preventing the CO_2 from leaving the reservoir.

For all investigated brine salinities, (3 wt%, 6 wt%, 10 wt% and 20 wt% NaCl brine), at a reservoir depth of 1373 m, 10 Mton of CO_2 were injected through a one injection well during a 10 years injection period at a rate of 1 Mt/year, which represents the highest Sleipner(Leung et al., 2014; Torp and Gale, 2004) and Quest(Bourne et al., 2014) CO_2 injection rate. This 10 years injection period was followed by a 200 year post-injection period to monitor CO_2 plume development following injection well shut-in. CO_2 plume migration, mobility and residual and dissolution trapping capacities were then computed for this period.

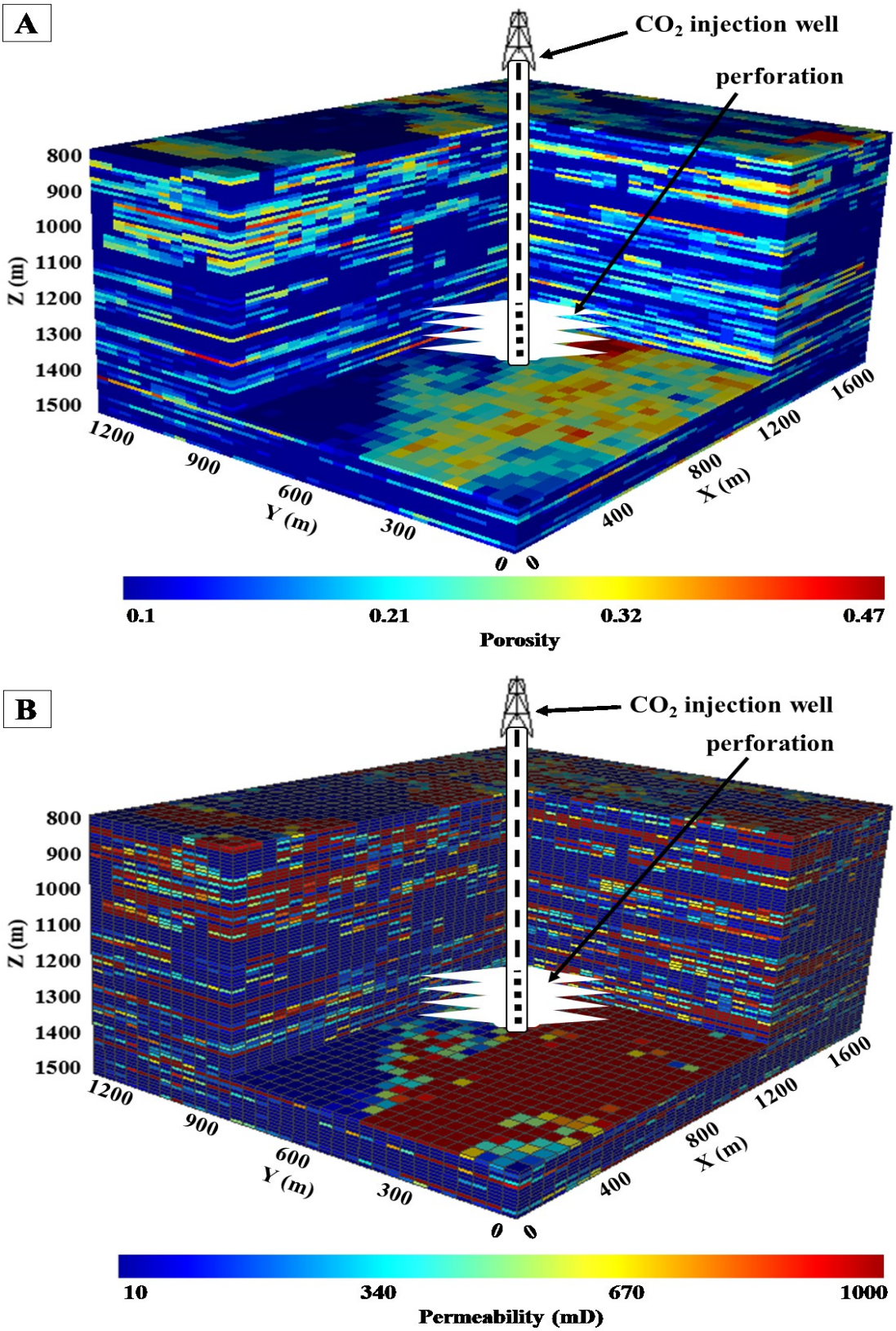

Figure 7-1 3-D reservoir model showing CO_2 injection well, perforation depth and model dimensions with: A) porosity distribution ; B) permeability distribution.

7.2.3 Implementation of different brine salinity scenarios

Variation in salinity has two effects: i) it influences the characteristics curves (i.e. capillary pressure and relative permeability), which have a significant influence on CO_2 migration (Doughty, 2007); and ii) it influences CO_2 solubility in the brine; higher solubilities can be achieved in less saline waters. (Rumpf et al., 1994; Duan and Sun, 2003; Spycher and Pruess, 2004; Iglauer, 2011; El-Maghraby et al., 2012) In terms of point i), Previous studies showed that relative permeability and capillary pressure curves are a function of the rock wettability (i.e. contact angle); while it is clear that brine salinity (and composition) changes the CO_2-rock wettability (increasing salinity reduces water wettability). (Al-Yaseri et al., 2016; Arif et al., 2016b; Chiquet et al., 2007; Espinoza and Santamarina, 2010; Farokhpoor et al., 2013; Jung and Wan, 2012; Saraji et al., 2014; Wang et al., 2012; Broseta et al., 2012; Sarmadivaleh et al., 2015) This shift in wettability (i.e. variation in the contact angle value) is thus the reason for the changes in relative permeability, (Al-Khdheeawi et al., 2017c; Al-Khdheeawi et al., 2017b; Levine et al., 2014; Krevor et al., 2012; Anderson, 1987b; Heiba et al., 1983; McCaffery and Bennion, 1974; Owens and Archer, 1971) capillary pressures,(Al-Khdheeawi et al., 2017c; Al-Khdheeawi et al., 2017b; Pini et al., 2012; Pini et al., 2013; Heiba et al., 1983; Batycky et al., 1981; Morrow, 1976; Melrose, 1965; Anderson, 1987a) and residual saturations. (Rahman et al., 2016; Al-Menhali et al., 2016; Ruprecht et al., 2014; Chaudhary et al., 2013; Akbarabadi and Piri, 2013; Iglauer et al., 2011; Pentland et al., 2011; Craig, 1993) Here, we implemented the impact of salinity via a pair of relative permeability and capillary pressure curves for each brine salinity. Thus, we modified here our recently developed relative permeability and capillary pressure curves for a water-wet system (Al-Khdheeawi et al., 2017c; Al-Khdheeawi et al., 2017b) by adjusting them for different CO_2-water wettabilities (i.e. for different salinities) using the Craig's rules of thumb(Craig, 1993) to consider different brine salinities.

We then modified these curves as follows to consider different brine salinities. (Craig, 1993)

Initially, for all salinity scenarios, water relative permeability (k_{rw}) was 1 and gas relative permeability (k_{rg}) was 0 to simulate a fully brine saturated aquifer (Figure 7-2; A). During CO_2 injection (drainage), k_{rw} decreased from 1 to 0 and k_{rg} increased from 0 to 1 at the endpoints (i.e. residual water and residual CO_2 saturations). During water

influx (imbibition) k_{rg} decreased again from 1 to 0 (at S_{gr}) and k_{rw} increased from 0 until it reached its maximum value at S_{gr} (Figure 7-2; B). Importantly, S_{gr} decreases with increasing brine salinity, because higher salinity increases CO_2-wettability (Al-Yaseri et al., 2016; Arif et al., 2016b; Chiquet et al., 2007; Espinoza and Santamarina, 2010; Farokhpoor et al., 2013; Jung and Wan, 2012; Saraji et al., 2014; Wang et al., 2012; Broseta et al., 2012; Sarmadivaleh et al., 2015) and S_{gr} is a function of wettability (i.e. increasing CO_2 wettability reduces S_{gr}).(Rahman et al., 2016; Al-Menhali et al., 2016; Ruprecht et al., 2014; Chaudhary et al., 2013; Akbarabadi and Piri, 2013; Iglauer et al., 2011; Pentland et al., 2011; Craig, 1993) Furthermore, lower salinity (i.e. lower CO_2-wettability) shifts the k_{rw} curves downwards, and the k_{rw}-k_{rg} intercept point towards the right (i.e. to a higher residual water saturation,(Craig, 1993) Figure 7-2).

The curves were subsequently implemented in the Van Genuchten-Mualem model,(Van Genuchten, 1980; Mualem, 1976) cp. also Figure 7-2:

$$k_{rw} = \sqrt{S^*}\left\{1-\left(1-[S^*]^{1/\lambda}\right)^{\lambda}\right\}^2 \quad \text{if } S_w < S_{ws} \tag{7.4}$$

$$k_{rw} = 1 \quad \text{if } S_w \geq S_{ws} \tag{7.5}$$

$$k_{rg} = 1 - k_{rw} \quad \text{if } S_{gr} = 0 \tag{7.6}$$

$$k_{rg} = \left(1-\hat{S}\right)^2\left(1-\hat{S}^2\right) \quad \text{if } S_{gr} > 0 \tag{7.7}$$

$$\left(P_{cap}\right) = P_0\left([S^*]^{-1/\lambda}-1\right)^{1-\lambda} \tag{7.8}$$

$$S^* = (S_w - S_{wr})/(S_{ws} - S_{wr}),\quad \hat{S} = (S_w - S_{wr})/(1 - S_{wr} - S_{gr}) \tag{7.9}$$

where:

k_{rg} = gas relative permeability, k_{rw} = water relative permeability,

S_{gr} = residual saturation for gas, S_w = water saturation,

S_{ws} = saturated water saturation (= 1), S_{wr} = residual saturation for water

P_c = CO_2-water capillary pressure, P_o = capillary pressure scaling factor.

λ = pore size distribution index (fitting parameter),

The influence of reservoir heterogeneity (i.e. porosity and permeability heterogeneity) on the capillary pressure curves for each grid cell was implemented via the Leverett J-function,(Leverett, 1941) cp. Figure 7-3:

$$J(S_w) = \frac{P_c}{\sigma \cos \Theta} \sqrt{\frac{k}{\phi}} \tag{7.10}$$

where

J = dimensionless capillary pressure, k = reservoir permeability,

ϕ = reservoir porosity, σ = CO_2-brine surface tension,

θ = CO_2-brine-rock contact angle.

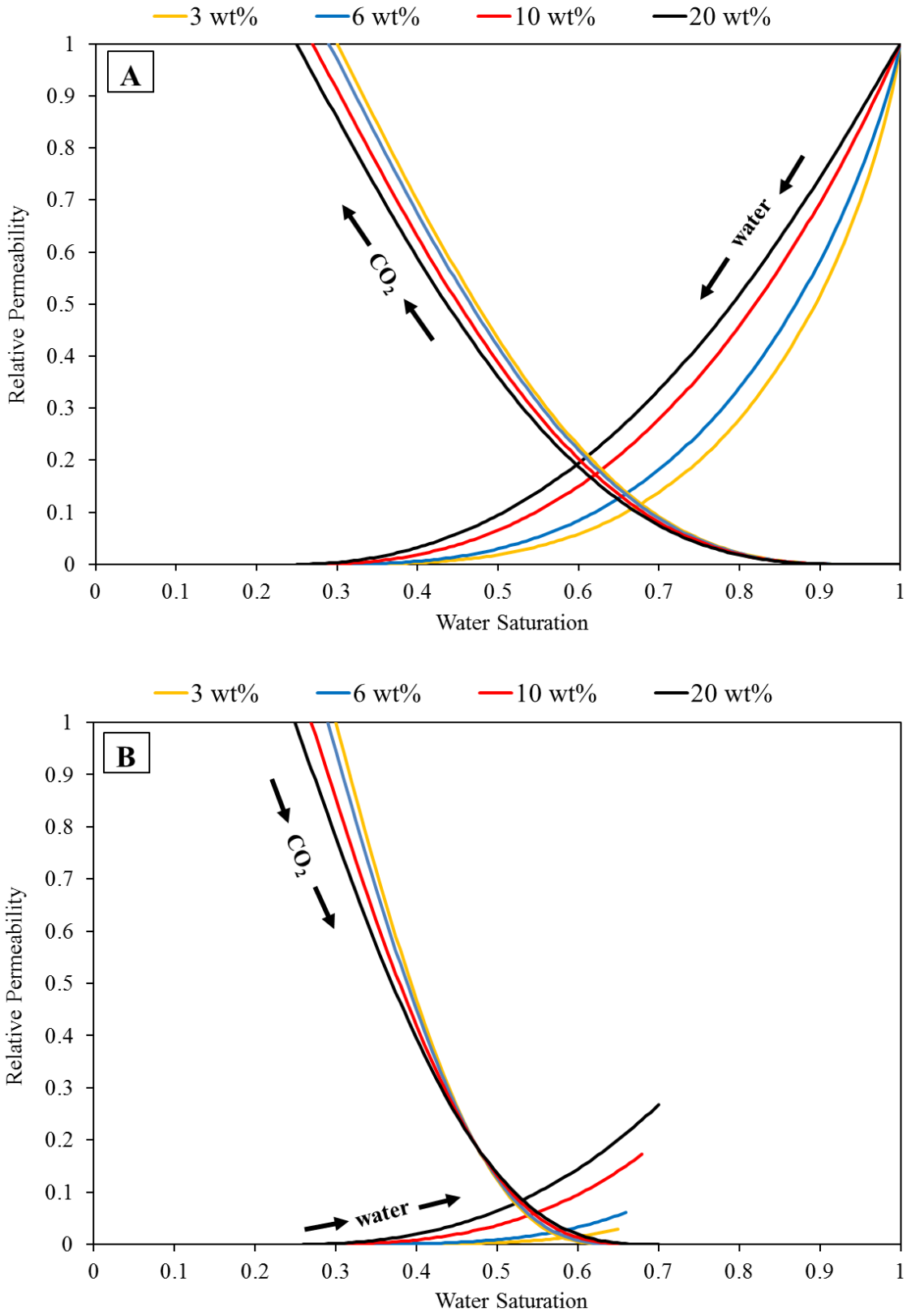

Figure 7-2 Relative permeability curves used for the different salinity scenarios: A) CO_2 injection (drainage); B) CO_2 storage (imbibition).

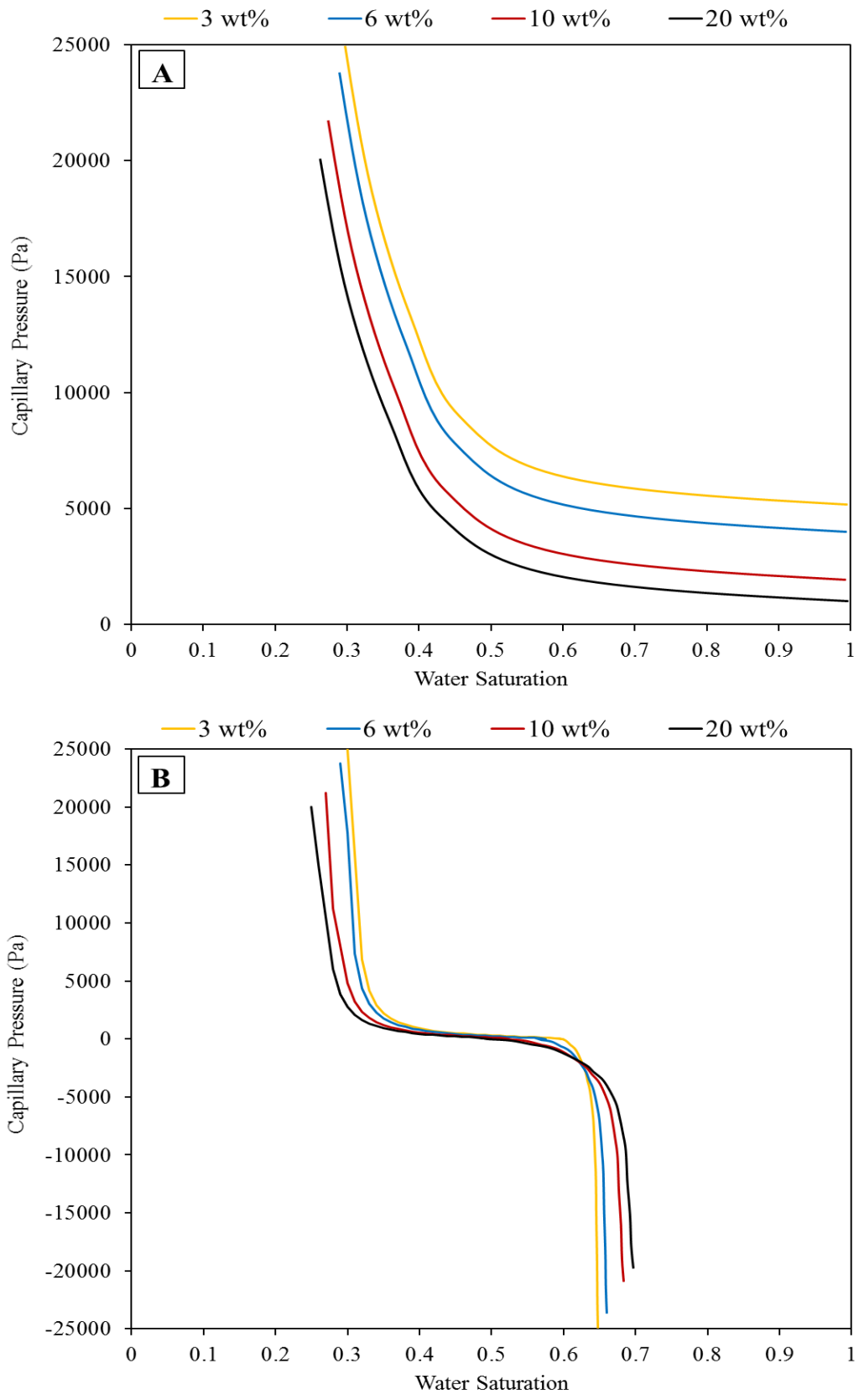

Figure 7-3 Capillary pressure curves used for the 4 different salinity scenarios: A) CO_2 injection (drainage); B) CO_2 storage (imbibition).

7.3 Results and discussion

7.3.1 Impact of salinity on CO_2-plume migration

Clearly, brine salinity has a significant impact on the plume shape and its migration distance (Figure 7-4). Specifically, lower brine salinities reduced vertical CO_2 plume migration distance during the whole storage period (0-200 years; for instance the highest CO_2 plume depth reached was 1090 m for 3 wt% salinity, 1069 m for 6 wt% salinity, 1012 m for 10 wt% salinity and 906 m for 20 wt% salinity; after 200 years, (Figure 7-5). This is equivalent to a vertical CO_2 plume migration distance of 283 m for 3 wt% salinity, 304 m for 6 wt% salinity, 361 m for 10 wt% salinity and 467 m for 20 wt% salinity (after 200 years storage time, (Figure 7-6).

This increase in migration distance with increasing salinity is caused by the shift in the characteristics curves (i.e. relative permeability and capillary pressure); recall that salinity affects the CO_2-rock wettability, and increasing brine salinity leads to reduced water wettability. (Al-Yaseri et al., 2016; Arif et al., 2016b; Chiquet et al., 2007; Espinoza and Santamarina, 2010; Farokhpoor et al., 2013; Jung and Wan, 2012; Saraji et al., 2014; Wang et al., 2012; Broseta et al., 2012; Sarmadivaleh et al., 2015)

This wettability shift causes the change in relative permeabilities (Figure 7-2) and capillary pressures (Figure 7-3), see discussion above. (Craig, 1993; Al-Khdheeawi et al., 2017c; Al-Khdheeawi et al., 2017b) Importantly, these characteristics curves have a significant influence on CO_2 migration.(Doughty, 2007) Furthermore, CO_2 migration increases with decreasing S_{gr} (Doughty, 2010) and thus with decreasing water-wettability (note that S_{gr} decreases when water wettability is reduced.(Rahman et al., 2016; Al-Menhali et al., 2016; Chaudhary et al., 2013)

In summary, our results indicate that brine salinity has a significant impact on CO_2 plume behaviour and its vertical migration distance; we conclude that lower brine salinity is preferable as it reduces CO_2 migration implying higher containment security.

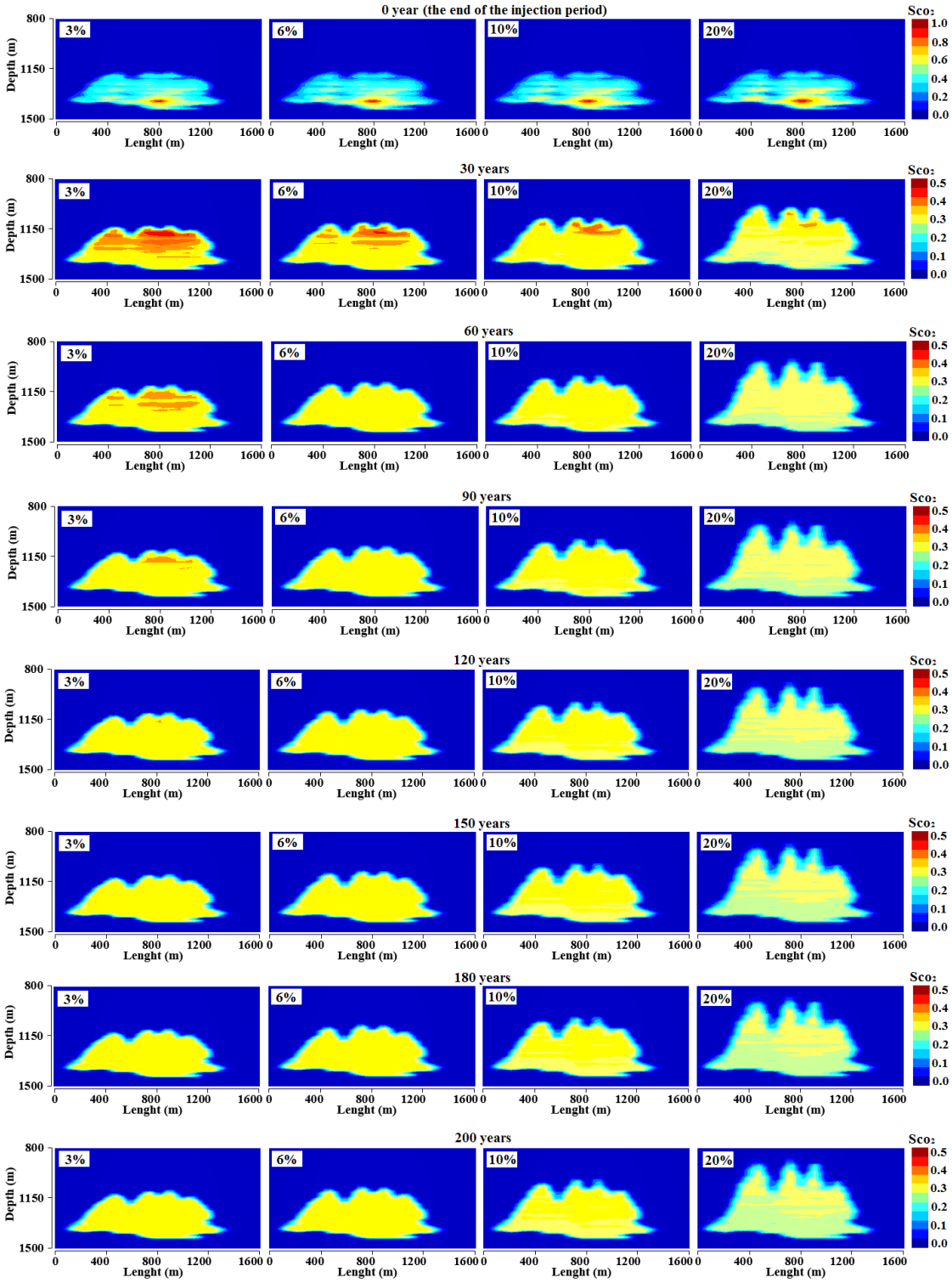

Figure 7-4 2D cross-sections through the middle of the storage reservoir. The CO_2 injection point is at a depth of 1373 m and a length of 800 m. CO_2 plume shape and migration are shown as a function of storage time and brine salinity; clearly salinity has a significant influence. 10 Mton of CO_2 were injected.

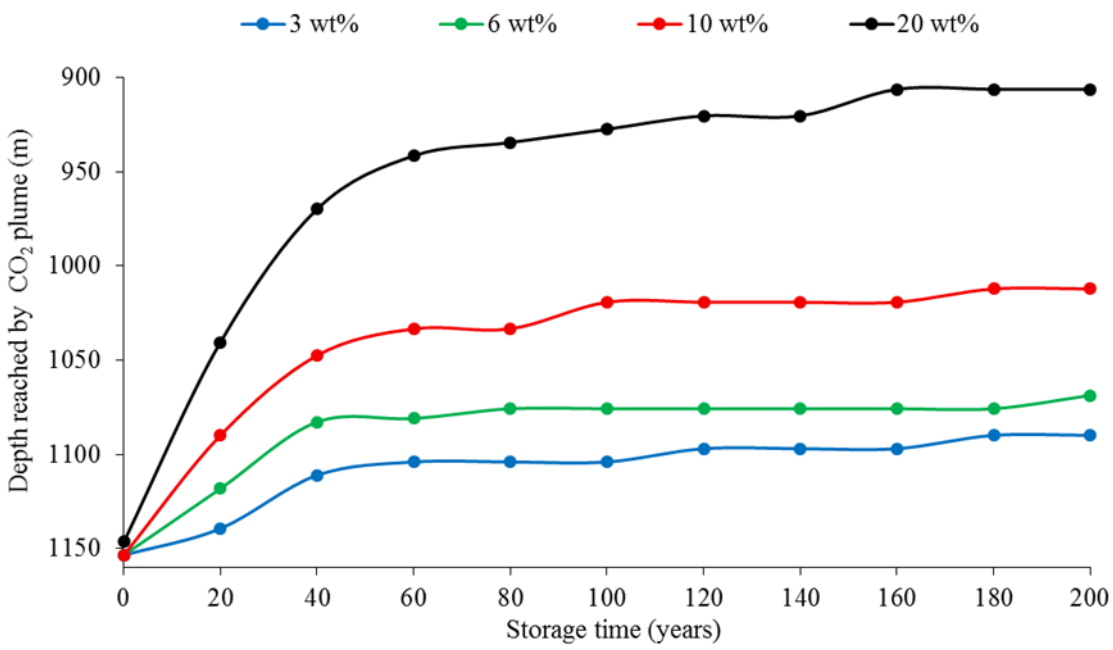

Figure 7-5 Reservoir depth reached by CO_2 plume as a function of storage time and salinity.

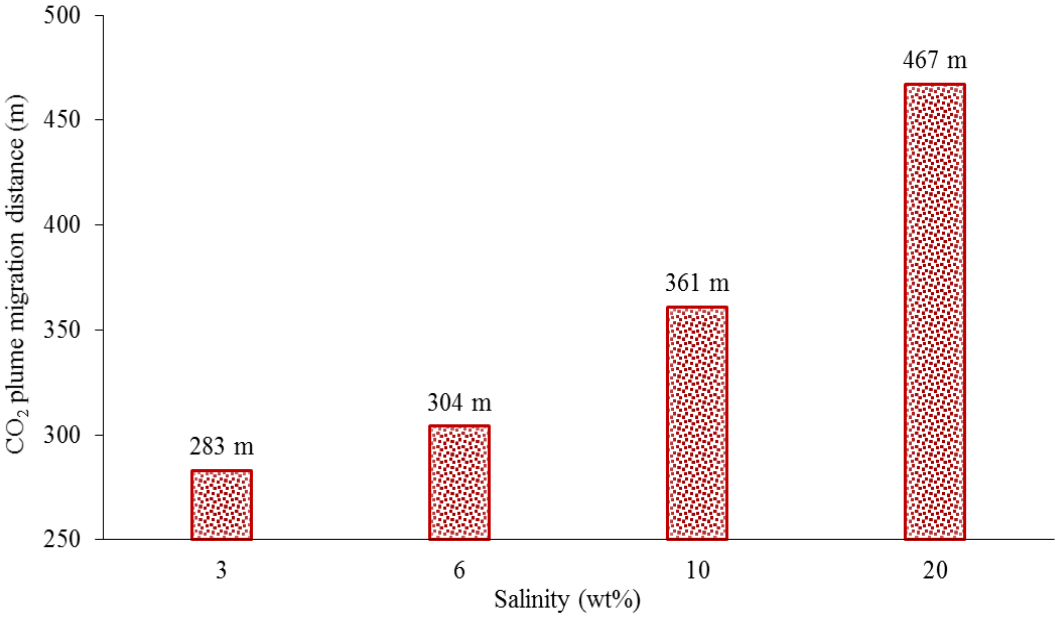

Figure 7-6. Total vertical CO_2 plume migration distance for the four salinity scenarios at the end of the storage period (after 200 years). The numbers indicate the exact distances.

7.3.2 Impact of salinity on CO_2 trapping capacity

Clearly, brine salinity has a considerable impact on solubility and residual (=capillary) trapping. Firstly, higher salinities lead to higher CO_2 mobility (following mobile CO_2 quantities were predicted after a 200 years storage period: 414 kton for 3 wt% salinity, 721 kton for 6 wt% salinity, 1135 kton for 10 wt% salinity, and 1760 kton for 20 wt% salinity; Figure 7-7 and Table 7-1), mainly due to the shifts in characteristics curves (see Figure 7-2 and discussion above). Related to this, capillary trapping capacities(Iglauer et al., 2011) are reduced in more saline brines (e.g. residual trapping capacity was 6445 kton for 20 wt% salinity, 6889 kton for 10 wt% salinity, 7219 kton for 6 wt% salinity and 7434 kton for 3 wt% salinity; at the end of the storage period after 200 years, Figure 7-8 and Table 7-1). This is consistent with our previous prediction that increased water wettability reduces the amount of mobile CO_2 and enhances residual trapping.(Al-Khdheeawi et al., 2017c; Al-Khdheeawi et al., 2017b)

Moreover, it is also clear that lower brine salinity enhances solubility trapping (e.g. solubility trapping capacity was 1795 kton for 20 wt% salinity, 1976 kton for 10 wt% salinity, 2060 kton for 6 wt% salinity and 2152 kton for 3 wt% salinity; at the end of the storage period after 200 years, Figure 7-9 and Table 7-1). This is mainly driven by the higher thermodynamic CO_2 solubility in lower salinity brine.(Rumpf et al., 1994; Duan and Sun, 2003; Spycher and Pruess, 2004; Iglauer, 2011; El-Maghraby et al., 2012)

Our results thus indicate that brine salinity has a major impact on CO_2 storage efficiency, and we conclude that lower salinities improve CO_2 containment security.

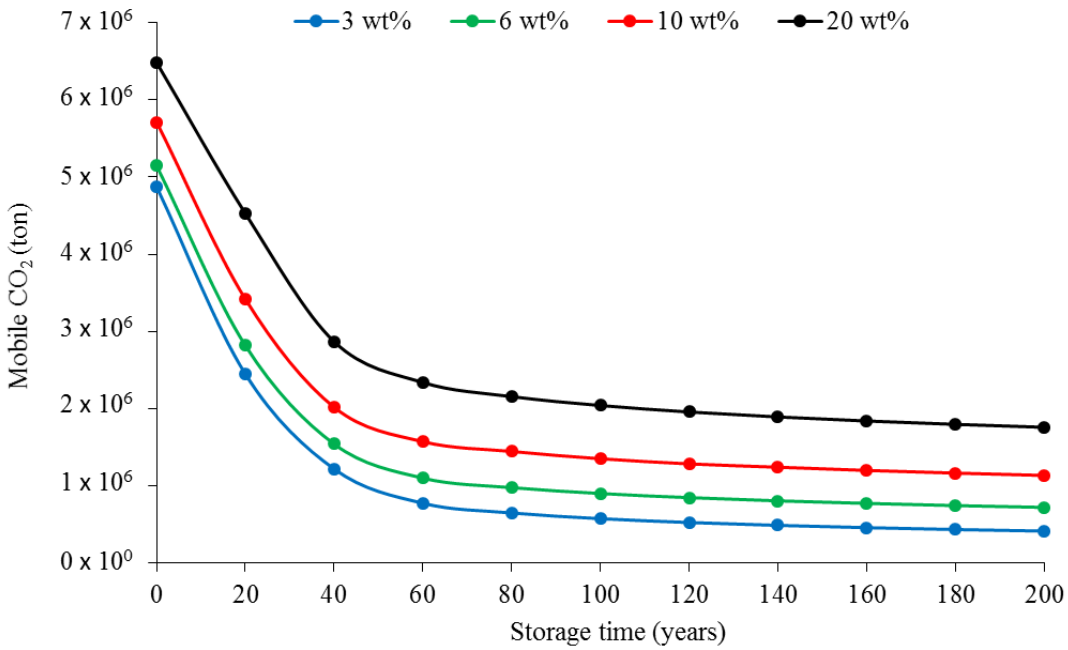

Figure 7-7 Amount of mobile CO_2 as a function of storage time and brine salinity. 10 Mton of CO_2 were injected.

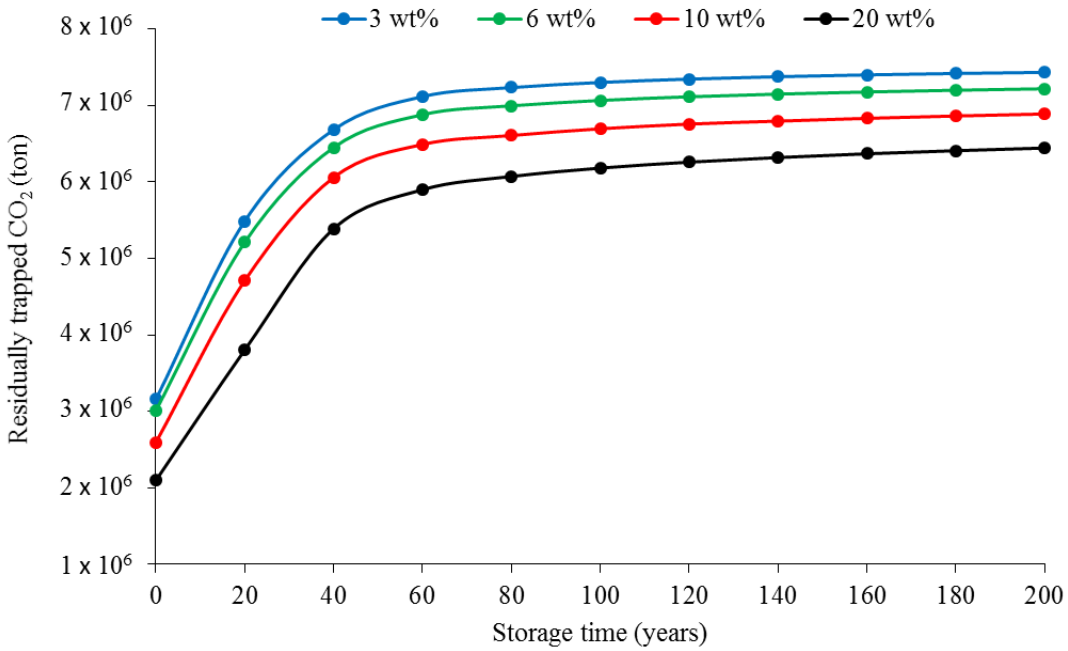

Figure 7-8 Amount of residually trapped CO_2 as a function of CO_2 storage time and brine salinity. 10 Mton of CO_2 were injected.

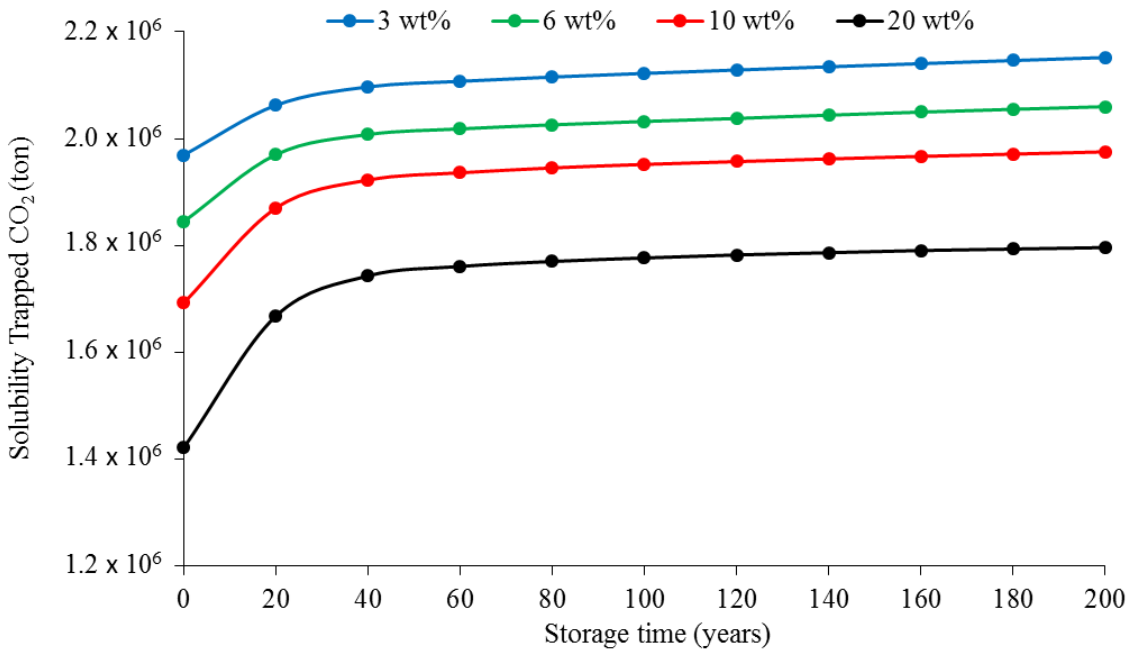

Figure 7-9 Amount of solubility trapped CO_2 as a function of storage time and brine salinity. 10 Mton of CO_2 were injected.

Table 7-1 Amounts of mobile and trapped CO_2 for different salinities after 200 years (at the end of the storage period). In all cases 10 Mt of CO_2 were injected

Salinity wt%	Solubility trapped CO_2 (kton)	Residually trapped CO_2 (kton)	Mobile CO_2 (kton)	Total CO_2 (kton)
3	2152	7434	414	10000
6	2060	7219	721	10000
10	1976	6889	1135	10000
20	1795	6445	1760	10000

7.4 Conclusions

Many factors influence CO_2 geo-storage efficiency, including permeability anisotropy,(Basbug et al., 2005) caprock properties,(Iglauer et al., 2015a) reservoir depth,(Zeidouni et al., 2015) injection well configuration,(Al-Khdheeawi et al., 2017d) stratum dip angle,(Wang et al., 2016a; Wang et al., 2016b) key model

parameters,(Zhang et al., 2016a) reservoir wettability, (Iglauer et al., 2015a; Iglauer et al., 2015b; Al-Khdheeawi et al., 2017c; Al-Khdheeawi et al., 2017b) and the reservoir porosity and permeability heterogeneity. (Doughty and Pruess, 2004; Hovorka et al., 2004; Obi and Blunt, 2006; Bryant et al., 2006; Flett et al., 2007; Ide et al., 2007; Saadatpoor et al., 2009; Zhou et al., 2010; Ambrose et al., 2008; Han et al., 2010; Hesse and Woods, 2010; Green and Ennis-King, 2010; Gershenzon et al., 2015; Gershenzon et al., 2016) One factor, which, however, has not received sufficient attention, is brine salinity, even though it is well established that brine compositions vary widely in prospective storage reservoirs. (Morton and Land, 1987; Bachu and Bennion, 2008; Chalbaud et al., 2010; Al-Khdheeawi et al., 2017a)

We thus computationally investigated the impact of brine salinity on CO_2 storage efficiency. To this end we developed a 3D highly heterogeneous reservoir model and predicted CO_2 migration distance, and the amounts of mobile, residually trapped and solubility trapped CO_2 for four salinity scenarios (i.e. 3 wt%, 6 wt%, 10 wt% and 20 wt% NaCl brines).

Our results indicate that brine salinity has a critical influence on the CO_2 plume migration distance, CO_2 mobility, and trapping capacities. Clearly, lower salinities lead to a reduction in a) the vertical CO_2 plume migration distance, and b) the amount of mobile CO_2; and lower salinities increase residual and solubility trapping capacities (by 10% and 4% over a 200 year storage period). This is consistent with previous predictions that lower water contact angles (i.e. more CO_2-wet rocks) lead to higher CO_2 mobility and less residual trapping (Al-Khdheeawi et al., 2017c; Al-Khdheeawi et al., 2017b).

We thus conclude that, from a trapping capacity and containment security perspective, low salinity reservoirs are preferential CO_2 geo-storage sinks.

Chapter 8 Enhancement of CO_2 Trapping Efficiency in Heterogeneous Reservoirs by Water Alternating Gas Injection

8.1 Introduction

Underground storage of carbon dioxide into geological formations is currently one proposed strategy to mitigate CO_2 emissions that result from various industrial activities (Benson and Cole, 2008; Bachu and Adams, 2003; Pruess et al., 2003). However, because of the density difference between the injected CO_2 (the lighter phase, even though CO_2 is in a supercritical state at the injection depth) and the formation water (the heavier phase), CO_2 moves upward with a risk of leakage through pathways such as faults, micro fractures or existing wells (Vialle et al., 2016). One way to mitigate this CO_2 leakage risk is to reduce the vertical CO_2 migration (which is induced by the above mentioned buoyancy forces) by increasing the efficiency of the different CO_2 trapping mechanisms. These mechanisms include structural trapping (caprock barrier) (Iglauer et al., 2015a; Hesse and Woods, 2010), capillary trapping (Iglauer et al., 2011; Iglauer and Wülling, 2016; Krevor et al., 2015; Pentland et al., 2011; Ruprecht et al., 2014; Suekane et al., 2008; Rahman et al., 2016), solubility trapping (Emami-Meybodi et al., 2015; Iglauer, 2011; Spycher et al., 2003) and mineral trapping (Bachu et al., 1994b; Gaus, 2010; Metz et al., 2005; Xu et al., 2003; Xu et al., 2004; Xu et al., 2005).

The effectiveness of the trapping mechanisms depends on various geological and hydraulic parameters, including geological reservoir heterogeneities (Al-Khdheeawi et al., 2017b; Ambrose et al., 2008; Doughty and Pruess, 2004; Flett et al., 2007; Gershenzon et al., 2015; Gershenzon et al., 2016; Gershenzon et al., 2017; Green and Ennis-King, 2010; Hovorka et al., 2004; Saadatpoor et al., 2009), caprock properties(Iglauer et al., 2015a; Naylor et al., 2011), CO_2-rock wettability (Al-Khdheeawi et al., 2017b; Al-Khdheeawi et al., 2017c; Al-Khdheeawi et al., 2017d; Iglauer et al., 2015b; Iglauer, 2017; Al-Menhali et al., 2015; Al-Khdheeawi et al., 2017e; Chaudhary et al., 2013), reservoir temperature (Al-Khdheeawi et al., 2018a), wettability heterogeneity (Al-Khdheeawi et al., 2018a) and brine salinity (Al-Khdheeawi et al., 2018; Al-Khdheeawi et al., 2017a). In addition, while many

geological parameters cannot be changed for a particular site, it has been shown that intelligent selection of CO_2 injection technology (e.g. the well configuration) can significantly improve storage capacity and containment security (Al-Khdheeawi et al., 2017d; Anchliya and Ehlig-Economides, 2009).

Here, we investigate and discuss a process that can be controlled, namely the CO_2 injection scheme. Specifically, we compare the efficiency of a Water-Alternating-Gas (WAG) injection with the traditionally implemented continuous CO_2 injection, used in most of the current CCS projects in the world such as the Sleipner project in Norway (Adam, 2001), and the Quest project in Canada (Bourne et al., 2014). WAG injection could indeed affect the CO_2 storage efficiency because of its well-known role in improving both the microscopic and macroscopic sweep efficiencies in oil reservoirs (Rogers and Grigg, 2001; Zheng and Yang, 2013). Even though WAG technology has been widely used in various industrial applications such as enhanced oil recovery (EOR) (Christensen et al., 2001; Dang et al., 2016; Fatemi and Sohrabi, 2013; Kulkarni and Rao, 2005; Laochamroonvorapongse et al., 2014; Sohrabi et al., 2004; Song et al., 2014b; Teklu et al., 2016), its effect on CO_2 trapping efficiency has not been addressed.

In this chapter, we therefore compare three different CO_2 injection scenarios, namely continuous CO_2 injection, intermittent CO_2 injection, and water alternating gas injection, using numerical multiphase flow simulations in a highly heterogeneous, hectometre-sized storage formation. For each injection scenario, we compute the vertical CO_2 plume migration distance, solubility trapping and capillary trapping capacities over a period of 100 years after the CO_2 injection has ceased. The results of this study show that WAG injection leads to significantly improved storage capacity and containment security: this is an important result for the commercial development and public acceptance of this technology.

8.2 Methodology

To test the efficiency of the different injection scenarios, (i.e. continuous, intermittent, and water alternating gas injection), hectometer scale reservoir simulations were conducted, and the predicted trapping parameters were quantified and compared. Note

that, for all tested injection scenarios, one geological scenario (i.e. heterogeneous reservoir) has been used.

8.2.1 Model characteristics

A heterogeneous reservoir with dimensions 1600 m × 1200 m × 700 m (with a regular Cartesian grid containing 37 × 33 × 80 = 97680 grid blocks) was employed. Geological reservoir heterogeneity parameters (i.e. porosity and permeability distribution) were taken from the SPE comparative solution project (Figure 8-1) (Christie and Blunt, 2001). This comparative solution project was initially developed for the PUNQ project (Floris et al., 1999). The model parameters are tabulated in Table 8-1.

Fluid flow was simulated using the nonisothermal multicomponent multiphase flow simulator TOUGH2 (Pruess et al., 1999) combined with the ECO2M module (Pruess, 2011). ECO2M computes the thermodynamic and thermophysical properties (e.g. viscosity, density and specific enthalpy) of H_2O, NaCl and CO_2 mixtures, including phase changes and compositions (Pruess, 2011).

In all injection scenarios, 5 Megatonnes (Mt) of CO_2 were injected at a depth of 1373 m over a 10 year period. For the continuous CO_2 injection, a continuous injection rate of 0.5 Mt/year was used. For the intermittent injection, 5 CO_2 injection cycles, at a rate of 1 Mt/year each was employed; each injection was followed by a 1 year shut-off period. In the WAG injection, 5 CO_2 injection cycles at a rate of 1 Mt/year were also carried out, but now each injection was followed by a 1 year water injection period at a rate of 3 Mt/year. All injections were followed by a 100 year observation period (post-injection period) for which the vertical CO_2 plume migration distance, solubility and capillary trapping capacities were computed and subsequently analysed.

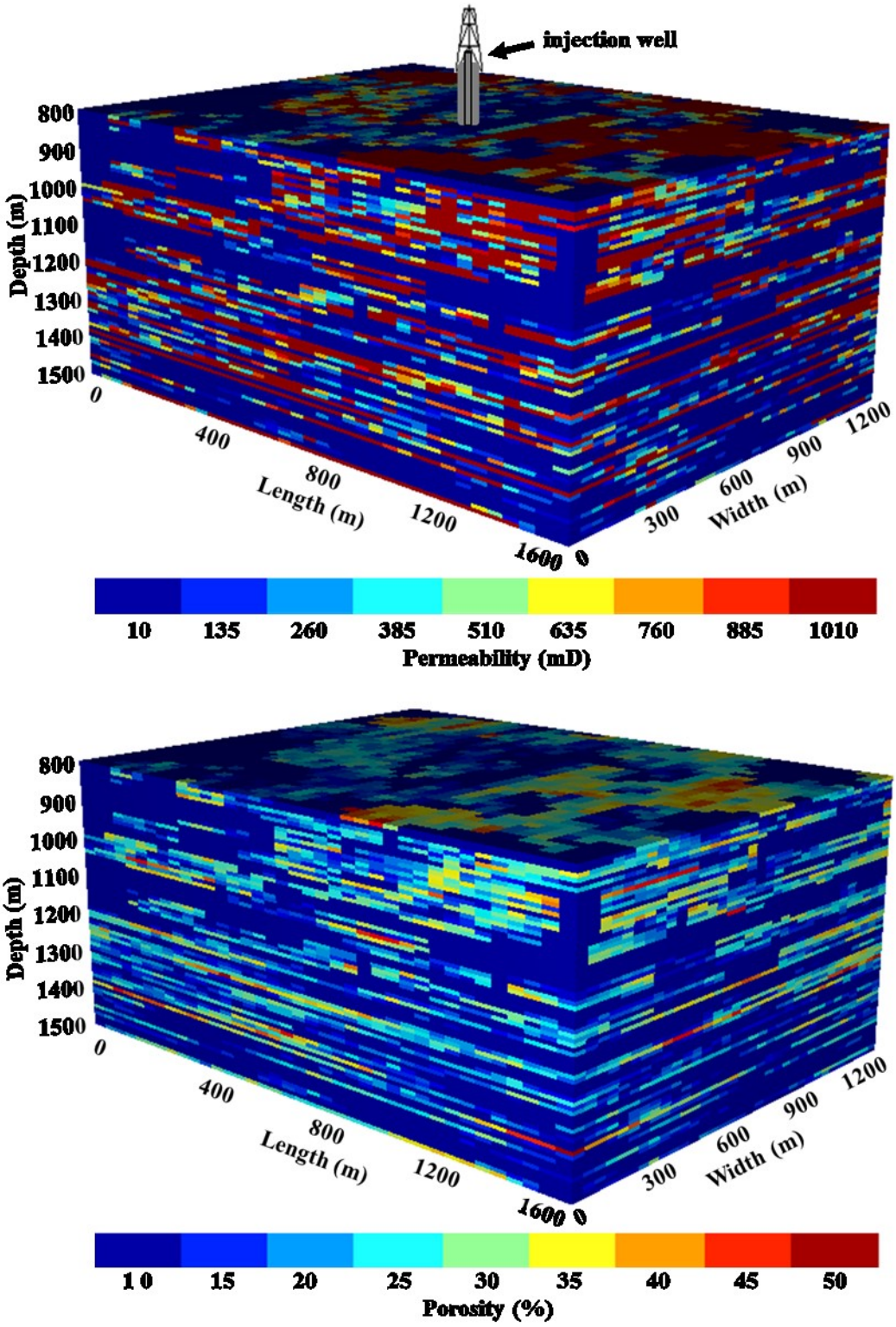

Figure 8-1 3D views of the heterogeneous model showing the location of the CO_2 and water injection well, model dimensions and permeability heterogeneity (on top) and porosity heterogeneity (on bottom).

Table 8-1 Reservoir model parameters

Property	**Value**
Length	1600 m
Width	1200 m
Thickness	700 m
Depth of the top of the reservoir	800 m
Depth of the bottom of the reservoir	1500 m
Grid block number	37 × 33 × 80 = 97680 grid blocks
k_v/ k_h in the storage reservoir	0.1
k_v/ k_h at the top layer of the reservoir[a]	10^{-6}
Boundary cells volume multiplier[b]	10^8
Brine salinity	60000 ppm
Initial pore pressure at 1200 m depth	12 MPa
Pressure gradient[c]	0.01 MPa/m
Reservoir temperature (isothermal)	333 K
Initial water saturation	100%
Injection depth	1373 m
Dip of the strata	0^0 (i.e. horizontal reservoir)

[a]The vertical to horizontal permeability ratio (k_v/k_h) is reduced to 10^{-6} at the top layer cells of the reservoir to simulate a barrier preventing the CO_2 from leaking out of the model (Al-Khdheeawi et al., 2017b; Al-Khdheeawi et al., 2017c; Al-Khdheeawi et al., 2017d; Hesse and Woods, 2010; Birkholzer et al., 2009; Zhou et al., 2008).

[b]The volumes of the bottom and side boundary cells have been multiplied by a factor of 10E8 to simulate constant pressure conditions at the reservoir outer boundaries (Nghiem et al., 2010).

[c]A pressure gradient of 0.01 MPa/m (Dake, 2007) was applied to simulate the hydrostatic pressure gradient in the reservoir.

8.2.2 Implementation of characteristics curves

It has been shown that characteristics curves (i.e. relative permeability and capillary pressure curves) have a significant impact on the CO_2-brine fluid dynamics in the reservoir (Woods and Farcas, 2009; Kopp et al., 2009; Hesse et al., 2008; Doughty, 2007). Thus, for simulating the continuous and intermittent CO_2 injections, we used previously developed relative permeability and capillary pressure curves for an intermediate-wet condition (Al-Khdheeawi et al., 2017b; Al-Khdheeawi et al., 2017c; Al-Khdheeawi et al., 2017d). These curves were built using experimental data (Anderson, 1987b; Anderson, 1987a; Craig, 1993; Batycky et al., 1981; McCaffery and Bennion, 1974; Melrose, 1965; Morrow, 1976; Owens and Archer, 1971). Intermediate-wet conditions were chosen as this is the most likely wettability scenario in CO_2-brine deep saline aquifer systems (Iglauer et al., 2014; Iglauer et al., 2015a; Iglauer et al., 2015b; Iglauer, 2017). In addition, rock wettability has a significant effect on the residual water and gas saturations (Anderson, 1987a; Anderson, 1987b; Craig, 1993; Iglauer et al., 2011). Specifically, for the construction of the relative permeability curves, we used McCaffery and Bennion's data (1974). We used Didger software (Golden Software Inc, 2013, Colorado) to digitize these curves and obtain data for the relative permeability values as a function of water saturation; we adjusted these curves using Craig's rules of thumb (Craig, 1993). Hence, to simulate the intermediate-wet wettability condition, we used the values of 0.22 for S_{wr} and 0.25 for $\boldsymbol{S_{co_2r}}$ as in our recent publications (Al-Khdheeawi et al., 2017b; Al-Khdheeawi et al., 2017c; Al-Khdheeawi et al., 2017d). In addition, the water saturation (S_w) at which the CO_2 relative permeability of CO_2 ($\boldsymbol{k_{rco_2}}$) and that of water (k_{rw}) are equal was selected to be 0.5 according to Craig's rule of thumb (Craig, 1993).[74] For all injection scenarios, initially k_{rw} is set to 1 and $\boldsymbol{k_{rco_2}}$ to 0, which corresponds to full (100%) water saturation. During the first CO_2 injection process k_{rw} reduces gradually, while $\boldsymbol{k_{rco_2}}$ increases until it reaches a maximum at the irreducible water saturation (S_{wr}).

Furthermore, and importantly, these characteristics curves, and the associated residual gas and water saturations (Herring et al., 2013; Herring et al., 2015; Herring et al., 2016; Skauge and Larsen, 1994; Akbarabadi and Piri, 2013; Benson et al., 2013; Krevor et al., 2011; Krevor et al., 2012; Pini et al., 2012; Reynolds and Krevor, 2015; Tokunaga et al., 2013) were modified based on Herring et al.'s data (Herring et al., 2016) for the WAG scCO_2-brine floods (Figure 8-2 and Figure 8-3). For the first WAG

cycle we used the values of the Sco_2r (residual CO_2 saturation) and Sco_2i (initial CO_2 saturation) of the intermediate-wet rock. Then for the cycles 2-5 the Sco_2r has been enhanced based on the experimental studies (Herring et al., 2013; Herring et al., 2015; Herring et al., 2016; Skauge and Larsen, 1994; Tokunaga et al., 2013). For all five WAG cycles the relationship of the Sco_2r versus Sco_2i followed Pentland's et al. measurements (Pentland et al., 2011). The Genuchten-Mualem model (Van Genuchten, 1980; Mualem, 1976) was then used to import the characteristics curves into the TOUGH2 code:

$$k_{rw} = \sqrt{S^*}\left\{1-\left(1-[S^*]^{1/\lambda}\right)^{\lambda}\right\}^2 \quad \text{if } S_w < S_{ws} \tag{8.1}$$

$$k_{rw} = 1 \quad \text{if } S_w \geq S_{ws} \tag{8.2}$$

$$k_{rco_2} = 1 - k_{rw} \quad \text{if } S_{co_2r} = 0 \tag{8.3}$$

$$k_{rco_2} = \left(1-\hat{\mathrm{S}}\right)^2\left(1-\hat{\mathrm{S}}^2\right) \quad \text{if } S_{co_2r} > 0 \tag{8.4}$$

$$\left(P_{cap}\right) = P_0\left([S^*]^{-1/\lambda}-1\right)^{1-\lambda} \tag{8.5}$$

$$S^* = (S_w - S_{wr})/(S_{ws} - S_{wr}),$$
$$\hat{\mathrm{S}} = (S_w - S_{wr})/(1 - S_{wr} - S_{co_2r}) \tag{8.6}$$

where:

k_{rco_2} = CO_2 relative permeability, k_{rw} = water relative permeability,

S_{co_2r} = CO_2 residual saturation, S_w = water saturation,

S_{ws} = saturated water saturation, S_{wr} = water residual saturation,

P_{cap} = CO_2-water capillary pressure, P_0 = capillary pressure scaling factor.

λ = pore size distribution index,

Moreover, the Leverett J-function (Leverett, 1941) was used to implement the effect of porosity and permeability heterogeneity on the capillary pressure curves for each grid cell:

$$J(S_w) = \frac{P_c}{\sigma \cos\Theta}\sqrt{\frac{k}{\phi}} \tag{8.7}$$

where:

$J(S_w)$ = dimensionless capillary pressure, k = rock permeability,

ϕ = rock porosity, σ = CO_2-water interfacial tension,

Θ = CO_2-water-rock contact angle. Pc = CO_2-water capillary pressure

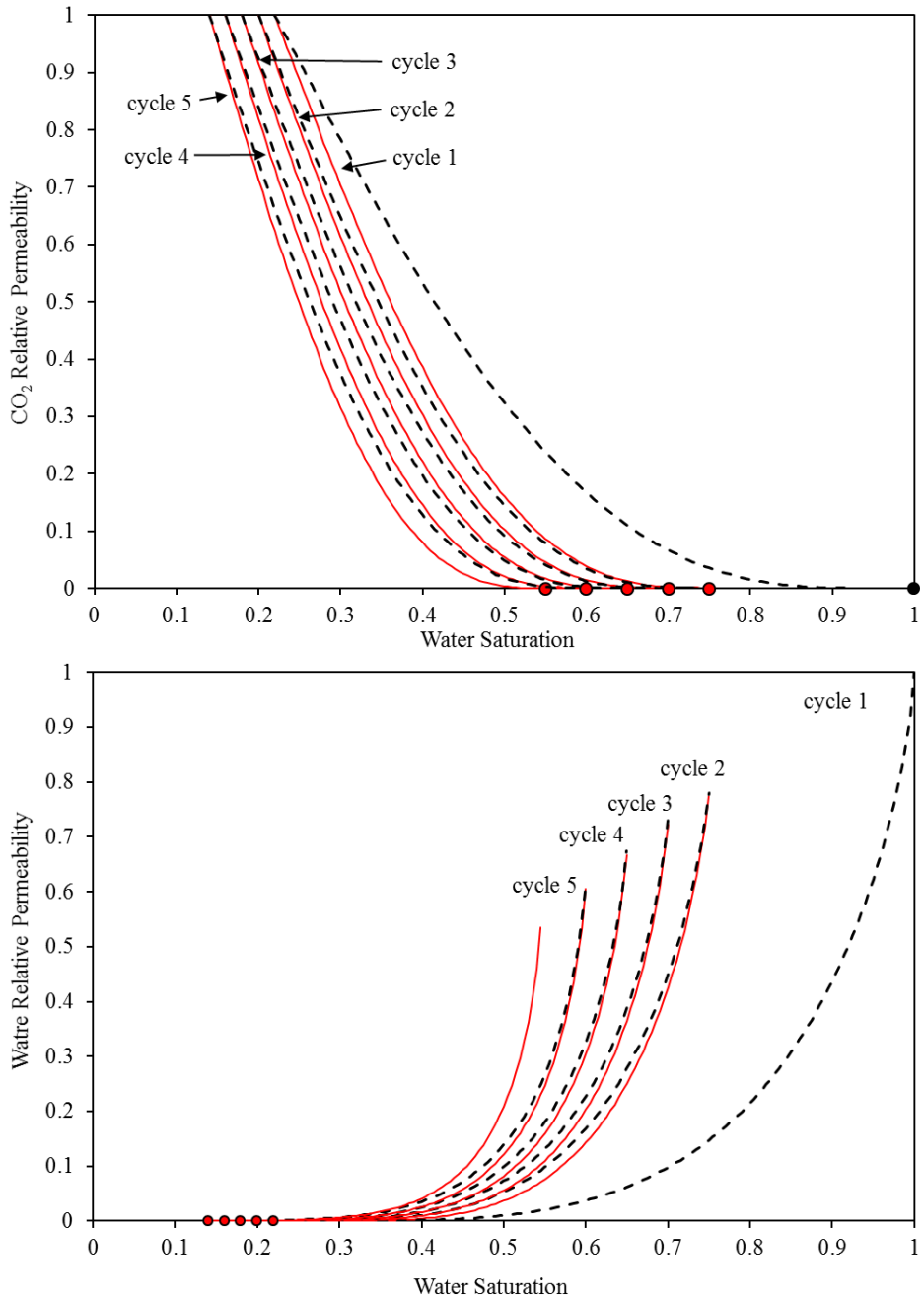

Figure 8-2 CO_2 and water relative permeability curves used for the five water-alternating gas injection cycles. The dashed black lines represent the CO_2 injection process and continuous red lines represent the water injection process. Note that cycle 1 represents the normal drainage and imbibition curves of the intermediate-wet rocks that have been used for the continuous and intermittent injection scenarios. Derived

from Al-Khdheeawi et al. (Al-Khdheeawi et al., 2017b; Al-Khdheeawi et al., 2017c; Al-Khdheeawi et al., 2017d) and extended for different WAG cycles based on the experimental studies (Herring et al., 2013; Herring et al., 2015; Herring et al., 2016; Skauge and Larsen, 1994; Tokunaga et al., 2013).

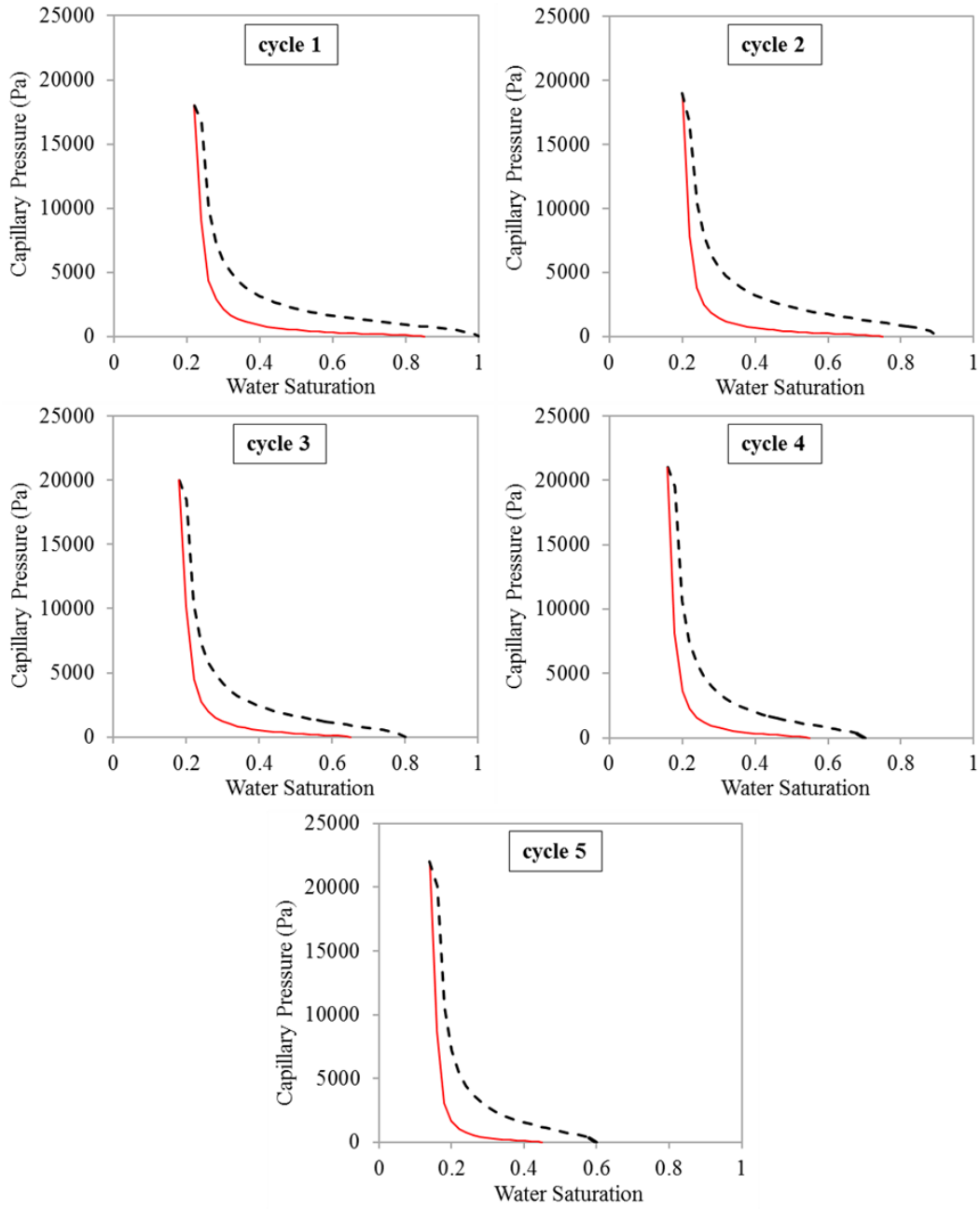

Figure 8-3 Capillary pressure curves used for the five water-alternating gas injection cycles. The dashed black lines represent the CO_2 injection process and continuous red lines represent the water injection process. Note: cycle 1 represents the intermediate-wet rock that underwent normal drainage and imbibition (used for continuous and intermittent injection). Derived from Al-Khdheeawi et al. (Al-Khdheeawi et al.,

2017b; Al-Khdheeawi et al., 2017c; Al-Khdheeawi et al., 2017d) and extended for different WAG cycles based on the experimental studies (Herring et al., 2013; Herring et al., 2015; Herring et al., 2016; Skauge and Larsen, 1994; Tokunaga et al., 2013).

8.3 Results and discussion

8.3.1 Storage capacity enhancement via WAG injection

Generally, in CO_2 geo-sequestration projects, higher vertical CO_2 migration is unwanted, because it increases CO_2 migration risk from the reservoir to the surface, while storage capacities need to be maximized. Here, we thus study the effect of continuous, intermittent and WAG injection on these storage parameters. Our results show that WAG injection had the lowest vertical CO_2 plume migration, less than half of the migration distance compared to continuous or intermittent injections, over the whole post-injection period of 100 years (

Figure 8-4 and Figure 8-5). For example, the results show that the total vertical CO_2 plume migration distance was 432 m for the intermittent injection, 453 m for the continuous injection, and only 198 m in case of WAG, after a 100 year storage period.

Mechanistically, this reduction in vertical CO_2 plume migration was caused by the relatively high residual CO_2 saturation (S_{co_2r}) in WAG (Herring et al., 2016), which diminished vertical CO_2 flow. Importantly, previous studies showed that vertical CO_2 plume migration distance is a function of the residual CO_2 saturation and that lower S_{co_2r} leads to an increase in CO_2 plume migration distance (Metz et al., 2005; Hesse et al., 2008; Doughty, 2010; Al-Khdheeawi et al., 2017b).

We thus conclude that WAG injection leads to a significant reduction in CO_2 leakage risk, implying superior containment security.

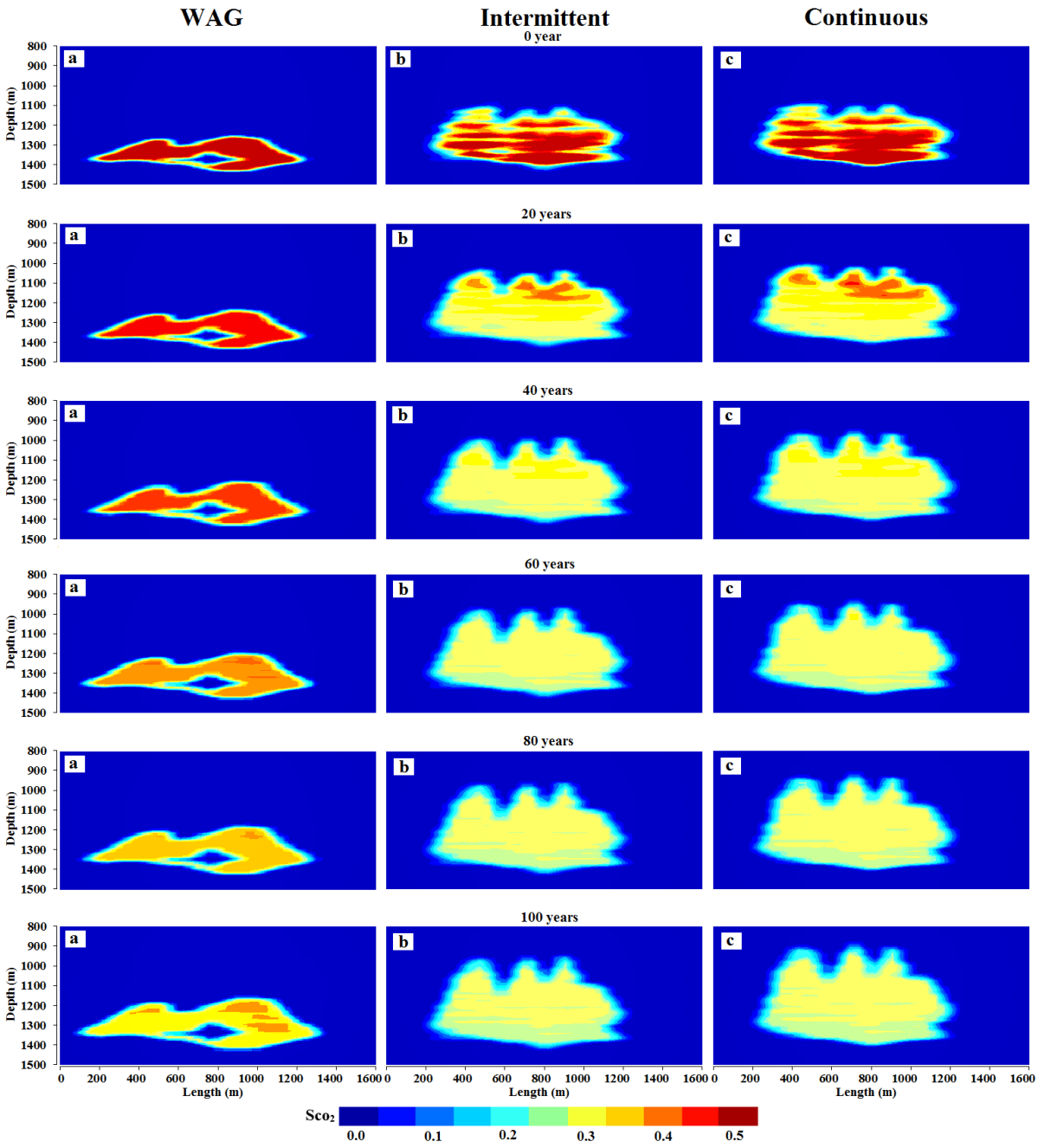

Figure 8-4 2D (X-Z) views through the center of the reservoir showing the CO_2 plume as a function of storage (post-injection) time and CO_2 injection scenario: a) WAG injection, b) intermittent injection, c) continuous injection. Sco_2 represents the supercritical CO_2 saturation.

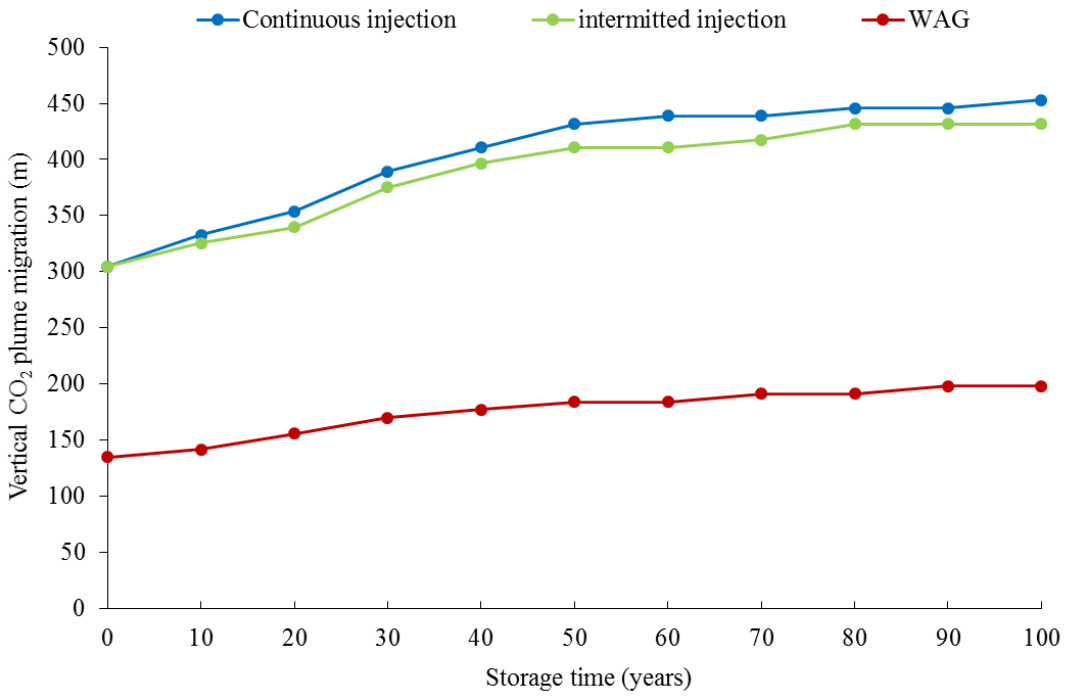

Figure 8-5 Vertical CO_2 plume migration distance as a function of storage time and injection scenario.

8.3.2 Maximising CO_2 trapping

Clearly, WAG injection significantly improves CO_2 trapping efficiency (Figure 8-6). Firstly, WAG maximises residual (capillary) trapping by increasing the residual CO_2 saturation for the imbibition cycle. For instance, after a 100 year storage period, 67% of the CO_2 was residually trapped in case of WAG, while only 52% and 49% (intermittent and continuous injection, respectively) were trapped otherwise. Recall, WAG significantly increases the residual CO_2 saturations (Figure 8-2 and Figure 8-3) (Herring et al., 2016).

Secondly, WAG injection also enhanced solubility trapping. This is of key importance as only CO_2 dissolved in water is truly safely stored and cannot leak back to the surface. As an example, after a 100 year storage period, 30% of the CO_2 was solubility trapped in WAG, while only 21% and 19% (intermittent and continuous injection, respectively) was solubility trapped in the other scenarios. In addition, the maximum mass fraction of CO_2 dissolved in the aqueous phase (XCO_2aq) after the end of the post-injection period (100 years) was ~0.05 for WAG scenario, compared to only ~0.025 for the intermittent and ~0.02 for the continuous CO_2 injection scenarios

(Figure 8-7). The reason for this is the larger lateral CO_2 spreading in cyclic WAG injection, which results in larger CO_2-water contact surface in WAG scenario (Doughty, 2010). Consequently, overall, WAG injection significantly reduces (unwanted) CO_2 mobility (i.e. the amount of free CO_2). In statistical terms, after 100 years the ratio of mobile to total injected CO_2 was only 3% for WAG while it was 27% for intermittent and 32% for continuous CO_2 injection (Figure 8-6).

Furthermore, our simulation results show that WAG injection has a higher overall CO_2 storage efficiency (via both residual and solubility trapping) than simultaneous water and gas injection (SWAG). For instance, after a 100 year storage period, the overall storage efficiency for WAG injection was 97% (i.e. only 3% of CO_2 is free) compared to only 75% (i.e. 25% of CO_2 is free) for the best SWAG injection scenario (Baz et al., 2016). Importantly, our results in terms of improving the storage efficiency by WAG injection are consistent with our previous study performed in homogeneous reservoirs (Al-Khdheeawi et al., 2018b), which concluded that, after a 200 years storage period, water alternating CO_2 ($WACO_2$) injection technology can enhance residual trapping by 13% and dissolution trapping by 14% when compared with the standard continuous CO_2 injection. It is important to mention that changing the boundary conditions may quantitatively affect the estimated trapping efficiencies. However, this change in boundary conditions will not change the basic difference between the different injection scenarios (i.e. the highest trapping efficiency will be obtained in the WAG scenario compared to the other two injection scenarios).

We thus conclude that WAG strongly enhances solubility and residual trapping and minimizes (detrimental) vertical CO_2 mobility, implying much better CO_2 geo-sequestration efficiency. WAG is therefore the preferred injection scheme.

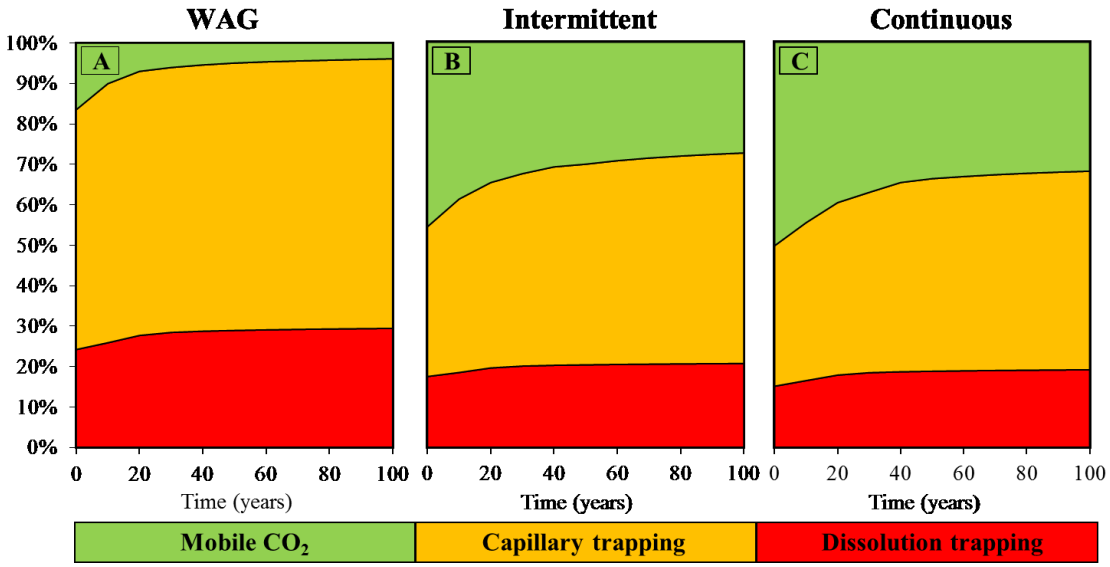

Figure 8-6 Percentage of mobile CO_2 (in green), capillary trapped CO_2 (in yellow) and solubility trapped CO_2 (in red) as a function of post-injection time and CO_2 injection scenario; A) WAG injection, B) intermittent CO_2 injection, C) continuous CO_2 injection. Clearly, WAG is the optimal CO_2 disposal scheme.

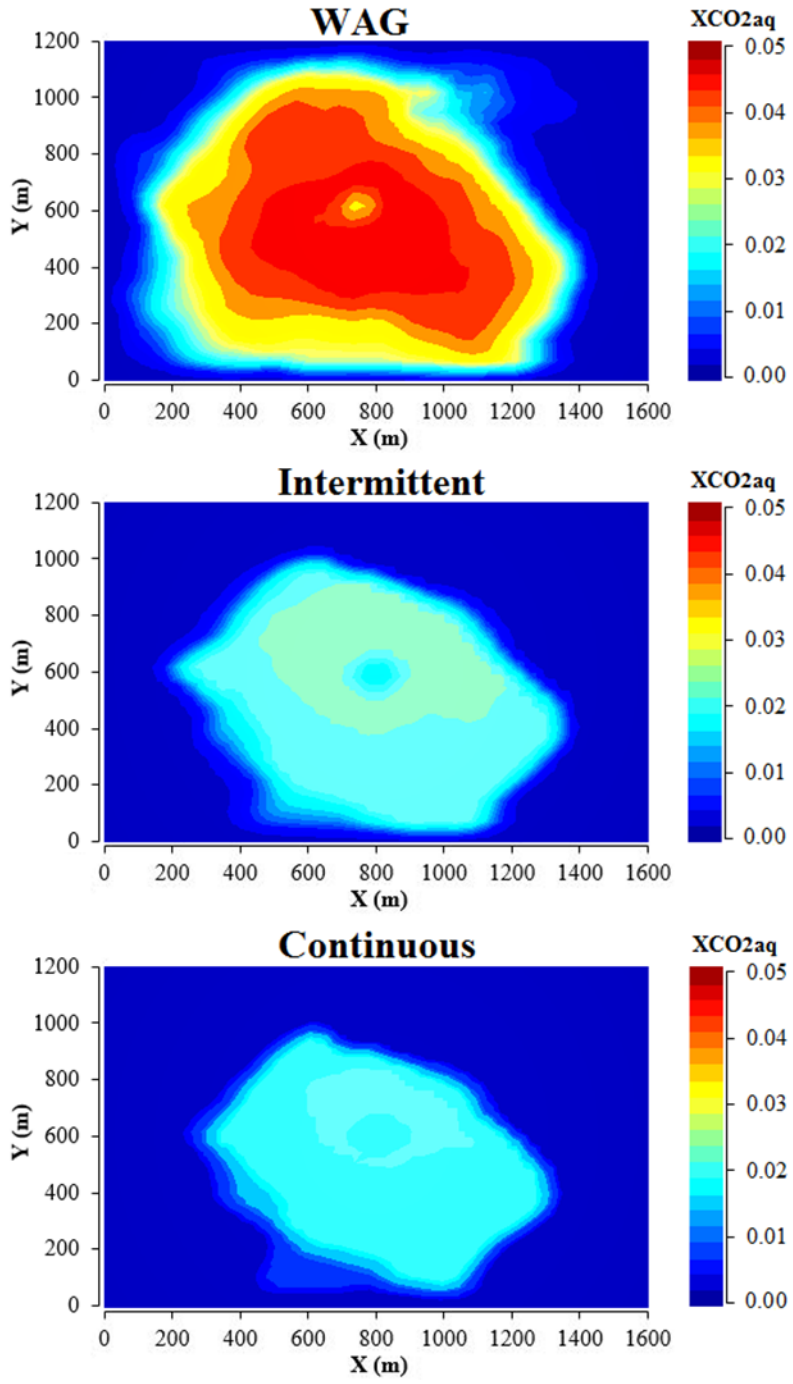

Figure 8-7 2D (X-Y) views through the reservoir at the CO_2 injection point at a depth of 1373 m showing the spreading of the dissolved CO_2 after the post-injection period (100 years) for the different injection scenarios: WAG injection (top), intermittent injection (middle), and continuous injection (bottom). Clearly, WAG has the largest lateral CO_2 spreading area and the highest mass fraction of dissolved CO_2 in aqueous phase (XCO_2aq).

8.4 Conclusions

Carbon dioxide storage in deep saline aquifers is currently considered as the most effective technology to mitigate climate change by reducing CO_2 emissions (Benson and Cole, 2008; Bachu and Adams, 2003; Pruess et al., 2003). The efficiency of CO_2 storage in saline aquifers can be improved either by the accurate evaluation of the various factors affecting CO_2 trapping mechanisms (e.g. reservoir heterogeneity, caprock properties, rock wettability and brine salinity) or by optimising the CO_2 injection technology (Al-Khdheeawi et al., 2017d; Anchliya and Ehlig-Economides, 2009). Although WAG technology has been widely used as an important method to improve the efficiency of enhance oil recovery process (EOR) (Christensen et al., 2001; Dang et al., 2016; Fatemi and Sohrabi, 2013; Kulkarni and Rao, 2005; Laochamroonvorapongse et al., 2014; Sohrabi et al., 2004; Song et al., 2014b; Teklu et al., 2016) and it affects residual gas and water saturations (Herring et al., 2013; Herring et al., 2015; Herring et al., 2016; Skauge and Larsen, 1994; Tokunaga et al., 2013), its effect on the CO_2 trapping efficiency is not completely understood.

Thus, here we investigated how WAG influences CO_2 storage efficiency in one heterogeneous reservoir scenario. Recall that the impact of the WAG injection on the relative permeability and capillary pressure curves, and the associated residual gas and water saturations were simulated based on previous experimental studies (Herring et al., 2013; Herring et al., 2015; Herring et al., 2016; Skauge and Larsen, 1994; Akbarabadi and Piri, 2013; Benson et al., 2013; Krevor et al., 2011; Krevor et al., 2012; Pini et al., 2012; Reynolds and Krevor, 2015; Tokunaga et al., 2013). Our results clearly showed that WAG injection reduced the total vertical CO_2 plume migration (by more than 50%), and that it also reduced CO_2 mobility (by > 24%) when compared with other injection scenarios (i.e. continuous and intermittent injections). In addition, WAG enhanced residual trapping (by ~ 17%) and solubility trapping (by ~ 9%) when compared with the conventional CO_2 injection process (i.e. continuous CO_2 injection).

Thus, we conclude that WAG injection can significantly enhance CO_2 storage efficiency and containment security, and WAG is thus the preferred injection scheme.

Our results have significant implications for enhancing the CO_2-geoseqestration efficiency, especially in CO_2 sequestration projects which rely on residual and

dissolution trapping (e.g. the South West Hub carbon capture and storage project in Western Australia) (Stalker et al., 2013).

Chapter 9 Conclusions, Recommendations and Outlook for Future Work

9.1 Conclusions

In the context of CO_2 geo-sequestration, the flow of CO_2 through porous media, as well as its storage capacity, are highly affected by different parameters. One key parameter, which has received little attention, is the rock wettability. This thesis, for the first time, investigated the influence of the rock wettability and wettability heterogeneity on CO_2 geo-sequestration efficiency and on CO_2 movements through porous media by performing various multiphase flow reservoir simulation models at a hectometre-scale. Importantly, in this thesis, and for the first time, five cases of CO_2-water-rock wettability have been implemented, from strongly water-wet to strongly CO_2-wet. To do so, a pair of relative permeability and capillary pressure curves for each wettability condition has been developed to simulate both CO_2 injection and storage processes. In addition, this thesis also included a sensitivity analysis of the effect of some other reservoir parameters, such as reservoir temperature, formation water salinity and permeability and porosity heterogeneity on CO_2 geo-sequestration efficiency. This thesis also covers the effect of engineering parameters on CO_2 geo-sequestration. Thus, the influence of using different CO_2 injection technologies such as injection well configurations (i.e. vertical and horizontal wells) and CO_2 injection scheme (i.e. continuous injection, intermittent injection, and water-alternating gas (WAG) injection) on CO_2 geo-sequestration efficiency have been investigated.

The thesis concludes that water-wet formations with homogeneous wettability improve the CO_2 geo-sequestration capacity and containment security. Water-wet formations with more homogeneous porosity and permeability distribution, lower formation water salinities, lower reservoir temperatures, and those instrumented with horizontal wells and WAG injection operations, were shown to be superior geo-sequestration candidates. Generally, the findings of this thesis lead to a better understanding of the important effect of rock wettability and wettability distribution, in addition to the effect other reservoir parameters and the used CO_2 injection technology on CO_2 geo-sequestration efficiency and CO_2 movements through porous media. The most significant findings of this thesis are summarized below:

1. Influence of wettability on CO_2 geo-sequestration in homogeneous saline aquifers
   - ❖ CO_2-wettability of rocks can vary tremendously, from strongly water-wet to strongly CO_2-wet
   - ❖ CO_2 is best retained in water-wet rock, while CO_2-wet reservoirs are relatively much more permeable to CO_2.
   - ❖ the shape of the CO_2 plume is also strongly affected by wettability, the plume is much more compact in case of water-wet rock, while it is vertically elongated in CO_2-wet rock.
   - ❖ The amount of residually trapped CO_2 is significantly higher in water-wet rock.
   - ❖ Dissolution trapping is more effective in CO_2-wet rock.
   - ❖ wettability significantly changes migration patterns and storage capacities, which is directly relevant to CO_2 geo-storage projects.
   - ❖ Strongly water-wet reservoirs are preferable CO_2 sinks due to their higher storage capacities and superior containment security.
   - ❖ This result has important implications for designing geoengineering solutions aiming at increasing CO_2 storage especially in situations where an efficient and continuous seal is absent.

2. Impact of reservoir wettability on CO_2 geo-sequestration in heterogeneous reservoirs
   - ❖ It has been confirmed that the effect of wettability on CO_2 geo-sequestration is valid for both the homogenous and heterogeneous reservoirs but the magnitude of these observations varies both in time and in space between the two cases.
   - ❖ CO_2-wet reservoirs have the highest CO_2 vertical migration, while water-wet reservoirs best retain CO_2.
   - ❖ Less residual CO_2 but more dissolved CO_2 is obtained in a CO_2-wet reservoir.
   - ❖ CO_2-wet reservoirs have the highest percentage of of mobile CO_2.

- ❖ Reservoir wettability has a critical impact on the CO_2 plume migration and trapping capacities, with water-wet reservoirs being preferable CO_2 sinks.
- ❖ Reservoir wettability needs to be accurately reflected in CCS reservoir simulations in order to reliably assess CO_2 storage capacities and containment security.

3. Influence of injection well configuration on CO_2 plume behaviour and CO_2 trapping capacity in heterogeneous reservoirs
   - ❖ The impact of the injection well configuration, horizontal versus three different vertical injection well scenarios (i.e. one, two and four vertical wells), on the CO_2 plume behaviour and CO_2 storage capacities for a wide range of rock wettabilities has been investigated, for the first time.
   - ❖ The injection well configuration has a major influence on CO_2 plume migration and on the amount of mobile, residual and dissolved CO_2.
   - ❖ Horizontal wells, for all wettability conditions, reduce CO_2 plume migration, CO_2 mobility and CO_2 solubility trapping.
   - ❖ Horizontal wells, for all wettability conditions, improve CO_2 residual trapping.
   - ❖ From a technical perspective horizontal injection wells are preferable as they increase storage capacity and containment security.
   - ❖ Using horizontal wells to inject the CO_2 leads to reduced costs associated with CO_2 geo-sequestration.
4. Effect of wettability heterogeneity on CO_2 storage efficiency in deep saline aquifers
   - ❖ The effect of heterogeneous wettability distribution (at isothermal and non-isothermal conditions) on the vertical CO_2 plume migration, and capillary and dissolution trapping capacities has been investigated, for the first time.
   - ❖ Spatial heterogeneities in wettability distribution lead to accelerated CO_2 upwards migration for both isothermal and non-isothermal conditions.
   - ❖ Simulations made with a homogeneous wettability distribution predicted a lower vertical migration distance than those assuming a heterogeneous wettability distribution.
   - ❖ Heterogeneously distributed wettability significantly increases CO_2 mobility and solubility trapping.
   - ❖ Wettability heterogeneity reduces residual trapping.

- ❖ Wettability heterogeneity is an important factor in the context of CO_2 geo-storage, and heterogeneous wettability reduces storage capacity for both isothermal and non-isothermal conditions.
- ❖ Wettability heterogeneity needs to be accurately modelled in reservoir-scale simulations in order to obtain reliable CO_2 storage predictions.

5. Impact of porosity and permeability heterogeneity on CO_2-plume migration and trapping capacity
   - ❖ The CO_2-plume vertical migration distance is larger in the homogeneous reservoir than in the heterogeneous reservoir, for all different wettability conditions.
   - ❖ For all wettability conditions and for all amounts of CO_2 injected, the CO_2 plume vertical migration distance in the homogeneous model is approximately two times more than that computed for the heterogeneous model.
   - ❖ More mobile CO_2 (the majority of this mobility following a horizontal movement not a vertical migration) is computed for the heterogeneous reservoir than for the homogeneous reservoir model, for all wettability conditions.
   - ❖ Porosity and permeability heterogeneity decreases the percentages of residually trapped and dissolved CO_2.
   - ❖ Porosity and permeability heterogeneity needs to be incorporated into reservoir simulations for accurate predictions of both CO_2 plume behaviour and CO2 storage capacities.
   - ❖ Not taking into account heterogeneities in the porosity and permeability distributions can lead to erroneous estimates of CO_2 storage capacities.
6. Effect of reservoir temperature on CO_2 storage efficiency in deep saline aquifers
   - ❖ Reservoir temperature affects vertical CO_2 migration, and the associated capillary and dissolution trapping mechanisms.
   - ❖ Higher reservoir temperatures significantly accelerated the vertical CO_2 plume movement.
   - ❖ Higher reservoir temperatures increase CO_2 mobility and solubility trapping.
   - ❖ Higher reservoir temperatures reduce residual trapping.

- ❖ Lower temperatures are preferred.

7. Impact of salinity on CO_2 containment security in highly heterogeneous reservoirs
   - ❖ A pair of relative permeability and capillary pressure curves for each brine salinity has been developed.
   - ❖ Lower brine salinities reduce CO_2 mobility and vertical CO_2 plume migration distance.
   - ❖ Lower brine salinity enhances capillary trapping and solubility trapping capacities.
   - ❖ Low salinity reservoirs are preferential CO_2 geo-sequestration sinks.
8. Enhancement of CO_2 trapping efficiency in heterogeneous reservoirs by Water Alternating Gas injection
   - ❖ The impact of the WAG injection on the relative permeability and capillary pressure curves were simulated based on previous experimental studies.
   - ❖ WAG injection leads to a significant reduction in CO_2 leakage risk.
   - ❖ WAG injection has less than half of the vertical migration distance compared to continuous or intermittent injections.
   - ❖ WAG maximises residual (capillary) trapping by increasing the residual CO_2 saturation for the imbibition cycle.
   - ❖ WAG injection also enhanced solubility trapping.
   - ❖ WAG injection significantly reduces (unwanted) CO_2 mobility
   - ❖ WAG is therefore the preferred injection scheme due to improve CO_2 geo-sequestration efficiency.

9.2 Recommendations and Outlook for future work

Based on the outcomes of this thesis, the following further studies are recommended to be conducted in future work:

- ❖ The influence of rock wettability on mineral reaction and mineral trapping mechanism is an open research area and needs to further research work. Thus, it is recommended to perform reservoir simulation model using TOUGHREACT or any other possible software to test the mineral trapping efficiency for the different wettability conditions.

- The influence of wettability on CO_2 geo-sequestration efficiency in hydrocarbon reservoirs (oil and gas reservoirs) is not well investigated. Thus, more simulation and experimental works are required. This will need to use three phase relative permeability and capillary pressure curves (oil/water and gas/oil) to simulate the different wettability conditions.
- The wettability variation during the CO_2 injection process and its effect on the CO_2 storage efficiency in reservoir scale is not well understood. This will need to develop new simulators that are able to predict the wettability variation during the CO_2 injection with time. Then, the new wettability condition should be automatically implemented in the simulation model.
- In this thesis, to simulate the wettability heterogeneity, and due to the fact that until now there is no particular correlation available in literature studies between wettability distribution and other petrophysical or geological parameters (i.e. permeability, porosity and mineralogy), separate probability distributions have been used to randomly assign the five wettability conditions to different cells. Thus, future studies should focus on investigating the relationship between wettability distribution and the other petrophysical or geological parameters.

References

Abdallah, W., Buckley, J. S., Carnegie, A., Edwards, J., Herold, B., Fordham, E., Graue, A., Habashy, T., Seleznev, N., and Signer, C. (1986). Fundamentals of Wettability. *Technology*, *38*, 1125-1144.

Adam, D. (2001). The North Sea bubble. *Nature*, *411*(6837), 518-519.

Adam, N. K., and Jessop, G. (1925). CCL.—Angles of contact and polarity of solid surfaces. *Journal of the Chemical Society, Transactions*, *127*, 1863-1868.

Akbarabadi, M., and Piri, M. (2013). Relative permeability hysteresis and capillary trapping characteristics of supercritical CO 2/brine systems: An experimental study at reservoir conditions. *Advances in Water Resources*, *52*, 190-206.

Al-Anssari, S., Barifcani, A., Wang, S., and Iglauer, S. (2016). Wettability alteration of oil-wet carbonate by silica nanofluid. *Journal of colloid and interface science*, *461*, 435-442.

Al-Khdheeawi, E. A., Vialle, S., Barifcani, A., Sarmadivaleh, M., and Iglauer, S. (2017a). Effect of brine salinity on CO_2 plume migration and trapping capacity in deep saline aquifers. *The APPEA Journal*, *57*(1), 100-109.

Al-Khdheeawi, E. A., Vialle, S., Barifcani, A., Sarmadivaleh, M., and Iglauer, S. (2017b). Impact of reservoir wettability and heterogeneity on CO 2-plume migration and trapping capacity. *International Journal of Greenhouse Gas Control*, *58*, 142-158.

Al-Khdheeawi, E. A., Vialle, S., Barifcani, A., Sarmadivaleh, M., and Iglauer, S. (2017c). Influence of CO_2-wettability on CO_2 migration and trapping capacity in deep saline aquifers. *Greenhouse Gases: Science and Technology*, *7*(2), 328-338. doi:10.1002/ghg.1648

Al-Khdheeawi, E. A., Vialle, S., Barifcani, A., Sarmadivaleh, M., and Iglauer, S. (2017d). Influence of injection well configuration and rock wettability on CO_2 plume behaviour and CO_2 trapping capacity in heterogeneous reservoirs. *Journal of Natural Gas Science and Engineering*, *43*, 190-206. doi:http://doi.org/10.1016/j.jngse.2017.03.016

Al-Khdheeawi, E. A., Vialle, S., Barifcani, A., Sarmadivaleh, M., and Iglauer, S. (2017e). Influence of Rock Wettability on CO_2 Migration and Storage Capacity in Deep Saline Aquifers. *Energy Procedia*, *114*, 4357-4365.

Al-Khdheeawi, E. A., Vialle, S., Barifcani, A., Sarmadivaleh, M., and Iglauer, S. (2018a). Effect of wettability heterogeneity and reservoir temperature on CO 2 storage efficiency in deep saline aquifers. *International Journal of Greenhouse Gas Control*, *68*, 216-229.

Al-Khdheeawi, E. A., Vialle, S., Barifcani, A., Sarmadivaleh, M., and Iglauer, S. (2018b). *Impact of Injection Scenario on CO 2 Leakage and CO 2 Trapping Capacity in Homogeneous Reservoirs.* Paper presented at the Offshore Technology Conference Asia.

Al-Khdheeawi, E. A., Vialle, S., Barifcani, A., Sarmadivaleh, M., Zhang, Y., and Iglauer, S. (2018). Impact of salinity on CO_2 containment security in highly heterogeneous reservoirs. *Greenhouse Gases: Science and Technology*, *8*(1), 93-105. doi:10.1002/ghg.1723

Al-Menhali, A. S., Menke, H. P., Blunt, M. J., and Krevor, S. C. (2016). Pore Scale Observations of Trapped CO_2 in Mixed-Wet Carbonate Rock: Applications to Storage in Oil Fields. *Environmental science & technology*, *50*(18), 10282-10290.

Al-Yaseri, A. Z., Lebedev, M., Barifcani, A., and Iglauer, S. (2016). Receding and advancing (CO 2+ brine+ quartz) contact angles as a function of pressure, temperature, surface roughness, salt type and salinity. *The Journal of Chemical Thermodynamics*, *93*, 416-423.

Al-Menhali, A., Niu, B., and Krevor, S. (2015). Capillarity and wetting of carbon dioxide and brine during drainage in Berea sandstone at reservoir conditions. *Water Resources Research*, *51*(10), 7895-7914.

Altunin, V. (1975). Thermophysical properties of carbon dioxide (Vol. 551). Moscow (in Russian): Publishing House of Standards Moscow Russia.

Ambrose, W., Lakshminarasimhan, S., Holtz, M., Nunez-Lopez, V., Hovorka, S., and Duncan, I. (2008). Geologic factors controlling CO_2 storage capacity and permanence: case studies based on experience with heterogeneity in oil and gas reservoirs applied to CO_2 storage. *Environmental Geology*, *54*(8), 1619-1633.

Anchliya, A., and Ehlig-Economides, C. A. (2009). *Aquifer management to accelerate* CO_2 *dissolution and trapping.* Paper presented at the SPE International Conference on CO_2 Capture, Storage, and Utilization.

Anderson, W. (1986a). Wettability literature survey-part 2: Wettability measurement. *Journal of Petroleum Technology*, *38*(11), 1,246-241,262.

Anderson, W. G. (1986b). Wettability Literature Survey- Part 1: Rock/Oil/Brine Interactions and the Effects of Core Handling on Wettability. *Journal of Petroleum Technology*, *38*(10), 1125-1144. doi:10.2118/13932-PA

Anderson, W. G. (1986c). Wettability literature survey-Part 3: The effects of wettability on the electrical properties of porous media. *Journal of Petroleum Technology*, *38*(12), 1,371-371,378.

Anderson, W. G. (1987a). Wettability literature survey-part 4: Effects of wettability on capillary pressure. *Journal of Petroleum Technology*, *39*(10), 1,283-281,300.

Anderson, W. G. (1987b). Wettability literature survey part 5: the effects of wettability on relative permeability. *Journal of Petroleum Technology*, *39*(11), 1,453-451,468.

Andrew, M., Bijeljic, B., and Blunt, M. J. (2013). Pore-scale imaging of geological carbon dioxide storage under in situ conditions. *Geophysical Research Letters*, *40*(15), 3915-3918.

Arif, M., Al-Yaseri, A. Z., Barifcani, A., Lebedev, M., and Iglauer, S. (2016a). Impact of pressure and temperature on CO 2–brine–mica contact angles and CO 2–brine interfacial tension: Implications for carbon geo-sequestration. *Journal of colloid and interface science*, *462*, 208-215.

Arif, M., Barifcani, A., Lebedev, M., and Iglauer, S. (2016b). Structural trapping capacity of oil-wet caprock as a function of pressure, temperature and salinity. *International Journal of Greenhouse Gas Control*, *50*, 112-120.

Aspenes, E., Graue, A., and Ramsdal, J. (2003). In situ wettability distribution and wetting stability in outcrop chalk aged in crude oil. *Journal of Petroleum Science and Engineering*, *39*(3), 337-350.

Babu, D., and Odeh, A. S. (1989). Productivity of a Horizontal Well (includes associated papers 20306, 20307, 20394, 20403, 20799, 21307, 21610, 21611, 21623, 21624, 25295, 25408, 26262, 26281, 31025, and 31035). *SPE Reservoir Engineering*, *4*(04), 417-421.

Bachu, S. (2000). Sequestration of CO 2 in geological media: criteria and approach for site selection in response to climate change. *Energy Conversion and Management*, *41*(9), 953-970.

Bachu, S. (2008). CO_2 storage in geological media: Role, means, status and barriers to deployment. *Progress in Energy and Combustion Science*, *34*(2), 254-273.

Bachu, S., and Adams, J. (2003). Sequestration of CO 2 in geological media in response to climate change: capacity of deep saline aquifers to sequester CO 2 in solution. *Energy Conversion and Management*, *44*(20), 3151-3175.

Bachu, S., and Bennion, D. B. (2008). Interfacial tension between CO_2, freshwater, and brine in the range of pressure from (2 to 27) MPa, temperature from (20 to 125) C, and water salinity from (0 to 334 000) mg· L− 1. *Journal of Chemical and Engineering Data*, *54*(3), 765-775.

Bachu, S., Gunter, W., and Perkins, E. (1994a). Aquifer disposal of CO_2: hydrodynamic and mineral trapping. *Energy Conversion and Management*, *35*(4), 269-279.

Bachu, S., Gunter, W., and Perkins, E. (1994b). Aquifer disposal of CO 2: hydrodynamic and mineral trapping. *Energy Conversion and Management*, *35*(4), 269-279.

Bartell, F., and Osterhof, H. (1927). Determination of the wettability of a solid by a liquid. *Industrial and Engineering Chemistry*, *19*(11), 1277-1280.

Basbug, B., Gumrah, F., and Oz, B. (2005). *Simulating the Effects of Deep Saline Aquifer Properties on CO_2 Sequestration.* Paper presented at the Canadian International Petroleum Conference.

Batycky, J., McCaffery, F., Hodgins, P., and Fisher, D. (1981). Interpreting relative permeability and wettability from unsteady-state displacement measurements. *Society of Petroleum Engineers Journal*, *21*(03), 296-308.

Baz, H., Noureldin, M., Allinson, W., and Cinar, Y. (2016). A field-scale investigation of residual and dissolution trapping of CO 2 in a saline formation in Western Australia. *International Journal of Greenhouse Gas Control*, *46*, 86-99.

Benner, F. C., Dodd, C. G., and Bartell, F. (1942). *Evaluation of Effective Displacement Pressures for Petroleum Oil-Water Silica Systems.* Paper presented at the Drilling and Production Practice.

Bennion, D. B., and Bachu, S. (2006). *Dependence on temperature, pressure, and salinity of the IFT and relative permeability displacement characteristics of CO_2 injected in deep saline aquifers.* Paper presented at the SPE Annual Technical Conference and Exhibition.

Benson, S., Pini, R., Reynolds, C., and Krevor, S. (2013). Relative Permeability Analysis to Describe Multi-Phase Flow in CO_2 Storage Reservoirs. *Global CCS Institute*.

Benson, S. M., and Cole, D. R. (2008). CO_2 Sequestration in Deep Sedimentary Formations. *Elements*, *4*(5), 325-331. doi:10.2113/gselements.4.5.325

Bertin, H., Hugget, A., and Robin, M. (1998). Two-phase flow through orthogonal composite cores with wettability heterogeneity. *Journal of Petroleum Science and Engineering*, *20*(3), 185-188.

Bickle, M. J. (2009). Geological carbon storage. *Nature Geoscience*, *2*(12), 815-818.

Bigelow, W., Pickett, D., and Zisman, W. (1946). Oleophobic monolayers: I. Films adsorbed from solution in non-polar liquids. *Journal of Colloid Science*, *1*(6), 513-538.

Bikkina, P. K. (2011). Contact angle measurements of CO 2–water–quartz/calcite systems in the perspective of carbon sequestration. *International Journal of Greenhouse Gas Control*, *5*(5), 1259-1271.

Birkholzer, J. T., Zhou, Q., and Tsang, C.-F. (2009). Large-scale impact of CO 2 storage in deep saline aquifers: a sensitivity study on pressure response in stratified systems. *International Journal of Greenhouse Gas Control*, *3*(2), 181-194.

Blunt, M. J. (1997). Pore level modeling of the effects of wettability. *Spe Journal*, *2*(04), 494-510.

Bobek, J., Mattax, C., and Denekas, M. (1958). Reservoir rock wettability-its significance and evaluation. JPT, 155-60; Trans., AIME, 213.

Bourne, S., Crouch, S., and Smith, M. (2014). A risk-based framework for measurement, monitoring and verification of the Quest CCS Project, Alberta, Canada. *International Journal of Greenhouse Gas Control*, *26*, 109-126.

Bretan, P., Yielding, G., Mathiassen, O. M., and Thorsnes, T. (2011). Fault-seal analysis for CO_2 storage: an example from the Troll area, Norwegian Continental Shelf. *Petroleum Geoscience*, *17*(2), 181-192.

Broseta, D., Tonnet, N., and Shah, V. (2012). Are rocks still water-wet in the presence of dense CO_2 or H2S? *Geofluids*, *12*(4), 280-294.

Bryant, S. L., Lakshminarasimhan, S., and Pope, G. A. (2006). *Buoyancy-dominated multiphase flow and its impact on geological sequestration of CO_2.* Paper presented at the SPE/DOE Symposium on Improved Oil Recovery.

Cain, J., Francis, D., Venter, R., and Neumann, A. (1983). Dynamic contact angles on smooth and rough surfaces. *Journal of colloid and interface science*, *94*(1), 123-130.

Calhoun, J. (1951). Criteria for determining rock wettability. *Oil Gas J*, *50*, 151-153.

Chalbaud, C., Robin, M., Bekri, S., and Egermann, P. (2007). *Wettability impact on CO_2 storage in aquifers: visualisation and quantification using micromodel tests, pore network model and reservoir simulations.* Paper presented at the International symposium of the society of core analysts, Calgary, Canada.

Chalbaud, C., Robin, M., Lombard, J.-M., Bertin, H., and Egermann, P. (2010). Brine/CO_2 interfacial properties and effects on CO_2 storage in deep saline aquifers. *Oil & Gas Science and Technology–Revue de l'Institut Français du Pétrole*, *65*(4), 541-555.

Chalbaud, C., Robin, M., Lombard, J., Martin, F., Egermann, P., and Bertin, H. (2009). Interfacial tension measurements and wettability evaluation for geological CO 2 storage. *Advances in Water Resources*, *32*(1), 98-109.

Chang, Y., Mohanty, K., Huang, D., and Honarpour, M. (1997). The impact of wettability and core-scale heterogeneities on relative permeability. *Journal of Petroleum Science and Engineering*, *18*(1-2), 1-19.

Chaouche, M., Rakotomalala, N., Salin, D., Xu, B., and Yortsos, Y. (1994). Capillary effects in drainage in heterogeneous porous media: continuum modelling, experiments and pore network simulations. *Chemical Engineering Science*, *49*(15), 2447-2466.

Chaudhary, K., Bayani Cardenas, M., Wolfe, W. W., Maisano, J. A., Ketcham, R. A., and Bennett, P. C. (2013). Pore-scale trapping of supercritical CO_2 and the role of grain wettability and shape. *Geophysical Research Letters*, *40*(15), 3878-3882.

Chaudhary, K., Guiltinan, E. J., Cardenas, M. B., Maisano, J. A., Ketcham, R. A., and Bennett, P. C. (2015). Wettability measurement under high P-T conditions using X-ray imaging with application to the brine-supercritical CO_2 system. *Geochemistry, Geophysics, Geosystems*, *16*(9), 2858-2864.

Chen, C., Wan, J., Li, W., and Song, Y. (2015a). Water contact angles on quartz surfaces under supercritical CO 2 sequestration conditions: Experimental and

molecular dynamics simulation studies. *International Journal of Greenhouse Gas Control*, *42*, 655-665.

Chen, C., Zhang, N., Li, W., and Song, Y. (2015b). Water contact angle dependence with hydroxyl functional groups on silica surfaces under CO_2 sequestration conditions. *Environmental science & technology*, *49*(24), 14680-14687.

Chiquet, P., Broseta, D., and Thibeau, S. (2007). Wettability alteration of caprock minerals by carbon dioxide. *Geofluids*, *7*(2), 112-122.

Christensen, J., Stenby, E., and Skauge, A. (2001). Review of WAG Field Experience. *SPE Reservoir Evaluation & Engineering*, *4*(02), 97-106.

Christie, M., and Blunt, M. (2001). *Tenth SPE comparative solution project: A comparison of upscaling techniques.* Paper presented at the SPE Reservoir Simulation Symposium.

Craig, F. F. (1993). *The reservoir engineering aspects of waterflooding* (Vol. 3): Richardson, TX: Henry L. Doherty Memorial Fund of AIME, Society of Petroleum Engineers.

Crocker, M., and Marchin, L. (1988). Wettability and adsorption characteristics of crude-oil asphaltene and polar fractions. *Journal of Petroleum Technology*, *40*(04), 470-474.

Dai, Z., Stauffer, P. H., Carey, J. W., Middleton, R. S., Lu, Z., Jacobs, J. F., Hnottavange-Telleen, K., and Spangler, L. H. (2014). Pre-site characterization risk analysis for commercial-scale carbon sequestration. *Environmental science & technology*, *48*(7), 3908-3915.

Dake, L. P. (2007). *Fundamentals of reservoir engineering* (Vol. 8): Elsevier.

Dang, C., Nghiem, L., Nguyen, N., Chen, Z., and Nguyen, Q. (2016). Evaluation of CO 2 Low Salinity Water-Alternating-Gas for enhanced oil recovery. *Journal of Natural Gas Science and Engineering*, *35*, 237-258.

Deel, D., Mahajan, K., Mahoney, C. R., McIlvried, H. G., and Srivastava, R. D. (2007). Risk assessment and management for long-term storage of CO_2 in geologic formations-United States Department of Energy R&D. *Systemics, Cybernetics and Informatics*, *5*(1), 79-84.

Denny, M. W. (1993). *Air and water: the biology and physics of life's media*: Princeton University Press.

DePaolo, D., Orr, F., Benson, S., Celia, M., Felmy, A., Nagy, K., Fogg, G., Snieder, R., Davis, J., and Pruess, K. (2007). *Basic Research Needs for Geosciences: Facilitating 21st Century Energy Systems*. Retrieved from

Dewhurst, D. N., Aplin, A. C., and Sarda, J. P. (1999). Influence of clay fraction on pore-scale properties and hydraulic conductivity of experimentally compacted mudstones. *Journal of Geophysical Research: Solid Earth*, *104*(B12), 29261-29274.

Dickson, J. L., Gupta, G., Horozov, T. S., Binks, B. P., and Johnston, K. P. (2006). Wetting phenomena at the CO_2/water/glass interface. *Langmuir*, *22*(5), 2161-2170.

Donaldson, E. (1981). Oil-water-rock wettability measurement. *Am. Chem. Soc., Div. Pet. Chem., Prepr.;(United States)*, *26*(CONF-810308-(Vol. 1)).

Donaldson, E. C., Kendall, R. F., Pavelka, E. A., and Crocker, M. E. (1980). *Equipment and procedures for fluid flow and wettability tests of geological materials*. Retrieved from

Donaldson, E. C., Thomas, R. D., and Lorenz, P. B. (1969). Wettability determination and its effect on recovery efficiency. *Society of Petroleum Engineers Journal*, *9*(01), 13-20.

Doughty, C. (2007). Modeling geologic storage of carbon dioxide: comparison of non-hysteretic and hysteretic characteristic curves. *Energy Conversion and Management*, *48*(6), 1768-1781.

Doughty, C. (2010). Investigation of CO_2 plume behavior for a large-scale pilot test of geologic carbon storage in a saline formation. *Transport in porous media*, *82*(1), 49-76.

Doughty, C., Freifeld, B. M., and Trautz, R. C. (2008). Site characterization for CO_2 geologic storage and vice versa: the Frio brine pilot, Texas, USA as a case study. *Environmental Geology*, *54*(8), 1635-1656.

Doughty, C., and Myer, L. R. (2009). Scoping calculations on leakage of CO_2 in geologic storage: the impact of overburden permeability, phase trapping, and dissolution. *Carbon Sequestration and Its Role in the Global Carbon Cycle*, 217-237.

Doughty, C., and Pruess, K. (2004). Modeling supercritical carbon dioxide injection in heterogeneous porous media. *Vadose Zone Journal*, *3*(3), 837-847.

Drelich, J., and Miller, J. D. (1994). The effect of solid surface heterogeneity and roughness on the contact angle/drop (bubble) size relationship. *Journal of colloid and interface science*, *164*(1), 252-259.

Duan, Z., and Sun, R. (2003). An improved model calculating CO 2 solubility in pure water and aqueous NaCl solutions from 273 to 533 K and from 0 to 2000 bar. *Chemical Geology*, *193*(3), 257-271.

Dullien, F. A. (1979). *Porous media: fluid transport and pore structure*: Academic press, Inc.

Economides, M., Deimbachor, F. X., Brand, C. W., and Heinemann, Z. E. (1991). Comprehensive-Simulation of Horizontal-Well Performance. *SPE formation evaluation*, *6*(04), 418-426.

El-Maghraby, R., Pentland, C., Iglauer, S., and Blunt, M. (2012). A fast method to equilibrate carbon dioxide with brine at high pressure and elevated temperature including solubility measurements. *The Journal of Supercritical Fluids*, *62*, 55-59.

Emami-Meybodi, H., Hassanzadeh, H., Green, C. P., and Ennis-King, J. (2015). Convective dissolution of CO 2 in saline aquifers: Progress in modeling and experiments. *International Journal of Greenhouse Gas Control*, *40*, 238-266.

Espinoza, D. N., and Santamarina, J. C. (2010). Water- CO_2-mineral systems: Interfacial tension, contact angle, and diffusion—Implications to CO_2 geological storage. *Water Resources Research*, *46*(7).

Farokhpoor, R., Bjørkvik, B. J., Lindeberg, E., and Torsæter, O. (2013). Wettability behaviour of CO 2 at storage conditions. *International Journal of Greenhouse Gas Control*, *12*, 18-25.

Fatemi, S. M., and Sohrabi, M. (2013). Experimental investigation of near-miscible water-alternating-gas injection performance in water-wet and mixed-wet systems. *Spe Journal*, *18*(01), 114-123.

Firoozabadi, A., and Myint, P. C. (2010). Prospects for subsurface CO_2 sequestration. *AIChE Journal*, *56*(6), 1398-1405.

Flett, M., Gurton, R., and Weir, G. (2007). Heterogeneous saline formations for carbon dioxide disposal: Impact of varying heterogeneity on containment and trapping. *Journal of Petroleum Science and Engineering*, *57*(1), 106-118.

Floris, F. J., Bush, M. D., Cuypers, M., Roggero, F., and Syversveen, A.-R. (1999). *Comparison of production forecast uncertainty quantification methods: an*

integrated study. Paper presented at the 1st Symposium on Petroleum Geostatistics, Toulouse.

Forster, A., Norden, B., Zinck-Jrgensen, K., Frykman, P., Kulenkampff, J., Spangenberg, E., Erzinger, J., Zimmer, M., Kopp, J., Borm, G., Juhlin, C., Cosma, C.-G., and Hurter, S. (2006). Baseline characterization of the CO2SINK geological storage site at Ketzin, Germany. *Environmental Geosciences*, *13*(3), 145-161.

Fowkes, F. M., and Harkins, W. D. (1940). The state of monolayers adsorbed at the interface solid—aqueous solution. *Journal of the American Chemical Society*, *62*(12), 3377-3386.

Gatenby, W., and Marsden, S. S. (1957). Some wettability characteristics of synthetic porous media. *Producers Monthly*, *22*(1), 5-12.

Gaus, I. (2010). Role and impact of CO 2–rock interactions during CO 2 storage in sedimentary rocks. *International Journal of Greenhouse Gas Control*, *4*(1), 73-89.

Gaydos, J., and Neumann, A. (1987). The dependence of contact angles on drop size and line tension. *Journal of colloid and interface science*, *120*(1), 76-86.

Gershenzon, N. I., Ritzi Jr, R. W., Dominic, D. F., Mehnert, E., and Okwen, R. T. (2016). Comparison of CO_2 trapping in highly heterogeneous reservoirs with Brooks-Corey and van Genuchten type capillary pressure curves. *Advances in Water Resources*, *96*(2016), 225-236.

Gershenzon, N. I., Ritzi, R. W., Dominic, D. F., Mehnert, E., and Okwen, R. T. (2017). Capillary trapping of CO 2 in heterogeneous reservoirs during the injection period. *International Journal of Greenhouse Gas Control*, *59*, 13-23.

Gershenzon, N. I., Ritzi, R. W., Dominic, D. F., Soltanian, M., Mehnert, E., and Okwen, R. T. (2015). Influence of small-scale fluvial architecture on CO_2 trapping processes in deep brine reservoirs. *Water Resources Research*, *51*(10), 8240-8256.

Ghanbari, S., Al-Zaabi, Y., Pickup, G., Mackay, E., Gozalpour, F., and Todd, A. (2006). Simulation of CO 2 storage in saline aquifers. *Chemical Engineering Research and Design*, *84*(9), 764-775.

Grant, M. A., and Bixley, P. F. (2011). Geothermal reservoir engineering.

Graue, A., Aspenes, E., Bognø, T., Moe, R., and Ramsdal, J. (2002). Alteration of wettability and wettability heterogeneity. *Journal of Petroleum Science and Engineering*, *33*(1), 3-17.

Green, C. P., and Ennis-King, J. (2010). Effect of vertical heterogeneity on long-term migration of CO_2 in saline formations. *Transport in porous media*, *82*(1), 31-47.

Gunter, W., Wiwehar, B., and Perkins, E. (1997). Aquifer disposal of CO 2-rich greenhouse gases: extension of the time scale of experiment for CO 2-sequestering reactions by geochemical modelling. *Mineralogy and Petrology*, *59*(1-2), 121-140.

Han, W. S., Lee, S. Y., Lu, C., and McPherson, B. J. (2010). Effects of permeability on CO_2 trapping mechanisms and buoyancy-driven CO_2 migration in saline formations. *Water Resources Research*, *46*(7).

Hardman, P. (1989). Beckingham 36 horizontal well. *SPE Drilling Engineering*, *4*(01), 17-23.

Hassanzadeh, H., Pooladi-Darvish, M., and Keith, D. W. (2009). Accelerating CO_2 dissolution in saline aquifers for geological storage□ Mechanistic and sensitivity studies. *Energy & Fuels*, *23*(6), 3328-3336.

Heiba, A., Davis, H., and Scriven, L. (1983). *Effect of wettability on two-phase relative permeabilities and capillary pressures.* Paper presented at the SPE Annual Technical Conference and Exhibition.

Herring, A. L., Andersson, L., Schlüter, S., Sheppard, A., and Wildenschild, D. (2015). Efficiently engineering pore-scale processes: The role of force dominance and topology during nonwetting phase trapping in porous media. *Advances in Water Resources*, *79*, 91-102.

Herring, A. L., Andersson, L., and Wildenschild, D. (2016). Enhancing residual trapping of supercritical CO_2 via cyclic injections. *Geophysical Research Letters*, *43*(18), 9677-9685.

Herring, A. L., Harper, E. J., Andersson, L., Sheppard, A., Bay, B. K., and Wildenschild, D. (2013). Effect of fluid topology on residual nonwetting phase trapping: Implications for geologic CO 2 sequestration. *Advances in Water Resources*, *62*, 47-58.

Hesse, M., Orr, F., and Tchelepi, H. (2008). Gravity currents with residual trapping. *Journal of Fluid Mechanics*, *611*(1), 35-60.

Hesse, M., and Woods, A. (2010). Buoyant dispersal of CO_2 during geological storage. *Geophysical Research Letters*, *37*(1).

Holloway, S. (2005). Underground sequestration of carbon dioxide—a viable greenhouse gas mitigation option. *Energy*, *30*(11), 2318-2333.

Holloway, S., and Savage, D. (1993). The potential for aquifer disposal of carbon dioxide in the UK. *Energy Conversion and Management*, *34*(9), 925-932.

Honari, A., Zecca, M., Vogt, S. J., Iglauer, S., Bijeljic, B., Johns, M. L., and May, E. F. (2016). The impact of residual water on CH 4-CO 2 dispersion in consolidated rock cores. *International Journal of Greenhouse Gas Control*, *50*, 100-111.

Houghton, J. T., Ding, Y., Griggs, D. J., Noguer, M., van der Linden, P. J., Dai, X., Maskell, K., and Johnson, C. (2001). Climate change 2001: the scientific basis.

Hovorka, S. D., Doughty, C., Benson, S. M., Pruess, K., and Knox, P. R. (2004). The impact of geological heterogeneity on CO_2 storage in brine formations: a case study from the Texas Gulf Coast. *Geological Society, London, Special Publications*, *233*(1), 147-163.

Humez, P., Lagneau, V., Lions, J., and Negrel, P. (2013). Assessing the potential consequences of CO_2 leakage to freshwater resources: A batch-reaction experiment towards an isotopic tracing tool. *Applied geochemistry*, *30*, 178-190.

Ide, S. T., Jessen, K., and Orr, F. M. (2007). Storage of CO 2 in saline aquifers: Effects of gravity, viscous, and capillary forces on amount and timing of trapping. *International Journal of Greenhouse Gas Control*, *1*(4), 481-491.

Iglauer, S. (2011). *Dissolution trapping of carbon dioxide in reservoir formation brine-a carbon storage mechanism*: INTECH Open Access Publisher.

Iglauer, S. (2012). Carbon capture and storage with a focus on capillary trapping as a mechanism to store carbon dioxide in geological porous media. *Advances in Multiphase Flow and Heat Transfer*, *3*, 177-197.

Iglauer, S. (2017). CO_2–Water–Rock Wettability: Variability, Influencing Factors, and Implications for CO_2 Geostorage. *Accounts of Chemical Research*, *50*(5), 1134-1142.

Iglauer, S., Al-Yaseri, A. Z., Rezaee, R., and Lebedev, M. (2015a). CO_2 wettability of caprocks: Implications for structural storage capacity and containment security. *Geophysical Research Letters*, *42*(21), 9279-9284.

Iglauer, S., Mathew, M., and Bresme, F. (2012). Molecular dynamics computations of brine–CO 2 interfacial tensions and brine–CO 2–quartz contact angles and their effects on structural and residual trapping mechanisms in carbon geo-sequestration. *Journal of colloid and interface science*, *386*(1), 405-414.

Iglauer, S., Paluszny, A., Pentland, C. H., and Blunt, M. J. (2011). Residual CO_2 imaged with X-ray micro-tomography. *Geophysical Research Letters*, *38*(21).

Iglauer, S., Pentland, C., and Busch, A. (2015b). CO_2 wettability of seal and reservoir rocks and the implications for carbon geo-sequestration. *Water Resources Research*, *51*(1), 729-774.

Iglauer, S., Salamah, A., Sarmadivaleh, M., Liu, K., and Phan, C. (2014). Contamination of silica surfaces: Impact on water–CO 2–quartz and glass contact angle measurements. *International Journal of Greenhouse Gas Control*, *22*, 325-328.

Iglauer, S., and Wülling, W. (2016). The scaling exponent of residual nonwetting phase cluster size distributions in porous media. *Geophysical Research Letters*.

Jafari, M., and Jung, J. (2016). The change in contact angle at unsaturated CO_2-water conditions: Implication on geological carbon dioxide sequestration. *Geochemistry, Geophysics, Geosystems*, *17*(10), 3969-3982.

Jahangiri, H. R., and Zhang, D. (2011). Effect of spatial heterogeneity on plume distribution and dilution during CO 2 sequestration. *International Journal of Greenhouse Gas Control*, *5*(2), 281-293.

Javanbakht, G., Sedghi, M., Welch, W., and Goual, L. (2015). Molecular Dynamics Simulations of CO_2/Water/Quartz Interfacial Properties: Impact of CO_2 Dissolution in Water. *Langmuir*, *31*(21), 5812-5819.

Joshi, S. (1988). Augmentation of well productivity with slant and horizontal wells (includes associated papers 24547 and 25308). *Journal of Petroleum Technology*, *40*(06), 729-739.

Joshi, S. (2003). *Cost/benefits of horizontal wells.* Paper presented at the SPE Western Regional/AAPG Pacific Section Joint Meeting.

Joshi, S. D. (1991). *Horizontal well technology*: PennWell Books.

Juanes, R., Spiteri, E., Orr, F., and Blunt, M. (2006). Impact of relative permeability hysteresis on geological CO_2 storage. *Water Resources Research*, *42*(12).

Jung, J.-W., and Wan, J. (2012). Supercritical CO_2 and ionic strength effects on wettability of silica surfaces: Equilibrium contact angle measurements. *Energy & Fuels*, *26*(9), 6053-6059.

Katz, D. L. V., and Lee, R. L. (1990). *Natural gas engineering: production and storage*: McGraw-Hill Economics Department.

Kaveh, N. S., Rudolph, E., Van Hemert, P., Rossen, W., and Wolf, K.-H. (2014). Wettability evaluation of a CO_2/water/bentheimer sandstone system: contact angle, dissolution, and bubble size. *Energy & Fuels*, *28*(6), 4002-4020.

Kaveh, N. S., Rudolph, E. S. J., Wolf, K.-H. A., and Ashrafizadeh, S. N. (2011). Wettability determination by contact angle measurements: hvBb coal–water system with injection of synthetic flue gas and CO 2. *Journal of colloid and interface science*, *364*(1), 237-247.

Kharaka, Y. K., Cole, D. R., Thordsen, J. J., Gans, K. D., and Thomas, R. B. (2013). Geochemical monitoring for potential environmental impacts of geologic sequestration of CO_2. *Reviews in Mineralogy and Geochemistry*, *77*(1), 399-430.

Kharaka, Y. K., Thordsen, J. J., Hovorka, S. D., Nance, H. S., Cole, D. R., Phelps, T. J., and Knauss, K. G. (2009). Potential environmental issues of CO_2 storage in deep saline aquifers: Geochemical results from the Frio-I Brine Pilot test, Texas, USA. *Applied geochemistry*, *24*(6), 1106-1112.

Kiriakidis, D. G., Mitsoulis, E., and Neale, G. E. (1993). Computer simulations of immiscible displacement in a porous medium containing a region of different wettability. *Journal of Canadian Petroleum Technology*, *32*(06).

Kopp, A., Class, H., and Helmig, R. (2009). Investigations on CO 2 storage capacity in saline aquifers: Part 1. Dimensional analysis of flow processes and reservoir characteristics. *International Journal of Greenhouse Gas Control*, *3*(3), 263-276.

Kossack, C., Kleppe, J., and Aasen, T. (1987). *Oil production from the Troll Field: A comparison of horizontal and vertical wells.* Paper presented at the SPE Annual Technical Conference and Exhibition.

Krevor, S., Blunt, M. J., Benson, S. M., Pentland, C. H., Reynolds, C., Al-Menhali, A., and Niu, B. (2015). Capillary trapping for geologic carbon dioxide storage–From pore scale physics to field scale implications. *International Journal of Greenhouse Gas Control*, *40*, 221-237.

Krevor, S., Pini, R., Li, B., and Benson, S. M. (2011). Capillary heterogeneity trapping of CO_2 in a sandstone rock at reservoir conditions. *Geophysical Research Letters*, *38*(15).

Krevor, S., Pini, R., Zuo, L., and Benson, S. M. (2012). Relative permeability and trapping of CO_2 and water in sandstone rocks at reservoir conditions. *Water Resources Research*, *48*(2).

Krevor, S., Reynolds, C., Al-Menhali, A., and Niu, B. (2016). The Impact of Reservoir Conditions and Rock Heterogeneity on CO 2-Brine Multiphase Flow in Permeable Sandstone. *Petrophysics*, *57*(01), 12-18.

Kulkarni, M. M., and Rao, D. N. (2005). Experimental investigation of miscible and immiscible Water-Alternating-Gas (WAG) process performance. *Journal of Petroleum Science and Engineering*, *48*(1), 1-20.

Kumar, A., Noh, M. H., Ozah, R. C., Pope, G. A., Bryant, S. L., Sepehrnoori, K., and Lake, L. W. (2005). Reservoir simulation of CO 2 storage in deep saline aquifers. *Spe Journal*, *10*(03), 336-348.

Kwok, D., Lin, R., Mui, M., and Neumann, A. (1996). Low-rate dynamic and static contact angles and the determination of solid surface tensions. *Colloids and Surfaces A: Physicochemical and Engineering Aspects*, *116*(1-2), 63-77.

Kyte, J., Naumann, V., and Mattax, C. (1961). Effect of reservoir environment on water-oil displacements. *Journal of Petroleum Technology*, *13*(06), 579-582.

Lackner, K. S. (2003). A guide to CO_2 sequestration. *Science*, *300*(5626), 1677-1678.

Laochamroonvorapongse, R., Kabir, C., and Lake, L. W. (2014). Performance assessment of miscible and immiscible water-alternating gas floods with simple tools. *Journal of Petroleum Science and Engineering*, *122*, 18-30.

Laroche, C., Vizika, O., and Kalaydjian, F. (1999). Wettability heterogeneities in gas injection: experiments and modelling. *Petroleum Geoscience*, *5*(1), 65-69.

Lebedev, M., Zhang, Y., Sarmadivaleh, M., Barifcani, A., Al-Khdheeawi, E. A., and Iglauer, S. (2017). Carbon geosequestration in limestone: Pore-scale dissolution and geomechanical weakening. *International Journal of Greenhouse Gas Control*, *66*, 106-119.

Leja, J., and Poling, G. (1960). *On the interpretation of contact angle.* Paper presented at the Proceedings of the 5th Mineral Processing Congress.

Leonenko, Y., and Keith, D. W. (2008). Reservoir engineering to accelerate the dissolution of CO_2 stored in aquifers. *Environmental science & technology*, *42*(8), 2742-2747.

Leung, D. Y., Caramanna, G., and Maroto-Valer, M. M. (2014). An overview of current status of carbon dioxide capture and storage technologies. *Renewable and Sustainable Energy Reviews*, *39*, 426-443.

Leverett, M. (1941). Capillary behavior in porous solids. *Transactions of the AIME*, *142*(01), 152-169.

Levine, J. S., Goldberg, D. S., Lackner, K. S., Matter, J. M., Supp, M. G., and Ramakrishnan, T. (2014). Relative Permeability Experiments of Carbon Dioxide Displacing Brine and Their Implications for Carbon Sequestration. *Environmental Science and Technology*, *48*(A-NETL-PUB-097).

Li, B., and Benson, S. M. (2015). Influence of small-scale heterogeneity on upward CO 2 plume migration in storage aquifers. *Advances in Water Resources*, *83*, 389-404.

Li, D. (1996). Drop size dependence of contact angles and line tensions of solid-liquid systems. *Colloids and Surfaces A: Physicochemical and Engineering Aspects*, *116*(1), 1-23.

Li, Q., and Liu, G. (2016). Risk Assessment of the Geological Storage of CO_2: A Review *Geologic Carbon Sequestration* (pp. 249-284): Springer.

Li, Z., Dong, M., Li, S., and Huang, S. (2006). CO_2 sequestration in depleted oil and gas reservoirs—caprock characterization and storage capacity. *Energy Conversion and Management*, *47*(11-12), 1372-1382.

Lin, F., Li, D., and Neumann, A. (1993). Effect of surface roughness on the dependence of contact angles on drop size. *Journal of colloid and interface science*, *159*(1), 86-95.

Lindeberg, E., and Wessel-Berg, D. (1997). Vertical convection in an aquifer column under a gas cap of CO 2. *Energy Conversion and Management*, *38*, S229-S234.

Liu, S., Yang, X., and Qin, Y. (2010). Molecular dynamics simulation of wetting behavior at v/water/solid interfaces. *Chinese Science Bulletin*, *55*(21), 2252-2257.

Macdonald, C. (1988). *Horizontal Wells: An Application in the North Sea.* Paper presented at the European Petroleum Conference.

Masalmeh, S. K. (2002). Studying the effect of wettability heterogeneity on the capillary pressure curves using the centrifuge technique. *Journal of Petroleum Science and Engineering*, *33*(1), 29-38.

McCaffery, F., and Bennion, D. (1974). The Effect OfWettability On Two-Phase Relative Pemeabilities. *Journal of Canadian Petroleum Technology*, *13*(04).

McCaughan, J., Iglauer, S., and Bresme, F. (2013). Molecular dynamics simulation of water/CO 2-quartz interfacial properties: Application to subsurface gas injection. *Energy Procedia*, *37*, 5387-5402.

Melrose, J. C. (1965). Wettability as related to capillary action in porous media. *Society of Petroleum Engineers Journal*, *5*(03), 259-271.

Metz, B., Davidson, O., De Coninck, H., Loos, M., and Meyer, L. (2005). IPCC, 2005: IPCC special report on carbon dioxide capture and storage. Prepared by Working Group III of the Intergovernmental Panel on Climate Change. *Cambridge, United Kingdom and New York, NY, USA, 442 pp*.

Mito, S., Xue, Z., and Ohsumi, T. (2008). Case study of geochemical reactions at the Nagaoka CO 2 injection site, Japan. *International Journal of Greenhouse Gas Control*, *2*(3), 309-318.

Mo, S., and Akervoll, I. (2005). *Modeling long-term CO_2 storage in aquifer with a black-oil reservoir simulator.* Paper presented at the SPE/EPA/DOE Exploration and Production Environmental Conference.

Mo, S., Zweigel, P., Lindeberg, E. G., and Akervoll, I. (2005). *Effect of geologic parameters on CO_2 storage in deep saline aquifers.* Paper presented at the SPE Europec/EAGE Annual Conference.

Morrow, N. R. (1970). Physics and thermodynamics of capillary action in porous media. *Industrial and Engineering Chemistry*, *62*(6), 32-56.

Morrow, N. R. (1976). Capillary pressure correlations for uniformly wetted porous media. *Journal of Canadian Petroleum Technology*, *15*(04).

Morrow, N. R. (1990). Wettability and its effect on oil recovery. *Journal of Petroleum Technology*, *42*(12), 1,476-471,484.

Morrow, N. R., Lim, H. T., and Ward, J. S. (1986). Effect of crude-oil-induced wettability changes on oil recovery. *SPE formation evaluation*, *1*(01), 89-103.

Morton, R. A., and Land, L. S. (1987). Regional variations in formation water chemistry, Frio formation (Oligocene), Texas Gulf Coast. *AAPG Bulletin*, *71*(2), 191-206.

Mualem, Y. (1976). A new model for predicting the hydraulic conductivity of unsaturated porous media. *Water Resour. Res*, *12*(3), 513-522.

Murphy, P. J. (1990). Performance of horizontal wells in the Helder Field. *Journal of Petroleum Technology*, *42*(06), 792-800.

Naylor, M., Wilkinson, M., and Haszeldine, R. (2011). Calculation of CO 2 column heights in depleted gas fields from known pre-production gas column heights. *Marine and Petroleum Geology*, *28*(5), 1083-1093.

Neumann, A., and Good, R. (1979). Techniques of measuring contact angles *Surface and colloid science* (pp. 31-91): Springer.

Nghiem, L., Shrivastava, V., Kohse, B., Hassam, M., and Yang, C. (2010). Simulation and optimization of trapping processes for CO_2 storage in saline aquifers. *Journal of Canadian Petroleum Technology*, *49*(08), 15-22.

Nghiem, L., Shrivastava, V., Tran, D., Kohse, B., Hassam, M., and Yang, C. (2009). *Simulation of CO_2 storage in saline aquifers.* Paper presented at the SPE/EAGE Reservoir Characterization & Simulation Conference.

Nilsen, H. M., Syversveen, A. R., Lie, K.-A., Tveranger, J., and Nordbotten, J. M. (2012). Impact of top-surface morphology on CO 2 storage capacity. *International Journal of Greenhouse Gas Control*, *11*, 221-235.

Obi, E. O. I., and Blunt, M. J. (2006). Streamline-based simulation of carbon dioxide storage in a north sea aquifer. *Water Resources Research*, *42*(3).

Ofori, A. E., and Engler, T. W. (2011). *Effects of CO_2 Sequestration on the Petrophysical Properties of an Aquifer Rock.* Paper presented at the Canadian Unconventional Resources Conference.

Oldenburg, C. M. (2007). Joule-Thomson cooling due to CO 2 injection into natural gas reservoirs. *Energy Conversion and Management*, *48*(6), 1808-1815.

Oldenburg, C. M. (2008). Screening and ranking framework for geologic CO_2 storage site selection on the basis of health, safety, and environmental risk. *Environmental Geology*, *54*(8), 1687-1694.

Oldenburg, C. M., and Unger, A. J. (2003). On leakage and seepage from geologic carbon sequestration sites. *Vadose Zone Journal*, *2*(3), 287-296.

Ortoleva, P., Dove, P., and Richter, F. (1998). *Geochemical perspectives on CO_2 sequestration.* Paper presented at the Manuscript prepared for US Department of Energy Workshop on "Terrestrial Sequestration of CO_2-An Assessment of Research Needs," Gaithersburg, MD, May.

Owens, W., and Archer, D. (1971). The effect of rock wettability on oil-water relative permeability relationships. *Journal of Petroleum Technology*, *23*(07), 873-878.

Pentland, C. H., El-Maghraby, R., Iglauer, S., and Blunt, M. J. (2011). Measurements of the capillary trapping of super-critical carbon dioxide in Berea sandstone. *Geophysical Research Letters*, *38*(6).

Pentland, C. H., Iglauer, S., Gharbi, O., Okada, K., and Suekane, T. (2012). *The influence of pore space geometry on the entrapment of carbon dioxide by capillary forces.* Paper presented at the SPE Asia Pacific Oil and Gas Conference and Exhibition.

Pini, R., Krevor, S., Krause, M., and Benson, S. (2013). Capillary Heterogeneity in Sandstone Rocks During CO 2/Water Core-flooding Experiments. *Energy Procedia*, *37*, 5473-5479.

Pini, R., Krevor, S. C., and Benson, S. M. (2012). Capillary pressure and heterogeneity for the CO 2/water system in sandstone rocks at reservoir conditions. *Advances in Water Resources*, *38*, 48-59.

Porter, R. T., Fairweather, M., Pourkashanian, M., and Woolley, R. M. (2015). The range and level of impurities in CO_2 streams from different carbon capture sources. *International Journal of Greenhouse Gas Control*, *36*, 161-174.

Preston, C., Monea, M., Jazrawi, W., Brown, K., Whittaker, S., White, D., Law, D., Chalaturnyk, R., and Rostron, B. (2005). IEA GHG Weyburn CO_2 monitoring and storage project. *Fuel Processing Technology*, *86*(14-15), 1547-1568.

Prevedel, B., Wohlgemuth, L., Legarth, B., Henninges, J., Schütt, H., Schmidt-Hattenberger, C., Norden, B., Förster, A., and Hurter, S. (2009). The CO 2 SINK boreholes for geological CO 2-storage testing. *Energy Procedia*, *1*(1), 2087-2094.

Pruess, K. (2005). Numerical simulations show potential for strong nonisothermal effects during fluid leakage from a geologic disposal reservoir for CO_2. *Dynamics of Fluids and Transport in Fractured Rock*, 81-89.

Pruess, K. (2011). ECO2M: a TOUGH2 fluid property module for mixtures of water, NaCl, and CO_2, including super-and sub-critical conditions, and phase change between liquid and gaseous CO_2. *Lawrence Berkeley National Laboratory*.

Pruess, K., and Garcia, J. (2002). Multiphase flow dynamics during CO_2 disposal into saline aquifers. *Environmental Geology*, *42*(2-3), 282-295.

Pruess, K., Oldenburg, C., and Moridis, G. (1999). TOUGH2 User's Guide Version 2. *Lawrence Berkeley National Laboratory*.

Pruess, K., Xu, T., Apps, J., and Garcia, J. (2003). Numerical Modeling of Aquifer Disposal of CO_2. *Spe Journal*, *8*(01), 49-60.

Qi, R., LaForce, T. C., and Blunt, M. J. (2009). Design of carbon dioxide storage in aquifers. *International Journal of Greenhouse Gas Control*, *3*(2), 195-205.

Rahman, T., Lebedev, M., Barifcani, A., and Iglauer, S. (2016). Residual trapping of supercritical CO 2 in oil-wet sandstone. *Journal of colloid and interface science*, *469*, 63-68.

Raza, S., Treiber, L., and Archer, D. (1968). Wettability of reservoir rocks and its evaluation. *Prod. Mon.;(United States)*, *32*(4).

Reiss, L. (1987). Production from horizontal wells after 5 years. *Journal of Petroleum Technology*, *39*(11), 1,411-411,416.

Reynolds, C., and Krevor, S. (2015). Characterizing flow behavior for gas injection: Relative permeability of CO_2-brine and N2-water in heterogeneous rocks. *Water Resources Research*, *51*(12), 9464-9489.

Rogers, J. D., and Grigg, R. B. (2001). A literature analysis of the WAG injectivity abnormalities in the CO_2 process. *SPE Reservoir Evaluation & Engineering*, *4*(05), 375-386.

Rumpf, B., Nicolaisen, H., Öcal, C., and Maurer, G. (1994). Solubility of carbon dioxide in aqueous solutions of sodium chloride: experimental results and correlation. *Journal of Solution Chemistry*, *23*(3), 431-448.

Ruprecht, C., Pini, R., Falta, R., Benson, S., and Murdoch, L. (2014). Hysteretic trapping and relative permeability of CO 2 in sandstone at reservoir conditions. *International Journal of Greenhouse Gas Control*, *27*, 15-27.

Saadatpoor, E., Bryant, S. L., and Sepehrnoori, K. (2009). Effect of capillary heterogeneity on buoyant plumes: A new local trapping mechanism. *Energy Procedia*, *1*(1), 3299-3306.

Saghafi, A., Javanmard, H., and Pinetown, K. (2014). Study of coal gas wettability for CO_2 storage and CH4 recovery. *Geofluids*, *14*(3), 310-325.

Sakurovs, R., and Lavrencic, S. (2011). Contact angles in CO 2-water-coal systems at elevated pressures. *International Journal of Coal Geology*, *87*(1), 26-32.

Saraji, S., Goual, L., Piri, M., and Plancher, H. (2013). Wettability of supercritical carbon dioxide/water/quartz systems: Simultaneous measurement of contact

angle and interfacial tension at reservoir conditions. *Langmuir*, *29*(23), 6856-6866.

Saraji, S., Piri, M., and Goual, L. (2014). The effects of SO 2 contamination, brine salinity, pressure, and temperature on dynamic contact angles and interfacial tension of supercritical CO 2/brine/quartz systems. *International Journal of Greenhouse Gas Control*, *28*, 147-155.

Sarmadivaleh, M., Al-Yaseri, A. Z., and Iglauer, S. (2015). Influence of temperature and pressure on quartz–water–CO 2 contact angle and CO 2–water interfacial tension. *Journal of colloid and interface science*, *441*, 59-64.

Schwartz, A. M., and Minor, F. W. (1959). A simplified thermodynamic approach to capillarity: I. Application to flow in capillary channels. *Journal of Colloid Science*, *14*(6), 572-583.

Shariatipour, S. M., Pickup, G. E., and Mackay, E. J. (2016). Simulations of CO 2 storage in aquifer models with top surface morphology and transition zones. *International Journal of Greenhouse Gas Control*, *54*, 117-128.

Shaw, J., and Bachu, S. (2002). Screening, evaluation, and ranking of oil reservoirs suitable for CO_2-flood EOR and carbon dioxide sequestration. *Journal of Canadian Petroleum Technology*, *41*(09).

Shi, J., and Durucan, S. (2005). CO_2 storage in deep unminable coal seams. *Oil & gas science and technology*, *60*(3), 547-558.

Sifuentes, W. F., Giddins, M. A., and Blunt, M. J. (2009). *Modeling CO_2 Storage in Aquifers: Assessing the key contributors to uncertainty.* Paper presented at the Offshore Europe.

Skauge, A., and Larsen, J. A. (1994). *Three-phase relative permeabilities and trapped gas measurements related to WAG processes.* Paper presented at the SCA 9421, proceedings of the International Symposium of the Society of Core Analysts, Stavanger, Norway.

Smithwich, R. W. (1988). Contact-angle studies of microscopic mercury droplets on glass. *Journal of colloid and interface science*, *123*(2), 482-485.

Smyth, R. C., Hovorka, S. D., Lu, J., Romanak, K. D., Partin, J. W., Wong, C., and Yang, C. (2009). Assessing risk to fresh water resources from long term CO_2 injection–laboratory and field studies. *Energy Procedia*, *1*(1), 1957-1964.

Sohrabi, M., Tehrani, D., Danesh, A., and Henderson, G. (2004). Visualization of oil recovery by water-alternating-gas injection using high-pressure micromodels. *Spe Journal*, *9*(03), 290-301.

Song, H., Huang, G., Li, T., Zhang, Y., and Lou, Y. (2014a). Analytical model of CO 2 storage efficiency in saline aquifer with vertical heterogeneity. *Journal of Natural Gas Science and Engineering*, *18*, 77-89.

Song, Z., Li, Z., Wei, M., Lai, F., and Bai, B. (2014b). Sensitivity analysis of water-alternating-CO 2 flooding for enhanced oil recovery in high water cut oil reservoirs. *Computers & Fluids*, *99*, 93-103.

Spinler, E., Baldwin, B., and Graue, A. (2002). Experimental artifacts caused by wettability variations in chalk. *Journal of Petroleum Science and Engineering*, *33*(1), 49-59.

Spycher, N., and Pruess, K. (2004). CO_2-H2O Mixtures in the Geological Sequestration of CO_2. II. Partitioning in Chloride Brines at 12-100oC and up to 600 bar. *Lawrence Berkeley National Laboratory*.

Spycher, N., Pruess, K., and Ennis-King, J. (2003). CO 2-H 2 O mixtures in the geological sequestration of CO 2. I. Assessment and calculation of mutual solubilities from 12 to 100 C and up to 600 bar. *Geochimica et cosmochimica acta*, *67*(16), 3015-3031.

Stalker, L., Varma, S., Van Gent, D., Haworth, J., and Sharma, S. (2013). South West Hub: a carbon capture and storage project. *Australian Journal of Earth Sciences*, *60*(1), 45-58.

Standnes, D. C., and Austad, T. (2000). Wettability alteration in chalk: 1. Preparation of core material and oil properties. *Journal of Petroleum Science and Engineering*, *28*(3), 111-121.

Stevens, S. H., Spector, D., and Riemer, P. (1998). *Enhanced coalbed methane recovery using CO_2 injection: worldwide resource and CO_2 sequestration potential.* Paper presented at the SPE International Oil and Gas Conference and Exhibition in China.

Suekane, T., Nobuso, T., Hirai, S., and Kiyota, M. (2008). Geological storage of carbon dioxide by residual gas and solubility trapping. *International Journal of Greenhouse Gas Control*, *2*(1), 58-64.

Syversveen, A. R., Nilsen, H. M., Lie, K.-A., Tveranger, J., and Abrahamsen, P. (2012). A Study on How Top-Surface Morphology Influences the Storage

Capacity of CO_2 in Saline Aquifers. In P. Abrahamsen, R. Hauge, & O. Kolbjørnsen (Eds.), *Geostatistics Oslo 2012* (pp. 481-492). Dordrecht: Springer Netherlands.

Tanaka, Y., Abe, M., Sawada, Y., Tanase, D., Ito, T., and Kasukawa, T. (2014). Tomakomai CCS Demonstration Project in Japan, 2014 Update. *Energy Procedia*, *63*, 6111-6119.

Teklu, T. W., Alameri, W., Graves, R. M., Kazemi, H., and AlSumaiti, A. M. (2016). Low-salinity water-alternating-CO 2 EOR. *Journal of Petroleum Science and Engineering*, *142*, 101-118.

Thomas, S. (2008). Enhanced oil recovery-an overview. *Oil & Gas Science and Technology-Revue de l'IFP*, *63*(1), 9-19.

Tokunaga, T. K., Wan, J., Jung, J. W., Kim, T. W., Kim, Y., and Dong, W. (2013). Capillary pressure and saturation relations for supercritical CO_2 and brine in sand: High-pressure Pc (Sw) controller/meter measurements and capillary scaling predictions. *Water Resources Research*, *49*(8), 4566-4579.

Torp, T. A., and Gale, J. (2004). Demonstrating storage of CO 2 in geological reservoirs: the Sleipner and SACS projects. *Energy*, *29*(9), 1361-1369.

Treiber, L., and Owens, W. (1972). A laboratory evaluation of the wettability of fifty oil-producing reservoirs. *Society of Petroleum Engineers Journal*, *12*(06), 531-540.

Turcotte, D., and Schubert, G. (2014). *Geodynamics*: Cambridge University Press.

Ukaegbu, C., Gundogan, O., Mackay, E., Pickup, G., Todd, A., and Gozalpour, F. (2009). Simulation of CO_2 storage in a heterogeneous aquifer. *Proceedings of the Institution of Mechanical Engineers, Part A: Journal of Power and Energy*, *223*(3), 249-267.

Underschultz, J., Boreham, C., Dance, T., Stalker, L., Freifeld, B., Kirste, D., and Ennis-King, J. (2011). CO_2 storage in a depleted gas field: An overview of the CO_2CRC Otway Project and initial results. *International Journal of Greenhouse Gas Control*, *5*(4), 922-932.

Van Genuchten, M. T. (1980). A closed-form equation for predicting the hydraulic conductivity of unsaturated soils. *Soil science society of America journal*, *44*(5), 892-898.

Van Lingen, P., Bruining, J., and Van Kruijsdijk, C. (1996). Capillary entrapment caused by small-scale wettability heterogeneities. *SPE Reservoir Engineering*, *11*(02), 93-100.

Vialle, S., Druhan, J. L., and Maher, K. (2016). Multi-phase flow simulation of CO_2 leakage through a fractured caprock in response to mitigation strategies. *International Journal of Greenhouse Gas Control*, *44*, 11-25.

Vivek, R., and Kumar, G. S. (2016). Numerical investigation on effect of varying injection scenario and relative permeability hysteresis on CO_2 dissolution in saline aquifer. *Environmental Earth Sciences*, *75*(16), 1192.

Vizika, O., and Duquerroix, J.-p. (1997). *Gas injection and heterogeneous wettability: what is the relevant information that petrophysics can provide.* Paper presented at the International Symposium of the Society of Core Analysts, Calgary, Canada, September.

Wang, F., Jing, J., Xu, T., Yang, Y., and Jin, G. (2016a). Impacts of stratum dip angle on CO_2 geological storage amount and security. *Greenhouse Gases: Science and Technology*, *6*(5), 682-694.

Wang, F., Jing, J., Yang, Y., Liu, H., Sun, Z., Xu, T., and Tian, H. (2016b). Impacts of injection pressure of a dip-angle sloping strata reservoir with low porosity and permeability on CO_2 injection amount. *Greenhouse Gases: Science and Technology*.

Wang, S., Edwards, I. M., and Clarens, A. F. (2012). Wettability phenomena at the CO_2–brine–mineral interface: implications for geologic carbon sequestration. *Environmental science & technology*, *47*(1), 234-241.

Wang, S., Tao, Z., Persily, S. M., and Clarens, A. F. (2013). CO_2 adhesion on hydrated mineral surfaces. *Environmental science & technology*, *47*(20), 11858-11865.

Wenzel, R. N. (1949). Surface roughness and contact angle. *The Journal of Physical Chemistry*, *53*(9), 1466-1467.

Wheaton, R. (2016). *Fundamentals of applied reservoir engineering: appraisal, economics and optimization*: Gulf Professional Publishing.

Wilhelmy, L. (1863). Ueber die Abhängigkeit der Capillaritäts-Constanten des Alkohols von Substanz und Gestalt des benetzten festen Körpers. *Annalen der Physik*, *195*(6), 177-217.

Woods, A. W., and Farcas, A. (2009). Capillary entry pressure and the leakage of gravity currents through a sloping layered permeable rock. *Journal of Fluid Mechanics*, *618*, 361-379.

Xie, X., and Economides, M. J. (2009). The impact of carbon geological sequestration. *Journal of Natural Gas Science and Engineering*, *1*(3), 103-111.

Xiuzhang, W. (2014). Shenhua Group's carbon capture and storage (CCS) demonstration. *Mining Report*, *150*(1-2), 81-84.

Xu, T., Apps, J. A., and Pruess, K. (2003). Reactive geochemical transport simulation to study mineral trapping for CO_2 disposal in deep arenaceous formations. *Journal of Geophysical Research: Solid Earth*, *108*(B2).

Xu, T., Apps, J. A., and Pruess, K. (2004). Numerical simulation of CO 2 disposal by mineral trapping in deep aquifers. *Applied geochemistry*, *19*(6), 917-936.

Xu, T., Apps, J. A., and Pruess, K. (2005). Mineral sequestration of carbon dioxide in a sandstone–shale system. *Chemical Geology*, *217*(3), 295-318.

Xue, Z., Tanase, D., and Watanabe, J. (2006). Estimation of CO_2 saturation from time-lapse CO_2 well logging in an onshore aquifer, Nagaoka, Japan. *Exploration Geophysics*, *37*(1), 19-29.

Yang, D., Gu, Y., and Tontiwachwuthikul, P. (2008a). Wettability Determination of the Crude Oil− Reservoir Brine− Reservoir Rock System with Dissolution of CO 2 at High Pressures and Elevated Temperatures. *Energy & Fuels*, *22*(4), 2362-2371.

Yang, D., Gu, Y., and Tontiwachwuthikul, P. (2008b). Wettability determination of the reservoir brine-reservoir rock system with dissolution of CO_2 at high pressures and elevated temperatures. *Energy & Fuels*, *22*(1), 504-509.

Yang, D., Tontiwachwuthikul, P., and Gu, Y. (2005). Interfacial tensions of the crude oil+ reservoir brine+ CO_2 systems at pressures up to 31 MPa and temperatures of 27 C and 58 C. *Journal of Chemical and Engineering Data*, *50*(4), 1242-1249.

Yang, Y., and Aplin, A. C. (2007). Permeability and petrophysical properties of 30 natural mudstones. *Journal of Geophysical Research: Solid Earth*, *112*(B3).

Yielding, G., Lykakis, N., and Underhill, J. R. (2011). The role of stratigraphic juxtaposition for seal integrity in proven CO_2 fault-bound traps of the Southern North Sea. *Petroleum Geoscience*, *17*(2), 193-203.

Yuan, Y., and Lee, T. R. (2013). Contact angle and wetting properties *Surface science techniques* (pp. 3-34): Springer.

Zeidouni, M., Nicot, J., Hovorka, S. D., and Nunez-Lopez, V. (2015). *Effect of Depth and Leakage-Pathway Flow Properties on Thermal Response to Leakage from* CO_2 *Storage Zone.* Paper presented at the Carbon Management Technology Conference.

Zhang, L., Dilmore, R. M., and Bromhal, G. S. (2016a). Effect of outer boundary condition, reservoir size, and CO_2 effective permeability on pressure and CO_2 saturation predictions under carbon sequestration conditions. *Greenhouse Gases: Science and Technology*, *6*(4), 546-560. doi:10.1002/ghg.1586

Zhang, Y., Lebedev, M., Sarmadivaleh, M., Barifcani, A., and Iglauer, S. (2016b). Swelling-induced changes in coal microstructure due to supercritical CO_2 injection. *Geophysical Research Letters*, *43*(17), 9077-9083.

Zhang, Z. (2016). Comparisons of various absorbent effects on carbon dioxide capture in membrane gas absorption (MGA) process. *Journal of Natural Gas Science and Engineering*, *31*, 589-595.

Zheng, S., and Yang, D. T. (2013). Pressure maintenance and improving oil recovery by means of immiscible water-alternating-CO_2 processes in thin heavy-oil reservoirs. *SPE Reservoir Evaluation & Engineering*, *16*(01), 60-71.

Zhou, Q., Birkholzer, J. T., Mehnert, E., Lin, Y. F., and Zhang, K. (2010). Modeling basin-and plume-scale processes of CO_2 storage for full-scale deployment. *Ground water*, *48*(4), 494-514.

Zhou, Q., Birkholzer, J. T., Tsang, C.-F., and Rutqvist, J. (2008). A method for quick assessment of CO 2 storage capacity in closed and semi-closed saline formations. *International Journal of Greenhouse Gas Control*, *2*(4), 626-639.

Appendix A: Attribution of Authorship

Paper "**Influence of CO_2-wettability on CO_2 migration and trapping capacity in deep saline aquifers**" Greenhouse Gases: Science and Technology, 2017, 7 (2), 328-338.

Authors and full affiliations: Emad A. Al-Khdheeawi[a,c,*], Stephanie Vialle[b], Ahmed Barifcani[a], Mohammad Sarmadivaleh[a], Stefan Iglauer[d]

[a] Department of Petroleum Engineering, Curtin University, 6151 Kensington, Western Australia, Australia.

[b] Department of Exploration Geophysics, Curtin University, 6151 Kensington, Western Australia, Australia.

[c] Petroleum Technology Department, University of Technology, Baghdad, Iraq

[d] School of Engineering, Petroleum Engineering discipline, Edith Cowan University, Joondalup Western Australia 6027, Australia.

	Conception and design	Acquisition of data and method	Data conditioning and manipulation	Analysis and statistical method	Interpretation and discussion	Final approval
Dr. Stephanie Vialle						✔
I acknowledge that these represent my contribution to the above research output. Signature: [redacted]						
Dr. Ahmed Barifcani						✔
I acknowledge that these represent my contribution to the above research output. Signature: [redacted]						
Dr. Mohammad Sarmadivaleh						✔
I acknowledge that these represent my contribution to the above research output. Signature: [redacted]						
Dr. Stefan Iglauer						✔
I acknowledge that these represent my contribution to the above research output. Signature: [redacted]						

Paper "**Impact of reservoir wettability and heterogeneity on CO_2-plume migration and trapping capacity"** International Journal of Greenhouse Gas Control, 2017, 58 (2017), 328-338.

Authors and full affiliations: Emad A. Al-Khdheeawi[a,c,*], Stephanie Vialle[b], Ahmed Barifcani[a], Mohammad Sarmadivaleh[a], Stefan Iglauer[d]

[a] Department of Petroleum Engineering, Curtin University, 6151 Kensington, Western Australia, Australia.

[b] Department of Exploration Geophysics, Curtin University, 6151 Kensington, Western Australia, Australia.

[c] Petroleum Technology Department, University of Technology, Baghdad, Iraq

[d] School of Engineering, Petroleum Engineering discipline, Edith Cowan University, Joondalup Western Australia 6027, Australia.

	Conception and design	Acquisition of data and method	Data conditioning and manipulation	Analysis and statistical method	Interpretation and discussion	Final approval
Dr. Stephanie Vialle						✔
I acknowledge that these represent my contribution to the above research output. Signature: [redacted]						
Dr. Ahmed Barifcani						✔
I acknowledge that these represent my contribution to the above research output. Signature: [redacted]						
Dr. Mohammad Sarmadivaleh						✔
I acknowledge that these represent my contribution to the above research output. Signature: [redacted]						
Dr. Stefan Iglauer						✔
I acknowledge that these represent my contribution to the above research output. Signature: [redacted]						

Paper "**Influence of injection well configuration and rock wettability on CO_2 plume behaviour and CO_2 trapping capacity in heterogeneous reservoirs**" Journal of Natural Gas Science and Engineering, 2017, 43 (2017), 190-206.

Authors and full affiliations: Emad A. Al-Khdheeawi[a,c,*], Stephanie Vialle[b], Ahmed Barifcani[a], Mohammad Sarmadivaleh[a], Stefan Iglauer[d]

[a] Department of Petroleum Engineering, Curtin University, 6151 Kensington, Western Australia, Australia.

[b] Department of Exploration Geophysics, Curtin University, 6151 Kensington, Western Australia, Australia.

[c] Petroleum Technology Department, University of Technology, Baghdad, Iraq

[d] School of Engineering, Petroleum Engineering discipline, Edith Cowan University, Joondalup Western Australia 6027, Australia.

	Conception and design	Acquisition of data and method	Data conditioning and manipulation	Analysis and statistical method	Interpretation and discussion	Final approval
Dr. Stephanie Vialle						✔
I acknowledge that these represent my contribution to the above research output. Signature: [redacted]						
Dr. Ahmed Barifcani						✔
I acknowledge that these represent my contribution to the above research output. Signature: [redacted]						
Dr. Mohammad Sarmadivaleh						✔
I acknowledge that these represent my contribution to the above research output. Signature: [redacted]						
Dr. Stefan Iglauer						✔
I acknowledge that these represent my contribution to the above research output. Signature: [redacted]						

Paper "**Effect of wettability heterogeneity and reservoir temperature on CO_2 storage efficiency in deep saline aquifers**" International Journal of Greenhouse Gas Control, 2018, 68 (2018), 216-229.

Authors and full affiliations: Emad A. Al-Khdheeawi[a,c,*], Stephanie Vialle[b], Ahmed Barifcani[a], Mohammad Sarmadivaleh[a], Stefan Iglauer[d]

[a] Department of Petroleum Engineering, Curtin University, 6151 Kensington, Western Australia, Australia.

[b] Department of Exploration Geophysics, Curtin University, 6151 Kensington, Western Australia, Australia.

[c] Petroleum Technology Department, University of Technology, Baghdad, Iraq

[d] School of Engineering, Petroleum Engineering discipline, Edith Cowan University, Joondalup Western Australia 6027, Australia.

	Conception and design	Acquisition of data and method	Data conditioning and manipulation	Analysis and statistical method	Interpretation and discussion	Final approval
Dr. Stephanie Vialle						✔
I acknowledge that these represent my contribution to the above research output. Signature: [redacted]						
Dr. Ahmed Barifcani						✔
I acknowledge that these represent my contribution to the above research output. Signature: [redacted]						
Dr. Mohammad Sarmadivaleh						✔
I acknowledge that these represent my contribution to the above research output. Signature: [redacted]						
Dr. Stefan Iglauer						✔
I acknowledge that these represent my contribution to the above research output. Signature: [redacted]						

Paper "**Impact of salinity on CO_2 containment security in highly heterogeneous reservoirs**" Greenhouse Gases: Science and Technology, 2018, 8(1), 93-105.

Authors and full affiliations: Emad A. Al-Khdheeawi[a,c,*], Stephanie Vialle[b], Ahmed Barifcani[a], Mohammad Sarmadivaleh[a], Yihuai Zhang[a], Stefan Iglauer[d]

[a] Department of Petroleum Engineering, Curtin University, 6151 Kensington, Western Australia, Australia.

[b] Department of Exploration Geophysics, Curtin University, 6151 Kensington, Western Australia, Australia.

[c] Petroleum Technology Department, University of Technology, Baghdad, Iraq

[d] School of Engineering, Petroleum Engineering discipline, Edith Cowan University, Joondalup Western Australia 6027, Australia.

	Conception and design	Acquisition of data and method	Data conditioning and manipulation	Analysis and statistical method	Interpretation and discussion	Final approval
Dr. Stephanie Vialle						✔
I acknowledge that these represent my contribution to the above research output. Signature: [redacted]						
Dr. Ahmed Barifcani						✔
I acknowledge that these represent my contribution to the above research output. Signature: [redacted]						
Dr. Mohammad Sarmadivaleh						✔
I acknowledge that these represent my contribution to the above research output. Signature: [redacted]						
Yihuai Zhang			✔			
I acknowledge that these represent my contribution to the above research output. Signature: [redacted]						
Dr. Stefan Iglauer						✔
I acknowledge that these represent my contribution to the above research output. Signature: [redacted]						

Paper "**Enhancement of CO_2 trapping efficiency in heterogeneous reservoirs by Water Alternating Gas injection**" Greenhouse Gases: Science and Technology, 2018, 8(5), 920-931.

Authors and full affiliations: Emad A. Al-Khdheeawi[a,c,*], Stephanie Vialle[b], Ahmed Barifcani[a], Mohammad Sarmadivaleh[a], Stefan Iglauer[d]

[a] Department of Petroleum Engineering, Curtin University, 6151 Kensington, Western Australia, Australia.
[b] Department of Exploration Geophysics, Curtin University, 6151 Kensington, Western Australia, Australia.
[c] Petroleum Technology Department, University of Technology, Baghdad, Iraq
[d] School of Engineering, Petroleum Engineering discipline, Edith Cowan University, Joondalup Western Australia 6027, Australia.

	Conception and design	Acquisition of data and method	Data conditioning and manipulation	Analysis and statistical method	Interpretation and discussion	Final approval
Dr. Stephanie Vialle						✔
I acknowledge that these represent my contribution to the above research output. Signature: [redacted]						
Dr. Ahmed Barifcani						✔
I acknowledge that these represent my contribution to the above research output. Signature: [redacted]						
Dr. Mohammad Sarmadivaleh						✔
I acknowledge that these represent my contribution to the above research output. Signature: [redacted]						
Dr. Stefan Iglauer						✔
I acknowledge that these represent my contribution to the above research output. Signature: [redacted]						

Appendix B: Copyright Agreements

Article: "Influence of CO_2-wettability on CO_2 migration and trapping capacity in deep saline aquifers" Greenhouse Gases: Science and Technology.

JOHN WILEY AND SONS LICENSE TERMS AND CONDITIONS

May 27, 2019

This Agreement between Mr. Emad Al-Khdheeawi ("You") and John Wiley and Sons ("John Wiley and Sons") consists of your license details and the terms and conditions provided by John Wiley and Sons and Copyright Clearance Center.

License Number	4597120068910
License date	May 27, 2019
Licensed Content Publisher	John Wiley and Sons
Licensed Content Publication	Greenhouse Gases: Science and Technology
Licensed Content Title	Influence of CO2-wettability on CO2 migration and trapping capacity in deep saline aquifers
Licensed Content Author	Emad A. Al-Khdheeawi, Stephanie Vialle, Ahmed Barifcani, et al
Licensed Content Date	Nov 18, 2016
Licensed Content Volume	7
Licensed Content Issue	2
Licensed Content Pages	11
Type of use	Dissertation/Thesis
Requestor type	Author of this Wiley article
Format	Print and electronic
Portion	Full article
Will you be translating?	No
Title of your thesis / dissertation	Influence of Rock Wettability on Reservoir-Scale CO2 Geo-Sequestration
Expected completion date	May 2019
Expected size (number of pages)	200
Requestor Location	Mr. Emad Al-Khdheeawi 26 Dick Perry Avenue Kensington, WA 6151 Australia Attn: Mr. Emad Al-Khdheeawi
Publisher Tax ID	EU826007151
Total	0.00 USD
Terms and Conditions	

Article: “Impact of reservoir wettability and heterogeneity on CO_2-plume migration and trapping capacity” International Journal of Greenhouse Gas Control.

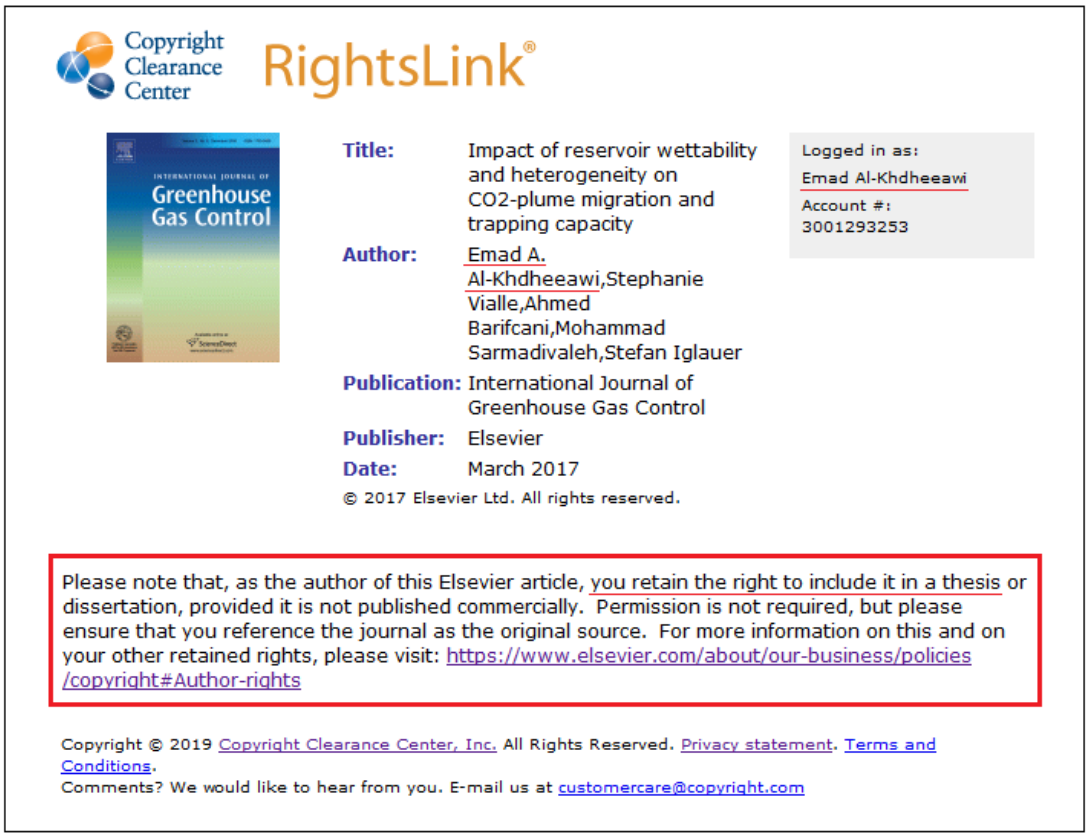

Copyright Clearance Center RightsLink®

Title: Impact of reservoir wettability and heterogeneity on CO2-plume migration and trapping capacity

Author: Emad A. Al-Khdheeawi,Stephanie Vialle,Ahmed Barifcani,Mohammad Sarmadivaleh,Stefan Iglauer

Publication: International Journal of Greenhouse Gas Control

Publisher: Elsevier

Date: March 2017

Logged in as:
Emad Al-Khdheeawi
Account #:
3001293253

Please note that, as the author of this Elsevier article, you retain the right to include it in a thesis or dissertation, provided it is not published commercially. Permission is not required, but please ensure that you reference the journal as the original source. For more information on this and on your other retained rights, please visit: https://www.elsevier.com/about/our-business/policies/copyright#Author-rights

Article: “Influence of injection well configuration and rock wettability on CO_2 plume behaviour and CO_2 trapping capacity in heterogeneous reservoirs” Journal of Natural Gas Science and Engineering.

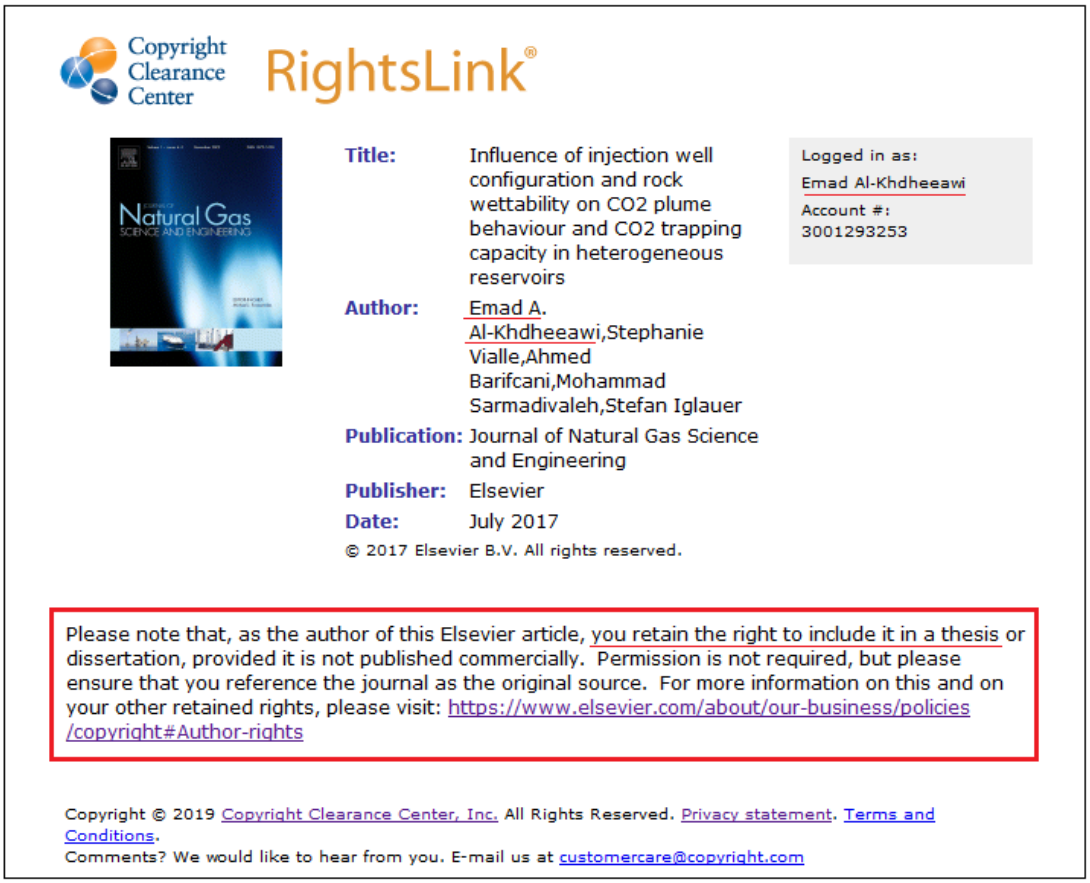

Copyright Clearance Center RightsLink®

Title: Influence of injection well configuration and rock wettability on CO2 plume behaviour and CO2 trapping capacity in heterogeneous reservoirs

Author: Emad A. Al-Khdheeawi,Stephanie Vialle,Ahmed Barifcani,Mohammad Sarmadivaleh,Stefan Iglauer

Publication: Journal of Natural Gas Science and Engineering

Publisher: Elsevier

Date: July 2017

© 2017 Elsevier B.V. All rights reserved.

Logged in as:
Emad Al-Khdheeawi
Account #:
3001293253

Please note that, as the author of this Elsevier article, you retain the right to include it in a thesis or dissertation, provided it is not published commercially. Permission is not required, but please ensure that you reference the journal as the original source. For more information on this and on your other retained rights, please visit: https://www.elsevier.com/about/our-business/policies/copyright#Author-rights

Copyright © 2019 Copyright Clearance Center, Inc. All Rights Reserved. Privacy statement. Terms and Conditions.
Comments? We would like to hear from you. E-mail us at customercare@copyright.com

Article: “Effect of wettability heterogeneity and reservoir temperature on CO_2 storage efficiency in deep saline aquifers” International Journal of Greenhouse Gas Control.

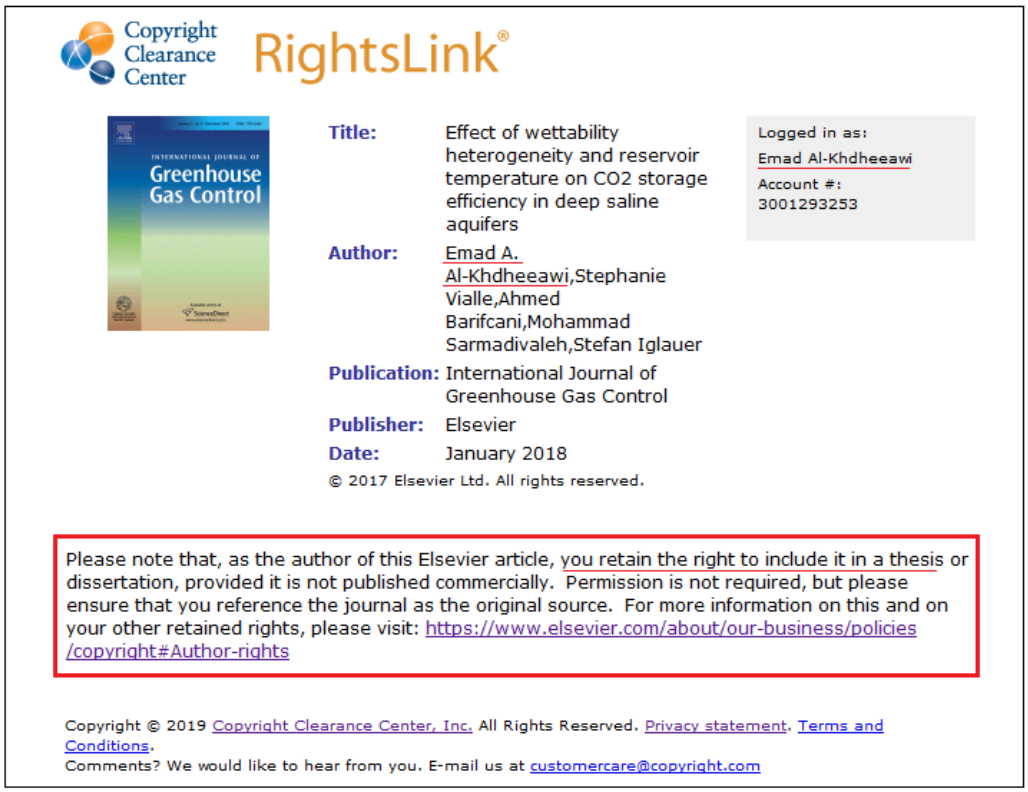

Copyright Clearance Center RightsLink®

Title: Effect of wettability heterogeneity and reservoir temperature on CO2 storage efficiency in deep saline aquifers

Author: Emad A. Al-Khdheeawi,Stephanie Vialle,Ahmed Barifcani,Mohammad Sarmadivaleh,Stefan Iglauer

Publication: International Journal of Greenhouse Gas Control

Publisher: Elsevier

Date: January 2018

© 2017 Elsevier Ltd. All rights reserved.

Logged in as:
Emad Al-Khdheeawi
Account #:
3001293253

Please note that, as the author of this Elsevier article, you retain the right to include it in a thesis or dissertation, provided it is not published commercially. Permission is not required, but please ensure that you reference the journal as the original source. For more information on this and on your other retained rights, please visit: https://www.elsevier.com/about/our-business/policies/copyright#Author-rights

Copyright © 2019 Copyright Clearance Center, Inc. All Rights Reserved. Privacy statement. Terms and Conditions.
Comments? We would like to hear from you. E-mail us at customercare@copyright.com

Article: “Impact of salinity on CO_2 containment security in highly heterogeneous reservoirs” Greenhouse Gases: Science and Technology.

JOHN WILEY AND SONS LICENSE TERMS AND CONDITIONS

May 27, 2019

This Agreement between Mr. Emad Al-Khdheeawi ("You") and John Wiley and Sons ("John Wiley and Sons") consists of your license details and the terms and conditions provided by John Wiley and Sons and Copyright Clearance Center.

License Number	4597120764228
License date	May 27, 2019
Licensed Content Publisher	John Wiley and Sons
Licensed Content Publication	Greenhouse Gases: Science and Technology
Licensed Content Title	Impact of salinity on CO2 containment security in highly heterogeneous reservoirs
Licensed Content Author	Emad A. Al-Khdheeawi, Stephanie Vialle, Ahmed Barifcani, et al
Licensed Content Date	Sep 8, 2017
Licensed Content Volume	8
Licensed Content Issue	1
Licensed Content Pages	13
Type of use	Dissertation/Thesis
Requestor type	Author of this Wiley article
Format	Print and electronic
Portion	Full article
Will you be translating?	No
Title of your thesis / dissertation	Influence of Rock Wettability on Reservoir-Scale CO2 Geo-Sequestration
Expected completion date	May 2019
Expected size (number of pages)	200
Requestor Location	Mr. Emad Al-Khdheeawi 26 Dick Perry Avenue Kensington, WA 6151 Australia Attn: Mr. Emad Al-Khdheeawi
Publisher Tax ID	EU826007151
Total	0.00 USD
Terms and Conditions	

Article: “Enhancement of CO_2 trapping efficiency in heterogeneous reservoirs by Water Alternating Gas injection” Greenhouse Gases: Science and Technology.

JOHN WILEY AND SONS LICENSE TERMS AND CONDITIONS

May 27, 2019

This Agreement between Mr. Emad Al-Khdheeawi ("You") and John Wiley and Sons ("John Wiley and Sons") consists of your license details and the terms and conditions provided by John Wiley and Sons and Copyright Clearance Center.

License Number	4597121102348
License date	May 27, 2019
Licensed Content Publisher	John Wiley and Sons
Licensed Content Publication	Greenhouse Gases: Science and Technology
Licensed Content Title	Enhancement of CO2 trapping efficiency in heterogeneous reservoirs by water-alternating gas injection
Licensed Content Author	Emad A. Al-Khdheeawi, Stephanie Vialle, Ahmed Barifcani, et al
Licensed Content Date	Jul 22, 2018
Licensed Content Volume	8
Licensed Content Issue	5
Licensed Content Pages	12
Type of use	Dissertation/Thesis
Requestor type	Author of this Wiley article
Format	Print and electronic
Portion	Full article
Will you be translating?	No
Title of your thesis / dissertation	Influence of Rock Wettability on Reservoir-Scale CO2 Geo-Sequestration
Expected completion date	May 2019
Expected size (number of pages)	200
Requestor Location	Mr. Emad Al-Khdheeawi 26 Dick Perry Avenue Kensington, WA 6151 Australia Attn: Mr. Emad Al-Khdheeawi
Publisher Tax ID	EU826007151
Total	0.00 USD
Terms and Conditions	